

**RUSSIAN ACADEMY OF NATURAL SCIENCES LOMONOSOV  
MOSCOW STATE UNIVERSITY**

---

**RUSSIAN ACADEMY of NATURAL SCIENCES  
LOMONOSOV MOSCOW STATE UNIVERSITY  
PEOPLES' FRIENDSHIP UNIVERSITY OF RUSSIA**

---

**MATERIALS**

**28th RUSSIAN CONFERENCE ON COLD TRANSMUTATION OF  
NUCLEI OF CHEMICAL ELEMENTS AND BALL LIGHTNING**

**PROCEEDINGS of  
the 28th RUSSIAN CONFERENCE on COLD NUCLEAR  
TRANSMUTATION of CHEMICAL ELEMENTS and BALL  
LIGHTNING**

**MOSCOW, September 30 - October 4, 2024**

**MOSCOW, September 30 - October 4, 2024**

---

**MOSCOW – 2024**

UDC 539.17 / 533.9  
BBK 22.383.5 / 22.333

**Problems of cold transmutation of nuclei of chemical elements and ball lightning:** Proceedings of the 28th Russian Conference on Cold Transmutation of Nuclei of Chemical Elements and Physics of Ball Lightning. Moscow, September 30 - October 4, 2024. Collection of materials. Ch. ed. A.G. Parkhomov, editor. L.B. Boldyreva, V.L. Bychkov V.N. Zatelepin., A.I. Klimov, A.A. Prosvirnov. M.: , 2024, 440 p.

From September 30 to October 4, 2024, the XXVIII Russian Conference on Cold Transmutation of Nuclei and Ball Lightning Physics (RCCNLP-28) was held online via the ZOOM system. Reports were heard and discussed in the following areas: experimental research in the field of Cold Transmutation of Nuclei (CTN) of chemical elements and Ball Lightning (BL), theoretical models of CTN and BL, prospects for practical applications of CTN and BL, theoretical, experimental and applied research into the interaction of physical fields and matter. The collection presents materials of reports accepted by the editorial board for publication.

UDC 539.17 / 533.9  
BBK 22.383.5 / 2.333

ISBN

## **Organizing Committee of the RKHTYA and SHM-28**

### **Chairman of the organizing committee:**

A.G. Parkhomov, Ph.D., Moscow, corresponding member. RANS

### **Members of the Organizing Committee:**

L.B. Boldyreva, Ph.D., Associate Professor

V.L. Bychkov, D.Sc. (Phys. and Mathematics), M.V. Lomonosov Moscow State University, Academician of the Russian Academy of Natural

Sciences V.N. Zatelepin, Ph.D. (Eng.), Inlis LLC, Moscow, Corresponding Member of the Russian Academy of Natural Sciences

A.I.Klimov, Doctor of Physical and Mathematical Sciences, OIVT RAS, Academician of the  
Russian Academy of Natural Sciences A.A. Prosvirnov, Scientific Secretary of VNIIAES

### **Dear colleagues!**

From September 30 to October 4, 2024, the XXVIII Russian Conference on Cold Nuclear Transmutation and Ball Lightning Physics (RKHTN and BL-28) was held. The conference was held in a way that has already become traditional: on the Internet via the ZOOM system without personal presence. The number of scientific reports made was 40. Among them, 8 reports from near and far abroad. 5 round tables were held with a discussion of the reports heard.

To ensure that everyone has a place at the Conference, in addition to the traditional sections "Cold transmutation of nuclei of chemical elements.

Experimental Research", "Theoretical Models" and "Ball Lightning" sections were organized: "Theoretical, Experimental and Applied Research of the Interaction of Physical Fields with Matter" and "Approaches to the Study of Little-Studied Natural Phenomena".

Of course, it's a pity that this time we couldn't communicate in person. But Internet conferences have their advantages. You don't have to spend a lot of money on travel and hotel accommodation. State borders cease to exist. an obstacle.

With video recordings of reports, as well as speeches at the Round Tables can be found on the Internet.

# Content

**Links to video recordings of RCCTN&BL – 28** Links to  
videorecord RCCTN&BL – 28 .....9

**The main speakers at the RCXTAISHM – 28**

.....10

## Review reports Overview reports

**Experimental prerequisites for the theory of cold nuclear transformations.** A.G.  
Parkhomov.

**Experimental prerequisites of the theory of cold nuclear transformations.**  
A. G. Parkhomov .....13

**LENR indicators.** V.A. Zhigalov **LENR**  
**indicators.** VA Zhigalov.....22

**Observational properties of ball lightning, data for 2024.** VL Bychkov .....38

## **Section "Cold transmutation of nuclei of chemical elements.**

### **Experimental studies"**

### **Section "Cold Nuclear Transmutation Of Chemical Elements.**

#### **Experimental Investigations»**

**Low-energy nuclear reactions in tungsten at the plasma focus PFM 72-m facility**

Savvatimova I.B., Klochkov A.N., Sidorov

P.P., Bashutin O.A.

**Low-energy nuclear reactions in tungsten at the PFM 72-m plasma focus**

**facility** Savvatimova IB, Klochkov AN, Sidorov PP, Bashutin

OA.....55

**The main results obtained at the PVR-V reactor in the period from 2022 to 2024.** A.I. Klimov.

**Main results obtained on PVR-V reactor in the period from 2022 to 2024** AI

Klimov.....71

<b>Study of the spectrum of spark electric discharge in water-air medium using antenna. Effect of electric field, magnetic field, laser on spectrum.</b> D.S. Baranov, V.N. Zatelepin, A.L. Shishkin.	
<b>Investigation of the spectrum of a spark electric discharge in an air-water environment using an antenna. The effect of an external electric field, magnetic field, and laser on the spectrum.</b> DS Baranov, VN Zatelepin, ALShishkin.....	82
<b>Formation of a solid phase by irradiating carbon dioxide with a laser beam, passed near the zone of spark electric discharge in the water-air environment.</b> D.S. Baranov, A. Kovacs, R. Grinye, V.N. Zatelepin V.N.	
<b>Formation of a solid phase when carbon dioxide is irradiated by a laser beam passing near the spark electric discharge zone in an air-water environment</b>	
Baranov DSAKovacs, R. Greenyer, VN Zatelepin .....	93
<b>Properties of strange radiation tracks. An attempt at explanation.</b> A.G. Parkhomov, V.A. Zhigalov	
<b>Properties of strange radiation tracks. An attempt at explanation</b>	
AG Parkhomov, VA Zhigalov.....	110
<b>Mass spectra of tungsten isotopes and their oxides and estimation of the number of massive electron pairs in modified tungsten atoms.</b> M.P. Kashchenko, M.A. Kovalenko, V.I. Pechorsky, N.M. Kashchenko	
<b>Mass-spectra of tungsten isotopes and of their oxidizes and estimation of quantity of massive electronic pairs in modified tungsten atoms.</b>	
M. P. Kashchenko, M. A. Kovalenko, V. I. Pechorskii, N. M. Kashchenko.....	124
<b>Lightning-like erosion structures activated by light, magnetic field and magnetorheological fluid</b>	
on the remaining magnetic charges in solid zirconium after their origin in nuclear transformations in electron melting. M.I. Solin	
<b>Lightning-like erosive structures of activating effects of light, magnetic field and magnetorheological fluid on preserved magnetic charges in solid zirconium after their emergence in nuclear transformations in electronic melting.</b> MI Solin.....	135
<b>Experiments with torsinds. The effect of accelerated rotation of a body on another stationary body.</b> V.A. Chizhov, I.N. Stepanov	
<b>Experiments with torsinds or the effect of accelerated rotation of a body on another stationary body.</b> VAChizhov, IN Stepanov .....	138

**Section "Cold transmutation of nuclei of chemical elements.  
Theoretical models"  
Section "Theoretical Models"**

**An approach to understanding the mechanism of low-energy nuclear transformations based on experimental premises.** A.G. Parkhomov

**An approach to understanding the mechanism of low-energy nuclear transformations based on experiments.** AG Parkhomov.....147

**Four steps of LENR reactions (multi-electron model of reactions).** V.F. Chibisov

**Four steps of LENR reactions (multi-electronic reaction model).** VF Chibisov...156

**Geometrical Theory of Nuclear Interactions and Its Practical Consequences.** E.A.Gubarev, A.N.Sidorov

**Geometric theory for the nuclear interaction and its practical consequences.**  
EAGubarev, ANSidorov.....177

**The Problem of Inertia and Rotation of Matter.** G.I. Shipov

**The problem of inertia and rotation of matter.** GI Shipov.....183

**Newton's First Law. The force of inertia and its manifestations (rotation of an accelerating body, change in weight rotating body).** L.B. Boldyрева

**The first law of Newton. The force of inertia and its manifestations (the rotation of a body moving with acceleration, changing the weight of a rotating body).**  
LB Boldyрева.....199

**From the properties of virtual photons to the corpuscular-wave dualism.** L.B. Boldyрева

**From properties of virtual photon to wave-particle duality.** LB Boldyрева.....213

**The mechanism of cavitation in solid, liquid, gas and ether (electric shock).** .V. Shestopalov

**The mechanism of cavitation in solids, liquids, gaseous and in the ether (electric shock).** AV Shestopalov.....225

**Why are LENR phenomena observed in hydrides of nickel, palladium and titanium? Where do protons and deuterons come from in metal hydrides?**

**What is the essence of low-energy nuclear interaction?** G.K. Savinkov

**Why are LENR phenomena observed in hydrides of nickel, palladium and titanium?**

**Where do protons and deuterons in metal hydrides come from?**

**What is the essence of low-energy nuclear interaction?** GK Savinkov.....245

## **Section "Ball Lightning" Section «Ball lightning»**

**Thermochemical Ball Lightning.** V.L.Bychkov, D.E.Sorokovskykh, D.N.Vaulin  
**Thermochemical ball lightning.** VLBychkov, DESorokovskykh, DN Vaulin.....263

**Interpretation of the experiments of D.S.Baranov, V.N.Zatelepin,  
A.L.Shishkin with spark discharges in a water-air medium from the  
position of unipolar ether. Types of ball lightning.** A.I.Mirkin  
**Interpretation of experiments conducted by DSBaranov, VN Zatelepin, AL  
Shishkin with spark discharges in water-air environment from  
the position of unipolar ether. Types of ball lightnings.** AI Mirkin.....273

**Cold Non-Nuclear Fusion and Ball Lightning.** A.V. Shestopalov  
**Cold non-nuclear fusion and ball lightning.** AVShestopalov.....284

**Ball Lightning Characteristics Help Us Understand the Strange Particles:  
Micro Ball Lightning.** Edward Lewis  
**Characteristics of Ball Lightning Provide an Understanding of Strange Particles:  
Microball Lightning.** Edward Lewis.....304

### **Section "Theoretical, experimental and applied research of the interaction of physical fields with matter"**

### **Section "Theoretical, experimental and applied studies of the interaction of physical fields with matter"**

**Dirac monopoles as entities of dynamic space. Magnetic field as an  
inertial characteristic of electromagnetic  
Reality as a stratification into a space of coordinates and a  
space of momenta** Strigin M.B.  
**Dirac monopolies as entities of dynamic space. The magnetic field  
as an inertial characteristic of an electromagnetic wave.  
Reality as a stratification into the space of coordinates  
and the space of impulses** Strigin MB.....318

**Theory and practice of measuring the characteristics of physical vacuum**  
E.M. Avsharov, E.A. Gubarev  
**Theory and practice of measuring the properties of physical vacuum.**  
EMAvsharov, EAGubarev.....330

**Etheric Vortex Mechanism of Toroidal-Cavitation Transmutation  
(EVTCT).** E.M. Avsharov  
**Ethereal Vortex mechanism of Toroidal Cavitation  
Transmutation.** EM Avsharov.....339

**Section "Approaches to the study of little-studied natural phenomena"  
Section "Approaches to the study of poorly studied natural phenomena"**

**Mechanical structure of the universe. Mechanical equivalent of electricity.** V.V. Afonin

**The Mechanical Structure of the Universe. The mechanical equivalent of electricity.**

VV Afonin.....363

**What is a de Broglie wave** V.N. Pakulin

**What is a de Broglie wave** VN Pakulin .....389

**The Nature of Thermal Background Radiation of the Universe.** S.I. Konstantinov

**The nature of thermal background radiation of the Universe** S.I. Konstantinov.....403

**What the History of Physics Helps Us Predict About the Development of the Microplasmoid**

**Field** Edward Lewis

**What the history of physics helps us predict about the development of the microplasmoid field.** Edward Lewis.....409

**Mechanico-mathematical substantiation of the main provisions of the poem**

**"On the Nature of Things" by Titus Lucretius Carus.** M.Ya. Ivanov

**Mechanical and mathematical justification of the main provisions of the poem "About the nature of things" by Titus Lucretius Carus.** M,Ya. Ivanov.....417

**Resolution on the work of the RCNT&B L**

..... 438

**Links to video recordings of RKHTYA and SHM – 28  
Links on videorecord RCCTN & BL – 28**

**September 30, 2024 September 30,**

**2024** 12 -14 Opening ceremony [https://disk.yandex.ru/i/VI\\_7D0IdGaDc1g](https://disk.yandex.ru/i/VI_7D0IdGaDc1g) 16 – 18 <https://disk.yandex.ru/i/ENHx9GpqJ1XuYQ> 19:00 Round table <https://disk.yandex.ru/i/3U4-sqqXuPvpbQ>

---

**October 1, 2024 October 1, 2024**

12 – 14 <https://disk.yandex.ru/i/1bZJ5QdUEbdzsw>  
16 – 18 <https://disk.yandex.ru/i/JF7PuT8zrl6eKQ>  
19:00 Round table <https://disk.yandex.ru/i/Libq11Dr-8lzfA>

---

**October 2, 2024 October 2,**

**2024** 12 – 14 <https://disk.yandex.ru/i/bOiA9MDPVk-AZA> 16 – 18 <https://disk.yandex.ru/i/TP6m7gwGIGzOTA> 19:00 Round table <https://disk.yandex.ru/i/D27QbfReNu2uzg>

**October 3, 2024 October 3,**

**2024** 12 - 14 <https://disk.yandex.ru/i/p9S4l5VWAyZWGQ> 16 - 18 <https://disk.yandex.ru/i/zQGjlto62Hux6g> 19:00 Round table [https://disk.yandex.ru/i/rV0ugkhAp\\_V0Qw](https://disk.yandex.ru/i/rV0ugkhAp_V0Qw)

**October 4, 2024 October 4,**

**2024** 12 – 14 <https://disk.yandex.ru/i/JuuQST7PMXpPGg> 16 – 18 [https://disk.yandex.ru/i/Sep\\_FQ\\_0h8gdmQ](https://disk.yandex.ru/i/Sep_FQ_0h8gdmQ) 19:00 Round table <https://disk.yandex.ru/i/wGnefHbyDwl5jg>

This collection contains articles prepared on the basis of reports given at the RKHTYA and SM-28, as well as reports at scientific seminars (webinars). 40 reports were given at the conference. We received 38 articles for publication in this collection. The editorial board decided to reject 3 articles due to non-compliance with the requirements for publication in the Collection.

In addition to the main time reports, many participants spoke at the Round Tables. Unfortunately, it is not possible to list them all. We can only publish information about the main time speakers (last name, first name, patronymic, place of residence, e-mail address). The names of the co-authors can be found in the titles of the published articles or in the program and abstracts of the reports published on the website <http://lenr.seplm.ru/konferentsii>.

## KEYNOTE SPEAKERS AT THE RKHTYA CONFERENCE AND SM-28

- Avsharov Evgeny Mikhailovich**, Moscow [ejen@course-as.ru](mailto:ejen@course-as.ru)  
**Alexandrov Dimitar**, Canada [dimiter.alexandrov@lakeheadu.ca](mailto:dimiter.alexandrov@lakeheadu.ca)
- Afonin Vladimir Viktorovich**, [aphoninvv@mail.ru](mailto:aphoninvv@mail.ru)
- Baranov Dmitry Sergeevich**, Moscow, [bds07@yandex.ru](mailto:bds07@yandex.ru)
- Boldyreva Lyudmila Borisovna**, Moscow, [boldyrev-m@yandex.ru](mailto:boldyrev-m@yandex.ru)
- Bychkov Vladimir Lvovich**, Moscow, [bychvl@gmail.com](mailto:bychvl@gmail.com)
- Voloshin A.S.** Novorossiysk, [riptop@inbox.ru](mailto:riptop@inbox.ru)
- Greenyer Robert (Greenyer Bob)**, Czech Republic, Brno, [bobgreenyer@gmail.com](mailto:bobgreenyer@gmail.com)
- Gryaznov Andrey Yurievich**, Moscow, [angrmsu@yandex.ru](mailto:angrmsu@yandex.ru)
- Gubarev Evgeniy Alekseevich**, Moscow, [e.gubarev.21@gmail.com](mailto:e.gubarev.21@gmail.com)
- Egorov Evgeny Ivanovi**, Omsk, [czl4otk9omsk@gmail.com](mailto:czl4otk9omsk@gmail.com)
- Zhilalov Vladislav Anatolyevich**, Kazakhstan, [zhigalov@gmail.com](mailto:zhigalov@gmail.com)
- Zatelepin Valery Nikolaevich**, Moscow, [zvn07@yandex.ru](mailto:zvn07@yandex.ru)
- Ivanov Mikhail Yakovlevich**, Moscow, [mikhivan@yandex.ru](mailto:mikhivan@yandex.ru)
- Mikhail Petrovich Kashchenko**, Ekaterinburg, [kashchenkomp@m.usfeu.ru](mailto:kashchenkomp@m.usfeu.ru)
- Klimov Anatoly Ivanovich**, Moscow, [klimov.anatoly@gmail.com](mailto:klimov.anatoly@gmail.com)
- Andras Kovacs**, Finland, [andras.kovacs@broadbit.com](mailto:andras.kovacs@broadbit.com)
- Konstantinov Stanislav Ivanovich**, St. Petersburg, [konstantinov.si@yandex.com](mailto:konstantinov.si@yandex.com)
- Lewis Edward**, USA, [e2023@fastmail.com](mailto:e2023@fastmail.com)
- Marin Mikhail Yurievich**, Khimki, Moscow region, [nvtitech@gmail.com](mailto:nvtitech@gmail.com)
- Nikitin Alexander Pavlovich**, Moscow, [anikitinaaa@mail.ru](mailto:anikitinaaa@mail.ru)
- Pakulin Valery Nikolaevich**, [valpak@yandex.ru](mailto:valpak@yandex.ru)

**Parkhomov Alexander Georgievich**, Moscow, alexparh@mail.ru  
**Jacques Ruer**, France, Paris, jsr.ruer@orange.fr **Savvatimova**  
**Irina Borisovna**, Podolsk, Moscow region, isavvatim@mail.ru **Savinkov Gennady**  
**Konstantinovich**, Kiev, sagk@rambler.ru **Savchenko Alexey**  
**Mikhailovich**, Moscow, sav-alex111@mail.ru **Solin Mikhail**  
**Ivanovich** solmiv@mail.ru **Stepanov Igor**  
**Nikolaevich**, Moscow, stepanovigorn@gmail.com **Strigin Mikhail**  
**Borisovich**, Chelyabinsk, strigin1969@gmail.com **Fomichev-Zamilov**  
**Maxim**, USA, Florida, maxfomitchevzamilov@gmail.com **Chepelev Vladimir**  
**Mikhailovich**, Moscow, chepelevv@mail.ru **Chibisov Viktor**  
**Fedorovich**, Novosibirsk, st.4p@mail.ru **Chizhov Vladimir**  
**Alesandrovich**, Moscow Chijov\_va@bk.ru **Chistolinov Andrey**  
**Vladimirovich**, Moscow, a-chi@yandex.ru **Shestopalov Anatoly**  
**Vasilievich**, Moscow, sinergo@mail.ru **Shipov Gennady**  
**Ivanovich**, Moscow, warpdrive09@gmail.com **Shishkin**  
**Alexander Lvovich**, Dubna, avkbeta@mail.ru **Shcherbak**  
**Valentin Stepanovich**, Krasnodar, sherbak\_w@bk.ru

## **Review reports**

---

## **Overview reports**

# Experimental prerequisites for the theory of cold nuclear transformations

A.G.Parhomov

[alexparh@mail.ru](mailto:alexparh@mail.ru)

Experiments show that low-energy nuclear transformations – the work of weak nuclear interactions, which can affect not only one atom, but also several atoms. This should underlie the explanation of the LENR phenomenon. It is necessary to explain not only the fundamental possibility of low-energy nuclear transformations, but also a number of experimentally discovered properties of this phenomenon: the enormous diversity of the resulting nuclides, the emission of soft X-rays instead of the hard gamma radiation usual for nuclear reactions, the low probability of the formation of radioactive nuclides, the appearance of new nuclides and other changes **outside** the active zone of reactors, including the appearance of tracks on smooth surfaces, the long-term continuation of changes at the nuclear level after the substance has been in and around LENR reactors.

## INTRODUCTION

If we count the time from the famous presentation of Fleischman and Pons, intensive research in the field of low-energy nuclear transformations has been conducted for 35 years. However, creating a theory of this phenomenon has proven difficult. Not because there is little experimental material. A lot of experimental material has been accumulated over these decades. The problem is that it is necessary to explain not only the fundamental possibility of low-energy nuclear transformations, but also the entire variety of empirical data, which in many ways contradict conventional ideas. At the first stage, the thinking of researchers was captivated by established ideas about the implementation of nuclear fusion by overcoming the Coulomb barrier. The only difference is that the traditional way is to impart sufficiently high energy to the

nuclei by heating to a high temperature. And here, overcoming the Coulomb barrier occurs in some other way, without **much** heating. Hence the original name of the phenomenon: "cold nuclear fusion". Analysis of changes in various substances has shown that not only does the synthesis of light nuclei to form heavier ones occur, but also the division of heavy nuclei into two lighter ones, as well as more complex nuclear transformations. Therefore, more appropriate terms for this phenomenon are "cold nuclear transformations (transmutations)" or "low-energy nuclear reactions" (LENR).

Transformations of matter at the nuclear level "under room conditions" is a phenomenon of interest not only for science. It promises very important practical applications. It was necessary to find an explanation for this phenomenon, which contradicts the established ideas about intranuclear processes. At present, for

Many hypotheses have been proposed to explain the LENR phenomenon. It is impossible to cover all of them within the framework of this article. We will focus on just a few.

## ATTEMPTS TO EXPLAIN COLD NUCLEAR TRANSFORMATIONS AT THE FIRST STAGE OF RESEARCH

**Deuterium is introduced into the crystal lattice of the metal. A high density of deuterium nuclei is achieved, which allows the fusion reactions  $D + D = T + p$ ,  $D + D =$  to occur. Fleischmann       $^3\text{He} + n$**

and Pons proceeded from these considerations when planning their experiment using a setup with palladium electrodes in which heavy water was electrolyzed [1]. They assumed that the low energy of the colliding nuclei could be compensated for by a high concentration of deuterium nuclei dissolved in palladium. And indeed, excess heat was recorded. But many orders of magnitude fewer neutrons and gamma quanta were emitted than if the process had followed a scheme similar to "hot" fusion. Only protons, tritium and helium should have been formed, but many other elements appeared. The process clearly did not correspond to the "hot fusion" scheme.

**The proton somehow leaks through the Coulomb barrier and as a result of a chain of radioactive decays produces a certain set of daughter nuclides**

This hypothesis was used by Piantelli, Focardi, Rossi [2-4], and the author of this article, when creating nickel-hydrogen reactors. It is easy to predict what will happen if nickel nuclei accept a proton. When nickel nuclei absorb a proton, nuclear reactions occur [5]:  $^{58}\text{Ni} + p \rightarrow ^{59}\text{Cu}^*$  ( $\tau = 1.3$  min)  $^{59}\text{Ni}^* \rightarrow$  ( $\tau = 8.104$  years)  $^{59}\text{Co}$  is stable

$^{60}\text{Ni} + p \rightarrow ^{61}\text{Cu}^*$  ( $\tau = 3.3$  min)  $^{61}\text{Ni}$  Stable

$^{61}\text{Ni} + p \rightarrow ^{62}\text{Cu}^*$  ( $\tau = 9.7$  min)  $^{62}\text{Ni}$  Stable

$^{62}\text{Ni} + p \rightarrow ^{63}\text{Cu}$  Stable

$^{64}\text{Ni} + p \rightarrow ^{65}\text{Cu}$  Stable Each

interaction is accompanied by the formation of a hard gamma quantum. But in reality, the intensity of gamma radiation during LENR is extremely weak. Positrons should be generated, which, during annihilation, produce gamma quanta with an energy of 511 keV. They were successfully registered, but the radiation intensity turned out to be many orders of magnitude lower than it should be if the process occurs according to the scheme shown above. Finally, the analysis of the elemental and isotopic compositions of the spent "fuel" revealed not only nickel, copper and cobalt, but also many other nuclides. Thus, this mechanism cannot explain "cold fusion".

### **Protons turn into neutrons, for which there is no Coulomb barrier**

Neutrons are captured by the nuclei of the surrounding matter. As a result of the chain of radioactive decays, a certain set of new nuclides is formed [6]. Here, first of all, the question arises: where does the energy of 780 keV, necessary for the transformation of a proton into a neutron, come from? And most importantly, if this were somehow

were carried out, the resulting neutrons would inevitably generate powerful capture gamma radiation. For example, nickel, when capturing 100 thermal neutrons, produces 267 gamma quanta with an energy of up to 10 MeV, aluminum produces 600 gamma quanta with an energy of up to 9 MeV [7]. But experiments consistently demonstrate that LENR reactors do not generate intense gamma radiation.

**An atom can, under certain conditions, transition to a compact state. This transition is accompanied by the release of large amounts of energy (e.g. the hydrino hypothesis, "dark hydrogen"). In addition, the properties of such an object are partly similar to those of a neutron, which makes it easier to overcome the Coulomb barrier.**

This approach also raises many questions and does not solve the problem of captured gamma radiation [5].

#### **The hypothesis of “ersion catalysis” by Yu.N. Bazhutov and G.M. Vereshkov [8,9]**

This hypothesis also did not explain the absence of hard gamma radiation and did not exclude the appearance of radioactive nuclides. In addition, experiments did not show the predicted advantage of deuterium over protium.

Thus, all hypotheses about the LENR phenomenon published in the first period after the experiments of Fleischmann and Pons, in which the reacting nuclei somehow overcame the Coulomb barrier, could not cope with explaining the information about the properties of this phenomenon that had already accumulated at that time. Other approaches are needed.

Note that theories in which hydrogen is an obligatory element cannot explain cold nuclear transformations in reactors that do not contain hydrogen at all. One can recall, for example, the experiment of Wendt and Irion (an electric explosion of a tungsten wire in a vacuum led to the appearance of helium) [10], or the appearance of calcium as a result of combustion of a thermite mixture [11], or LENR

when melting zirconium in an electron beam furnace (a phenomenon discovered by Solin) [12], or the formation of various elements in our experiments with incandescent lamps [13,14].

Hypotheses in which the occurrence of cold nuclear transformations required a crystalline structure of matter also turned out to be untenable. Experiments show the possibility of transformations not only in solids, but also in liquid media, as well as in dense low-temperature plasma.

### **EXPERIMENTAL PREREQUISITES FOR THE THEORY OF LOW-ENERGY NUCLEAR TRANSFORMATIONS**

Important results were obtained soon after Fleischmann and Pons Karabut, Kucherov, Savvatimova on a gas discharge setup [15]. All the main properties of the phenomenon were revealed in these experiments. In addition to excess heat generation, the formation of many initially absent nuclides was detected. And if the process had proceeded in the same way as in “hot fusion,” only tritium, hydrogen, and helium should have formed. In reality, many elements emerged, from lithium and boron to silver and indium. These nuclides

were formed not by the synthesis of light elements, but by the division of heavy ones. In these studies, soft X-ray radiation was first recorded and its spectrum measured. Subsequently, soft X-ray radiation near installations where the LENR process takes place was studied in detail by A.I. Klimov [16].

We encountered an abundance of emerging nuclides (not just an abundance, but an astonishing abundance) when working with nickel-hydrogen reactors. Table 1 shows, as an example, the results of mass-spectral analysis of a ceramic tube — the shell of one of the nickel-hydrogen reactors [17].

	До	После	После/ до		До	После	После/ до
<sup>10</sup> B	0.0008	0.0318	41.8	<sup>114</sup> Cd, Sn	0.0005	0.0064	11.9
<sup>11</sup> B	0.0054	0.1277	23.4	<sup>116</sup> Cd, Sn	0.0022	0.0275	12.8
<sup>29</sup> Si	0.3709	4.2603	11.5	<sup>117</sup> Sn	0.0011	0.0129	12.0
<sup>43</sup> Ca	0.0158	0.2638	16.7	<sup>118</sup> Sn	0.0024	0.0422	17.9
<sup>44</sup> Ca	0.2123	3.1461	14.8	<sup>119</sup> Sn	0.0014	0.0165	11.7
<sup>45</sup> Sc	0.0507	2.0384	40.2	<sup>120</sup> Sn, Te	0.0034	0.0670	19.5
<sup>46</sup> Ti, Ca	0.0074	0.0836	11.3	<sup>122</sup> Te	0.0007	0.0101	15.0
<sup>51</sup> V	0.0028	0.2151	78.0	<sup>127</sup> I	0.0062	0.1589	25.7
<sup>53</sup> Cr	0.0057	0.0753	13.3	<sup>128</sup> Te	0.0002	0.0046	22.8
<sup>64</sup> Ni, Zn	0.0186	0.2224	12.0	<sup>124</sup> Te	0.0008	0.0092	11.4
<sup>66</sup> Zn	0.0099	0.1102	11.1	<sup>130</sup> Te	0.0006	0.0101	16.7
<sup>67</sup> Zn	0.0014	0.0211	15.0	<sup>182</sup> W	0.0076	4.3168	567.8
<sup>68</sup> Zn	0.0080	0.0808	10.1	<sup>183</sup> W	0.0035	2.3489	671.7
<sup>72</sup> Ge	0.0001	0.0037	27.2	<sup>184</sup> W	0.0076	5.0087	658.8
<sup>75</sup> As	0.0001	0.0138	102.2	<sup>185</sup> Re	0.0006	5.9469	9827.0
<sup>76</sup> Ge, Se	0.0115	0.1976	17.2	<sup>186</sup> W, Os	0.0089	4.7748	537.6
<sup>77</sup> Se	0.0001	0.0055	82.2	<sup>198</sup> Hg	0.0001	0.0321	238.5
<sup>78</sup> Se, Kr	0.0028	0.0542	19.7	<sup>199</sup> Hg	0.0007	0.0248	33.5
<sup>79</sup> Br	0.0028	0.0560	20.3	<sup>200</sup> Hg	0.0004	0.0560	138.9
<sup>81</sup> Br	0.0040	0.0790	19.6	<sup>202</sup> Hg	0.0005	0.0606	128.8
<sup>83</sup> Kr	0.0001	0.0009	13.7	<sup>203</sup> Tl	0.0015	0.1498	101.2
<sup>107</sup> Ag	0.0067	0.0863	13.0	<sup>204</sup> Pb, Hg	0.0010	0.0101	10.0
<sup>109</sup> Ag	0.0071	0.1020	14.3				
<sup>113</sup> Cd, In	0.0001	0.0009	13.7				

**Table 1.** Relative content of nuclides (atomic %) in a ceramic tube before and after operation of the KV3 reactor.

The table shows the nuclides whose content increased more than 10 times, starting with boron and ending with lead. Only cobalt and

copper. The table shows the changes not in the nickel-hydrogen core of the reactor (many new nuclides appeared there too), but in the shell. It looks as if the reactor core is releasing

something that causes nuclear transformations not only in the core of the reactor, but also in surrounding substance.

Appearance sets new elements from deuterium and tritium to lead were also

discovered at the Vachaev and Ivanov "Energoniva" installation, where water or other liquids were passed through a special electric discharge [18]. Let's consider what could have happened using the

example of iron formation from water. There are exactly as many nucleons in three water molecules as in the nucleus of one of the stable isotopes of iron 54Fe. Let's assume that they somehow combined. But this will not produce iron, but 54Zn. Such a nuclide does not exist even in a radioactive state. To produce iron, it is necessary to reduce the charge of the nucleus by 4 units. This can happen if you add 4 electrons to the merging nuclei, fortunately, there are plenty of electrons in any substance.

But even here, not everything is in order. When a single particle is formed as a result of a nuclear reaction, the law of conservation of momentum cannot be fulfilled. On the other hand, the lepton charge contributed by the electrons remains uncompensated. Both of these

problems are solved if we assume that the formation of an iron nucleus is accompanied by the emission of neutrinos:  $\gamma^{54}\text{Fe} + 26 + 4\bar{\nu} + 87.81$

**analysis MeV**  $3\text{H}_2\text{O} + 4e^-$  - Thus, the of experimental results shows that the formation of iron from water is impossible without the participation of electrons and neutrinos. And nuclear reactions in which electrons and neutrinos participate are *reactions of weak nuclear interaction*.

Элемент, соединение	в твердой фазе, г/кг	в жидкой фазе, мг/л
Li, Be	0,006	Следы
C	6,7	-
B	1,1	0,1
Si	4,4	0,2
Cr	0,9	0,1
Mg	0,1	0,1
Fe	6,6	Следы
Mn	0,1	-
Ni	0,4	-
V	0,7	-
Sn	5,5	-
Zn	2,0	0,4
Al	2,1	1,1
Cu	0,4	-
Ti	0,4	-
P	0,1	-
S	-	-
Bi	0,1	0,01
Se	0,1	-
Pb	0,8	-
Te	-	-
$\text{D}_2\text{O}$	-	0,06
$\text{T}_2\text{O}$	-	0,05
pH	-	6,0

**Table 2.** Elements resulting from the flow of distilled water through the Energoniva reactor.

An analysis of nuclides arising in various LENR reactors indicates that not only the formation of iron, discussed above, but also all cold nuclear transformations in general are associated with weak nuclear interaction. This conclusion was reached long ago by L.I. Urutskoev and D.V. Filippov [19, 20], Yu.L. Ratis [21], G.V. Myshinsky and others [22].

It should be noted that when iron is formed from water, the emitted neutrinos carry away the bulk of the energy. The iron nucleus receives approximately 1/1000 of the released energy – only about 120 keV. It is this energy that gives the excess heat release. If we relate it to one nucleon, we get 2.2 keV. (For comparison: in the “hot” synthesis of

deuterium into helium, where neutrinos do not “steal” energy, about 1 MeV is released per nucleon). But even such heat release is more than three orders of magnitude higher than in chemical reactions.

On the other hand, the small energy received by the emerging nucleus makes it impossible to excite nuclei with subsequent emission of hard gamma quanta. The energy of the first excitation level for heavy nuclei is several hundred keV, and for light nuclei it is several MeV. Although nuclear transformations are also

possible in which neutrinos are not emitted and do not carry away much energy. For example, in the Vachaev-Ivanov reactor, in addition to iron, a lot of silicon and deuterium were formed. This could have happened as a result of

interactions of two oxygen nuclei, an electron and an antineutrino:  $^{16}\text{O} + ^{16}\text{O} + \text{e}^- + \bar{\nu} \rightarrow ^{30}\text{Si} + ^2\text{D} + 1.83 \text{ MeV}$ .

In this nuclear reaction, the excess heat release is 1.83 MeV per transmutation act (60 keV per nucleon). And here the energy received by the emerging nuclei (deuteron and silicon) is insufficient for their excitation. Therefore, no gamma radiation.

We have considered what happens when iron is formed as a result of the combination of six protons and three oxygen nuclei contained in three water molecules, as well as four electrons. But from the standpoint of existing concepts, this is completely impossible. All these particles are separated by significant distances and Coulomb barriers. The probability of a proton overcoming the Coulomb barrier under the conditions existing in LENR reactors is negligible. The situation with heavier nuclei is even worse. Nevertheless, experiments show that this **happens**. And this happens **precisely in the process of weak nuclear interaction**. Thus, we have to admit that weak nuclear interaction has an amazing property of combining nuclear particles, ignoring the Coulomb barrier. Note that this happens without violating the laws of conservation of energy, momentum, electric, baryon and lepton charges.

Although this happens at a very low rate. For example, in our nickel-hydrogen reactors the power of excess heat generation reached 1000 watts [23]. It can be calculated that even with such a very significant heat generation, approximately one atom of the reactor substance out of a million undergoes cold transmutation per day. The low rate of the process is compensated by the large

energy release in each act of transmutation. It should be noted

that L.I. Urutskoev was the first to come to the conclusion that the process of low-energy nuclear transformations affects many atoms. A certain set of atoms is transformed into an energetically more favorable set of other atoms. His report at the 25th Russian Conference in October 2018 was called: "**On the Collective Nature of the Physical Mechanism of LENR**" [24].

Another surprising effect is the long-term continuation of nuclear transformations in the substance that has been in the LENR reactor. This was demonstrated by experiments in the laboratory of I.N. Stepanov and in the INLIS laboratory [25]. The long-term continuation of cold nuclear transmutations was observed by V.V. Evmenenko [26], this was noted by A.I. Klimov, L.I. Urutskoev, F.S. Zaitsev, V.S. Shcherbak and V.A. Chizhov. In our experiments, which were reported at the Klimov-Zatelepin webinar in April 2024, a short-term reactor activation led to long-term changes in the results of amplitude spectra measurements

scintillation counter. The lead nozzle weakens the background, but after short-term switching on of the reactor itself becomes a source of radiation with energy of 60-70 keV. In addition, a prolonged increase in the count rate of  $^{239}\text{Pu}$  and  $^{137}\text{Cs}$  radiation was detected after a short-term reactor shutdown.

### **THE BASIS ON WHICH THE THEORY OF COLD NUCLEAR TRANSFORMATIONS SHOULD BE BUILT**

When creating a theory of cold nuclear transformations, it is necessary to proceed from the fact that this is the work of weak nuclear interactions, which can affect not only one atom, but also several atoms. Moreover, the participation of hydrogen in this process is not necessary. The theory must explain not only the fundamental possibility of low-energy nuclear transformations, but also a number of experimentally discovered properties of this phenomenon. Such as:

- a huge variety of emerging nuclides,
- the possibility of LENR occurring both in solids and in liquid media and in dense low-temperature plasma,

- soft X-ray and optical radiation characteristic of highly excited multi-charged ions, instead of the hard gamma radiation typical of nuclear reactions,
- low probability of formation of radioactive nuclides,
- formation of new nuclides and other changes ***outside*** the active zone reactors, including the appearance of "tracks" on smooth surfaces,
- long-term continuation of changes at the nuclear level and soft X-ray emission ***after*** the substance has been in and around LENR reactors.

It is important to note that these are not speculative postulates, but conclusions that follow from the analysis of various experiments.

### **LITERATURE**

1. Fleischmann M. and Pons S. Electrochemically Induced Nuclear Fusion of Deuterium. *J.Electroanal. Chem.*, 1989, 261: 301-308.
2. Focardi S., Habel R. and Piantelli F. Anomalous Heat Production in Ni-H Systems. *Nuovo Cimento*, 1993, 107A 163. 1994, vol. 107 A (1):163-167.
3. Focardi S. *et al.* Large excess heat production in Ni-H systems. *Nuovo Cimento*, 1998, 111A(11):1233-1242. <https://cloud.mail.ru/public/xBZM/ANrwBCcpH>
4. Focardi S., Rossi A. A new energy source from nuclear fusion. *Journal of nuclear Physics*, March 22, 2010
5. Parkhomov A.G. Cold transmutation of nuclei: strange results and attempts to explain them. *Journal of Emerging Directions of Science (JFNS)*, 2013, 1(1):71-76.

6. Widom A., Larsen L. Ultra Low Momentum Neutron Catalyzed Nuclear Reactions on Metallic Hydride Surfaces. *The European Physical Journal*, 2006, 46(1): 107–111.
7. Komar D.I. et al. Source of capture gamma radiation with energies up to 7 MeV and up to 10 MeV based on a neutron radiation verification facility. *Ves. Nat. Acad. Sci. Belarusi. Ser. Phys.-Eng. Sci.*, 2017, 2: 96–103.
8. Bazhutov Yu.N., Vereshkov GM A Model of Cold Nuclear Transmutation by the Erzion Catalysis, *Proceedings of ICCF-4*, Hawaii, 1993, v.4, 8-1.
9. Bazhutov Yu.N. Erzion interpretation of the results of experiments with hydrogenation of various metals. Proceedings of the 19th Russian Conference "Cold Transmutation of Nuclei of Chemical Elements and Ball Lightning" (RKHTYAiShM-19) , 2012, 55-63.
10. Wendt GL, Irion CE Experimental attempts to decompose tungsten at high temperatures. Amer. Chem. Soc. 44, (1922). Experimental attempts to decompose tungsten at high temperatures. Trans. Zhigalov V.A.: *J. Phys. Nauk*, 4(2):100–104, 2014 <https://www.unconv-science.org/n4/wendt>
11. Gromov A.A., Gromov A.M., Popenko E.M. et al. On the formation of calcium in combustion products of iron-aluminum thermites in air. *Russian Journal of Physical Chemistry*, 2016, 90(10):1578–1580
12. Solin M.I. Experimental facts of spontaneous generation of a condensate of soliton charges with the formation of nuclear fusion products in liquid zirconium. *Physical Thought of Russia*, 2001, 1: 43–58.
13. Parkhomov A.G., Karabanov R.V. LENR as a manifestation of weak nuclear interactions. A new approach to creating LENR reactors. *RENSIT: Radioelectronics. Nanosystems. Information technologies*, 2021, 13 (1): 45-58.
14. Parkhomov A.G. Nuclear transmutations and excess heat in reactors with incandescent lamps. *Proceedings of RKHTYAiShM -27*, 2022, 25-34.
15. Karabut AB, Kucherov YR and Savvatimova IB Nuclear product ratio for glow discharge in deuterium. *Phys. Lett. A*, 1992, 170: 265.
16. Klimov A.I., Belov N.K., Tolkunov B.N. Soft X-ray radiation created by nano-cluster plasmoids. *Proc. RKHTYAiShM -23*, 2016, 127-138.
17. Parkhomov A.G., Alabin K.A., Andreev S.N. etc. Nickel-hydrogen reactors: heat release, isotopic and elemental composition of fuel. *RENSIT*, 2017, 9 (1): 74-93.
18. Vachaev A.V., Ivanov N.I., Ivanov A.N., Pavlova G.A. A method for obtaining elements and a device for its implementation. *RF Patent No. 2096846, MKI G 21 G 1/00, H 05 H 1/24. Claimed 31.05.94// Inventions*. 1997. No. 32. P. 369.

19. Filippov DV, Urutskoev L.I On the possibility of nuclear transformation in low-temperature from the viewpoint of conservation laws plasma. *Annales de la Fondation Louis de Broglie*, 2004, 29(3): 1187-1205.
20. Urutskoev L.I., Filippov D.V. Is it possible to transform nuclei into low-temperature plasma from the point of view of conservation laws? *Applied Physics*, 2004, 2:30-35.
21. Ratis Yu.L. Cold nuclear fusion. Problems and models. [http://www.second-physics.ru/reviews/dineutron\\_review\\_f4.pdf](http://www.second-physics.ru/reviews/dineutron_review_f4.pdf)
22. Kuznetsov V., Mishinsky G., Penkov F., Arbuzov V., Zhemenik V. Low Energy Transmutations of Atomic Nuclei of Chemical Elements. *Annales de la Fondation Louis de Broglie*, 2003, 28(2):173-213.
23. Parkhomov A.G., Zhigalov V.A., Zabavin S.N., Sobolev A.G., Timerbulatov T.R. Nickel-hydrogen heat generator that operated continuously for 7 months. *J. Phys. Science*, 2019, 23-24(7):57-63.
24. Urutskoev L.I. On the collective nature of the physical mechanism LENR *Presentation of the report at the conference RKHTYAiSHM-25 (2018)*. <https://cloud.mail.ru/public/BgLk/x8pjgfFsR>
25. Baranov D.S., Zatelepin V.N., Stepanov I.N., Shishkin A.L. Registration X-ray spectrum by NaI detector in the vicinity of high-pressure steam generator. *Proc. RKHTYAiShM -27, 2022*, 74-82.
26. Evmenenko V.V., Malakhov Yu.I., Parkhomov A.G. Radiation of nickel-hydrogen reactor. *ZhFNN*, 2019, 25(7): 55-57.

## **Experimental prerequisites of the theory of cold nuclear transformations**

**AGParkhomov**  
[alexparh@mail.ru](mailto:alexparh@mail.ru)

Experiments show that low-energy nuclear transformations are the work of weak nuclear interactions, which can affect not only one atom, but also several atoms. This should be the basis for explaining the LENR phenomenon. It is necessary to explain not only the fundamental possibility of low-energy nuclear transformations, but also a number of experimentally discovered properties of this phenomenon: huge variety of emerging nuclides, emission of soft X-rays instead of the usual hard gamma radiation for nuclear reactions, low probability of the formation of radioactive nuclides, appearance of new nuclides and other changes outside the reactor core, long-term continuation of changes at the nuclear level after the substance was in and around the reactors.

# LENR indicators

V.A. Zhigalov

Satbayev University, Almaty, Kazakhstan

[zhigalov@gmail.com](mailto:zhigalov@gmail.com)

Conventional methods for measuring the intensity of nuclear reactions (measuring the flux of neutrons and other particles) are not suitable for explaining LENR. The reason is the absence of significant fluxes of neutrons, gamma quanta and other ionizing particles from low-energy nuclear reactions. However, without measuring the intensity of their occurrence, it is impossible to build technically applicable reactors, and it is very difficult to study the phenomenon itself in laboratory conditions. The reasons for the difficulty in indicating and measuring LENR are determined by the current stage of studying this phenomenon. There is still no generally accepted model for the occurrence of this class of nuclear reactions. Many proposed theories and hypotheses involve some nuclear-active agent: neutronium, magnetic monopole, ultracold neutrinos, dark hydrogen, etc. If such an agent is responsible for the occurrence of LENR, then the indication and measurement of the reaction intensity can be based on measuring the fluxes of this agent. The report provides an overview of the experimental results that can be considered as detection of such an agent: these are the results of N.A. Kozyrev and his followers, A.G. Parkhomov, I.M. Shakhpashov and others. An attempt is made to link these and other results with the LENR theme. The report also considers methods of LENR indication by excess heat release, element transformation, strange radiation tracks, etc.

## 1. Introduction

Despite the rich experimental data accumulated in the field of low-energy nuclear reactions, the mechanism of these reactions has not yet been clarified. The abundance of theories, none of which is universally accepted, suggests that we are not at the final stage of studying this phenomenon, but rather in the middlegame. Much remains to be learned from experiments, so that then, based on phenomenological models, the LENR theory that many are waiting for will be born.

If we consider the many attempts to theoretically explain the LENR process, we can see a common denominator in some theories: some material nuclear-active agent is introduced that causes low-energy reactions. Examples of such approaches are: neutronium [1], magnetic monopole [2], ultracold neutrinos [3], dark hydrogen [4], transatoms [5], etc. Such a concept can be called nuclear catalysis.

Slow progress in this area is not only due to the lack of a theory that would allow predicting efficient reactor modes. Work is also slowed by the lack of convenient and reliable methods for measuring the intensity or even indicating LENR. It is unlikely that traditional nuclear reactors could

could have been created in a limited time in the middle of the 20th century if a) the mechanism of uranium fission using a neutron flux had not been understood, and b) convenient neutron counters had not been created. Today we are forced to work blindly: counters of neutrons, gamma quanta and other familiar ionizing particles cannot be indicators of LENR, since they usually do not leave the reactors during their operation.

Without measuring the rate at which low-energy nuclear reactions occur, it is impossible to build technically feasible reactors, and it is very difficult to study the phenomenon itself in laboratory conditions. If you can't measure it, you can't control it.

## **2. Possible methods of LENR indication**

What methods of indication can be used, if we start from the fact that we are talking about nuclear transformations that are accompanied by the release of energy? Obviously, calorimetric methods, as well as methods of elemental and isotopic analysis, separately and together, can indicate, and if they are developed, measure the intensity of LENR.

### **2.1 Calorimetry and elemental analysis**

Calorimetry allows for the rapid assessment of the volume of heat release and thus the intensity of ongoing nuclear reactions. However, there are pitfalls associated with the fact that the processes that lead to the emergence of LENR are also conventional sources of thermal energy. For example, electrical discharges, cavitation, heating of conductors, electrolysis, electric explosions and others themselves release a large amount of heat without ongoing nuclear processes. In addition, we must not forget about the phenomenon of biological transmutation, in which there is no significant energy release.

Elemental and isotopic analysis is suitable for post-mortem studies, i.e. after the reactor has been in operation. Comparison of fuel composition before and after reactor operation shows the transformation of elements into each other. But the methods used in this case (EDS, ICPMS, SIMS, etc.) are not related to operational methods of indication, they require expensive equipment and are difficult to use, in addition, they often do not allow for reliable quantitative analysis.

The author is not aware of any works where the methods of analytical chemistry would promptly indicate the appearance of new elements. Apparently, such an approach is only waiting for researchers. For example, there are simple methods for indicating the presence of iron, calcium and other elements in solutions, which usually appear during reactor operation.

### **2.2 LENR indication using ultrapure materials**

A.G. Parkhomov proposed an interesting method for indicating the occurrence of LENR: samples of semiconductor devices (diodes, transistors, etc.) are placed near the active zone of the reactor. Their volt-ampere characteristics are measured before and after exposure. Preliminary experiments [6] show that, indeed, the reverse current of the diodes changes as they are exposed near LENR reactors. This can be explained by the fact that the nuclear-active agent that causes nuclear

transformations in the working substance of the reactor, comes out and at the same time causes transmutations in silicon or germanium. In semiconductor devices, the composition of the semiconductor impurities is strictly standardized and any change in them should lead to changes in the electrical characteristics, which, apparently, Parkhomov observed in his experiments. Here, testing semiconductors with a large area, such as solar cells, or pure silicon wafers, is promising.

A similar scheme of using pure substances can be applied to water. Distilled water is a poor conductor (as are pure semiconductors). If we assume that nuclear reactions will occur in water under the action of a nuclear-active agent, then the newly created elements will participate in the formation of ionic conductivity. It is known that such elements as calcium, sodium, iron are often found in LENR products. The appearance of even small impurities of these and other metals can lead to a change in the conductivity of the water cell. It is possible to use other schemes of experiments with pure and ultrapure substances.

## **2.3 Characteristic electromagnetic radiation**

Many researchers have noticed soft X-rays accompanying LENR. They are usually easily screened by reactor shells. Their appearance is explained by the fact that during transmutation the nuclei must be re-dressed with electron shells, and such a process must be accompanied by characteristic electromagnetic radiation when electrons "fall" into the orbitals of new atoms. This phenomenon can be used to create operational LENR indicators. But, as in calorimetry, more trivial sources must also be taken into account, for example, X-ray radiation in some types of electric discharge. Apparently, over time, the isolation of certain characteristic radiation lines and their operational comparative analysis will be developed here - what usually happens in the EDS method. In addition to X-ray radiation, other parts of the spectrum may also contain characteristic radiation lines.

## **2.4 Strange radiation**

It is known that the operation of LENR reactors is accompanied by radiation that leaves "strange tracks" on the surface of various materials. Can it be used as a characteristic indicator of LENR? Strange radiation has a very large

variability in time and unevenness in space, and the rate of track formation is extremely low. This complicates its use as a direct indicator: with stable operation in the same mode of LENR reactors, tracks are sometimes formed in large quantities, sometimes they are practically not formed, and it is necessary to collect large statistics with long exposures. In addition, the labor intensity of counting tracks makes this method unpromising in its current form. Here there is hope for clarifying the nature of strange tracks (see, for example, [7]), with the fact that

so that the operation of indicators is based, for example, on the forces that arise on the surface of materials when tracks are formed by solid particles.

### 3. Evidence of a nuclear-active agent

The idea of nuclear catalysis was mentioned above: let us assume that the LENR process consists of two stages – the formation of a nuclear-active agent and its actual operation in the reactor working substance (Fig. 1). This idea is confirmed in some types of reactors, in particular, in Parkhomov reactors based on incandescent lamps [8].

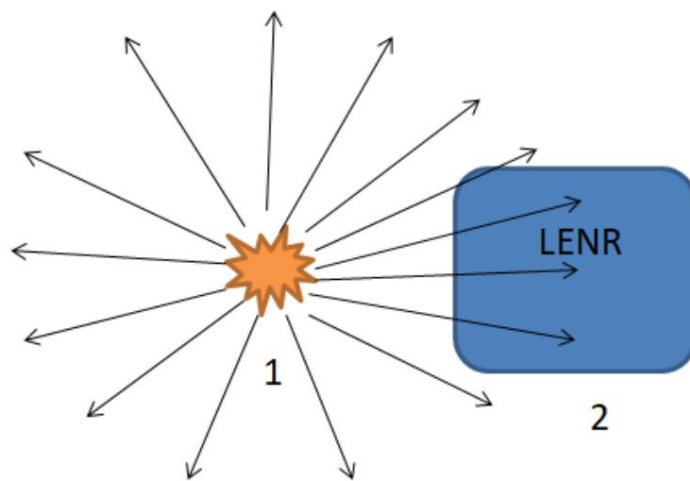


**Fig. 1.** Concept of nuclear catalysis. The agent source (1) is separated from the working substance (2). LENR occurs in the working substance (2).

Whatever the nature of this physical agent, this idea makes us take a fresh look at some interesting experimental results that have been almost forgotten and have no generally accepted explanation. Let us list some of them.

#### 3.1 Kozyrev and followers

Soviet astronomer N.A. Kozyrev is known primarily for his theory of the nature of time [9], first published in 1958. But even many professional astronomers are unaware of his later works from the 1970s, in which flows of a certain physical agent from celestial sources were discovered, which were concentrated by reflecting telescopes and acted on some sensitive systems. In a number of experiments, visible light from these sources was blocked by opaque screens, but the sensitive systems continued to register responses. Kozyrev made a large number of observations with a sensitive system representing an ordinary metal-film resistor MLT as part of a measuring bridge. This resistor was placed at the focus of a reflecting telescope. The response of such a system was registered from dozens of celestial objects [10].

Two Soviet groups of astronomers, replicating Kozyrev's research, confirmed his results. M.M. Lavrentyev's group observed the same objects (stars, nebulae) on the same 50-inch telescope as Kozyrev in 1989-1991 [11, 12]. A.F. Pugach's group observed the same and other objects on several telescopes in 1991 [13]. The response of the resistor resistance when pointing the telescope at the vicinity of stars, as well as at other places in the celestial sphere where there were no stars, was confirmed (Fig. 2).

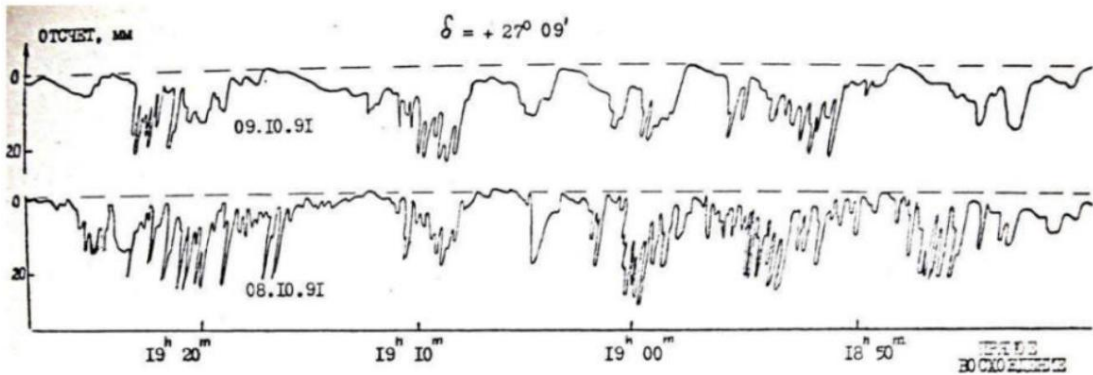


**Fig. 2.** Comparison of recordings of the same strip of sky, made on adjacent dates (A.F. Pugach) [13].

The presence of a signal from celestial objects corresponds to a decrease in the resistor resistance. Researchers emphasized the presence of an aftereffect: after a series of impacts, the detector's sensitivity decreased, and it had to be given a "rest" for 1-2 days. Another subtlety of the technique

experiment: "the sensor should not come into contact with massive parts of the telescope, but should be mounted on the thinnest possible mounts" due to the transmission of the agent through conductors [10].

In a recent study by S.N. Andreev's group, a similar response was demonstrated for a differential measuring system, implemented on a modern element base, when pointing a telescope at a star [14].

### 3.2 Parkhomov: bursts of beta activity

In the 1990s and 2000s, A.G. Parkhomov, in a similar experiment setting, observed short bursts of radioactivity, sometimes exceeding the average count by several orders of magnitude, when placing a beta source and a Geiger counter at the focus of a reflector telescope [3]. Such bursts were not observed outside the focus of the reflector. 2D scans of the celestial sphere showed a dynamic picture, in

where the locations from which the radiation causing the bursts emanated, although not 100% identical on adjacent dates, formed similar areas (Fig. 3).

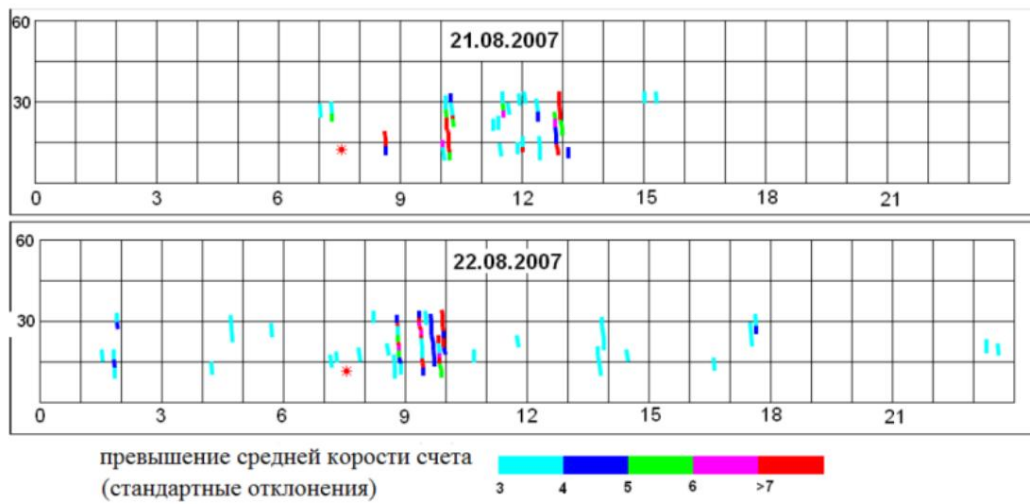
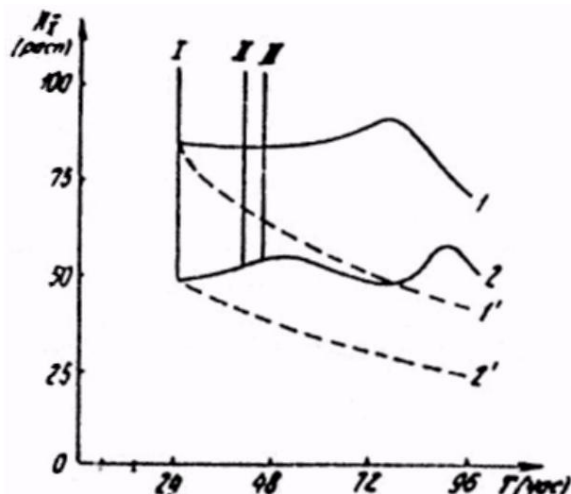


**Fig. 3.** Bursts of the count rate during two-dimensional scanning of the celestial sphere on August 21 and 22, 2007 (A.G. Parkhomov). The horizontal axis is Moscow summer time, the vertical axis is declination (degrees). The swing range is 8..34 degrees [3].

These results indirectly confirmed the results of Kozyrev and his followers, although with the help of a fundamentally different sensitive system. This makes us assume the nuclear activity of a physical agent that comes from Space and can be reflected by mirrors. According to the hypothesis of A.G. Parkhomov, such an agent is relic ultracold neutrinos and antineutrinos, which can move in a wide range of speeds and be gravitationally lensed by stars.

### 3.3 Shakharponov: "Kozyrev-Dirac radiation"

In a completely different experimental setup, I.M. Shakharponov obtained results on the impact on radioactive sources. With the help of some exotic electromagnetic generators, Shakharponov created radiation, which he called "Kozyrev-Dirac radiation". Fig. 4 shows the result of the impact of this radiation on  $^{131}\text{I}$  preparations. After the impact



The half-lives of the two drugs are irreversible.  
Shakharponov also obtained results on the change in the gamma spectrum of uranium [15].

**Fig. 4.** Effect on the decay of  $^{131}\text{I}$  Shakharponov emitter [15]. The dotted line is the normal activity curve. The solid lines are actual curves after exposure.

### 3.4 Balyberdin et al.: "Penetrating radiation of cavitation caverns"

A group of researchers from Kharkov used the Kozyrev sensor (a resistor in the bridge) when observing a local source through a reflecting telescope some radiation, which they called "penetrating radiation of cavitation caverns" [16]. The source was the process of water cavitation in the cavitation nozzle. The sensor showed deviations that coincided with the inclusion of the movement of water and salt solutions in the circuit where cavitation was caused (Fig. 5).

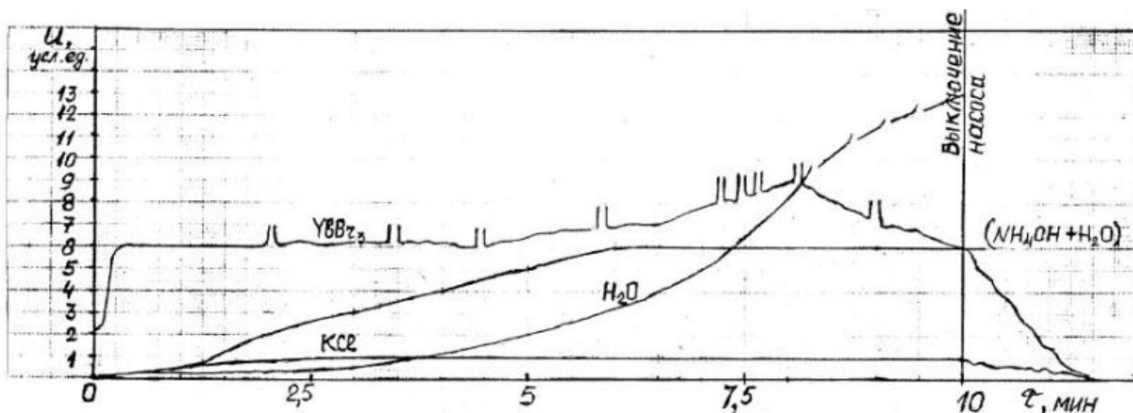


**Fig. 5.** Time course of the change in the signal value from the Wheatstone bridge resistor for aqueous solutions of ytterbium bromide ( $\text{YbBr}_3$ ), ammonium hydroxide ( $\text{NH}_4\text{OH}$ ), potassium chloride ( $\text{KCl}$ ) and pure distilled water ( $\text{H}_2\text{O}$ ) [16].

### 3.5 Kinderevich: change in the activity of radioactive samples

Kiev physicist A.V. Kinderevich invented an electromagnetic device, in which the activity of radioactive sources changed when placed (Fig. 6). Thus, for  $^{90}\text{Sr}$ ,  $^{135}\text{Cs}$ , exposure for tens of hours led to a decrease in activity by tens of percent [17]. These results may seem impossible, but the measurement protocols were signed by representatives of specialized physics institutes in Kiev and Moscow.

Kinderevich's device is electrically a capacitor in which the outer lining is cylindrical, the inner one is star-shaped in cross-section, and between them are inserted prisms made of ferromagnetic material. Two conical "plugs" at the top and bottom are connected to the same alternating voltage as the capacitor and are also filled with a ferromagnet. A container with radioactive samples is located along the axis. Kinderevich also used Kozyrev's sensor (a resistor in the bridge) to debug his devices.

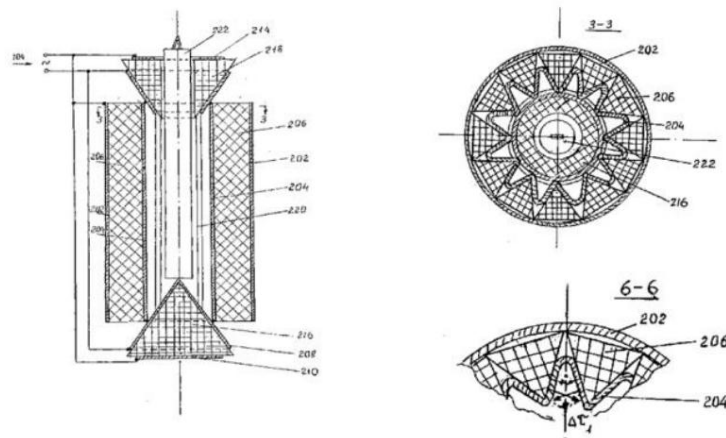


**Fig. 6.** Schematic diagram of the generator by A.V. Kinderevich [17].

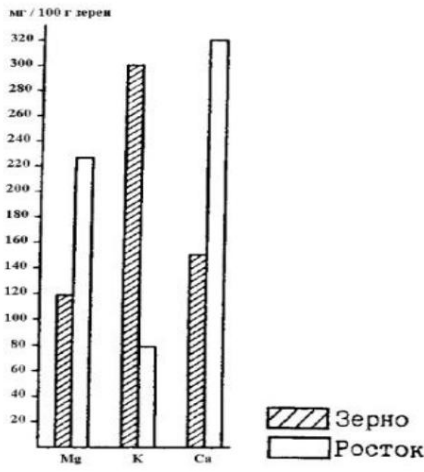
### 3.6 Kanzhen, Komrakov: transmission of biologically active radiation

Systems that focus some biologically active radiation have been used for many years by Jiang Kanzhen to transfer specific and non-specific information from one biological organism to another [18]. Studies have been conducted that show that concentrated radiation from germinating plants causes a strong rejuvenating effect on mice and humans. These results are confirmed by the results of Yevgeny Komrakov, a follower of Jiang Kanzhen [19] (Fig. 7).



**Fig. 7.** Exposure of mice to E. Komrakov's biotron increases their lifespan. Three groups of 12 mice each were studied [19].

His devices use reflective segments of spheres and cylinders. Biologically active radiation from plants in one focal area is transmitted to a person who is located in another focal area. Perhaps these results show the regulation of LENR reactions in the body under the influence of a focused agent.



### 3.7 LENR in biology

In long-term studies of CL

Kervran [20] demonstrated that during the germination of oat seeds, a transmutation of elements occurs: potassium is converted into calcium (Fig. 8).

**Fig. 8.** Changes in Mg, K, Ca during germination of Nuprim oats over 6 weeks of cultivation (K.L. Kervran) [20]

Numerous experiments by A.A. Kornilova and V.I. Vysotsky with microorganisms confirmed the phenomenon of biological transmutation [21]. Review

JP Biberian [22] provides a historical perspective on this area of research, including the results of JP Biberian himself [23].

### 3.8 Paradoxical seasonality

In the work of Indian physicists [24], a cyclical nature of the potassium content during the germination of mung bean seeds was discovered: the potassium content in the sprouts followed the lunar cycle, changing several times (Fig. 9). One can also assume a connection with the biological transmutation of elements. The review [22] also contains negative results of testing biological transmutation. Let us imagine that some experimenters conducted the experiment during a period of low values of K formation, and some during a period of high values (Fig. 9). Such

periodicity, if confirmed, can explain the poor reproducibility of the results in this area.

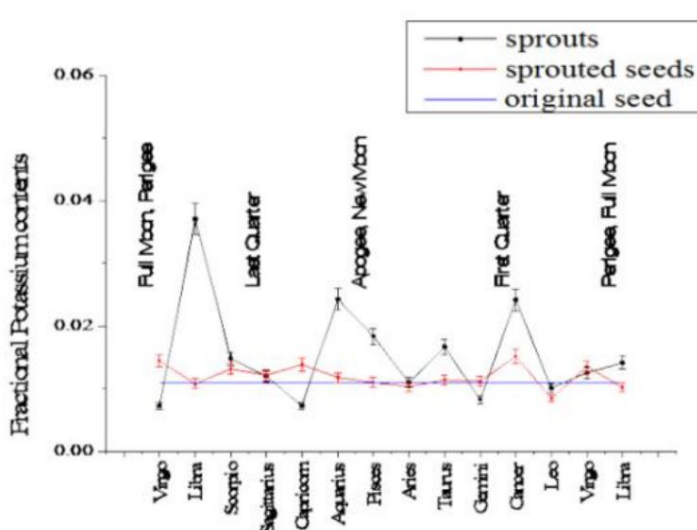


**Fig. 9.** Potassium content in original/germinated seeds/sprouts with moon phases (K.Deep, R.Mittal) [24].

Paradoxical seasonality was also discovered in many other biophysical experiments, in particular, in the mirror cytopathic effect discovered by V.P. Kaznacheev and L.P. Mikhailova [25]. In this effect, specific information about the pathology of cell cultures was transmitted in the presence of optical contact between cultures separated by a hermetic partition. The effect had a bright

expression in August-September (up to 80%) and was almost not reproduced in November (20%) – over the course of 10 years of experiments (Fig. 10).

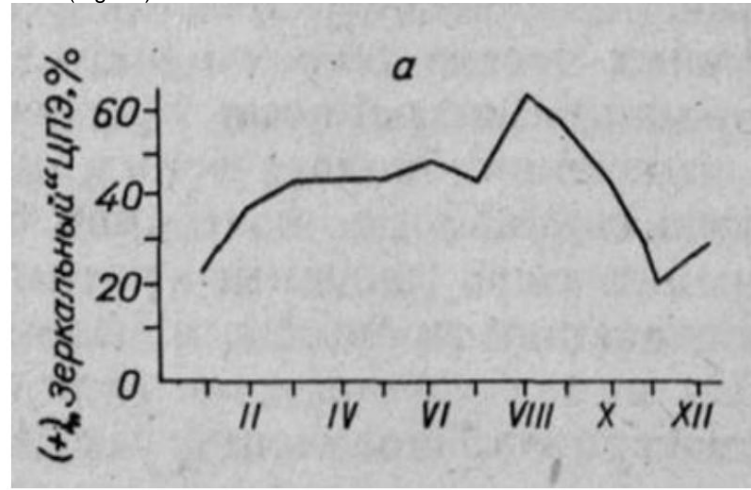


Fig. 10. Manifestation of the mirror CPE by month over 10 years (1966 – 1976) [25].

Another surprising seasonality was discovered during the study of the properties of magnetized aqueous solutions [26]. Thus, the magnetic susceptibility of a nickel sulfate solution changed radically with the annual period (Fig. 11).

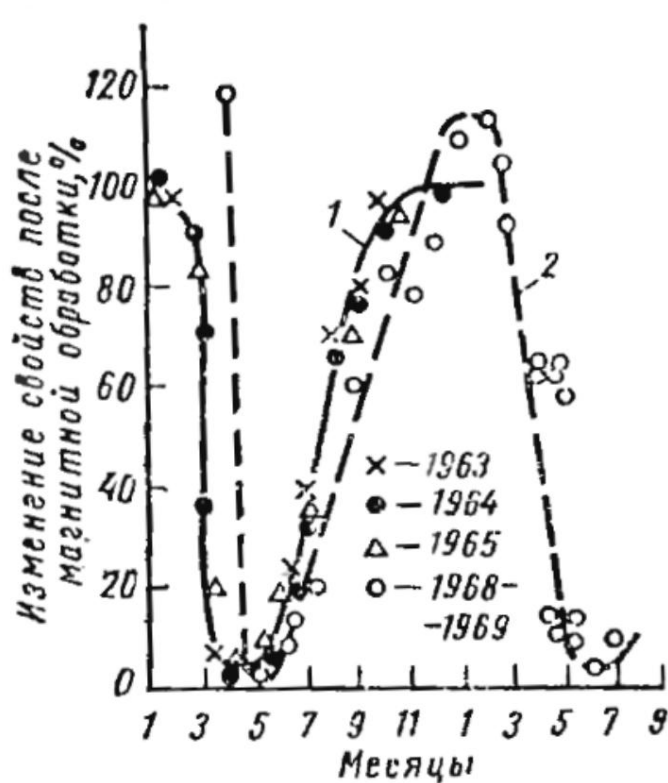
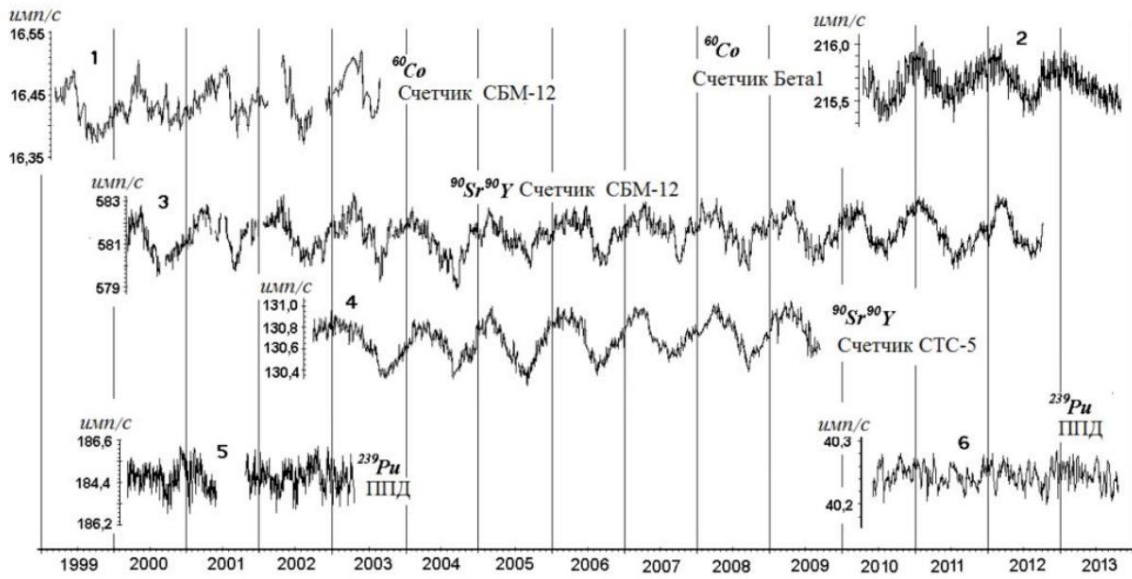


Fig. 11. Changes in the properties of water solutions after magnetization depending on the time of year: 1 – change of magnetic susceptibility of nickel sulfate solution; 2 – change in the density of sulfuric acid solution [26].

Returning to the results of A.G. Parkhomov, it can be noted that he also identified an annual

periodicity of beta decay intensity during synchronous observations of several sources (Fig. 12) [3]. No periodicity in the count rate was detected during the study of alpha sources.



**Fig. 12.** The count rate of beta sources  $^{60}\text{Co}$  (1 and 2) and  $^{90}\text{Sr}-^{90}\text{Y}$  (3 and 4), measured by Geiger counters, corrected for the decrease in activity with half-lives of 5.26 and 27.7 years, as well as the count rate of the alpha source  $^{239}\text{Pu}$  (5 and 6), measured by semiconductor detectors (A.G. Parkhomov) [3].

\*\*\*

These results, considered together, suggest the existence of some cosmophysical factor that has escaped the attention of physicists and that acts on many physical processes, from biophysics to nuclear processes, and that this factor is amenable to both screening and concentration, and it can be generated locally.

If we combine these exotic results with the concept of nuclear catalysis, we can assume the identity of the agent discovered by astrophysical methods by N.A. Kozyrev and the agent that causes LENR in a variety of processes. A number of emerging hypotheses can be experimentally verified, although they require serious efforts.

#### 4. The concept of LENR indicators

Let us return to the processes in LENR reactors and the need to ensure reliable LENR metrology. If we assume the existence of a nuclear-active agent causing nuclear transformations in the reactor working substance, the concept of LENR indicators can be introduced as a logical development of this idea.

LENR indicator is a small LENR reactor, the purpose of which is not to produce excess energy, but to indicate the presence and, in the future, to measure the flows of the agent causing low-energy nuclear reactions (Fig. 13). The indicator itself can use the methods mentioned in the second part of this article, and as the physical nature and properties of the agent are clarified, other physical principles. The main purpose of LENR indicators is to provide experimenters with reliable measuring instruments, similar to

The Geiger counter has served physicists for a hundred years to measure the intensity of traditional nuclear reactions.

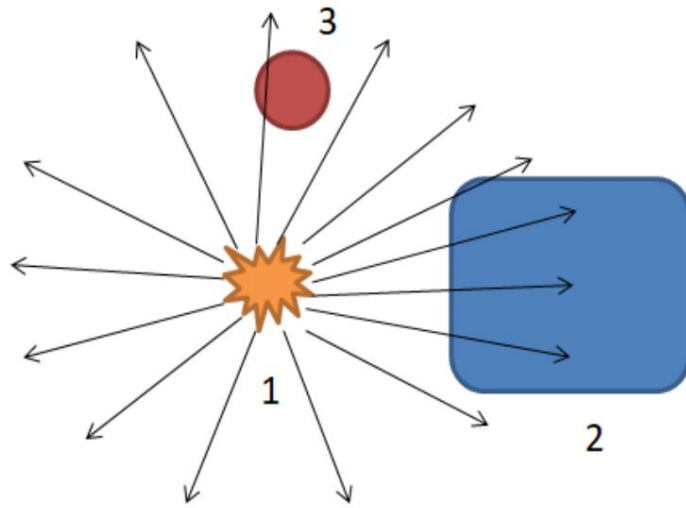


**Fig. 13.** The concept of the LENR indicator. The LENR indicator (3) detects/measures the agent flow from the source (1). The main LENR process occurs in the working fluid (2).

The problem of concentration of flows of nuclear-active agent should be solved separately. For this purpose, reflection, the so-called form effect, and possibly concentration methods using active devices can be used [27]. This will also increase the intensity of LENR flow in reactors and thereby increase their energy efficiency.

It should not be forgotten that this physical agent is biologically active (see works [28-31], in which similar biological effects operate). LENR indicators are also a way to provide experimenters with systems for warning of undesirable consequences for their health.

## 5. Conclusion

Consideration of a variety of experimental results from astrophysics to biophysics allows us to assume the existence of some physical agent that is responsible for the LENR process and is involved in many as yet unexplained phenomena. A physical model of such an agent must inevitably take into account the following features:

1. This agent does not correspond to any known radiation; it is a new object for physics.  
Attempts to "pull in" for explanations, for example,  
electromagnetic radiation does not stand up to criticism.
2. The agent is nuclear active. It can change the properties of radioactive nuclides and  
cause low-energy reactions.
3. It is characterized by the effect of accumulation in the substance, which leads to the  
phenomenon of aftereffect, well known to experimenters in the field of LENR.

4. Agent flows can be screened, reflected and concentrated. This gives references to the phenomenology of the effect of forms.
5. The agent has a changeable cosmophysical component.
6. The agent is biologically active.

Properties 3–5 greatly complicate the work of isolating this agent, since even in the same laboratory at different times, apparently, different flows of this agent and its different concentrations in materials are created. This leads to low reproducibility of the results of many experiments, and property 6 creates additional risks for experimenters. However, the fundamental isolation of such an agent as an object of targeted study is an important step for progress in this area of research. LENR indicators are designed to solve the problem of studying its physical properties.

## 6. Acknowledgments

The author expresses gratitude to V.A. Romanovsky for fruitful discussions.

### Literature

1. *Ratis Yu.L.* On the possibility of the existence of a long-lived exoatom “neutronium”. Journal of Emerging Directions of Science, 2(1), pp. 27-42, 2013.
2. *Lochak G.* Theory of the Leptonic Monopole. [http://lochak.com/Z-files/livre\\_monopole.pdf](http://lochak.com/Z-files/livre_monopole.pdf)
3. *Parkhomov A.G.* Space. Earth. Man. New Facets of Science. Moscow: Nauka, 2009. 272 p. Second edition: M, 2020, 285 p. <https://cloud.mail.ru/public/pbfN/c21VsXtVU>
4. *Baranov D.S., Zatelepin V.N., Panchelyuga V.A., Shishkin A.L.* Transfer of “dark hydrogen” by atomic matter. Methods for diagnosing “dark hydrogen”. RENSIT, 2021, 13(3):319-328. DOI: 10.17725/rensit.2021.13.319.
5. *Myshinsky G. V., Kuznetsov V. D., Starostin V. I.* Natural nucleosynthesis. Radioelectronics. Nanosystems. Information technologies. – 2022. – V. 14. – No. 4. – P. 473-496.
6. *Parkhomov A.G.* Nuclear transmutations and excess heat in reactors with incandescent lamps. Proceedings of the 27th Russian Conference on Cold Transmutation of Nuclei of Chemical Elements and Physics of Ball Lightning (2022) pp. 25–34. <https://cloud.mail.ru/public/Mwqk/xJH5jLqrP>
7. *Parkhomov A.G., Zhigalov V.A., Nevolin V.K.* Tracks of strange radiation. Their properties. An attempt at explanation. RENSIT: Radioelectronics. Nanosystems. Information Technologies, 2024, 16(1):79-88.

8. Parkhomov A.G., Karabanov R.V. LENR as a manifestation of weak nuclear interactions. A new approach to creating LENR reactors. RENSIT, 2021, 13(1):45-58.
  
9. Kozyrev N.A. Selected works. L.: Leningrad University Publishing House. 1991 - 448 p. See also <https://www.nkozyrev.ru> 10.
  
- Kozyrev N.A., Nasonov V.V. New method for determining trigonometric parallax based on measuring the difference between the true and apparent position of the star. Astrometry and celestial mechanics. – M., L., 1978, pp. 168-179. <http://www.nkozyrev.ru/bd/002.php>
  
11. Lavrentyev M.M., Eganova I.A., Lutset M.K., Fominykh S.F. About remote the effect of stars on a resistor. Reports of the Academy of Sciences. – Russian Academy of Sciences, 1990. – V. 314. – No. 2. – P. 352-355.
  
12. Lavrentiev M.M., Eganova I.A., Medvedev V.G., Oleynik V.K., Fominykh S.F. O scanning the starry sky with the Kozyrev sensor. Reports of the USSR Academy of Sciences, v. 323 (No. 4), pp. 649-652 (1992).
  
13. Akimov A.E., Kovalchuk G.U., Medvedev V.G., Oleynik V.K., Pugach A.F. Preliminary results of astronomical observations of the sky using the method of N.A. Kozyrev. Academy of Sciences of Ukraine, Main Astronomical Observatory // Preprint of the Main Astronomical Observatory of the Academy of Sciences of Ukraine GAO-92-5R. Kyiv. – 1992.
  
14. Andreev S. N., Voropinov A. V., Tsipenyuk D. Yu. Creation and testing four-channel setup for testing at a modern experimental level the controversial astronomical observations of N.A. Kozyrev. Radioelectronics. Nanosystems. Information technologies. – 2017. – Vol. 9. – No. 2. – P. 139-146.
  
15. Shakhpargonov I.M. Interaction of Kozyrev-Dirac radiation with radionuclides.
  
16. Balyberdin V.V., Glyanko V.T., Zhuk N.A., Kolpakov N.D., Nechaev A.V., Chernyshov S.I. Penetrating radiation of cavitation caverns. In the collection. V.A. Atsyukovsky. Principles of etherodynamic natural science. Book 6. Modern etherodynamic experiments and technologies.
  
17. Kinderevich A.V. Solution to the problem of accelerated deactivation of radioactive elements. Proceedings of the conference "Torsion fields and information interactions - 2009".
  
18. Jiang Kanzheng Yu.V. Mastering the potential of life by bioelectromagnetic field. "The Asia-Pacific Region in Global Politics, Economics and Culture

- XXI century". International scientific conference October 22-23, 2002, materials of reports. Khabarovsk 2002. pp. 118-120. ([http://replay.waybackmachine.org/20070403012426/http://www.jiang.ru/ru/dok/do\\_k040.shtml](http://replay.waybackmachine.org/20070403012426/http://www.jiang.ru/ru/dok/do_k040.shtml))
19. *Komrakov E.* Control of focusing of ultra-weak fields. Publishing solutions, 2023. - 224 p.
20. *Kervran K.L.* Arguments in the biology of transmutations at weak energies. <http://prosolver.kiev.ua/biblio.html> 21.
- Vysotsky V.I., Kornilova A.A.* Nuclear reactions and transmutation of isotopes in biological systems (prehistory, current state, prospects). Journal emerging areas of science. – 2017. – Vol. 5. – No. 17-18. – P. 34-42.
22. *Biberian JP* Biological transmutations: historical perspective. Journal of Condensed Matter Nuclear Science. – 2012. – T. 7. – No. 1. – pp. 11-25.
23. *Biberian JP* Biological transmutations // Journal of Condensed Matter Nuclear Science. – 2019. – T. 28. – No. 1. – pp. 21-27.
24. *Deep K., Mittal R.* Macronutrient K variation in mung bean sprouts with lunar phases. European Scientific Journal. – 2014. – T. 10. – No. 9.
25. *Kaznacheev V.P., Mikhailova L.P.* Ultraweak radiation in intercellular interactions. – 1981.
26. *Klassen V.I.* Magnetization of water systems. – M.: Chemistry, 1978. – 240 p.
27. *Zhilalov V.A.* Characteristic effects of non-electromagnetic radiation. "The Second Physics, 2011
28. *Shakhparonov I.M.* Kozyrev-Dirac radiation and its influence on animals.
29. *Pryakhin EA, Tryapitsina GA, Urutskoyev LI, Akleyev AV* Assessment of the biological effects of "strange" Radiation // Annales de la Fondation Louis de Broglie, Volume 31 no 4, 2006 (<http://www.ensmp.fr/aflb/AFLB-314/aflb314m514.pdf>).

---
30. *Pryakhin E.A. Urutskoyev L.I., Styazhkina E.V., Tryapitsyna G.A., Aldibekova A.E., Peretykin A.A., Pryakhin E.E., Alabin K.A., Pilia N.D., Chikovani N.Z., Voitenko D.A., Arshba R.M.* Biological detection of physical factors associated with high-current electric explosion of conductors in vacuum. Bulletin of the Russian Academy of Sciences. Physical Series. - 2020. - Vol. 84. - No. 11. - P. 1560-1568.
31. *Panov V.F., Testov B.V., Klyuev A.V.* Reaction of mice to torsion radiation. Scientific foundations and applied problems of energy-information interactions in nature and society: Proceedings of the International Congress "InterENIO-99". - M.: Publishing house VIU, 2000.

## LENR indicators

**V. A. Zhigalov**

Satbayev University, Almaty, Kazakhstan

[zhigalov@gmail.com](mailto:zhigalov@gmail.com)

The generally accepted methods of measuring the intensity of nuclear reactions (measuring the flux of neutrons and other particles) are not suitable for LENR. The reason is the absence of significant fluxes of neutrons, gamma quanta and other ionizing particles from low-energy nuclear reactions. However, without measuring the intensity of their occurrence, it is impossible to build technically applicable reactors, and it is very difficult to study the phenomenon itself in laboratory conditions. The reasons for the difficulty in indicating and measuring LENR are caused by the current stage of studying this phenomenon. There is still no generally accepted model for the mechanism of this class of nuclear reactions. Many proposed theories and hypotheses involve some nuclear-active agent: neutronium, magnetic monopole, ultracold neutrinos, dark hydrogen, etc. If such an agent is responsible for the LENR process, then the indication and measurement of the reaction intensity can be based on the measurement of the flows of this agent. The report provides an overview of the experimental results that can be considered as the detection of such an agent: these are the results of NA Kozyrev and his followers, AG Parkhomov, IM Shakhpashov and others. An attempt is made to link these and other results with the LENR topic. The report also considers methods for indicating LENR by excess heat release, element transformation, strange radiation tracks, etc.

# Observational properties of ball lightning, data, 2024

V.L. Bychkov, D.N. Vaulin, Bychkov D.V.

Moscow State University named after M.V. Lomonosov, Moscow, Russia bychvl@gmail.com

---

Observational data on ball lightning are presented, collected on the basis of information on the Internet and by surveying observers in the period 2023-2024. The main observations are from Russia. The information is provided with comments.

## 1. Moscow. 2023, July. Nadezhda Petrovna Savenkova, Ph.D., VNS, Andrey Mokin, Ph.D., Senior. Rev. , Faculty of Computer Science, Moscow State University,

We saw ball lightning in Moscow in the Pokrovskoye-Streshnevo Park during a thunderstorm. The weather was bad, rainy. We were standing under a tree, and in front of us, five meters away, was a metal fence of the park. A glowing ball appeared suddenly, hissed and moved along the top of the fence above the sharp ends of the rods. The diameter of the ball was 4 cm. The surface glowed brightly. The light was the same as that of an electric arc. Inside, the ball seemed dark. We watched the ball for no more than 5 seconds. Then it jumped off the fence, flew above the ground into the bushes and exploded! All this lasted for several seconds, we did not even have time to get scared.

Comment: What is unusual about the description is that the ball moved along the top of the fence above the sharp ends of the bars. This emphasizes that the SM was not plasma, but most likely had a shell.

---



## 2. .10.2023. Ufologist made contact with plasmoids.

Source: Notes of Osvaldo Prospero.

Fig.1. Photo source: progomel.by

Stepan Mikhailovich Sapogov was an outstanding researcher phenomenon – ball lightning (BL). The enthusiast worked for a long time with the Ufologist Felix Yuryevich famous Zigel. Stepan Mikhailovich was born in the city of Zhirny, later Zhirnovsk. S.M. Sapogov

dedicated his life studying ball lightning. It so happened that the largest anomalous zone in Russia, the Medveditskaya Ridge, was located just a few kilometers from the researcher's home settlement.

The Medveditskaya Ridge is a unique place. People with different levels of perception feel differently, sometimes even perceive reality differently from each other. The anomalies of the Medveditskaya Ridge are very diverse: "chrono-mirages", UFO flights, "UFO landings", "different flows of time", underground tunnels made of white ceramics that go for hundreds of kilometers, SM.

SM is changeable. There are known cases when these clots of energy "chase" people. "Chased" them from a certain territory and flew away, but as soon as they got closer, the attack began again.

S.M. Sapogov often spent weeks and even months on the Medveditskaya Ridge. There is a place here called the SM slope. Each tree on it is covered with round burnt holes - ball lightning moved along the same trajectories and burned through holes in the tree trunks. The researcher tried to contact the SM. According to his stories, it happened that he chased them, but more often he ran away from them. However, several times he managed to establish communication with the help of a powerful flashlight. He waited until it got dark and went to the lightning slope. There, upon seeing an object, the man sent signals with a flashlight. Most often there was no feedback. But the researcher repeatedly recorded a response glow. The SM seemed to contract and unclench, becoming brighter, then dimmer. At the same time, the frequency of the glow change repeated the frequency of flashes of a flashlight in the person's hands.

In 1970, S. M. Sapogov recorded a fiery BL on the lightning slope. The clot of energy combined tongues of flame and electrical discharges. The man wanted to observe it, but suddenly the object disintegrated - into BL and fiery sparks, which quickly died out. In 1979, S. M. Sapogov went to the

lightning slope for the last time. Stepan did not return from this trip. Four days later, his tent and personal belongings were found. The researcher himself disappeared. **Commentary.** S. M. Sapogov recorded a fiery ball lightning. The clot of energy combined tongues of flame and electrical discharges.

### **3. 11-10-2023 13:31. In 1985, a UFO attacked a civilian aircraft. What the pilots and passengers of the Kyiv-Tallinn airliner said. Albert Olimidin**

Today I would like to share with you information about the events of 1985 that took place in Minsk. A civilian aircraft was flying on the Kyiv-Tallinn route. Something inexplicable happened to the aircraft over the territory of Belarus. The result was an emergency landing at the Minsk airport. The excellent training of the Soviet pilots allowed them to land the plane on an alternate runway in an extreme situation. Here is what they and the passengers on board the plane said.

"Flying over the border of the Ukrainian SSR and the Byelorussian SSR, we noticed a spherical white object appear in the distance, with two golden rings circling around it. This ball followed us from Gomel to Rogachev, after which it came closer and released several white rays. The skin and one of the engines were damaged. We could not fly to Tallinn in these conditions and requested a reserve runway in Minsk. The airfield in Mogilev was closer, but my colleague and I knew the Minsk airfield like the back of our hand, so we decided to land there,"

pilot Alexey reported after a successful landing.

During the flight, Alexey noticed a flash ahead and to the left of the course. "It looked like a bright light bulb, and there were rings spinning around it. I managed to notice that the object was not flying like us, but in jerks. It would fly a few dozen meters, stop abruptly. It would fly, stop again. Pilots often see different things, but for a civilian aircraft to be attacked... I don't remember that. At first, the object was to the side or

far ahead. But at some point he headed straight for the plane. And then either there was a collision, or he fired something. I still don't understand," Victor said.

"There were no balloons visible from my side. But I heard people talking and looking out the windows. Something must have been happening in the sky," said one of the passengers.

"It was some kind of shiny, snow-white ball. It seemed that it was not a device, but a clot of some kind of energy, like ball lightning. But the rings around it were clearly made of metal. Initially, it looked like a small ball, but as it approached, it became less dense and larger. Many of those on board saw it, and it was scary. We thought it was some new American weapon," another passenger testified.

An examination conducted under the supervision of the country's top leadership revealed serious damage. Something had burned two 20-centimeter-diameter holes in one of the plane's turbines and in the nose. Moreover, it had burned through everything evenly - the skin, internal parts, wiring, mechanisms. The newspapers of the time published an article that the plane had been struck by lightning, but there was no thunderstorm in the clear sky.

In the early 2000s, retired pilot Viktor Olesko said that they were forced to retract their words about the mysterious ball. Otherwise, their profession was at stake. Because of this, they had to publicly retract their testimony after the examination and admit that it was ball lightning. However, civilian passengers cannot be fooled. They saw everything and shared their impressions immediately after the incident. Among the opinions, there were suggestions about a partial similarity to ball lightning, but the fact that the object followed the plane for many kilometers and then attacked it completely denies the possibility that it was ball lightning. It was probably a UFO, and the reason for its aggression towards a passenger airliner still remains a mystery.

**Comment:** Description of an object that is not typical for ball lightning.

#### **4. September 3, 2019, 10:53 — IA Regnum. Bokhan settlement, Irkutsk region.**

**Ball lightning left more than 3,000 residents of the Angara region without power.**

Today, September 3, Irkutsk power engineers are forced to eliminate the consequences of an emergency at an electrical substation that occurred in the morning at 06:35 local time in **the Bokhansky district**. As reported by the press service of the **Irkutsk energy sales company**, a complete switchgear broke due to a SM strike. 3,395 residents of ten settlements were left without power. Also, 20 socially significant facilities were de-energized.

**Comment.** The impact of the SM broke the complete switchgear of the electrical substation

#### **5. October 16, 2023, 09:30 <https://msk1.ru/text/gorod/2023/10/16/72806252/>**

**What secrets does the Moscow Kremlin keep? An unidentified object and a celestial sphere.** If we are to believe the archival records of that time, we can say that the appearance of SM was noticed very often on the territory of the Kremlin. In 1997, four SM were noticed here at once. A survey of witnesses showed that the first one with a diameter of about

one meter appeared about two hundred meters above the Grand Kremlin Palace. Later, the ball broke up into three others, and each of them moved toward Ivanovskaya Square, Tainitsky Garden and the Archangel Cathedral. In December 2009, an equally strange phenomenon occurred:

an object in the shape of a tetrahedron was spotted above the center. Moreover, this event made a lot of noise at the time. TV and newspapers covered the incident in every possible way, and every self-respecting Internet user put forward his own hypothesis. It is still unclear whether it was a UFO

or something else.

Thanks to the work of the historian Sizov, records were found that told about an identical situation on the territory of the Kremlin four hundred years ago.

**Comment:** Frequent occurrence of ball lightning in the Moscow Kremlin area

**6. 12/28/2023** A rare phenomenon was captured on video in Florida. Day.Az, the footage was published on Telegram.



**Fig.2.** During a thunderstorm, a ball lightning ran along the wires. **Comment.**

Movement along wires is encountered in SM observations

**7. 11.09.23.** Newspaper "Pravda Severa" Nikolay Chesnokov. **Memory of the**

#### **Heart: Ball Lightning**

Every summer, grandson Senya visited Baba Tasya - a naughty child who did poorly at school. Once, during just such a dry thunderstorm, the old woman heard his voice from the next room: "Baba, baba, look, what kind of a ball is flying above me?!"

Taisiya Vasilyevna looked into the room and was stunned. She had never seen such miracles in her life: a reddish ball was flying in circles around her grandson's head. It was as if a halo had shone over Senka... The ball was hissing and throwing out sparks, like a Bengal fire in a village club on New Year's. And Granny Tasya seemed to have been paralyzed – she stood rooted to the spot. Then she

gathered her courage and said barely audibly: "Senya, my dear, don't move! Don't wave your arms, don't try to catch that ball! Maybe the devil will pass you by!" And Senya obeyed, lowered his arms, and stood up quietly, as Granny Tasya had ordered.

SM, as if hearing the old woman's order, changed its orbit, rushing towards the window, and instantly seeped through the glass. On the street, it hopped along the path into the neighboring yard, and then flew into the keyhole of the front door. It flew around the rooms, choosing a victim for itself and attached itself to a large samovar standing on a copper tray in the middle of the table. It repeated the exercise familiar to us - it made a circle or two, and the water instantly boiled, which was indicated by the shrill copper whistle of the samovar. It circled, as if around Senya's head, and then began to disfigure. SM for a start

snapped the copper handles, then sparked with electric welding at the tap, soldering this most important part. But, apparently, having spent all its charge, the lightning thundered like a burst wedding balloon, and instantly disappeared, leaving the remains of the "samovar massacre" on the tray

**Comment.** The SM leaked through the glass. The SM flew into the keyhole of the front door. The SM snapped the copper handles, then sparked with an electric welder at the tap, soldering this part.

#### 8. 06.09.2023 **Ghosts, UFOs, life after death, earth hum, intuition and much more.** Source <https://zabavniks.com>

According to news reports, in January 1984, a Russian aircraft was struck by a lightning bolt mid-flight. The bolt hovered over the heads of the stunned passengers in the tail section of the plane before it split into two glowing crescents, which then rejoined and left the plane almost silently. In the incident with the plane, the bolt left one hole in the plane. **Comment.** The bolt split into two glowing crescents, which then rejoined and left the plane almost silently. The bolt left a hole in the plane.

#### 9. 10/06/23 **Ghosts, UFOs, life after death, the hum of the earth, intuition and much more.** Russian Seven. History A controversial issue is the frequency of ball

lightning. In 1966, NASA researchers surveyed **two thousand people** and asked them to answer two questions: had they seen BL, and if yes, was the phenomenon accompanied by standard lightning discharges? Scientists tried to determine the frequency of BL compared to linear discharges. Of those surveyed, only 409 people observed linear lightning in close proximity, while only 200 respondents encountered BL. Scientists were lucky: among the participants in the experiment, there was even one "lucky one" who **observed the "fireball" eight times**. His testimony added to the treasury of indirect evidence that ball lightning is not such a rare phenomenon.

phenomenon...

**Comment.** One witness observed SM 8 times. **10. 09:32, March 2, 2023.**

**World. In Japan**

**another mysterious ball found**

**of unknown origin**

**Fig. 3.** MBC: A second hollow sphere measuring 1.5 meters in diameter has been discovered on the southern island of Tokunoshima in Japan. Image: Minaminihon Broadcasting Co.



Another ball of unknown origin was found on the southern island of Tokunoshima in Japan, its diameter is 1.5 meters. The second ball found was reported by the Japanese TV channel MBC. It is reported that the ball

was found on February 28, law enforcement agencies and experts concluded that it was not dangerous. On February 21, a ball with a diameter of 1.5 meters, presumably made of iron, was found on Enshuhama Beach in the city of Hamamatsu (Shizuoka Prefecture in Japan).

**Comment:** The observation is interesting in connection with the possibility of the formation of SM with a solid and metallic shell.

11. Sun 4 Aug 2024. ramis.tns@gmail.com **Ramis Akhmetov**, on July 31, two ball lightnings flew into my house, both exploded in the air and burned almost all the low-voltage electronics, some by breakdown from secondary to primary circuits, and some simply by high EMI. All the windows and doors in the house were closed. And here the question arises, how could they get into the house? A video was sent, in which you can see through the window how (2s) white ball lightning, 3-4 cm in diameter, flies.



**Fig. 5.** Photo of glass.

Comment: Observation of two SM.

12. S.V. Bogomolov. Prof. of the Faculty of Computational Mathematics and Cybernetics, Moscow State University. Moscow, August 2023. Impact of SM on window glass. Ball Lightning. Photos of a trace on a window pane are presented. During the day, an observer saw a hole in the balcony glazing.

**Fig.4** Photo from the observer's window.

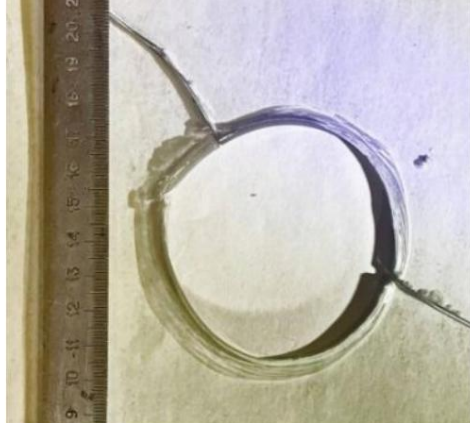


**Fig.6.**

Photo

holes  
in glass

Please pay attention  
attention  
on the thin  
edge  
glass.

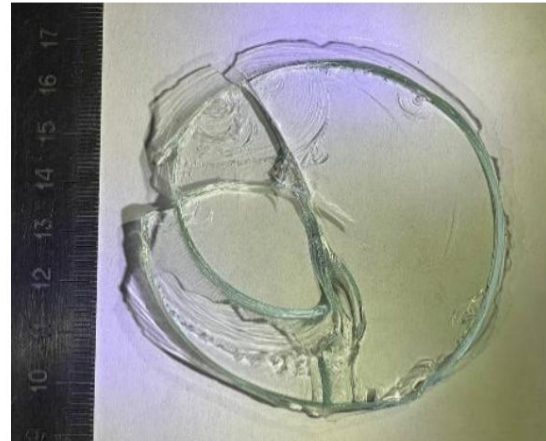


Fig. 7 shows glass after exposure to a high-temperature plasma jet (up to 6000K). The formation of a thin glass layer in the form of a fringe of molten glass is visible.

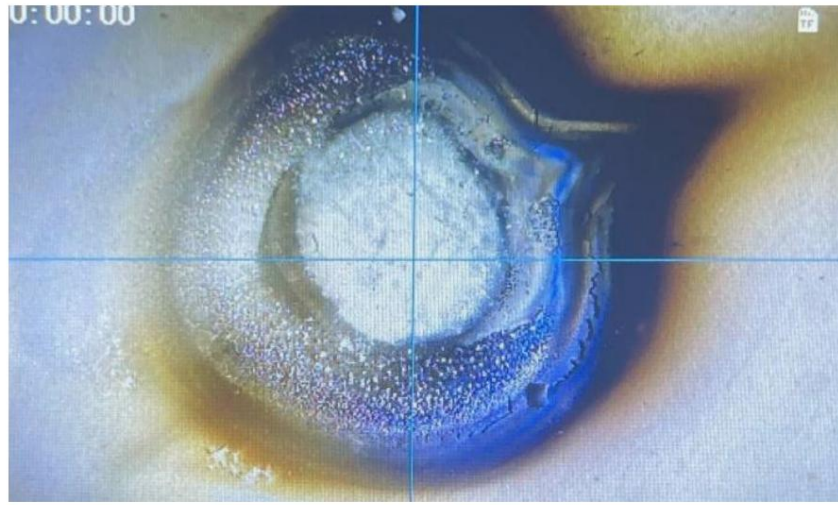


Fig.7.

**13. April 29, 2024 Omsk.** Andrey Shchedrin, SM researcher. In the city of Tyukalinsk, Oktyabrsky settlement, April 28, 2024, a SM hit a house. No one

was in the house at the time of the impact. The TV and router were damaged and burned down. Neighbors reported that there was a strong explosion. In the comments, people wrote that it was not a SM, but a linear one. However, the presence

grounded antenna mast and a tall spruce nearby (see photo) almost excludes the passage of a linear lightning channel along the wall, and even horizontally (the object left a charred trace on the wall of the house). The only option is poor grounding of the mast and if some wire went horizontally from it in the direction of the left corner of the building.



Then this wire could have worked as a fuse when linear lightning discharged through it onto a gas pipe or an overhead power line wire, which is visible there on the insulator.

Comment: Horizontal trace from the SM.

Fig.8

**14. February 2024 12:00 Author:** Elena Volkova ўIZHLIFE **Rare natural phenomena in Udmurtia.** In August 2014, information

about BL in Udmurtia appeared for the first time. Residents of the village of Mul'shur in the Uvinsky district heard a thunderstorm and left the hayfield, and already at home they happened to hear a lightning discharge. According to eyewitnesses, the lightning was so strong that even the walls and roof of the house shook. To see the lightning, people ran out into the street and saw that it was literally destroying their house: BL hit right into the extension, breaking the roof. Fortunately,

There were no casualties, and the budding fire was quickly extinguished.

**Comment:** Multiple destruction caused by SM

### 15. December 22, 2023 THEORIES, VERSIONS, HYPOTHESES. Look and think.

Alexander Chumichev observed SM in his childhood. We were standing with my mother in the kitchen by the window, 1st floor. There was a blanket lying on the ground in front of the window. It was being hailed. Suddenly there was a flash above the blanket. We recoiled from the window. A small sparkling ball flew in through the window. It flew around the kitchen like a curious little animal, small but deadly dangerous, and also left through the window to the street. Zinfira Davletova SM, which visited me (70 years have

passed) she charged me, being at a distance and made it clear that her energy passes without touching, but at a distance, I thought that she was intelligent, she moved very well, as if examining me!

Mikhail. A SM flew into a village house of elderly relatives through a window, and the glass remained intact, that is, it somehow passed through it. Then it went down the wall along a wooden cornice into a sideboard with dishes, passing by the electrical wiring and the meter, in the sideboard it chipped a couple of wine glasses at the stem, came out from there, went down lower, floated past the hostess sitting at the table, walked inside the sofa with springs on which the owner was lying at that time. **Comment.** A selection of SM observations. In one observation, a SM flew into a village house through a window, and the glass remained intact.

### 16. 14.07.01.2024 Orlando, Florida. USA Politikus.info

Video shared by Orlando residents. At first, eyewitnesses (100 people) thought they were seeing the Moon. But then smaller objects emerged from this sphere.



Fig.9

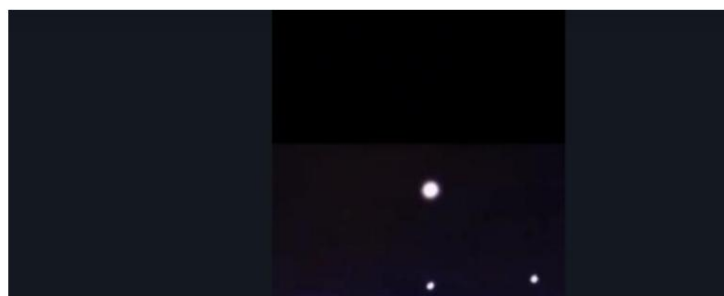


Fig.10

The lifetime of a large sphere is up to a minute. The lifetime of small spheres is several tens of seconds.

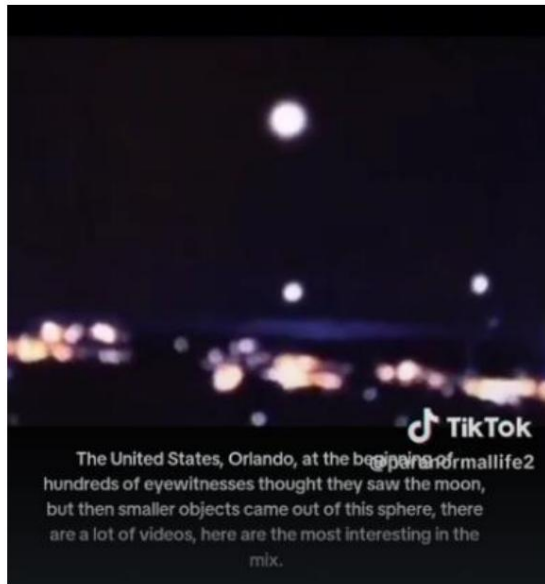


Fig.11

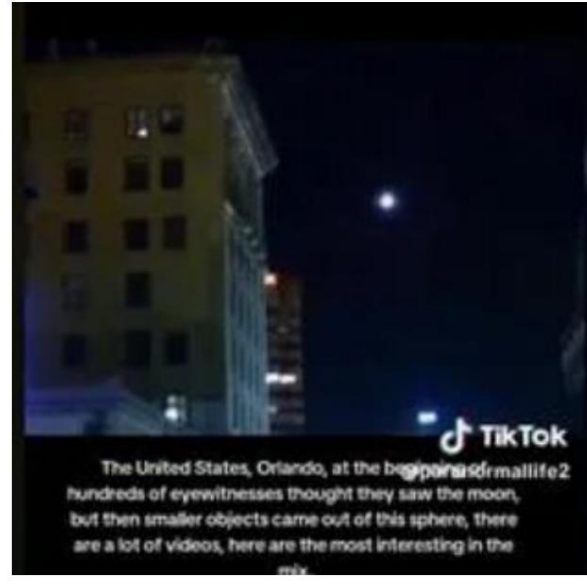


Fig.12

**Comment:** Multiple occurrences of SM.

**17. om1.ru April 30, 2024, 15:47. Incidents in Omsk.** Lev Mindalev. Two days earlier, ball lightning hit a house in Tyukalinsk.

It didn't cause a fire, but it did cause a TV and router to burn in the house, and the neighbors heard a loud explosion. Luckily, there was no one in the house.

**Comment:** Destruction of SM objects.

**18. Newsland 04/28/24** "Ball lightning. My God, what a wild thing."

"I was 14 and I saw her running along the train tracks. After she disappeared, there was a loud bang and I'm not sure if she exploded or hit something."

**Comment:** The death of the SM with an explosion.

**19. May 29, 2024, 19:21 Karel inform.**

A fire started near Petrozavodsk due to SM. Yesterday in Pinguba, SM was presumably the cause of a fire on private property. Rescuers and gas service employees worked at the scene. A private bathhouse and an outbuilding in the SNT "Pribrezhny" were on fire. It took 2.5 hours to fight the fire. Judging by the footage, the buildings burned out completely. Eyewitnesses of the incident told the Telegram channel "Karelsky Dvorik" that the fire occurred after a gas cylinder exploded. They also mentioned that a ball hit the building a moment before the explosion

lightning.

**Comment:** Destruction of SM objects

**20. Reteyum A. Prof. of the Faculty of Geography of Moscow State University**

In early June 1999, a balloon was flying from the Zailiyskiy Alatau mountains over the city of Alma-Ata at an altitude of 300-500 m and a distance of about 1 km from the observer, at an inclined trajectory, at the speed of a landing airplane. Because of the usual haze for the city, I did not see the end of the path. The balloon was light orange, and flew completely silently. Apparently, its diameter was about 1 m. The weather was partly cloudy. There were no unusual effects, but the phenomenon made a strong impression on me, it is difficult to say why. It is comparable to the sensations from the catastrophic Khait earthquake (M 7.6), which I experienced at the age of 7 in the mountains of Tajikistan, when not far from our village about 30 thousand people instantly died (a mountain fell). By the way, I found the recorded memories of a pilot who had flown into the city the day before with a load of money for wages. He writes that before the earthquake there was fog and drizzle, and 2 days before there were local showers (we don't have that). This is in the summer, with a dry atmosphere - signs of hydrogen emission. I found similar precursors in many cases in Iran according to weather stations.

**Comment:** At an altitude of 300-500 m and a distance of about 1 km from the observer, a ball was flying at the speed of a landing airplane, along an inclined trajectory.

#### **21. June 11, 2011 20:42 REX correspondent reports**

An explosion thundered in one of the courtyards of the Shevchenkivskyi district of Kyiv on June 11 at about 18:30 local time. According to residents, it was caused by a BL that hit a tree branch. Residents who were in the courtyard and near the windows saw a bright flash, which was accompanied by a sound wave. Due to the explosion, the windows in the house shook, the glass in one of the apartments cracked, and car alarms went off. No other consequences were observed, there was no smoke or fire. arose.

Eyewitnesses said they saw a spherical substance and a blue flash in the air, then an explosion occurred. At the time of the explosion, no one was setting off fireworks nearby, no repair or welding work was being carried out. However, given that the territory of a military base is nearby, this version was not the only one. The Main Directorate of the Ministry of Emergency Situations of Kyiv stated that at the moment they have not received any statements about the explosion in the microdistrict.

**Comment.** Explosion of the SM.

#### **22. 05.07.2007 14:12 INCIDENTS. UNIAN.**

In the Dniprovsy district of Kyiv, the roof of a four-story residential building caught fire as a result of a ball lightning strike. Rescuers who arrived at the scene found that the roof insulation had caught fire on the technical floor, and they extinguished the fire in a matter of minutes. As one of the residents of the building told the rescuers, watching from the window during the rain, she saw "some strange fireball that rose up." At the same time, according to her, a powerful explosion was heard upstairs, and she saw smoke coming from the roof of the building. As a result of the explosion, the pipelines in the building were damaged and residents had significant problems with the water supply. In addition, electrical equipment in some apartments failed.

**Comment.** Explosion of the SM.

**23. 10 JUNE, 19:24 2024. MOLDOVA,**

Source: <https://bloknot-moldova.ru/news/vzryv-byl-bolshoy-sharovaya-molniya-udarila-v-dets> Society, 06/29/2018

18:31

"The explosion was big": A ball hit a kindergarten in Transnistria. In the Grigoriopol district, a ball hit a kindergarten, completely destroying the roof of the building. A powerful cyclone passed over the republic last night. Showers and strong winds raged in all cities and districts. The village of Bychok was also damaged. There, a ball hit the kindergarten building. There was a powerful explosion. People who came to the kindergarten in the morning were faced with a horrifying picture: destroyed structures, cracked plaster, broken windows, pieces of slate lying everywhere. A witness to the incident was the kindergarten security guard Alexey Lyutov: - I went there and back. When I was returning, I heard a strong blow. A big explosion. At first, the lighting was yellow, and then a rustling sound was heard, like a dry leaf, -

Alexey said.

After the SM explosion, the kindergarten building, which is also the school, was left without a roof. The security guard immediately called for help. The man was not injured, but the shock he had to endure will not be forgotten soon. **Comment.** SM explosion.

**24. 12.06.2024. Ball lightning flew into a house on Dvinskaya Street in Novosibirsk** Telegram Fedor Burov



Fig.13. Photos provided by Infopro54

A natural phenomenon that looks like a ball glowing in the air has broken through a wall. A through brick

Novosibirsk family suffered from a visit to their home by SM. The owner of the mansion on Dvinskaya Street is still assessing the damage caused by SM and eliminating the consequences. Sergey M. told Infopro54 journalists that it happened late in the evening on June 6. "My wife was in the shower, the

child was in his room, and I was making up the bed and getting ready to go to bed. Suddenly, I heard a crash on the roof. It banged so loudly that half the city could hear it. Then something flew right over my head and collided with a wire in the room. I thought they were bombing us. Stones and plaster started falling. The fire alarm went off on the first floor. I ran to the gas boiler room. There was already a fire there. I somehow reached the pipe and turned off the gas. I burned my hands. Then I noticed that the water pipe was broken."



**Fig.14**

The natural disaster that raged under the roof of the mansion pierced the brick wall and started a fire in the gas boiler room.



**Fig.15 . Fig.16.**

Surprisingly, all these events happened literally in a matter of seconds. Lightning struck the electrical panel, all electrical appliances instantly turned off, and light bulbs exploded. Having visited one house, the natural elements moved on. Neighbors say that they also saw a glowing ball and their home and household appliances burned out.

My seven-year-old son was very scared, he started having hysterics. Firefighters and an ambulance arrived. The child had to be taken to relatives. The Caucasian Shepherd named Harley in the yard was in complete shock, she was showered with bricks and sparks. She didn't even come out when the Ministry of Emergency Situations entered the yard. There were two small dogs in the house, terrified

made puddles. Even the robot vacuum cleaner hid under the table out of fear, says Sergey.

An hour after the outbreak, the man's mobile phone broke. And in the morning, the more serious scale of this catastrophe became clear. It turned out that the gas boiler was broken, the pipeline was punctured, the freezer burned out, two computers and other equipment.

My neighbors had more appliances burnt out. Their 15-year-old girl saw the lightning itself and cried for a long time. My son couldn't come to his senses for three days. Now we are restoring everything. According to the most conservative estimates, the damage is more than one hundred thousand rubles. But, thank God, everyone is alive. "We didn't lose our house and celebrated our birthday," says the victim.

After his encounter with lightning, Sergei drew certain conclusions for himself.

Now I understand that in heavy rain and thunderstorms it is worth disconnecting all household appliances in the house from the socket, and even better, immediately turn off the electricity in the panel. Just in case, you need to close the windows and doors. Although in my situation, lightning broke through the wall and destroyed 4 rows of brickwork.

Residents of Novosibirsk are sharing their impressions on social networks that they also saw ball lightning these days. Several more houses in the private sector on Vysotsky Street were allegedly damaged.

**Comment:** Destruction of SM objects.

#### **25. 01/06/2024, 18:19 Author: Alena Pyatenok**

The SM was spotted in the village of Malinovka, Chistoozerny District, Novosibirsk Region. The electrical wiring was damaged, but household appliances remained intact. Elderly people live on one side of the two-apartment house, and the Gavrilov family lives on the other. There is one electrical input to the house.

Here is what Igor Gavrilov said: "At three o'clock in the morning, lightning flashed, and suddenly it was as if someone had fired a gun in the house, a light bulb lit up by itself, and a glowing ball darted to the side. My wife and I jumped up and saw that the curtain was burning and the window sill was slightly melted. We ran to check everything to make sure nothing was on fire. Lime was falling off the walls in places. We were scared, of course. We didn't sleep a wink until dawn, we were afraid. In the morning, it turned out that all the household appliances weren't working. We called electricians, and it turned out that all the wiring had burned out, but the appliances were intact. But the neighbors' TV had burned out and wasn't working."

**Comment:** Destruction of SM objects.

#### **26. June 30 14:46 Elizaveta Kostishina**

"As if headlights illuminated the windows": near Yaroslavl, a lightning bolt hit a house. **The house burst into flames like a match.** Emergency in the Yaroslavl Region: in the village of Tvorogova, a lightning bolt hit a house. - I saw with my own eyes a huge stream of light, followed by a strong lightning strike, as if headlights illuminated the windows, - said Olga Panueva.

Residents say the fire broke out a minute after a bolt of lightning struck a window. The incident occurred on Sunday morning, June 30,

in the village of Tvorogovo on Krasny Perekop in Yaroslavl. The incident occurred during a severe thunderstorm. The owners of the house were away at the time of the incident.

**Comment:** Fire caused by SM.

## 27. Sib. fm yesterday 08:21 SOCIETY

### INCIDENTS

SM hit a residential building in the Novosibirsk region.

The photo was provided by an eyewitness. On June 25, 2024, a heavy downpour with thunder and lightning occurred in the region, as a result of which some buildings, trees and houses. Thus, residents of the village of Kamenka in the weather, a SM hit their house, Novosibirsk region suffered from the elements. reported that during the terrible after which the premises immediately caught fire and a fire started. Fig. 18



**Comment:** Fire caused by SM.

## 28. 2.07.2024 12:10

[https://gk.tu/news/131821.ns\\_Regions.ru\\_Pavlovsky](https://gk.tu/news/131821.ns_Regions.ru_Pavlovsky)

Posad. Author: Victoria Gordeeva In the village of Argunovka, Pavlovsky Posad urban district, a SM hit a private house. Everyone is alive, but the house burned to the ground.

**Fig. 17.** Photo: vk.com/Anna Peshkina

A major fire occurred in the SNT. Eyewitnesses

said that a private house caught fire like a match after a SM strike. "We live opposite the burnt house. The elements were playing out on the street - a thunderstorm, lightning, heavy rain. Suddenly we were blinded by a bright flash, and at the same time something went boom. A few minutes later we saw the neighboring house burning,"

commented the residents of the SNT.

**Fig. 18**



**Comment:** Fire caused by SM.

## 29. Anton BELKA. Source: Youth newspaper Tags:

#thunderstorm#heat#forest#lightning#fire#danger#fire#emergency

A couple of years ago, a fire broke out in a private house in the Leninsky district. Then the bad weather raged. Lightning struck the roof overhang of the two-story brick house. After that, a resident of the house saw a small glowing ball the size of

with a soccer ball. It only appeared for a few seconds. - *It was like electric ball,*" said the owner of the house, **Eduard.** " *Where did it come from?*" *It's unclear. A hole formed on the roof. The SM either came out through it or came in.* *The woman felt like she flew in through the window. A few seconds later, something happened.* *there was a blow and the whole room was filled with smoke.*

The bedroom caught fire in a matter of seconds. The owners immediately called the fire department. The family was lucky. That day, several fire trucks were on their way to training and drove past the emergency site, so they arrived in just a minute and put out the fire. ignition.

**30.** <https://www.baikal-daily.ru/news/20/481833/Proishhestviya>, 13.07.2024 10:58

**Photo:** "Eravna-info.24/7" The incident occurred during a thunderstorm.

In the village of Sosnovo-Ozerskoye in the Yeravninsky District of Buryatia, a SM flew into the chimney of a residential building's stove and exploded. The incident occurred the day before during a thunderstorm, the group "Yeravna - info.24/7" reports.

The SM discharge hit the electrical wiring. As a result, the cable insulation melted, and the light and sockets literally exploded. Fortunately, there was no further fire. There was no one in the house at the time, so there were no casualties. Full version: <https://www.baikal-daily.ru/news/20/481833/>



Fig.19



Fig. 20



**Fig. 21**



**Fig. 22**

## **Observational properties of ball lightning, data 2024**

**VL Bychkov, DN Vaulin, DV Bychkov**, Lomonosov

Moscow State University, Moscow, Russia, [bychvl@gmail.com](mailto:bychvl@gmail.com)

Observational data on ball lightning collected on the basis of information on the Internet and during a survey of observers in the period 2023-2024 are presented. The main observations are collected in Russia. The information is provided with comments.

## **Cold nuclear transmutation chemical elements**

### **Experimental research**

---

### **Cold Nuclear Transmutation Of Chemical Elements**

### **Experimental Investigations**

## **Low-energy nuclear reactions in tungsten at the plasma focus PFM72-m facility**

**Savvatimova I.B., Klochkov A.N., Sidorov P.P., Bashutin O.A.**

National Research Nuclear University MEPhI

isavvatim@mail.ru

The article presents the results of mass spectrometric analysis obtained at the SIMS after the action of deuterium plasma flows on the PFM72-m plasma focus (PF) facility on samples of single-crystal tungsten and polycrystalline tungsten foil. A significant increase in the concentration of "light" elements with a mass less than the mass of the matrix material W (Li, Na, K, Ca, Mg) was detected in the zone of direct PF action, as well as in the shielded and peripheral areas of single-crystal and polycrystalline tungsten samples by 5 to 100 times for various elements. Moreover, in the peripheral and shielded areas of the analyzed samples, remote from the plasma focus axis, up to millions of pulses (ions) are recorded compared to thousands in the central area of the PF. That is, a significant increase in the concentration of "light" isotopes is observed in areas remote from the axis of the installation, where their dispersion and "ejection" by the shock plasma wave is less or does not occur at all, and where the energy of the particles ranges from units to tens of electron volts and various nuclear-chemical reactions can occur.

### **Introduction**

Research into low-energy nuclear reactions (other definitions include cold fusion processes, nuclear chemical processes) is apparently entering a new phase, as the outright rejection of the very possibility of such nuclear transformations by many professionals is being replaced by a certain interest in such processes. More than 30 years of efforts by disparate groups have yielded convincing experimental data that have made it possible to reverse the situation, and today some leading physics journals [1-5] are publishing the problems.

results                          By                          this

At the same time, however, questions about the mechanism of these processes remain unclear due to the unusually low (6 orders of magnitude lower) energies, which are not at all characteristic of nuclear physics, as well as the practical absence of dangerous ionizing radiation during the nuclear transmutations that occur. But it should be noted that some steps in understanding the phenomenon of cold fusion have already been made earlier on the basis of

studies of nuclear chemical processes initiated under conditions of low-temperature nonequilibrium plasma (in glow discharge in protium- and deuterium-containing plasma [6], in laser ablation of metals in inlet solutions [7]. Under glow discharge conditions, most of the experiments were carried out on palladium using deuterium as the plasma-forming gas. Since the first publications in the 90s, attention has been drawn in almost every publication to the local distribution of impurity elements appearing after the experiments. In particular, it was shown that "hot

"dots" with locally concentrated new elements were revealed, as when scanning on a Hitachi SEM with the "Link Analytical" attachment [8]

by subtracting the spectra of new impurity elements before and the spectra after irradiation in a glow discharge plasma in D, H, Ar+Xe plasma. And it was shown that the maximum effect was achieved using deuterium as a plasma-forming gas, smaller effects by the number of new

impurity elements when using hydrogen and argon with xenon. Therefore, the main data array was obtained for the Pd-D system [9]. In addition, "hot spots" were intensively recorded by radiography methods in ion-irradiated palladium samples and even in the underlying layers of titanium and palladium foils that were not directly subjected to glow discharge ion bombardment [10]. It was also established that artificial radioactivity can be initiated under the influence of low-temperature nonequilibrium plasma flows. This was shown by the change in the blackening density curve of the X-ray film in

depending on the duration of time after the end of the experiment, the existence of hot spots in complex multilayer cathode samples was emphasized both on the directly irradiated surfaces and on the surfaces of underlying Pd and Ti located under the irradiated sample, as well as in zones shielded from the direct impact of bombarding ions. When analyzing the isotopic and elemental composition in the near-surface region of Pd and Ni cathodes, both initial and after 40-hour plasma treatment, changes in the isotopic ratios for impurity isotopes of Pt and Pb in the Pd cathode and Fe, Cu and Zn in the Ni cathode were recorded, as well as a significant reduction in the amount of these impurity elements in the cathodes and the formation of W isotopes in the Pd cathode [11, 12]. In the course of such studies, it was shown that the unusual nature of the very phenomenon of initiation of nuclear-chemical

processes in conditions of low-temperature nonequilibrium plasma is also manifested in the fact that in such processes, in addition to the formation of heavy isotopes, "light" nuclei are also formed. Such anomalies, not manifested during radioactive decays, natural and initiated during interactions with protons or alpha particles, are associated with the formation of a disrupted nucleon structure of nuclear matter, compound nuclei formed in such processes and the subsequent implementation of a kind of "quark-cumulative mechanisms" of the transformations that occur [13].

The main objective of this work, which investigated the effects of low-temperature plasma flows formed in pulsed discharges on W samples in a plasma focus facility, was to establish the capabilities of such facilities for studying the initiation of nuclear-chemical processes, especially since the characteristics of low-temperature plasma in plasma focus facilities and glow discharges differ significantly. In the works cited above, devoted to studies of materials irradiated

with glow discharge plasma ions, the voltage supplied to the electrodes does not exceed 1.5 kV, the current density was 5-150 mA/cm<sup>2</sup>, and in the PF installation the supplied voltage reached 27 kV and the current in a short-term pulse was 350 kA. That is, the temperature and density of the plasma were significantly higher, the pulses were shorter.

The presented study set the task of studying these effects using a new interesting method, both for TN and CN, a method which consists of creating a high-energy beam of high-density charged particles with nanosecond pulses using a plasma focus type installation. [14].

The aim of the work was to study the interaction of the plasma focus discharge in a deuterium medium with a tungsten surface. The analysis was carried out after the impact on the tungsten surface of deuterium plasma with a particle energy of 1 keV in a pulsed mode with a plasma exposure time of particle density  $(2-4) \times 10^{17} - (6-8) \times 10^{18} \text{ cm}^{-3}$  and a pulse duration of about 20 microseconds per pulse for a series of 30 pulses.

Plasma focus generates hard and soft X-rays, plasma flows, produces a shock plasma wave, thermal and neutron radiation.

The capabilities of a specific plasma focus installation PFM72-m are described in detail in [14].

### Plasma Focus Experiment Technique on the PFM72-m installation

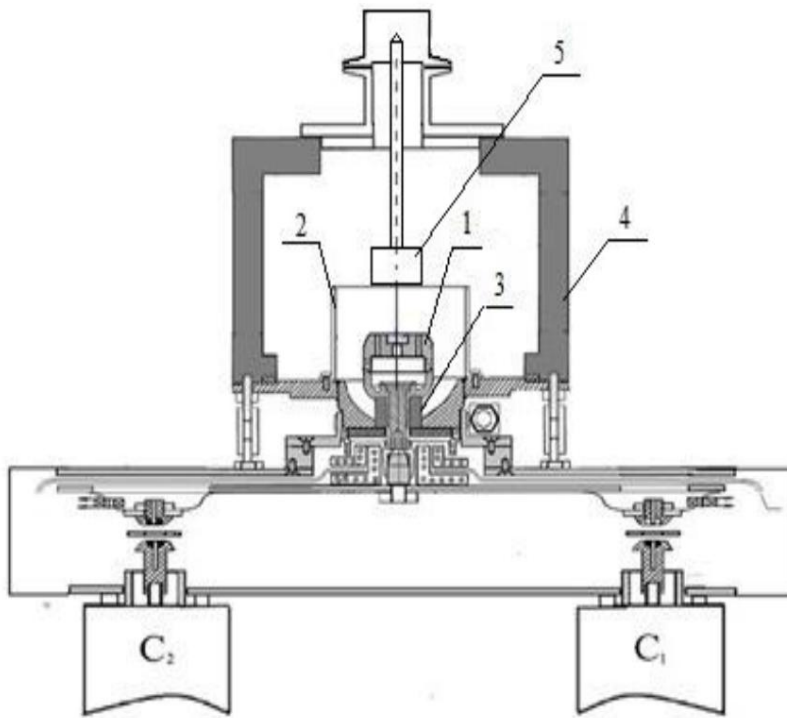
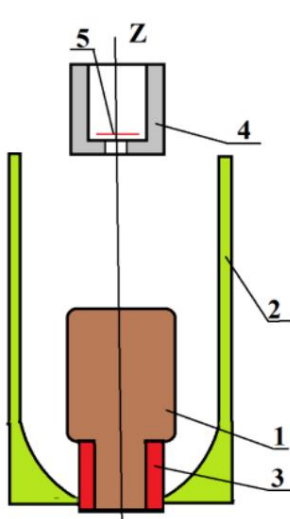


**Fig. 1.** Schematic diagram of the Plasma Focus (PFM 72-m) setup 1-anode, 2-cathode, 3-insulator, 4-vacuum plasma chamber, 5 - sample W single crystal +W foil ~100 μm thick, located under the W single crystal



The diagram shows the arrangement of samples during the irradiation process with deuterium plasma flows; the distance from the cathode – sample to the end of the anode is ~ 50 mm.

**Fig. 2.** Sample arrangement diagram: 1 - Cu anode, 2 - cathode, 3 - Al<sub>2</sub>O<sub>3</sub> insulator, 4 - W single crystal sample, 5 - W sample – polycrystalline foil

The sample made of a tungsten single crystal is a cup (a cylinder with a bottom) with dimensions of diameter  $\ddot{\gamma} = 12$  mm, height  $H = 10$  mm, the thickness of the bottom facing the anode of the plasma focus is ~ 2 mm, the central hole in the bottom of the tungsten sample is

glass is  $\ddot{y} = 2.5$  mm. A tungsten foil with a thickness of  $\sim 100 \mu\text{m}$  was located under the tungsten single crystal and was shielded except for the central zone with a diameter of 2.5 mm under the hole in the tungsten single crystal cathode-cup.

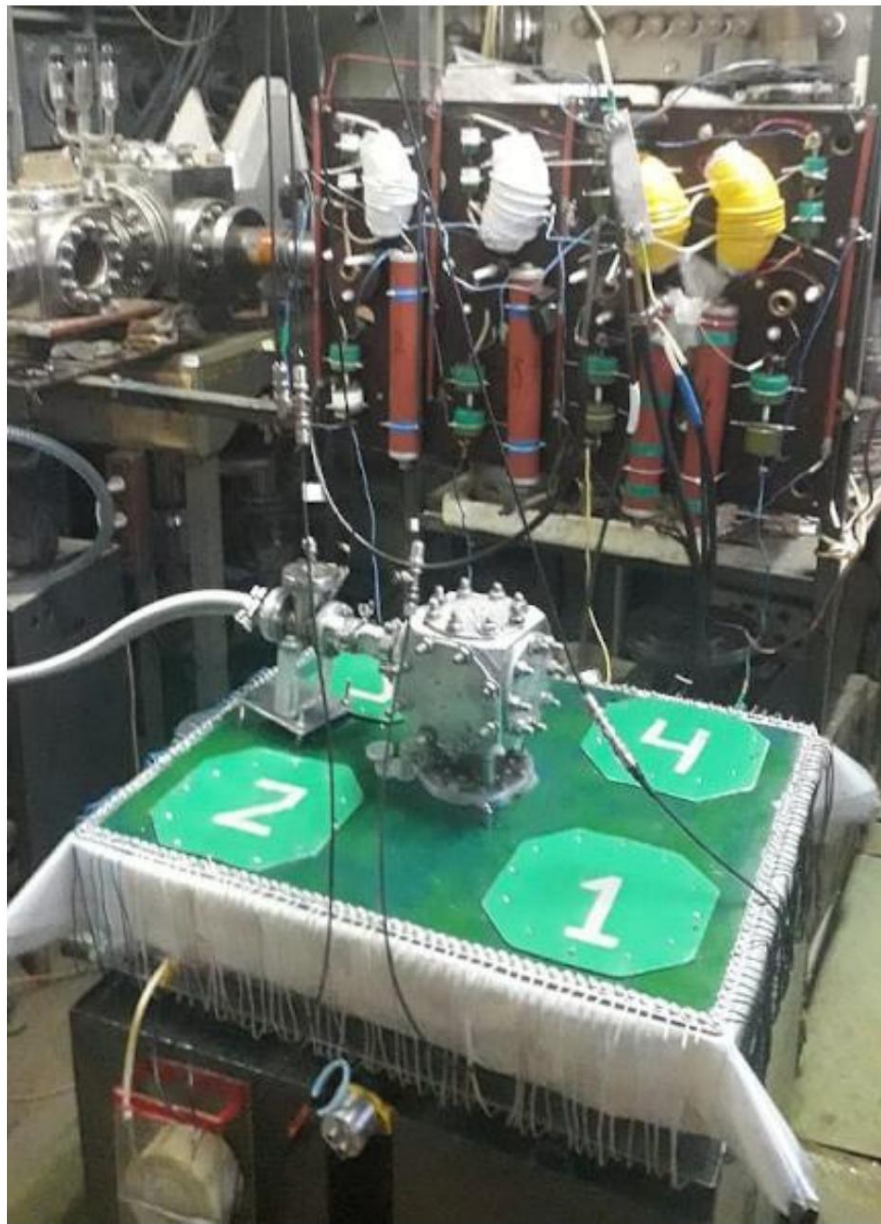


**Fig. 3.** External view of the PFM 72-m installation

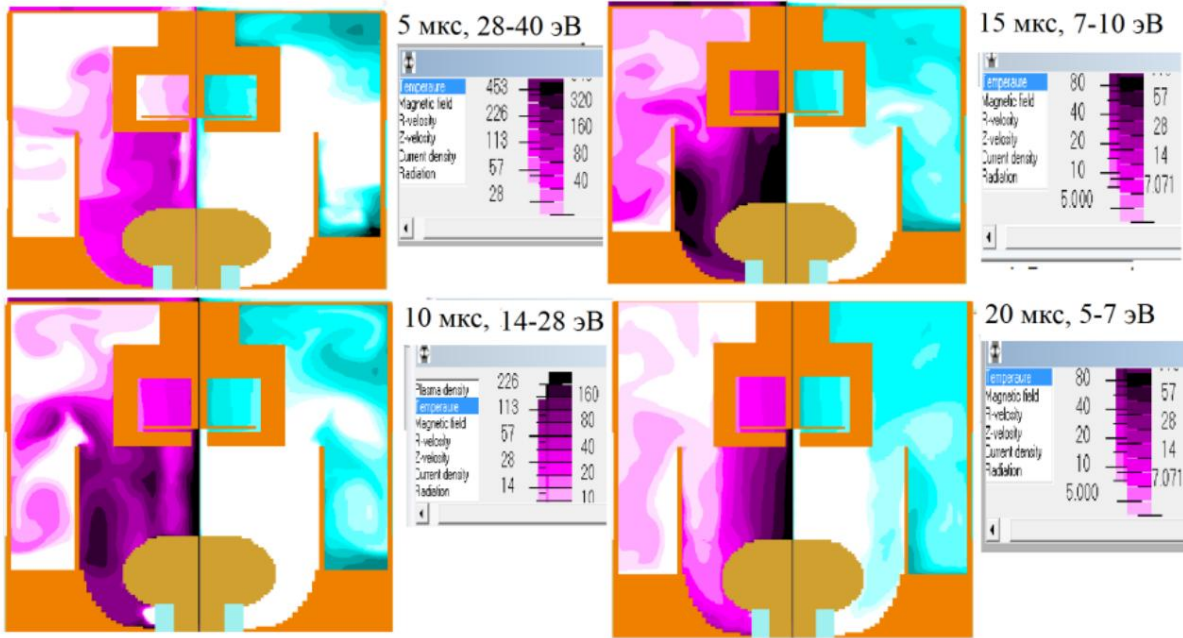


**Fig. 4.** Plasma movement to the tungsten target-cathode during the pulse process according to the ideal model of V.V. Vikhrev.

1. t = 5  $\mu$ s, 28 - 40 eV, 2. t = 10  $\mu$ s, 14 - 28 eV, 3. t = 15  $\mu$ s, 7-10 eV, 4. t = 20  $\mu$ s, 5-7 eV (on the right - plasma temperature - eV)

Fig. 4 shows schematically the movement - propagation of plasma from the anode to the cathode according to the MHD PF model of V.V. Vikhrev [15] with samples located on the cathode 5 - foil and 4 - tungsten single-crystal cup with a hole in the center, through which plasma with a density of  $(2 - 4) \times 10^{17} \text{ cm}^{-3}$

spreads into the interior of the tungsten cup and covers the tungsten foil with a stream of particles, lifting it. As a result, the plasma in the central part of the foil, as in the tungsten single crystal, has a higher particle density and energy, and at the periphery of the PF, energy is lost. Energy is also lost inside the tungsten cathode as a result of reflections between the bottom of the W single crystal and the W polycrystalline foil.

### Deuterium plasma flow irradiation mode

The plasma chamber was evacuated to a residual pressure of  $5 \times 10^{-6}$  Torr, then filled with plasma-forming gas – deuterium to a pressure of 5-7 Torr. For the plasma focus creation modes used in the experiment,

The spectrum of hard X-ray radiation (HXR) reaches 1 MeV [14]. There are 4-6 orders of magnitude fewer high-energy electrons than low-energy ones.

The maximum neutron yield ( $Y_n$ ) at a current of 360 kA was  $\sim 4 \times 10^7$  n per pulse [14]. The duration of the neutron pulse and HXR was about  $\sim 20$  nanoseconds per pulse. The duration of each pulse of irradiation with plasma flows was 20 microseconds,

- 1st series of pulses - 20 pulses Ucharge=26 kV, I<sub>max</sub> = 345 kA, Y<sub>n</sub> <106 n/imp.
- 2nd series of pulses - 5 pulses with the same parameters.
- 3rd series of pulses - 5 pulses Ucharge=27 kV, I<sub>max</sub> = 360 kA, 107 <Y<sub>n</sub> <4·107 n/imp. It should be noted that the number of neutrons in a pulse hitting the samples is relatively small (does not exceed 1000 neutrons for foil and 20,000 for a single crystal for the entire irradiation time [14]), therefore this value can be neglected for the processes of fusion-decay.

It should be emphasized that the foil W, when interacting with the flow of charged deuterium particles in the region of formation of the plasma focus on the axis of the installation, in the center of the sample was subjected through the hole in the single crystal to practically the same effect in terms of energy and flux density of deuterium plasma as the single crystal W. And the area of the foil in the zone shielded from the direct impact of the flow was exposed to plasma with significantly lower density and energy.

Ions propagating along the Z axis of the plasma focus (PF) setup have an energy of up to 300 keV [14], while the peripheral plasma has a significantly lower particle energy (D+, D0 D-, , D\*) from 1 keV to units of eV, i.e. there is a possibility for low-energy nuclear chemical reactions to occur.

During the SIMS (secondary ion mass spectrometry) studies it was found that the maximum effects were observed in the cold plasma region located in the peripheral part of the samples at a distance of 5 - 10 mm from the plasma focus axis.

### **Tungsten structure after pulsed plasma focus action**

Surface structure of a tungsten single crystal after plasma focusing in deuterium when examined under an optical microscope is shown in Fig. 5.

In the photo in Fig. 5a, one can see the surface structure of single-crystal tungsten, close to the central part of the plasma focus, with clearly defined decorated grain subboundaries, where the maximum energy and particle density, and, accordingly, temperature, were in the center of the plasma focus. In Fig. 5b and Fig. 5c, the particle energy and thermal conditions have already changed, so we see a structure with solidified molten tungsten droplets, and in Fig. 5d, on the structure remote from the center of the PF, there are already "ejected" from the central and near-central parts of the formation, solidified and settled in "flight" on the peripheral part of the formation. In Fig. 5e - Fig. 5g, directed radial emissions are illustrated in the peripheral and boundary areas

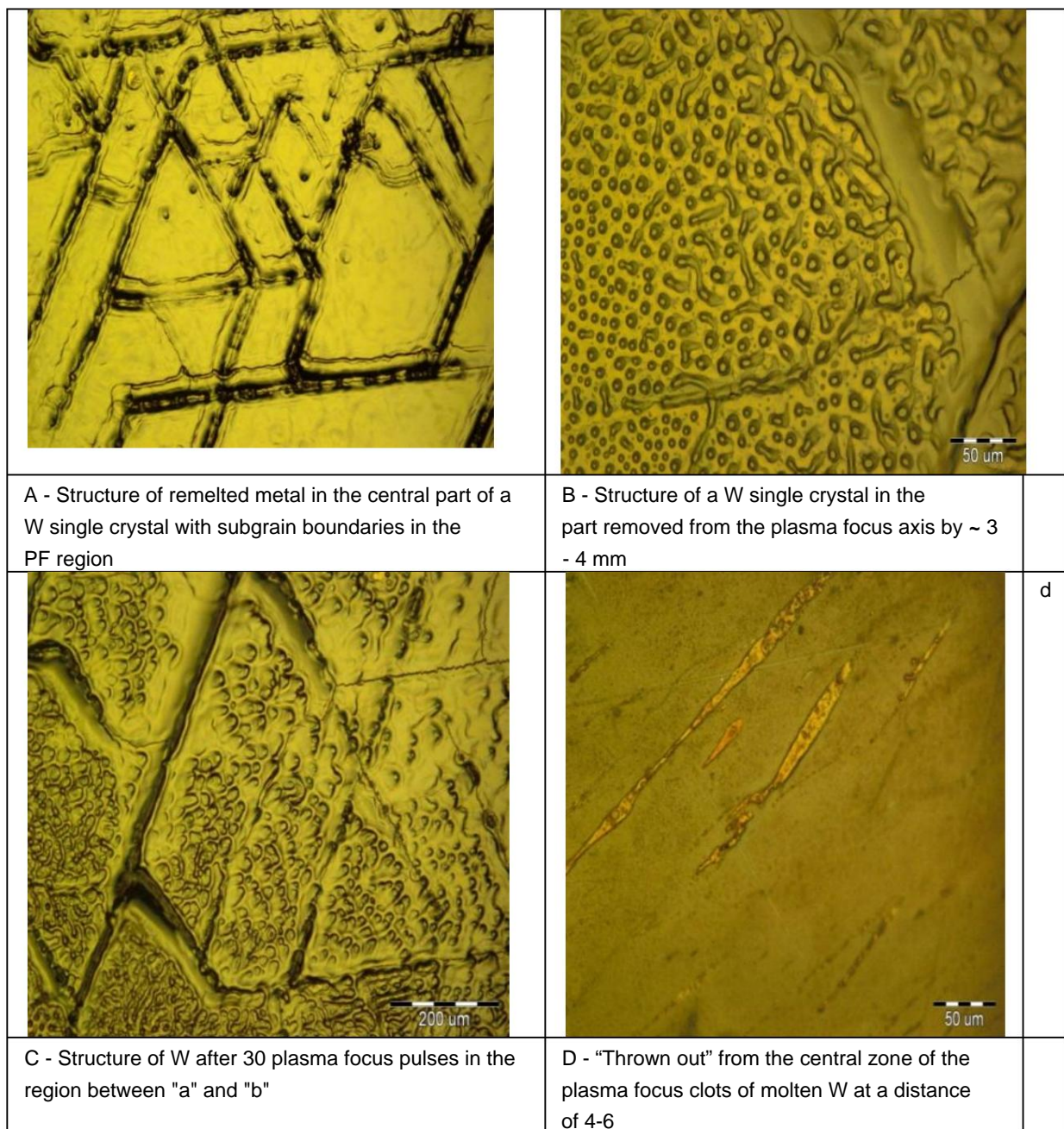
with the PF. One can also note the appearance of traces of particles with chaotic movement - Fig. 5e and spiral traces of movement -

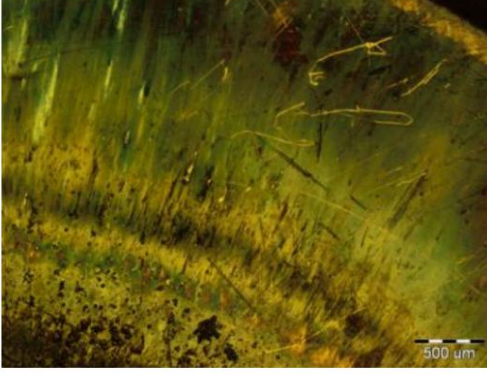
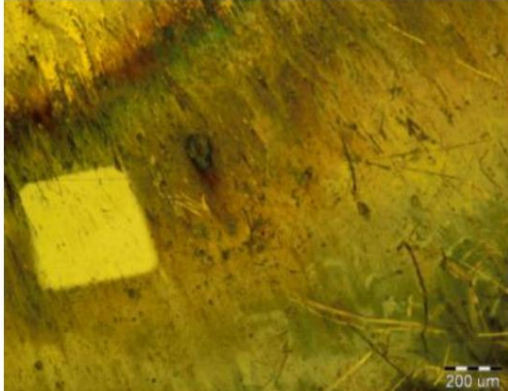
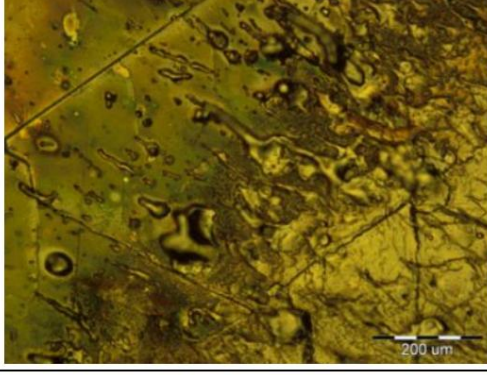
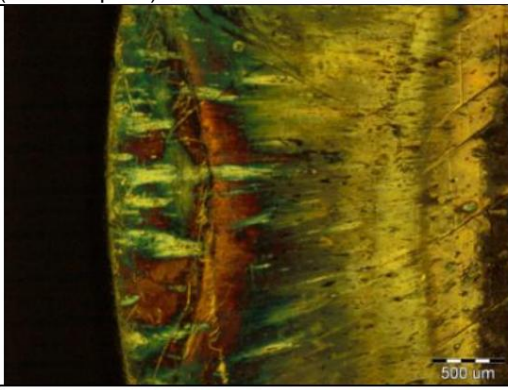
Fig.5g in the peripheral area.

The presented photographs of the structure of the samples analyzed by the SIMS method show why the quantitative data for the same zones of the samples differ. It is clear that structural changes of the macroscopic scale have a very significant effect. Thus, in Fig. 5d, the analysis was carried out in the area without pronounced structural macroeffects. Other places for SIMS analysis were also selected.

The structure of the central part differs from the peripheral part due to different physical processes of plasma interaction with the surface (Fig. 5). High-energy electrons, due to the structure of magnetic fields, propagate along the Z axis of the setup and lose energy interacting with W atoms. And tungsten is located both in the anode insert on the end of the anode and on the sample-cathode. Figure 4 explains the difference in temperature effects depending on the distance from the setup axis.

**Fig. 5.** Surface structure of a single-crystal W sample after exposure to plasma focus in deuterium



	mm from PF axis	
		
E - Surface structure of a single-crystal W sample after exposure to a plasma focus in deuterium at a periphery of 5-6 mm from the PF axis.	F - Light square spot - scanning zone of SIMS analysis on a surface relatively clean from molten metal emissions  (150x150 $\mu\text{m}^2$ )	
		
G – boundary with characteristic emissions from the PF region	H-periphery with characteristic emissions on the left and a pronounced structure of a single crystal on the right	
		
I - peripheral zone with directed radial emissions of matter from the central zone of the PF and traces of chaotic motion of particles	G- peripheral directed zone with radial emissions of matter from the central zone of the PF and spiral motion of particles  traces	

### **Methodology of VIMS research**

The analysis of the surfaces of single-crystal tungsten and polycrystalline tungsten foil was carried out by secondary ion mass spectrometry (SIMS) on a TOF.SIMS 5 mass spectrometer.

The TOF.SIMS 5 secondary ion mass spectrometer provides detailed information on the isotopic, elemental and molecular composition of the surface and near-surface layers of the sample. SIMS analysis was performed by bombardment with 30 keV Bi<sup>3+</sup> ions and etching the samples with a 2 keV Cs ion beam, which ensured measurement of depth profiles.

The measurement of the number of knocked out secondary ions was carried out in positively charged secondary ions. The counting time in pulses per second was 400 seconds for each scan.

The surface scanning was performed in the central and peripheral parts exposed to the plasma focus of the W single crystal and the polycrystalline foil partially located under the W single crystal.

### **Results of the VIMS studies**

The results of mass spectrometric analysis of the surfaces of single-crystal tungsten and polycrystalline tungsten foil obtained at SIMS after exposure to deuterium plasma flows in the plasma focus are presented.

During the research it was discovered that the maximum effects of increasing the concentration of elements that are "light" relative to the main matrix material of tungsten were observed in the area of "spreading" cold plasma located in the peripheral part of the samples (at a distance of 5–6 mm from the axis).

An increase in the concentration of light elements with a mass less than the mass of the matrix material of the W sample (Li, Na, K, Ca, Mg) in the shielded and peripheral areas of the monocrystalline and polycrystalline tungsten samples by 5 to 100 times for various elements was detected. Moreover, in the peripheral and shielded areas of the analyzed samples, up to millions of pulses (ions) are recorded compared to thousands in the central area. That is, a significant increase in the concentration of "light" isotopes is observed in areas remote from the axis of the installation, where their sputtering either does not occur at all, or the "ejection" by the shock plasma wave is less, or a process of multiple reflection with re-sputtering of the resulting light elements occurs.

Spectra of individual elements on the surface of a single crystal of W and polycrystalline foil W, recorded by SIMS, are shown in Figure 6.

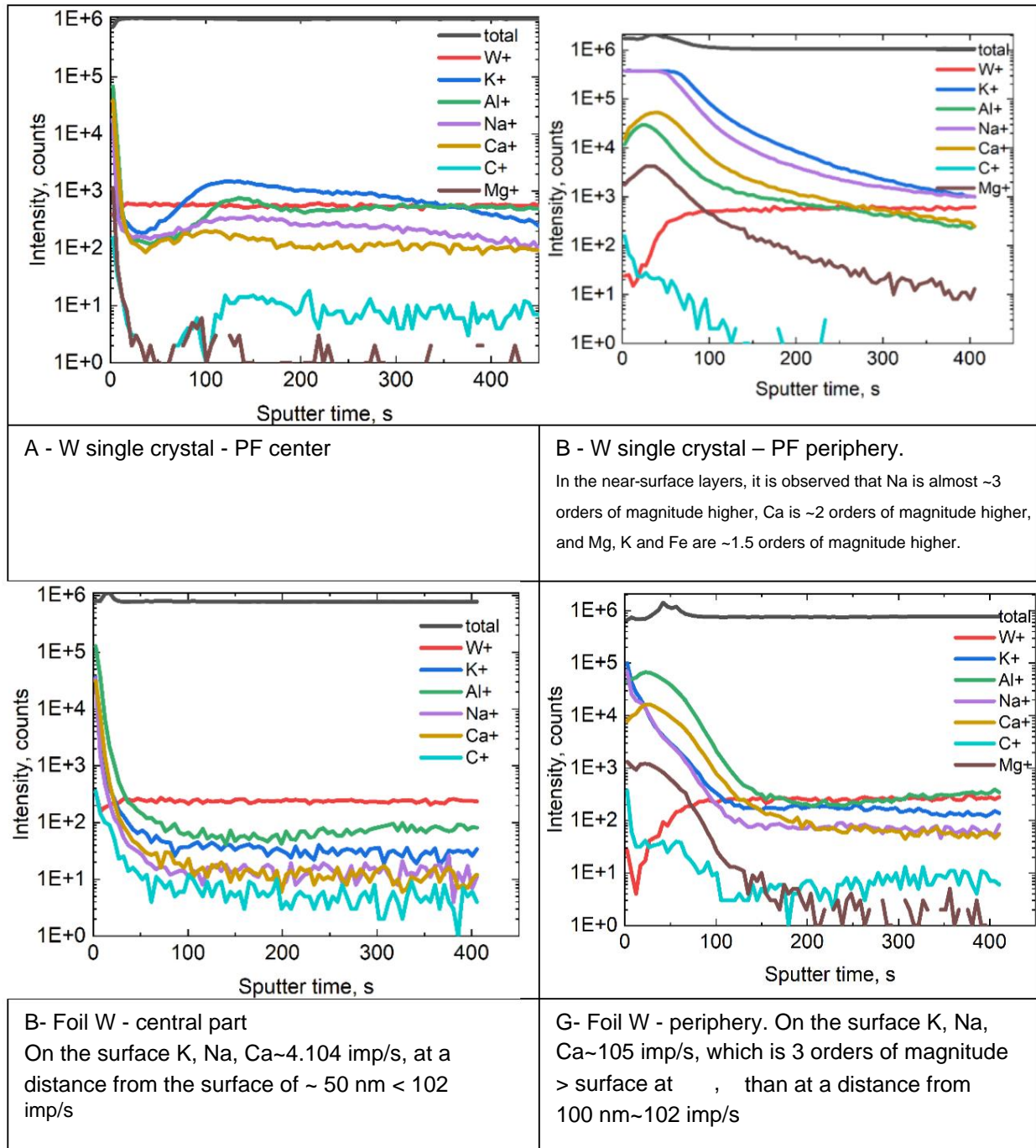


**Fig. 6.** Spectra of individual elements on the surface of a W single crystal and a W polycrystal foil, recorded by SIMS

**Table 1** "Light" elements in W single crystal and polycrystalline foil after plasma focus in deuterium

Element m/z	W1	mono center	W2 mono center	W mono Edge 1	Wmon o Edge 2	W foil Center 1	W foil Edge 1	W foil Edge 2
1	2	3	4	5	6	7	8	9
N	0.99	1186	1020	5040 16	924	545	7124	2565
Li6 7.5% 6.07	278		228	1359 15	43	263	6876	379
Li7 92.5% 6.95		763	1322	<u>13</u> <u>362</u>	<u>14</u> 754	1190	<u>75</u> 482	3066
C12	11.96	1003	2098	798	1704	1407	2159	1454
O16	16.04	478	680	3533 62	74	362	4 389	1 103
Na23	22.99 39	297 49	986	5 641 388 3 547	031	38 713 4 252	542 194 540	
Mg 26	26.01	692	1 315	7 973 1	072	782	4 382	2 398
K39 93.3% 12	39.88	545 69,289	7,035,144		5 530286	43231 6 855	759 264 414	
Ca40 97% 39.89	53 873	192 033 72	32	72	1 522747	42 392 381	152	178 970
K41 6.7% 41	405 11,095	7,431 1,006			439819	5702	548 696	22 829
Ca44 2% 43	82 4 498		4 681	19 011	34 274	1 833	10 132	4 929
2 Na23 46	45.85	1675	421	51 104	10 253	575	18787	771

Table 1 presents the results of mass spectrometric analysis obtained on SIMS after exposure to deuterium plasma flows in digital format. Column 1 is the analyzed isotope, column 2 is the

mass of this isotope, columns 3-6 are the number of registered ions is 3-6 for a tungsten single crystal and 7-9 for a polycrystalline foil. Columns 3-4 are for the central part of the single crystal, 5-6 are for the peripheral zone. Column 7 is for the central part of the foil, and columns 8 and 9 are for the peripheral shielded part of the foil. As can be seen, the increase in the concentration of light elements with a mass less than the mass of the matrix material of the sample W (Li, Na, K, Ca, Mg) in the shielded and peripheral areas of the samples of monocrystalline and polycrystalline tungsten is from 5 to 100 times for various elements. Moreover, in the peripheral and shielded areas of the analyzed samples, up to millions of pulses (ions) are recorded compared to thousands in the central area. That is, a significant increase in the concentration of "light" isotopes is observed in areas remote from the axis

installations where their dispersion and "ejection" by a shock plasma wave is less or does not occur at all.

For the material of the Cu and Al structural elements, such an effect is not observed. Changes in their content in the samples in the center of the plasma focus and on the periphery, and in the shielded zone either do not change, or change several times, and not tens and hundreds of times. And the isotopic ratios for structural materials also remain unchanged.

## Discussion

### Facts to note:

1. Li7 up to 15,000 pulses (ions) per second in a W single crystal and up to 75,000 pulses (ions) per second in a tungsten foil in a zone remote from the center of the plasma focus - peripheral and "shielded" at the edges of W samples 5 times more.
2. Na - at the center of the plasma focus, ~ 40 - 50 thousand pulses are recorded at the center W of the single crystal and foil, and at the periphery of the single crystal and in the shielded zone of the foil ~ 3 - 5 million pulses, i.e. > ~ 75 - 100 times.
3. A similar result is observed for K: in the center of the W single crystal samples, the content of potassium K39 is tens of thousands of pulses ~ 70 - ~ 90 thousand, and in the peripheral areas by ~ 5 - 7 million pulses, i.e. ~ 100 times more, for the W foil the result of comparing the central zone of the plasma focus and the periphery is repeated. For K41, the multiplicity of increase in the content of this isotope in the zone remote from the center is also preserved. Potassium is absent in the design elements!!! But on the SIMS, millions of pulses (ions) per second are recorded!!! The natural ratio K39/K41 = 14; for Wmono

---

at the edge of the sample = 7 and 12.5; in the center of the sample = 8 and 9.3; in the foil 12.5. Perhaps the lighter isotope K39 is "carried out" by the plasma shock wave. The appearance of potassium must be understood and explained.

4. For the isotope Ca40 in the center of the PF action the intensity of the ion number registration was (~ 50 - ~ 19) thousand pulses, and at the periphery from ~ 700 thousand pulses to ~ 1.5 million pulses (~ 30 - 35 times more). For the isotope Ca44 (2%) the increase in content was observed in ~ 5.
5. Mg - changes in the analysis zones by ~3-5 times, the content of this element recorded during the analysis is ~50 times less than Na, and in ceramic insulators - structural elements, the content of Mg is 6 times greater than Na. That is, it is impossible to explain the appearance of magnesium by the spraying of the element from structural parts.
6. At the edges of the samples of single-crystal W and W foil in the "shielded" zone at the periphery of the plasma focus, 10 - 20 - 100 times more "lighter" elements appear than at the center of the focus. That is, either they are also formed, but are less sprayed and "thrown out", or the energy conditions in these peripheral areas are more favorable for their formation.
7. With Al and Cu, which are elements of the design, such an effect is not observed (either we have no difference at all in the content of these elements along the edge and center of the foil, or we have a difference of several times, but not tens and hundreds of times, as for Li and Na).

8. Si 28 – the content of this isotope in the foil after plasma focus is 2-5 times less in the foil at the periphery, and in the center there are similar values in the single crystal and polycrystalline foil.

When analyzing tungsten after plasma focus exposure using the SIMS method, various complexes are detected along with the elements with masses less than the mass of the matrix element. In particular, these are the WO, **WO<sub>2</sub>**, WCs complexes, the totality of which should be taken into account when determining the value of "Total W", as well as some other CsZn, 2Na complexes that were successfully recorded and understood. The constancy of the isotopic ratios of the measured isotope intensities for the main matrix elements and their complexes (WCs, 2CsCu) indicates the reliability of the measurements.

**Table 2.** Ratio of measured intensities of WCs complexes

Complex	nature no	Wmono center1	Wmono center2	Wmono Edge 1	Wmono Edge 2	W foil center 1	W foil edge 1	W foil edge 2	Average meaning
<sup>182</sup> W <sup>133</sup> Cs	1.80	1.80		1.82	1.82	1.84	1.82	1.84	1.82±0.02
<sup>183</sup> W <sup>133</sup> Cs	1	1		1	1	1	1	1	1
<sup>184</sup> W <sup>133</sup> Cs	2.15	2.12		2.11	2.11	2.13	2.13	2.12	2.12±0.01
<sup>186</sup> W <sup>133</sup> Cs	2	1.97		1.96	1.96	1.99	1.98	1.97	1.974±

\* W complex      Cs taken as 1

**Table 3.** Ratio of measured intensities of 2CsCu63 and 2CsCu65 complexes

Mass Complex	m/z	W mono center1	W mono center2	W mono Edge 1	W mono Edge 2	W foil center 1	W foil Edge 1	W foil Edge 2
2CsCu63	329 36351		36930	130117 155235		22725 40264		148834
2CsCu65	331 18071		17394	60260	70526	11338 19097		67755
2CsCu63/ 2CsCu65		2.01	2.12	2.15	2.20	2.00	2.10	2.19

The diagnostics of changes in the composition of the tungsten surface under the influence of the "plasma focus" using the SIMS method indicate a variety of nuclear-chemical processes that are predominantly initiated in areas with reduced Ee kinetic energy of electrons (we assume ~ Ee < 10 eV) [1-3]. Possible nuclear-chemical processes that explain the phenomena under study are considered in detail in [11, 12, 13].

## Conclusion

1. Plasma focus as a method of matter transformation can be included in the scope of LENR interests, since under plasma focus conditions there is room for low-energy nuclear-chemical reactions.
2. The main result of this work is the confirmation of the basic idea [11, 12, 13] about the determining role of nonequilibrium electrons with kinetic energy  $E_e \sim 3\text{-}5 \text{ eV}$  in the initiation of non-nucleon metastable excitations of nuclear matter during the interaction of electrons with the base nuclei of low-temperature plasma and the atomic nuclei of the metal cathode. Electrons of high kinetic energies mainly lose their energy to the ionization of atoms of the walls of the working chambers.
3. We believe that the recorded increase in the content of light atoms is a consequence of possible nuclear-chemical reactions [11, 12, 13], initiated by the action of pulsed plasma flows on the cathode of the plasma focus installation. To specify such processes and compile a set of possible nuclear-chemical processes, subsequent studies are required to establish nuclei of heavier masses formed in the processes under study.

## Literature

1. *Trilochan Gadly, Suhas Phapale, Sunita Gamre et al.* Experimental and theoretical validation for transmutation of palladium at electrochemical interfaces. *Scientific Reports.* 2024 Sep 11;14(1):21270.
2. *Fomitchev-Zamilov M.* Observation of Neutron Emission During Acoustic Cavitation of Deuterated Titanium Powder // *Scientific Reports.* 2024. V. 14. Article paper 11517
3. *Pines V., Pines M., Chait A. et al.* Nuclear Fusion Reactions in Deuterated Metals. *Phys. Rev. C.* 2020. V. 101. P. 044609.
4. *Schenkel T., Persaud A., Wang H. et al.* Investigation of Light Ion Fusion Reactions with Plasma Discharges. *J. Appl. Phys.* 2019. V. 126. P. 203302.
5. *Vysotsky V.I., Kornilova A.A., Vysotsky M.V.* Features and mechanisms generation of neutrons and other particles in the first laser experiments synthesis. *JETP.* 2020. T. 158, No. 4. pp. 645–651.
6. *Karabut AB, Kucherov Ya.R., Savvatimova IB* "Nuclear product ratio for glow discharge in deuterium". *Physics Letters A.* 170, 265-272 (1992).
7. *Savvatimova, Ya. Kucherov, and A. Karabut,* Cathode Material Change after Deuterium Glow Discharge Experiments // *Transaction of Fusion Technology* 26, 4T, 389 (1994); *Savvatimova I., Kucherov Y. and A. Karabut // Proc. ICCF4 3, (1993), p 169* [www.lenr-canr.org/acrobat/EPRproceedingb.pdf](http://www.lenr-canr.org/acrobat/EPRproceedingb.pdf)
8. *Barmina EV, Timashev SF, Shafeev GA* Laser-Induced Synthesis and Decay of Tritium under Exposure of Solid Targets in Heavy Water // *J. Phys.: Conf. Ser.* 2016. V. 688. P. 012106; [http://arxiv.org/abs/1306.0830\[physics.gen-ph\]](http://arxiv.org/abs/1306.0830[physics.gen-ph]).
9. *I. Savvatimova, A. Senchukov, and I. Chernov, ICCF6*, Progress in new hydrogen energy. Japan (1996), p. 575.
10. *Savvatimova I.B., Karabut A.B.* Radioactivity of palladium cathodes after irradiation in a glow discharge// *Surface.* 1996. No. 1. P. 76–84.

11. S.F. Timashev, I.B. Savvatimova, S.S. Poteshev, S.M. Ryndya, N.I. Kargin. Physics of elementary particles and atomic nuclei. 2022, Vol. 53. Issue 1, p. 110.
12. S. F. Timashev, I. B. Savvatimova, S. S. Poteshev, S. M. Ryndya, N. I. Kargin. Initiation of artificial radioactivity of impurity elements in a lead cathode under glow discharge conditions. J. Phys. Chemistry, 2023, v. 97, no. 7, pp. 915-924
13. Timashev SF Non-Nucleon Metastable Excitations in Nuclear Matter and e- Catalysis As a Quark-Cumulative Mechanism for Initiating Low-Energy Nuclear Chemical Processes: Phenomenology. Russ. J. Phys. Chem. A, 2024. Vol. 98, No. 6, pp. 1147–1152; ArXiv\_2406.10293v1.
14. Bashutin O.A., Sidorov P.P., Kozlovsky K.I., Salakhutdinov G.Kh. Radiative characteristics of the plasma focus PFM-72m // In the book: Laser, plasma research and technologies LaPlas-2024. Collection of scientific papers of the X International Conference. Moscow, 2024. P. 204.
15. Vikhrev V.V. // Journal of Plasma Physics. 1977. Vol. 3. P. 981

## **Low-Energy Nuclear Reactions in Tungsten on the Plasma Focus PFm72-M Equipment**

Savvatimova IB, Klochkov AN, Sidorov PP, Bashutin OA  
National Research Nuclear University MEPhI

The paper presents the results of mass spectrometric analysis obtained at SIMS after the action of deuterium plasma flows in a PFM72-m plasma focus (PF) facility on samples of single-crystal tungsten and polycrystalline tungsten foil.

A significant increase in the concentration of "light" elements with a mass less than the mass of the matrix material W (Li, Na, K, Ca, Mg) was detected in the zone of direct PF action, as well as in the shielded and peripheral areas of single-crystal and polycrystalline tungsten samples by 5 to 100 times for various elements.

Moreover, in the peripheral and shielded areas of the analyzed samples, remote from the plasma focus axis, up to millions of pulses (ions) are recorded compared to thousands in the central area of the PF. That is, a significant increase in the concentration of "light" isotopes is observed in areas remote from the axis of the installation, where their dispersion and "ejection" by the shock plasma wave is less or does not occur at all, and where the energy of the particles ranges from units to tens of electron volts and various nuclear-chemical reactions can occur.

## Main results obtained at the PVR-V water reactor in the period from 2022 to 2024

A.I. Klimov, S.E. Altunin, O.M. Kulakovskiy

<sup>1</sup> Scientific and technical center "Prometheus", Bryansk

[klimov.anatoly@gmail.com](mailto:klimov.anatoly@gmail.com)

Our team has created a number of plasmoid vortex reactors (PVR) based on LENR in heterogeneous working mixtures: argon + water vapor and water vortex flow [1-3]. The created PVR reactors allow obtaining excess thermal energy of the order of 1-3 kW, several times exceeding the consumed electrical energy spent on the creation of heterogeneous plasma in the reactor. In addition, the specific energy released in LENR reaches 1-10 keV/atom of hydrogen (or metal). This work is a continuation of the above-mentioned works [1-3].

### Introduction

The history of the development of plasmoid vortex reactors (PVR) began quite a long time ago at the Joint Institute for High Temperatures of the Russian Academy of Sciences, at least 40 years ago. Let us recall that in studies on plasma aerodynamics (PA) it was shown that the experimentally discovered features of the dynamics and structure of the shock wave (SW) in a weakly ionized nonequilibrium plasma (WNP) can be explained within the framework of a physical model of possible *detonation processes and the release of significant additional energy behind the shock wave front in such a medium* [1, 2]. In the language of modern LENR physics, in order to clarify the physical features of the SW in WNP, it would be necessary to introduce the parameter of energy efficiency SOR (the ratio of the released energy behind the SW to the electrical energy spent on creating a pulsed discharge). It was shown that in the aforementioned PA experiments, the maximum value of SOR reached the order of **SOR = 4** [1, 2]. Therefore, the physical mechanism of such a significant release of energy behind the SW front in WNP had to be sought *in the change in the internal energy of the gas excited by the electric discharge*

*and passed through the shock wave front.* Therefore, plasma technologies were used as the basis for the design of the PVR reactor.

Further, in our studies on PA, the problem of interaction of the SNP with a vortex gas flow was studied in detail. Important results were obtained on the generation of a stable extended heterogeneous plasmoid in a vortex flow, the electric discharge plasma spontaneously concentrated in the axial region of the vortex and was significantly heated. This vortex plasmoid was simultaneously a trap for nano-cluster metal particles (the result of electrode erosion). Note that the first mentioned property of the vortex plasmoid made it possible to solve the problem of thermal insulation of hot plasma from the reactor walls, and the second property made it possible to increase the efficiency of the interaction of hydrogen atoms and ions with

nano-clusters of metals on its axis. It is these properties of vortex plasmoids that made it possible to use them in the creation of highly efficient PVR designs.

## Main experimental results

A number of heterogeneous plasmoid vortex reactors *PVR-G with a working gas flow* and *PVR-V with a working water flow* were created at the Prometheus Scientific and Technical Center , Figure 1, [2, 3]. Typical values of the energy conversion coefficient COP in the PVR reactor are 2 - 6 (the ratio of the output excess thermal energy of the heterogeneous plasma flow to the electrical energy expended in its creation).

Simultaneously, calibration experiments were conducted with two types of PVR using an electric heater. It was found that the value of heat losses in the PVR is **K<sub>p</sub> = 0.6- 0.8**. The value of K<sub>p</sub> was determined as the ratio of the thermal power of the working gas (water) flow in the reactor to the electric power spent on heating the electric heater. It was shown that the main heat losses in the reactor were associated with heating the PVR structural elements with hot heterogeneous plasma. Note that the results of measuring the COP value in the PVR-G and PVR-V reactors are reliable. Various

*independent diagnostic methods* were used to measure the output thermal power from the PVR (including contact and non-contact calorimetric methods:

- a method of gas (water) calorimetry using thermocouples and simultaneous measurement of the flow rate of the working gas (water),
- use of an outlet water heat exchanger in a gas PVR,
- measurement of temperature fields in a heterogeneous plasma flow at the outlet of the PVR-G reactor nozzle using a non-contact optical interferometry method,
- measurement of the temperature field in the heterogeneous plasma flow at the outlet of the reactor nozzle PVR-G using non-contact optical spectroscopy method,
- measurement of the temperature field in the heterogeneous plasma flow at the outlet of the reactor nozzle PVR-G using the optical pyrometry method,

It is important to note that each of the above methods additionally measured the velocity field in the heterogeneous plasma flow using the PIV method. It was shown that the COP values measured using the above methods were close to each other, with an accuracy of up to 15%.

Hence, a conclusion was made about the reliability of the experimental results obtained using the above methods. The optimal gas flow modes in the reactor in which the

stable combustion of a pulse-periodic discharge in it.

Experimental dependences of the COR value on the gas flow rate, composition of the working gas mixture, and the swirl parameter of the swirling flow were obtained. The role of cold gas suction from the atmosphere when the hot vortex flow exits the reactor outlet nozzle and its effect on the COR parameter were studied.

In this paper we will consider in detail the latest experimental results obtained on *the water PVR-V*. On the physics of the water PVR-V operation and

gas PVR-G differ significantly. This device has accumulated all the positive reserves previously obtained during the creation of PVR-G reactors. In the PVR-V reactor, many technical difficulties identified during the operation of previous PVR-G with a working gas environment were overcome. In the water PVR-V, a denser working environment is used - a water vortex flow. The most important distinguishing feature of the PVR-V from

the PVR-G is the following: - the presence and location of the water heat exchanger near the zone of the electric discharge itself. As our previous studies have shown, the value of the energy efficiency coefficient SOR significantly drops in the heterogeneous plasma flow after it leaves the PVR nozzle due to recombination processes in the heterogeneous plasma itself (the process of evaporation - disintegration of charged water clusters during their neutralization) and the suction of cold air from the atmosphere. Therefore, the decision to use the working water flow simultaneously as a working fluid and a heat exchanger is important and necessary. The PVR-V reactor is described in detail in [3].

The PVR-V reactor is described in detail in [3]. In the gas cavity of the water vortex in the PVR-V reactor, water molecules are evaporated by a powerful pulsed current. The pressure in the steam cavity can reach tens and even hundreds of bars. Such hydraulic shocks are easily measured by a hydrophone. Therefore, the working medium in the steam-gas cavity is dense. It is known that the productivity of any plasma-chemical reactor increases significantly with an increase in the density of the working medium (or its pressure), as well as its heating (an increase in the temperature of the working medium). Direct measurements of the temperature in the heterogeneous plasma in the PVR-V using the optical spectroscopy method convincingly prove this position. Let us recall that the typical temperature in the PVR-G reached 3000-4000K, [2]. The temperature value in the heterogeneous plasma in the PVR-V reactor can reach 10000K (see below). Therefore, the productivity of transmuted elements and hydrogen in a dense working water medium increased significantly (see below). In addition, the PVR-V reactor has a *closed water circuit*. In such a circuit, additional production and accumulation of transmuted chemical elements occurs. At the same time, their concentration in the plasma gap increases significantly, which allows switching to a weak electrode erosion mode (weaker discharge current mode) after reactor acceleration. This result allowed us to increase the service life of the electrodes in the reactor without replacing them.

However, the PVR-V reactor has a weak point - *the presence of electrolysis in water* in the pre-breakdown period during charging of the storage capacity of the modulator C, (Fig. 1). As a result, the integral energy efficiency of the SOR reactor is significantly reduced. However, this technical difficulty has been successfully overcome at present.

The PVR-V circuit is shown in Fig. 1. The experiment uses a stabilized DC source with an output voltage of UDC = 8 kV and a maximum current of IDC = 2 A. An LC circuit with variable parameters is mounted in front of the discharge gap. The circuit parameters varied within the range: L = 20-200  $\mu$ H, C = 0.01-0.1  $\mu$ F. The oscillatory circuit allowed

implement a relaxation oscillation mode on the discharge gap with frequencies of 100-10000 kHz.

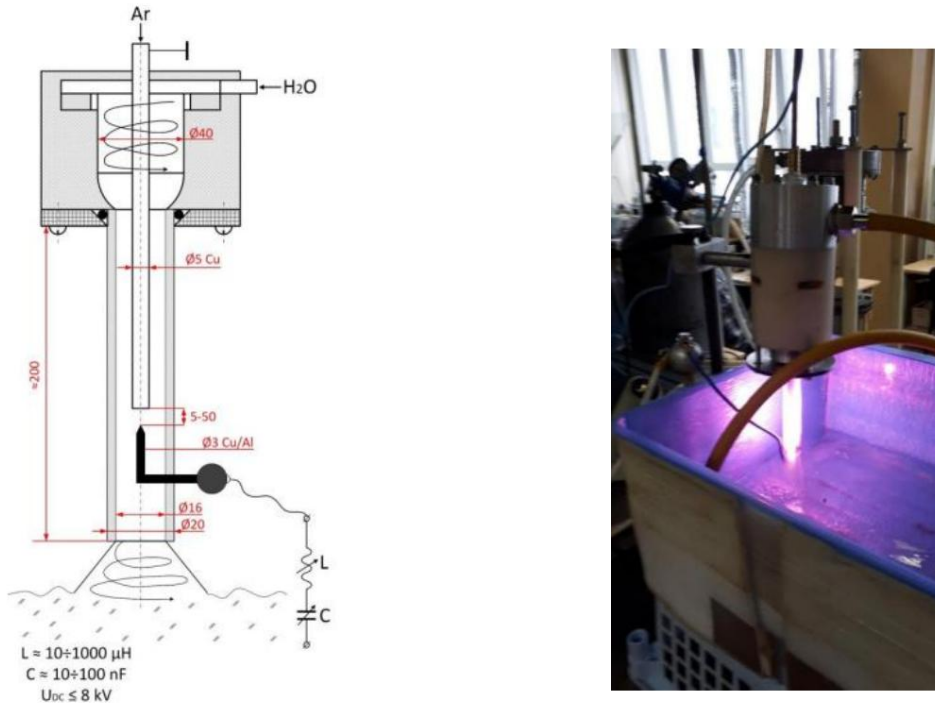


**Fig. 1.** The PVR-V installation diagram and the LC circuit - modulator used in its power supply (left). General view of the PVR-V (right)

Electrical parameters (current, voltage), as well as electrical power and energy on the discharge gap are measured using calibrated high-voltage probes (Tektronix P-6015) and current probes (TRCP0300). The temperature in the pool is measured before the experiment  $T_n$  and after it is carried out  $T_k$ . The mass of distilled water poured into the pool  $MH_2O$  was measured at the beginning and end of the experiment.

Typical results obtained in the experiment are shown in Table 1 and Fig. 1, 2. They show that the voltage to which the modulator capacitor C was charged did not exceed 3 kV. The typical value of the pulse current at the moment of the discharge gap breakdown reached 150 A. The frequency of relaxation oscillations varied from 400 Hz to 10000 Hz (depending on the parameters of the LC circuit). In the period between power pulses, the storage capacitor of the modulator C is charged and, at the same time, an undesirable process of water electrolysis occurs. The electrolysis current can reach 0.5 - 1 A. At a high charging voltage of the capacitor C, about 1 - 4 kV, there is a significant consumption of input electric power of about 1 - 2 kW, spent on the process of water electrolysis during this period.



**Fig. 2.** Volt-ampere signals on the discharge gap of the PVR-V. Mode of developed relaxation self-oscillations. Green - voltage  $U_d$  on the discharge gap, yellow - current  $I_d$ , red - electric power  $N_e = U_d(t)I_d(t)$

From the analysis of Table 1 it follows that in the first two experiments, when there were no relaxation oscillations (the LC circuit was absent), the value of the SOR did not exceed 0.73 – 0.8. In this mode, there was no erosion of the electrodes and no production of powder from transmuted elements in water.

In the mode of developed relaxation oscillations (experiments 4–7), the value of the COP coefficient increased to 1.62–2.82.

**Table 1**

$\dot{y}$ MH <sub>2</sub> O, G	T <sub>y</sub> , °C	$\ddot{y}$ , s	$N_e$ , W QH <sub>2</sub> O, kJ	Qe, kJ COP
1 4000	18.0	218 690	120.4 150.4	0.80 25.2
2 4000	23.6	174 790	100.3 137.5	0.729.6
3 5000	26.7	90 970	144.2 87.3	<b>1.65</b> 33.6
4 5000	32.2	90 700	171.3 63.0	<b>2.72</b> 40.4
5 6000	17.5	60 727	122.9 43.6	<b>2.82</b> 22.4
6 6000	26.8	55 1071	125.4 58.9	<b>2.13</b> 31.8
7	8000	28.2 90	1540 224.0	<b>1.62</b> 49.1

where MH<sub>2</sub>O is the mass of water in the water pool, T<sub>y</sub>, °C is the initial temperature of the water, T<sub>y</sub>, °C is final water temperature,  $\ddot{y}$ , s - experiment time,  $N_e$ , W - average electric power spent on creating heterogeneous plasma, QH<sub>2</sub>O, kJ - output thermal energy in PVR-V, Qe, kJ - electric energy spent on creating heterogeneous plasma,  $\ddot{y}\ddot{y} = QH_2O/Qe$

It should be noted that the calculations of QH<sub>2</sub>O and COP values did not take into account the heating of the water pool body itself, connecting pipes, pump, the mass of the outgoing water vapor and the production of hydrogen. Taking these factors into account leads to an increase in the indicated values by at least 1.5 times.

**Analysis of the obtained frames of high-speed video film obtained in the experiment on  
PVR-V**

*The purpose of the experiment.* Visualization of the dynamics of a pulsed water discharge funnel and the structure of the heterogeneous plasma zone.

*Experimental conditions.* In our experiments we used a high-speed video camera Phantom CV. The shooting frequency was 30 kHz, the frame exposure time was 1.2 µsec.

Operating mode of PVR-V	conventional, axial electrode arrangement
Modulator capacitance value C	3 µF
Inductance value L	225 µH
Electrode material Argon	aluminum 0.4
consumption Water	
consumption	g/s
Water loading	10 l/min
in heat exchanger	4000g

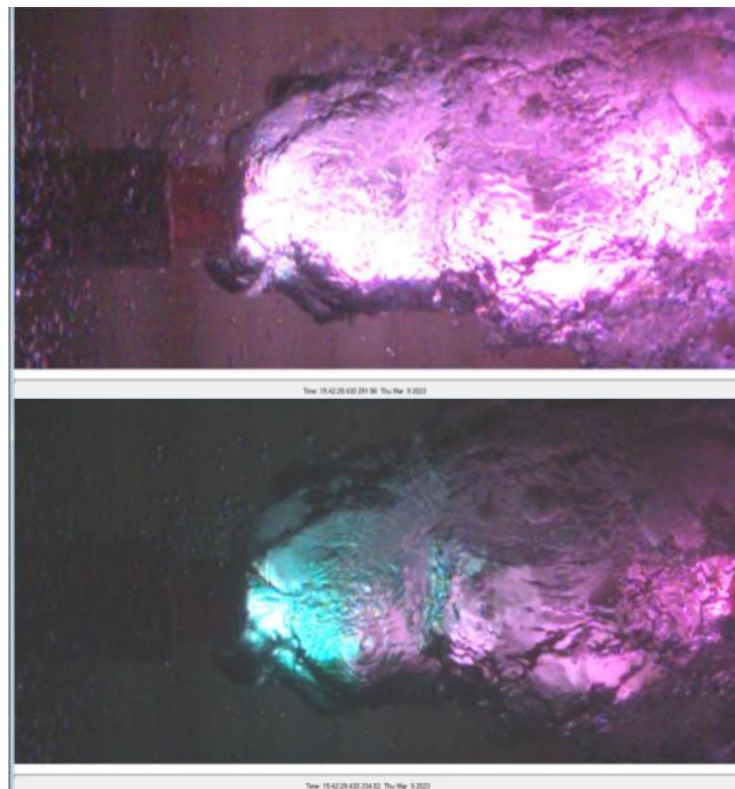


**Fig. 3.** Longitudinal IPR in the PVR-V reactor. Typical frames of a high-speed video film. *Left: - anode - aluminum tube with a diameter of 4 mm. Right: - along the reactor axis - cathode made of nickel. Distance between electrodes - 22 mm*

*Analysis of the presented frames.* It is evident that in all the frames (Fig. 3) the electric discharge occurs *in the gas bubble*, the dimensions of which reach 10-15 mm and significantly exceed the diameter of the initial funnel core, about 4 mm (without discharge). *Conclusion:* - a powerful electric discharge (at a pulse current > 100A) moves apart the funnel walls due to the high pressure of the gas heated during the power pulse. The presented frames of the high-speed video film show that numerous small bubbles (less than mm in diameter) are formed near the upper electrode located in the water flow, before entering the discharge area, and the surface of the large bubble. We believe that these bubbles are formed by water electrolysis near this electrode. They may play a significant role in the process of forming the electrical breakdown itself and the large bubble (especially in the mode without argon supply). 1. It is evident that the hydrogen production phase (red glow) precedes the erosion phase of the aluminum electrode (blue glow). This fact indicates the decisive role of the bombardment of the aluminum electrode surface with hydrogen atoms and ions in the process of its erosion.

2. The electric discharge channel has a strongly curved appearance (in contrast to the rectilinear channel in PVR-3). It can be assumed that individual charged gas inhomogeneities of the water bubble can lead to such instability of the discharge channel.
3. During the extinction of the pulse discharge, local dark areas appear in the water bubble. In appearance, they resemble cloudy formations with transmuted elements (electrode erosion material), visually observed during the experiment on the surface of the water in the pool in the form of cloudy formations.
4. On the surface of the gas bubble, many turbulent disturbances are visible. In the electric discharge itself, there are various instabilities of its channel (curvature, constrictions, etc.)

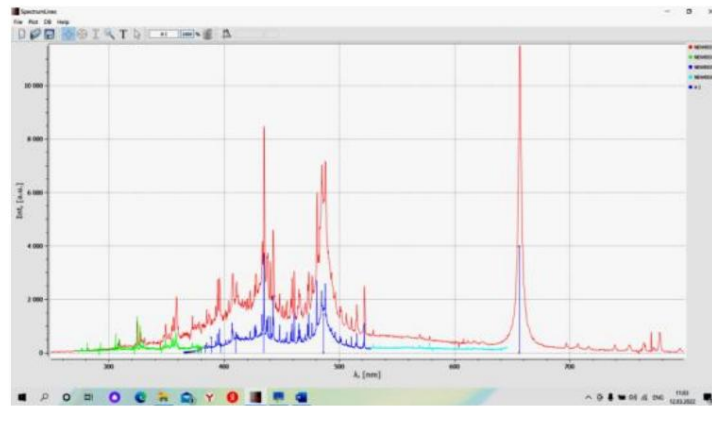
*General conclusion to the section.* The presented frames of high-speed video films clearly show various gas-hydrodynamic instabilities, turbulence of the water flow, as well as instabilities of the plasma channel itself. All these instabilities and non-uniformities certainly affect and are reflected in the nature of the discharge current-voltage characteristic and the value of the SOR. In addition, *the poor reproducibility of the experimental results* obtained in different experiments under equal initial conditions becomes clear.

#### **Optical spectra in heterogeneous plasma in PVR-V**

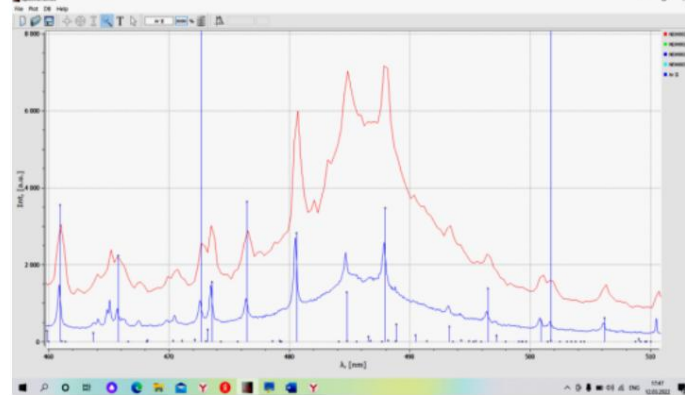
Typical overview and detailed optical spectra obtained in heterogeneous plasma in PVR-V are shown in Fig. 4. Note that the lines in the UV and IR parts of the spectrum are poorly resolved due to the presence of the walls of the water funnel and the glass tube. The transmittance of plasma radiation in these regions is low. From the analysis of the spectra it follows that there is an intense continuous spectrum and a rich line spectrum. The Balmer series of hydrogen (H) shines most brightly . *The argon lines ArI and ArII are clearly visible in the spectra . H*

ÿ , H ÿ , ÿ

The lines of copper  $Cu\text{ I}$  and aluminum  $Al\text{ I}$  are distinguishable. However, most of the optical lines *have not been identified so far*. Note that the excitation energy of the lines of the excited argon ion  $Ar\text{ II} > 15.6$  eV. It is well known that such a high excitation energy of argon in an arc discharge with a typical pulsed current above 100 A and a low value of the reduced electric field  $E/p = 0.2$  V/cm Torr is impossible, and the optical lines of  $Ar\text{ II}$  should not be observed [4]. Therefore, it can be assumed that in a heterogeneous plasma in a water vapor + argon mixture, there are highly inhomogeneous and nonequilibrium processes due to the presence of high-energy LENR. Processing of the continuous spectrum (within the framework of the blackbody model) made it possible to determine the glow temperature of cluster particles at a level of **10,000 K**.



Marked hydrogen  $H\text{ I}$  lines



The marked lines of the argon ion  $Ar\text{ II}$

**Fig. 4.** Typical overview and detailed optical spectra in heterogeneous plasma PVR-V. The vertical lines with circles indicate the calculated lines from the NIST database.

### Chemical analysis of sediment in PVR-V, performed using the EDS method

In this work, chemical analysis measurements were performed on the powder from transmuted elements obtained in the PVR-V. The powder productivity on such a setup was many times higher than on the PVR-G gas setup, and reached about 1 cm<sup>3</sup> for a typical reactor operation time of 1 min. The chemical composition of the powder was studied using the X-ray spectroscopy method (EDS method). Typical results of such analysis using a copper cathode and an aluminum anode are shown in Fig. 5-6. It is evident that the typical size of the powder particles varies from 100 µm to the submicron level, Fig. 5.

Important conclusions follow from the analysis of EDS spectra, Fig. 6. The appearance of both *heavy chemical elements and light elements* (in comparison with the atomic weight of the electrodes themselves) is observed. In the EDS spectra, both expected elements such as zinc **Zn** and iron **Fe** (products of possible transmutation of the copper electrode), silicon **Si** and magnesium **Mg** (products of possible transmutation of the aluminum electrode) are observed; as well as completely unexpected elements such as carbon **C** in large quantities and many others. In further experiments, a thorough analysis of the isotopic composition of these elements is necessary. A possible difference of such a composition from the natural one can finally confirm the hypothesis of the artificial origin of these elements.

**EDAX TEAM**

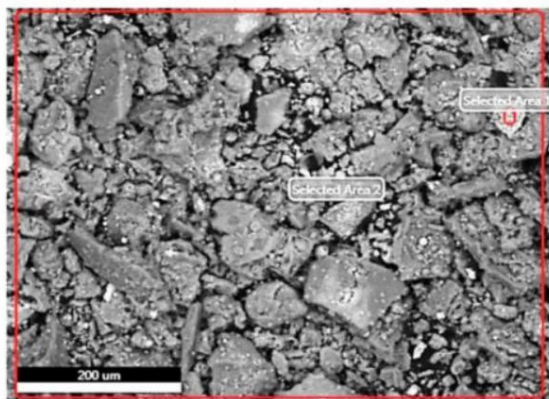
*Page 1*

#### Powders 2022

Author: supervisor

Sample Name: B1

##### Area 1



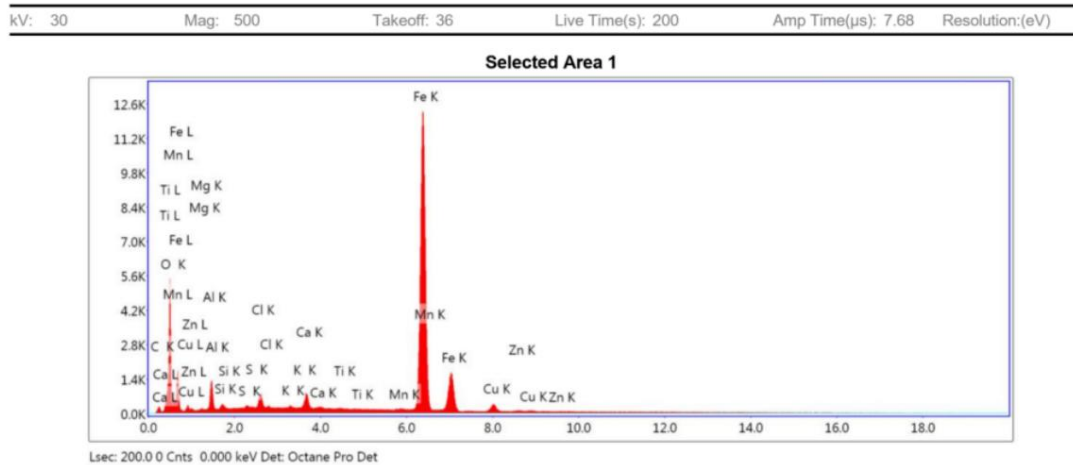
Notes:

**Fig. 5.** Structure of the studied powder obtained at PVR-V

EDAX TEAM

Page2

## Selected Area 1

eZAF Smart Quant Results

Element	Weight %	Atomic %	Error %
C K	4.76	10.96	19.44
O K	30.86	53.29	8.02
MgK	0.98	1.11	14.85
AlK	4.67	4.78	9.94
SiK	0.51	0.50	17.29
S K	0.19	0.17	27.89
ClK	1.17	0.91	9.31
K K	0.15	0.11	27.30
CaK	1.24	0.86	6.07
TiK	0.05	0.03	56.83
MnK	0.24	0.12	26.83
FeK	52.96	26.20	1.15
CuK	1.98	0.86	10.45
ZnK	0.24	0.10	56.25

**Fig. 6.** X-ray EDS spectra of the studied powder.

## Conclusion

The latest experimental results obtained on the PVR-V water plasma reactor are considered. Reliable results on measuring the energy efficiency value using a closed-type water calorimeter are obtained. The typical value of the SOR reached  $SOR = 2 - 4$  without taking into account the heat losses in the reactor.

Optical spectra in water heterogeneous plasma created in PVR-V were obtained and analyzed. The Balmer series of hydrogen shines most brightly. Argon lines ***ArI*** and ***ArII*** are ***clearly visible in the spectra***. Most of the optical lines *have not been identified so far*. It was suggested that highly excited ***ArII*** complexes appear in heterogeneous plasma during the implementation of LENR in it.

The chemical composition of the powder from transmuted elements obtained in PVR-V was measured using EDS spectroscopy. The EDS spectra show both expected elements such as zinc ***Zn*** and iron ***Fe*** (products of possible transmutation of the copper electrode), silicon ***Si*** and magnesium ***Mg*** (products of possible transmutation of the aluminum electrode); and completely unexpected elements such as carbon ***C*** in large quantities and many others.

---

## LITERATURE

1. Avramenko R.F., Klimov A.I., Mishin G.I., et al., Diploma for scientific discovery No. 007 dated March 25, 1985. Anomalous supersonic flow around bodies in weakly ionized nonequilibrium plasma. State Committee of the USSR for Inventions and Discoveries
2. Klimov A. Energy Release and Transmutation of Chemical Elements in Cold Heterogeneous Plasmoids. J. Condensed Matter Nucl. Sci. 19 (2016), pp.1-9
3. Klimov A., Altunin S., Kulikovskii O. Highly Efficient Water Plasma Vortex Reactor for Obtaining of Extra Thermal Energy and Transmuted Chemical Elements, J. Condensed Matter Nucl. Sci. 38 (2024), pp. 287–295
4. Raiser Yu.P. Physics of gas discharge. Moscow: Nauka, 1987, p.592

## Main results obtained at the PVR-W reactor in the period from 2022 to 2024

**AI Klimov, SE Altunin, OM Kulakovskiy1**

1Research Center "Prometheous", Bryansk

[klimov.anatoly@gmail.com](mailto:klimov.anatoly@gmail.com)

Our team has created a number of heterogeneous plasmoid vortex reactors (PVR) based on LENR in a working mixture of argon + water vapor or water vortex flow using nickel electrodes [1-3]. The created PVR reactors allow obtaining excess thermal energy of the order of 1-3 kW, several times exceeding the input electrical energy used on creating the heterogeneous plasma itself in this reactor. Typical value of the energy conversion coefficient COP in the PVR reactor reaches  $COP = 2 - 6$ , where COP is the ratio of the output excess thermal energy of the heterogeneous plasma flow to the input electrical energy spent on its creation. The specific energy released in LENR reaches 1-10 keV/hydrogen atom (or metal). This work is a continuation of the above-mentioned works [1-3].

## **Formation of a solid phase when carbon dioxide is irradiated by a laser beam that passes near the zone of a spark electric discharge in a water-air environment.**

**Baranov D.S.<sup>1</sup>, Zatelepin V.N.<sup>1</sup>, Kovacs A.<sup>2</sup>, Greenyer R.<sup>3</sup>,**

Laboratory INLIS, Moscow,

<sup>2</sup> BroadBit Energy Technologies, Helsinki,

<sup>3</sup> Martin Fleischmann Memorial Project

The article presents data on experiments with irradiation of a gas volume filled with carbon dioxide CO<sub>2</sub> by a laser beam passing near a spark discharge. The experimental setup consists of an electric spark gap (30 kV) placed in a closed dielectric volume; a low-power green (532 nm) laser (5 mW); a fiber optic line with a total length of 10 m, along which the laser beam passes; a sealed glass container filled with carbon dioxide with room parameters. Most of the length of the fiber optic line, along which the laser beam passes, is wound into a coil and surrounds the electric spark gap. The laser beam emerging from the fiber optic line is directed to a sealed glass container filled with CO<sub>2</sub> in the gas phase. The duration of the discharge and laser irradiation of the container with CO<sub>2</sub> is about 60 min. After completion of the experiment, a layer of a white solid substance was formed on the bottom of the glass container filled with CO<sub>2</sub>. In the solid substance formed during the irradiation of the container with CO<sub>2</sub>, up to 30% aluminum, up to 23% silicon, up to 4% titanium were found. The report considers the version that during the formation of the solid phase, not standard nuclei, for example Al, are formed, but a nuclear molecule of nuclear size, consisting of C and H nuclei, and having a binding energy of the order of keV. The unification of nuclei into a nuclear molecule is facilitated by a neutron-like particle formed in an electric discharge. This version allows us to explain the change in the composition of the sample during long-term (more than 10 sec) irradiation with an electron beam in EDS

analysis.

### **Introduction**

Experiments published in [1] showed that irradiation of a closed volume with room air by a laser beam passing near the electric discharge zone leads to a decrease in pressure in the volume. These experiments were conducted in 2018-2021. The experiments [1] were not conducted by chance. In the INLIS laboratory, for several years, purposefully various experiments have been conducted to confirm the hypothesis about the formation of "unknown particles" in cold transmutation reactions of elements, which have physical properties that contribute to the initiation of the transmutation process.

The transformation of the substance in the gas filling the sealed volume located near the discharge is probably the reason for the decrease in pressure in this volume. One of the possibilities to decrease the gas pressure is

condensation of the solid phase in the gas volume. That is, in the irradiated gas volume, transmutation of the gas composition may occur with the formation of substances that condense into a solid phase under room conditions. To confirm this hypothesis, work on irradiating gas volumes with a laser beam passing near the discharge zone was continued in 2022 - 2024. The results of these experiments are reported in this article.

### Experimental setup

This paper presents the results of experiments with laser beam irradiation of a gas volume filled with carbon dioxide CO<sub>2</sub> or air. Fig. 1 shows the composition of the experimental setup.

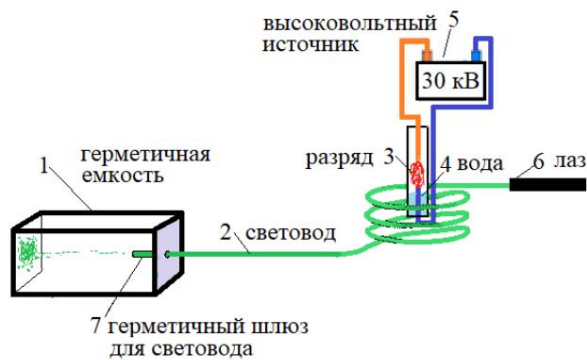


**Fig.1** Experimental setup stand

The experimental setup consists of a 30 kV source (5), an electric discharger (3) placed in a closed dielectric volume containing a small amount of water, a low-power (5 mW) green (532 nm) laser (6), a fiber optic line with a total length of 10 m (2), a sealed container (1), and a sealed gateway for introducing the fiber optic into the container (1).

The setup operates as follows. The container (1) is filled with either atmospheric air or carbon dioxide. The container is hermetically sealed. The output end of the fiber optic line is inserted into a hermetically sealed gateway for the light guide (7) attached to the container. As a result, the laser beam coming out of the fiber optic line illuminates the gas in the container without violating the hermetic seal of the container. Most of the length of the fiber optic line (2), along which the laser beam passes, is wound into a coil and surrounds the electric discharger (3). The laser beam coming out of the fiber optic line illuminates the gas in the hermetically sealed container. It is expected that the effect of the laser beam passing near the discharge will lead to a change in the composition of the gas in the hermetically sealed container.

Two types of experiments were conducted:

- I - a sealed container made of plexiglass is filled with atmospheric air and illuminated by a laser beam,
- II - a sealed glass container is filled with carbon dioxide and illuminated laser.

Experiment I showed that, as expected, a substance in the solid phase was formed in small quantities in the volume of the cuvette. We assumed that the formation of the solid phase was due to the presence of a small amount of carbon dioxide in the atmospheric air. Experiment II was conducted to test this idea.

with carbon dioxide in a sealed container.

**Experiment 1 –  
a sealed container with atmospheric air is irradiated with a laser beam that has passed near the  
discharge**

Fig. 2 shows a sealed organic glass container used in Experiment I. The walls of the 20\*10\*15 cm container are made of 10 mm thick organic glass. The walls are tightened with metal bolts to ensure tightness. Fig. 2 shows the wires that are connected to the container from above and from the left. These wires make it possible to measure the temperature and pressure in the container. Data on measuring the temperature and pressure are not provided in this paper, since the purpose of Experiment I was to detect solid particles.

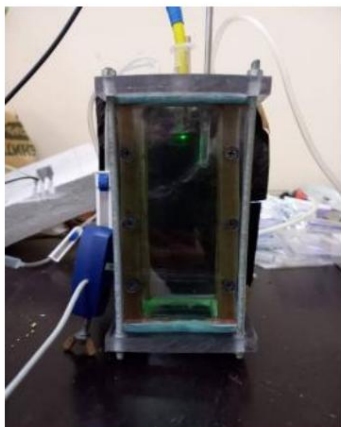


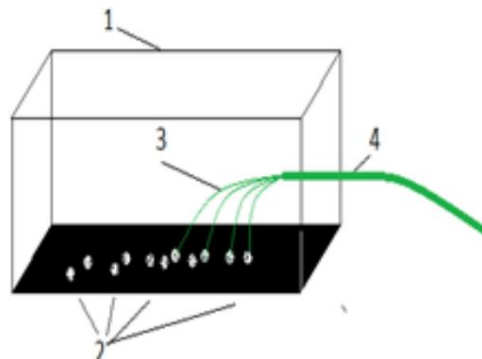
**Fig. 2** Photo of a sealed cuvette that is irradiated by a laser beam that has passed near an electric discharge

Experiment I showed that the assumption about the formation of a solid phase during irradiation of the container by a laser beam passing near the discharge was confirmed. Traces of a solid substance were found on the bottom wall of the container (1). The traces of the solid substance were located in such a way as if the condensation of the solid substance occurred along the laser beam exiting the optical fiber and passing further through the air to the opposite wall. Fig. 3 shows a diagram of the flight of particles of the condensed solid phase, which explains how the traces of the solid phase were formed on the bottom wall

of the container.

**Fig. 3.** Diagram of a sealed container with atmospheric air of an unknown substance with spots formed by irradiating the air in the container with a laser.

Of course, the solid phase particles do not move along with the laser beam along the optical fiber. According to our version, an electrically neutral particle of "dark hydrogen" with a magnetic moment moves along the optical fiber under the action of the magnetic field of the laser beam. After this particle enters the air environment of the container (1), it begins to become overgrown with a transmuted substance formed from



air molecules. As a result, a macroscopic particle is formed, which falls onto the lower surface of the container (1) under the action of gravity. The length of the flight of macroscopic particles of the transmuted substance depends on the speed. Using the known relationships for the motion of bodies in the Earth's gravitational field, the speed of these macroscopic particles can be calculated. Fig. 4 shows a photograph of the lower wall of the container (1) after an experiment with laser irradiation of the air in the container.

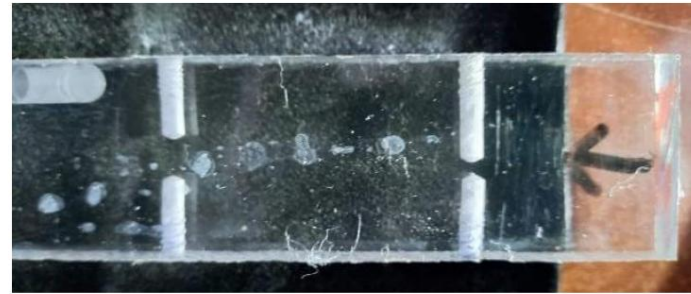


**Fig. 4.** Photo of the lower transparent wall (plexiglass) of the container (1) with traces of white round spots, which are an accumulation of a huge number of macroscopic condensed particles of transmuted matter.

Fig. 4 shows the transparent (plexiglass) lower wall of the container (1). The black arrow drawn with a felt-tip pen indicates the direction of the laser beam. The white round spots consist of a huge number of submicron particles of condensed matter. The white straight lines located across the wall are holes drilled in the plexiglass to attach the walls of the container to each other. The laser beam enters the container at a height of 2 cm from the lower wall, which we see in Fig. 4. The average length of the flight of the particles that formed the spots on the wall is approximately 7 cm. Hence, the speed of the macroscopic particles of the transmuted substance is on average 2 cm/s. It is interesting that the line of traces of the round spots shown in Fig. 4 is not straight, but curves along the horizontal surface of the lower wall. We believe that this shows the influence of external magnetic fields on the particles of the transmuted substance. That is, the particles of the transmuted substance are magnetoactive. Figure 5 shows two enlarged photographs of round marks on the bottom wall of the container, taken under a microscope.

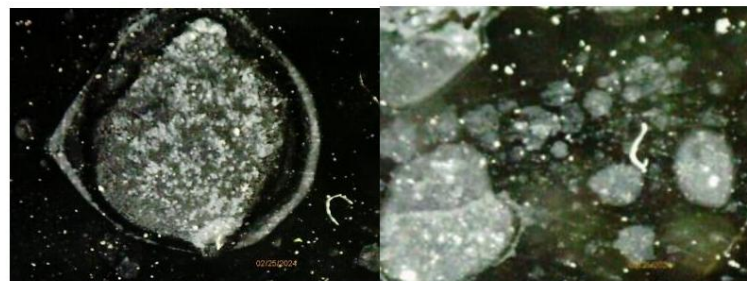


**Fig. 5.** Two photographs of rounded tracks. Magnification approximately 40 times.

In Fig. 5 it is clearly seen that the rounded traces consist of a large number of white particles deposited on the lower wall of the container. We observed similar white particles in many experiments with LED disks located near discharges or irradiated by a laser beam that passed near the discharge. In Fig. 5 the bright white particles have a size of about 10 - 20  $\mu\text{m}$ . The foggy areas between the bright white particles are filled with even smaller particles of condensed matter. The rounded border around the spot shown on the left side of Fig. 5 consists of very small and relatively large (10-20  $\mu\text{m}$ ) particles.

Various variations of Experiment I, the description of which would increase the volume of this article considerably, led us to the conclusion that the transmutation of the elements, as a result of which the condensed substance on the spots in the container (1) was formed, is connected with the presence of small quantities of carbon dioxide in the atmospheric air. Experiment II was carried out to confirm this hypothesis.

### Experiment 2 –

#### a sealed container with carbon dioxide CO<sub>2</sub> is irradiated with a laser beam that has passed near the discharge

Experiment II used the same setup as Experiment I (Fig. 1), supplemented with a system for filling the volume with carbon dioxide. Also, in Experiment II, unlike Experiment I, a glass jar with a tightly closed and glued (to improve the tightness) metal lid was used as a sealed container. Two thin hoses were hermetically mounted in the metal lid. Carbon dioxide was supplied through one hose, which went down to the bottom of the jar. Air was removed from the jar through the other hose when it was filled with carbon dioxide.

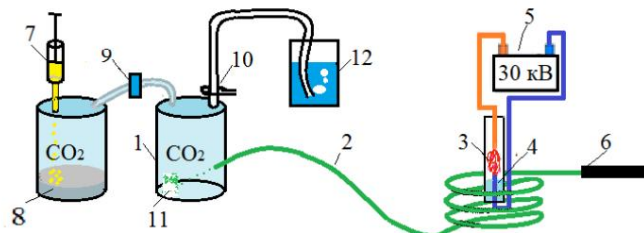


**Fig. 6.** Schematic diagram of the setup in Experiment II, showing the process of filling the container (1) with carbon dioxide.

Fig. 6 shows the process diagram of filling the tank (1) with carbon dioxide, and shows the tank (1) diagram in more detail. To obtain carbon dioxide, the reaction of baking soda with hydrochloric acid  $\text{NaHCO}_3 + \text{HCl} \rightarrow \text{NaCl} + \text{H}_2\text{O} + \text{CO}_2$  was used. Hydrochloric acid is fed into the tank with soda (8) using a syringe (7) before turning on the discharge. In the tank (8), during the reaction of hydrochloric acid with soda, carbon dioxide is produced, which is fed through a hose (9) through a filter into the tank (1). A hose (10) comes out of the top of the tank (1), through which air from the tank (1) exits into a water seal (12), and then the atmosphere. On all hoses

There are shut-off valves that ensure tightness. After feeding hydrochloric acid into the container with soda (8), observing the bubbling of gas through the water seal (12), we control the displacement of air from the container (1). The process of filling the container (1) with carbon dioxide continues for 3-5 minutes, after which all the valves on the hoses are closed. Of course, such a procedure does not guarantee that there is no air or water vapor left in the container (1). But the main goal has been achieved - we have significantly increased the concentration of carbon dioxide in the container (1). Other elements of the stand: (2) - fiber optic line (light guide). (3) and (4) - discharge gap and water in a plastic cylinder with a discharge, (5) high voltage source, (6) - a continuous radiation laser with a power of 5 mW with a wavelength of 532 nm.

Having switched on the discharge (3), we direct the output end of the fiber optic line to the glass wall of the container (1) of the laser beam. By the scattering of the green laser beam on the opposite wall of the container (1), we understand that the laser beam passes through the volume of the container (1) filled with carbon dioxide. The joint work of the discharge and the laser irradiating the container (1) continues for about 30 minutes. During this experiment, we have the opportunity to measure both the pressure and the temperature in the container (1). In order for the electronic temperature and pressure sensors to work stably during the discharge, the container (1) is removed 2 m from the discharge zone.

## Results of Experiment II

Many experiments were conducted on irradiating a container with carbon dioxide with a laser beam passing near the discharge. In most experiments, a decrease in pressure in the container (1) from fractions of % to 4-5% and an increase in the gas temperature in the container (1) by fractions of a degree Celsius were recorded. After completing one of the experiments, we found that a layer of white solid substance had formed on the bottom of the glass container (1).



**Fig. 7.** Photo of particles of a solid substance formed when a sealed container with gaseous CO<sub>2</sub> was irradiated by a laser beam that passed near a discharge in a water-air mixture.

In Fig. 6 this place is marked (11). The appearance of this layer resembled sediment in a solution when water dries. But there was no water in the container (1), and it could not "dry out", because the container was hermetically sealed. The thickness of the layer of the substance on the bottom of the container (1) is fractions of a mm. Fig. 7 shows a photograph of pieces of the layer of this substance, which we collected from the bottom of the container (1). The size of the largest piece in Fig. 7 is about 2 mm.

The particles that appeared at the bottom of the container (1) were collected and handed over to A. Kovacs and R. Gheenye. R. Greenyer analyzed the composition of the obtained samples using an electron microscope and the EDS method (ThermoFisher Phenom XLelectron microscope and the EDS method). In EDS analysis, a microscope was used simultaneously, which shows the area of the sample in which the composition analysis is performed. When analyzing the composition of the sample, an area of 211  $\mu\text{m}$  is irradiated

electron beam with an energy of 15 keV. The analysis of the composition of the selected area, and the irradiation of this area with an electron beam is carried out for 50 seconds. Table 1 shows the results of determining the composition in a certain area of the sample.

**Table 1**

Time, s	2,149	5,528	15,544	20,55	42,125	47,336
<b>Carbon. C</b>	24,18	18,28	31,10	40,64	37,49	30,89
<b>Atomic %</b>						
<b>Oxygen O</b>	47,53	51,29	54,7	36,69	49,23	54,07
<b>Atomic %</b>						
<b>Aluminium</b>	23,74	30,42	14,15	6,2	12,81	15,03
<b>Atomic %</b>						

The first row of Table 1 shows the moments of time at which the composition is determined. A total of 6 moments of time are selected. The left column shows the substances whose atomic percentages are determined at a given moment of time in a certain area of the sample. In the solid substance formed during laser irradiation of a container with CO<sub>2</sub>, new elements were found that were not contained in the initial composition of the gas that filled the container (1) before the start of the experiment: up to 30% aluminum, up to 23% Si, up to 4% Ti. Silicon and titanium found during the analysis are not shown. Fig. 8 shows the results collected in Table 1 in the form of a graph of the dependence of the atomic percentage of the composition of substances in the sample on time.

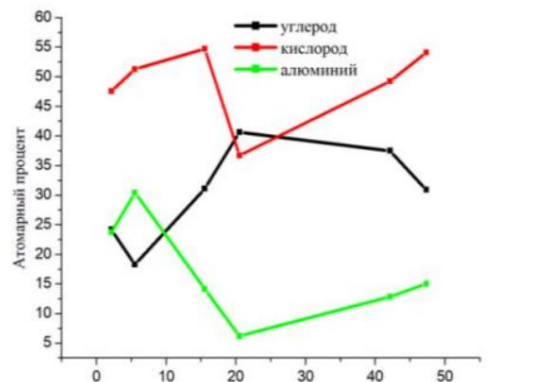


**Fig. 8** Dependence of the atomic percentage of substances in the sample on time.

The abscissa axis shows the time of composition determination in seconds from the start of measurement, the vertical axis shows the atomic percentage of the composition. In addition to the amazing fact that aluminum, which was not present in the initial gases filling the container (1) before the experiment, was registered in the composition of the solid phase condensed on the bottom of the container (1), the behavior of the composition depending on time is surprising. A.Kovacs drew the attention of the authors of the work to the peculiarities of this dependence. Firstly, it is interesting that the course of the black curve (carbon C) and the green curve (aluminum Al) are mutually opposite. The sum of the atomic compositions of these substances changes slightly with time. If there is more aluminum, then at this moment less carbon is registered. And vice versa, less aluminum - more carbon. It seems that one of the substances is transformed into another substance. In addition, an increase (or decrease) in the amount of aluminum occurs simultaneously with an increase (or decrease) in the amount of oxygen in the sample. It seems that aluminum is oxidized and binds oxygen at the measurement point.

It should be noted that the initial compositions of the substances do not match the compositions at the end of the measurement after 50 seconds. This may indicate that the process of transmutation of the substance in this experiment generates unstable new substances that disintegrate over time. The disintegration of the transmuted substance indicates that during transmutation in this experiment, there is not a process of formation of new nuclei, for example, aluminum nuclei, but a process of formation of some other structures that are perceived as aluminum nuclei.

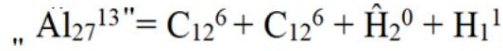
There is another explanation for the change in the composition recorded by the device. ThermoFisher Phenom XL. The fact is that when a certain area is irradiated with an electron beam with an energy of 15 keV, the substance may begin to melt. As a result, over time, the device will provide data obtained from different points of the sample by depth. R Greenyer drew attention to this possibility.

### **Two possible mechanisms of transmutation: formation of "nuclear molecules"; shielding of the nucleus by an electron pair**

The decay of the transmuted substance may indicate that the transmutation in this experiment is not a process of forming new nuclei, such as aluminum nuclei, but a process of forming some other structures that are perceived as aluminum nuclei. In this section, we propose a mechanism for the transmutation of elements in Experiment II that is based on the formation of combined structures from the nuclei of the original substances that will have a characteristic X-ray signal that coincides with the signal of an ordinary nucleus. The idea of the existence of "nuclear molecules" was probably first put forward in [1], and in application to the processes of "cold transmutation of nuclei" in [2]. Standard nuclear physics believes that combined structures from nuclei, which can be called

"nuclear molecules" can exist only for a very short time, less than 10<sup>-22</sup> s. We have previously suggested [3] that the

"dark hydrogen" we introduced can act as a "glue" that allows nuclei to come closer together for a long time at a distance significantly smaller than the characteristic atomic size, and to hold the nuclei together for a comparatively long time. Two properties of "dark hydrogen" allow it to hold nuclei at almost nuclear distances. The word "almost nuclear" is very important, since "dark hydrogen" has a characteristic size of 10<sup>-13</sup> – 10<sup>-14</sup> and brings nuclei together at a distance of 10<sup>-13</sup> – 10<sup>-14</sup>, which is significantly larger than the size of a nucleus (10<sup>-15</sup> m), but significantly smaller than the size of an atom (10<sup>-10</sup> m). The second important property of "dark hydrogen" is a magnetic moment equal to 2 Bohr magnetons, which is a thousand times greater than the typical magnetic moment of a nucleus. It is the magnetic moment that allows the nuclei to be brought together at a distance of 10<sup>-14</sup>, which allows the formation of the electronic structure of "transmuted aluminum", similar to the structure of real aluminum. The molecule of "transmuted aluminum" was formed according to our model by the following reaction:



where " Al27 13" is the nuclear molecule of transmuted "aluminum", C12<sup>6</sup> - core - ordinary carbon, H1<sup>1</sup> – the nucleus of ordinary hydrogen (proton), H2<sup>0</sup> designation "dark hydrogen". Reactions of nuclei of chemical elements with the formation of nuclear

molecules according to such a model using the unique properties of "dark hydrogen" can be called second-order chemistry. The typical energy of a single act of reactions second-order chemistry ( $> 10$  keV) is approximately a thousand times greater than the typical energies of ordinary atomic-molecular chemistry. The term "second-order chemistry" has already been used before (Vigier) at Russian and international conferences. We believe that it is worth returning this term to scientific literature.

It is most likely that the formation of "Transmuted Aluminum" will be accompanied by the release of energy. In Experiment II, we recorded a slight increase in the temperature of the container (1) in which the transmutation reaction occurs. Fig. 9 shows the possible geometric structure of the nuclear molecule of transmuted aluminum,

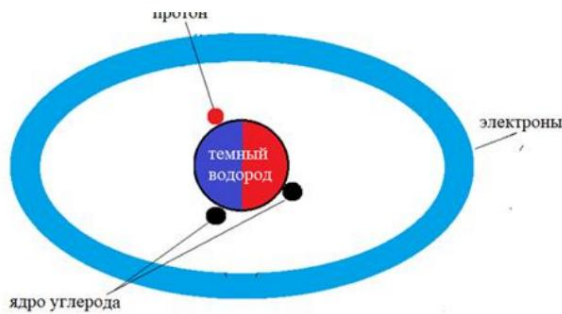


**Fig. 9.** Model of the nuclear molecule of "transmuted aluminum" formed with the help of "dark hydrogen"

Electrostatic interaction of the formed electrons, the "nuclear molecule" of "transmuted aluminum" will not differ from the electron shell in ordinary aluminum. It is this circumstance that is misleading when using electromagnetic spectral methods for studying the composition. We believe that in order to distinguish "transmuted aluminum" from ordinary aluminum, it is necessary to use accurate mass spectrometric methods.

The considered mechanism of formation of the "nuclear molecule" during formation of "transmuted aluminum" resembles the reaction of nuclear synthesis, since the "nuclear molecule of transmuted aluminum" is formed with the participation of two carbon nuclei. A. Kovacs noted that a thorough analysis of the X-ray spectrum obtained by R. Grinye

reveals a peak in the region of 104 eV. This energy is very close to the energy of the characteristic radiation of beryllium Be (108 eV). It can be assumed that the interaction of "dark hydrogen" with one nucleus, for example, carbon, can lead to the detachment of protons of "dark hydrogen". The electron pair remaining from the "dark hydrogen", due to its large mass and magnetic interaction with the carbon nucleus, will be located in a significantly lower orbit around the carbon nucleus than the orbit of an ordinary electron with  $n=1$ . The remaining four electrons of carbon will give a characteristic spectrum similar to the spectrum of beryllium, since the electron pair in a low orbit will screen the Coulomb field of the nucleus acting on these 4 electrons. This mechanism of transmutation of carbon nuclei by the change of characteristic spectrum resembles the reaction of nuclear decay. Let us recall that some experimenters point out that, when working with superunit reactors, there is a feeling that reactions of not only nuclear synthesis but also nuclear decay are possible.

The reactions of transmutation of nuclei of chemical elements with the formation of nuclear ones using the unique electron properties of "dark hydrogen" or molecules, shielding of nuclei using the magnetic properties of the pair can be called "**second-order chemistry**". The typical energy of a single act of second-order chemistry reactions ( $> 10$  keV) is approximately a thousand times greater than the typical energies of conventional atomic-molecular chemistry. The term "Second-order chemistry" has already been proposed by the French physicist Jean-Pierre Vigier at Russian and international conferences. We believe that it is worth returning this term to scientific literature.

### Conclusions

1. It has been shown that irradiation of some gases (air and CO<sub>2</sub>) with a laser beam passing near a spark electric discharge leads to the formation of solid phase.
2. EDS analysis of the solid phase revealed the appearance of characteristic spectra similar to those of aluminum, silicon, and titanium, which may indicate the formation of these "new substances." A change in the intensity of the spectra of the "new substances" was recorded during long-term irradiation of the sample with an electron beam during EDS analysis.
3. It has been suggested that the appearance of characteristic spectra of "new substances" is associated not with the formation of new nuclei, but with the formation of "nuclear molecules" that have electrostatic properties similar to the properties of "new substances".
4. A model of the formation of "nuclear molecules" using "dark hydrogen" atoms is proposed. This type of transmutation can be interpreted as pseudo-nuclear synthesis.
5. A model of the transmutation of elements using the magnetic properties of an electron pair remaining from a decayed "dark hydrogen" atom is proposed. This type of transmutation can be considered as pseudo-nuclear decay.
6. It is proposed to use the term "second-order chemistry" to denote the reaction of transmutation of nuclei of chemical elements with a characteristic energy of a single act of the order of 10 keV or more.

### Literature

1. Baranov DS, Zatelepin VN, Panchelyuga VA, Shishkin AL Transfer of "dark hydrogen" by atomic matter. Diagnostic methods of "dark hydrogen", RENSIT, 2021, 13(3):319-328
2. Bromley D. Nuclear molecules. Uspekhi Fizicheskikh Nauk. Vol. 131. No. 4 (1980).
3. Baranov DS, Baranova OD Evidence of the Formation and Decay of Giant Long-lived Nuclear Molecules. INTERN. SYMP. ON EXOTIC NUCLEI (EXON2012). (October, 2012, Vladivostok) CONFERENCE PROCEEDINGS P 209-212. <http://exon2012.jinr.ru>
4. Baranov D.S., Zatelepin V.N. Mechanism of formation and physicochemical properties Proceedings of the 26th Russian Elements and Ball Lightning, Conference on Cold "Dark Hydrogen". Transmutation of Nuclei of Chemical Moscow, September 28 – October 2, 2020, pp.64–86.

## Formation of a solid phase when carbon dioxide is irradiated by a laser beam passing near the spark electric discharge zone in an air-water environment

Baranov DS<sup>1</sup>, Kovacs A.<sup>2</sup>, Greenyer R.<sup>3</sup> Zatelepin VN<sup>1</sup>

<sup>1</sup> INLEAS Laboratory, Moscow, <sup>2</sup> BroadBit Energy Technologies, Helsinki,

<sup>3</sup> Martin Fleischmann Memorial Project

Experiments published in [1] showed that irradiation with a laser beam passing near the electric discharge zone of a closed volume with room air leads to a decrease in pressure in the volume. These experiments were conducted in 2018-2021. The reason for the decrease in pressure remained unclear. One of the possibilities to reduce the gas pressure is to initiate condensation of the solid phase in the gas volume. Ie, in the irradiated gas volume, the gas composition may be transmuted to form substances that condense into the solid phase under room conditions. To confirm this hypothesis, work on irradiation of gas volumes with a laser beam that has passed about the discharge zones were continued in 2022-2024.

This paper presents data on experiments with laser irradiation of a gas volume filled with CO<sub>2</sub> carbon dioxide. The experimental setup consists of: an electric spark gap (30 kV) placed in a closed dielectric volume; a low-power green (532nm) laser (5 MW); a fiber-optic line with a total length of 10 m, through which a laser beam passes; a glass sealed container into which carbon dioxide is injected with room parameters. Most of the length of the fiber-optic line along which the laser beam passes is wound into a bay and surrounds an electric spark gap. The laser beam coming out of the fiber optic line is directed to a sealed glass container filled with CO<sub>2</sub> in the gas phase. The duration of discharge and laser irradiation of a CO<sub>2</sub> container is about 60 minutes. After the experiment was completed, a white solid layer formed at the bottom of a glass container filled with CO<sub>2</sub>. The left side of the photo shows pieces of this substance collected from the bottom of a glass container. The typical size of large pieces is about 1-2 mm.



R.Greenyer analyzed the composition of the obtained samples using an electron microscope and the EDS method. Up to 30% aluminum (right part of the photo), up to 23% Si, and up to 4% Ti were found in the solid formed by irradiation of a container with CO<sub>2</sub>. The report considers the version that during the formation of the solid phase, not standard nuclei, such as Al, are formed, but a nuclear molecule having a nuclear size, consisting of C and H nuclei, and having a binding energy of the order of keV. The fusion of nuclei into a nuclear molecule is facilitated by a neutron-like particle formed in an electric discharge. This version allows us to explain the change in the composition of the sample during prolonged (more than 10 seconds) irradiation with an electron beam in a microscope.

1. Baranov DS, Zatelepin VN, Panchelyuga VA, Shishkin AL Transfer of "dark hydrogen" by atomic matter. Diagnostic methods of "dark hydrogen", RENSIT, 2021, 13(3):319-328

**Study of spark electric discharge in water-air environment using antenna.  
Effect of electric field, laser, magnetic field on amplitude spectrum of pulses in  
antenna**

**D.S. Baranov<sup>1</sup> ,V.N. Zatelepin<sup>1</sup> , A.L. Shishkin<sup>2</sup>**

<sup>1</sup>INLIS Laboratory, Moscow

<sup>2</sup>Laboratory AVK BETA, Dubna

A spark electric discharge in a closed volume with dielectric walls was studied in two types of media: dry air or air with high humidity (about 100%), pure argon or argon with water vapor. To record the electromagnetic signal generated by the discharge, an antenna made of copper wires in the form of the Latin letter V with a characteristic size of 10 cm was located at different distances from the discharge. The signal from the antenna was fed to an analog-to-digital converter (ADC Theremino), which selects and records unipolar signals taking into account the signal amplitude. The signal from the ADC was accumulated on a computer, which makes it possible to construct a distribution of the number of registered signals depending on the signal amplitude (discharge spectrum). The effect of various devices located near the antenna on the recorded discharge spectrum was studied: a high-voltage air capacitor; irradiation of the antenna with a laser beam passing near the discharge; a magnet and a magnetic film. The analysis of the obtained results leads to the conclusion that the discharge in a water-air or water-argon medium generates, in addition to the electromagnetic signal, unknown particles with electrical and magnetic properties. The passage of these particles near the antenna creates an additional signal to the electromagnetic wave from the discharge, which significantly changes the spectrum of the discharge. It can be assumed that the role of these unknown particles is played by the "dark hydrogen" [1], introduced earlier by the authors, which is created in the discharge in the water-air medium and which has both electrical and magnetic properties.

### **Introduction**

The authors of this paper have been studying X-ray spectra in the vicinity of spark discharges in air with high humidity for many years. Over several years of experiments with spark discharges in the INLIS Laboratory, we have developed several methods that show whether the processes of cold transmutation of elements (CTE) have been launched during the next spark discharge in humid air. Of course, the most reliable method for determining the launch of the CTE reaction is to register the appearance of new elements. But the methods of mass spectrometry or electromagnetic spectrometry are complex and do not allow for the rapid and reliable determination of the appearance of new elements. Therefore, cheap and simple methods for registering secondary manifestations of CTE are very helpful in determining

initiation of the process of cold transmutation. We include the following processes among such secondary manifestations of CTE:

- formation of craters and deposits on the CD disk located next to the discharge in the form of white crumbs with a diameter of one micron and above,
- formation of deposits in the form of white crumbs on a CD disc, remote from the discharge, but irradiated by a laser beam that passed through an optical fiber near the discharge,
- reduction of the activity of the radioactive source of X-ray radiation, located next to the discharge,
- electrification of the electroscope, provided that one of the electrodes is located electroscope near the discharge,
- changes in the background X-ray spectrum in the laboratory after completion of spark discharge tests in a water-air environment,
- change in the mass of water in a sealed volume when the volume is located next to discharge,
- formation of a special type of spectrum when measuring during a discharge on an X-ray spectrograph with a sensor based on NaI and a photomultiplier tube (PMT), with the sensor located in a zone up to 1.5 m from the discharge.

Results of experiments on changing the mass of water in a sealed volume at  
The results of the study on the location of the volume near the discharge were so intriguing that a discussion of these experiments (and similar experiments by other researchers) was devoted to the Round Table "Transformation of matter in the vicinity of cold fusion reactors" at the Klimov-Zatelepin webinar on May 15, 2024. A video recording of this Round Table can be viewed at the link <https://disk.yandex.ru/i/xVQWlzHYK5lxKQ>.

---

At this Round Table we reported that one of the unexpected incidental results of the experiments on changing the mass of water in a sealed volume was that when recording X-ray radiation during a discharge it was discovered that a special type of X-ray spectrum with the formation of peaks on the spectrum is recorded by a photomultiplier tube (PMT) even without using a NaI crystal. After the Round Table was over, L.I. Urutskoev verbally informed us that a similar situation with recording peaks on the X-ray spectrum was reported in [2]. In [2], the method of passing hydrogen under

pressure through an iron oxide foil with an admixture of potassium was used to initiate the process of cold transmutation. In [2], as in our experiments, an X-ray signal was recorded without the participation of a NaI crystal, only in the presence of a PMT in the recording device. It became clear to us that the registration of the X-ray signal in our experiments using a photomultiplier without using a NaI crystal is not an error, but reflects some important feature of the process of cold transmutation of elements. This work is devoted to studying the features of registration of the electromagnetic signal during a spark discharge in a water-air medium.

The sequence of experiments presented in this paper is not random. The experiments are aimed at showing that spark discharges in air saturated with water vapor result in the formation of material

particles, the flow of which, when passing through the antenna, generates an electromagnetic signal. To register the flow of these particles, it is not necessary to use X-ray detectors. These particles generate a voltage pulse on the radio antenna.

In connection with the fact that the operation of some types of reactors for cold transmutation of elements may be accompanied by the formation of unknown particles, which were mentioned above, it is important to recall that in theoretical models for CTE, two directions can be distinguished:

- CTE is a process of transformation of nuclei of initial chemical elements, with the formation of new nuclei of a new composition of chemical elements,
- CTN is primarily a process of formation of nuclear molecules from nuclei of initial chemical elements. Nuclear molecules are not nuclei of new chemical elements, but in mass spectrometry and electromagnetic spectrometry they exhibit properties similar to the properties of nuclei of new elements. We believe that it is the formation of nuclear molecules that is the main process in CTN. Perhaps, for the first time in the literature, the term "nuclear molecules" appeared at the end of the 20th century in the article [3] to describe short-lived nuclear formations.

In the work [4], this term was first used to describe the processes of "cold fusion". Without developing theoretical models of the process of formation of nuclear molecules in CTN in this work, we point out that, in our opinion, the formation of "nuclear molecules" occurs with the participation of an unknown particle of nuclear scale. That is, it is possible that the formation of unknown particles of nuclear scale, contributing to the formation of "nuclear molecules", is not just a consequence of CTN, but also one of the main reasons for the interaction of nuclei at low temperatures. In this case, the methods of registering such particles, which are the subject of this work, become extremely important in the study of CTN.

In the future, in this work we will use the following terms: - the peak of the spectrum of electromagnetic unipolar pulses, which is recorded by the antenna in the vicinity of the spark discharge, will be called a **"special electromagnetic pulse"**.

- the material particle that presumably generates a **"special electromagnetic pulse"** will be called an **"unknown particle"**.

## Experimental stand

The registration of the "unknown particle" formed in the discharge zone, unlike the registration of the X-ray signal, does not require the use of a NaI crystal. We assumed that it is the action of the flow of such particles on the PMT that leads to the registration of an electromagnetic signal, which we perceive as an electromagnetic spectrum of a special shape. Thinking in this direction, we realized that the PMT is essentially an antenna consisting of several electrodes. Therefore, in the experiments presented in this work, we abandoned the use of the PMT as a recorder and used an antenna in the form of the Latin letter V, formed by two copper wires approximately 5 cm long and 0.5 mm in diameter, covered with an insulator. Fig. 1 shows the experimental

a stand where the physical properties of signals recorded by an antenna when a spark discharge is switched on were studied.

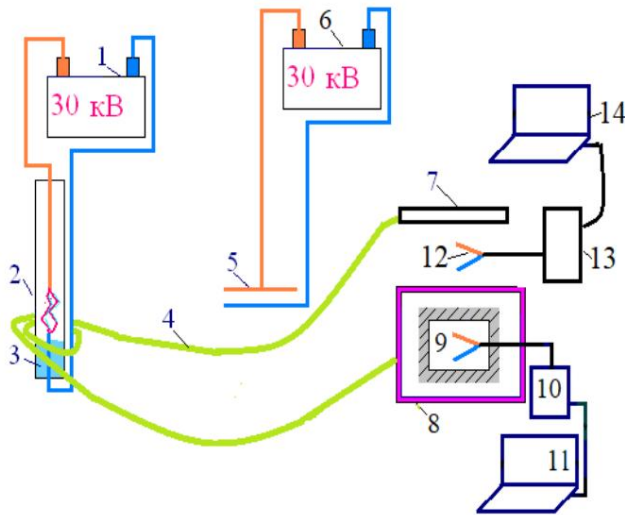


**Fig. 1.** The main experimental setup: 1 and 6 – high (30 kV) voltage sources, 2 – a closed container made of transparent plastic with electrodes on which a spark discharge occurs, 3 – water poured into this container. 4 – fiber optic cable, 5 - air condenser, 7 - green laser 532 nm, 8 - magnetic plastic film, 9 – antenna placed in a lead box, 10 – Theremino analog-to-digital converter, 11 – computer for recording spectrogram, 12 – unshielded oscilloscope, 14 – computer for recording oscillogram.

antenna, 13 -

The setup operates as follows. A high voltage of 30 kV is applied to the electrodes placed in a closed container (2) containing atmospheric air and water. A spark discharge is ignited on the electrodes, which is essentially non-stationary. On average, the voltage across the discharge gap during a spark discharge is 12-20 kV. The breakdown frequency in a spark discharge in our experiments exceeds 10 discharges per second. Visually, with such a breakdown frequency, the discharge is perceived as a continuously burning discharge. An antenna placed in a lead box is located at different distances from the discharge (from 60 to 120 cm). The lead box isolates the antenna from recording the electromagnetic signal. Grounding the lead box does not change the spectrum of the signal recorded by the antenna. For more accurate modeling of the operating conditions of the photomultiplier, a voltage of 659 V is applied to the antenna. It is this voltage of 659 V that we applied to the photomultiplier when the photomultiplier was used to record the signal.

The signal received by the antenna is fed to the Theremino analog-to-digital converter, which records only unipolar signals. Unipolar electromagnetic signals are typical for particle registration. This is extremely important, since it allows excluding the registration of conventional electromagnetic bipolar oscillatory processes. After the ADC, the signal is fed to the computer (10), which records the histogram - the dependence of the number of pulses on the voltage on the antenna during the pulse. To obtain an oscillogram of pulses (the dependence of the voltage on the antenna on time), an unshielded antenna (12) was used, the signal from which was fed to the oscilloscope (13) and to the recording computer (14).

The stand contains several auxiliary devices: laser (7) with optical fiber (4); air capacitor (5); magnetic film (8). Using these devices

simultaneously with the discharge in the spark gap will help to confirm the generation of "unknown particles" in the discharge zone, and also to understand some properties of these. Below, in the relevant section, it is described how particles. the stand works with using assistive devices

### 1. Spark gap

Fig. 2 shows a photo of one of the spark gaps that we used in the experiments.



**Fig. 2. Photograph of the spark gap.**

The discharger is made on the basis of a medical syringe. The photo on the left shows the syringe rod, in which the discharger anode is fixed, made of steel wire. The photo on the right shows the syringe cylinder, through the lower part of which a steel cathode wire is inserted, at the end of which a piece of carbon is fixed. The cathode in the discharger, as a result, is carbon. Using a syringe allows you to achieve

completed from

several purposes: - the discharge occurs in a closed volume, ozone does not spread from the discharge zone in the laboratory, which is very important during long launches, - we pour water into the syringe cylinder, which allows us to obtain saturated water vapor in the discharge zone. As will be shown in this work, a mixture of water vapor and air is the most important condition for the generation of a "special electromagnetic pulse" during a spark discharge. - the movement of the rod along the syringe cylinder allows precise adjustment of the volume electrode gap, obtaining similar conditions in different experiments.

### 2. The determining role of water vapor in the discharge region in the formation of "special electromagnetic pulses" on the antenna

At the beginning of the work, it was decided to check whether the presence of water vapor is a necessary condition for registering a "special electromagnetic pulse", i.e. a signal that is registered not only by an X-ray detector, but also by a conventional electrical antenna. Among experimenters working in the field of cold nuclear transmutation (CNT), the role of hydrogen is debated. Some believe that the presence of hydrogen is not necessary for starting the CNT process. We believe that it is hydrogen that is involved in starting the CNT process. This section describes two experiments showing that the presence of water vapor during a spark discharge is critically important for obtaining a "special electromagnetic pulse" on the antenna. We believe that the registration of a "special electromagnetic pulse" is a harbinger of the start of the CNT reaction, i.e.

information about the influence of water vapor on the generation of a "special electromagnetic pulse" is information about the influence of water vapor on the initiation of the CTE reaction.

The experiment presented in this section shows that when discharging in pure argon, the antenna does not register "special electromagnetic pulses". But when discharging in a mixture of argon and water vapor, the antenna registers a huge number of "special electromagnetic pulses". We have made a modification of the arrester shown in Fig. 3.

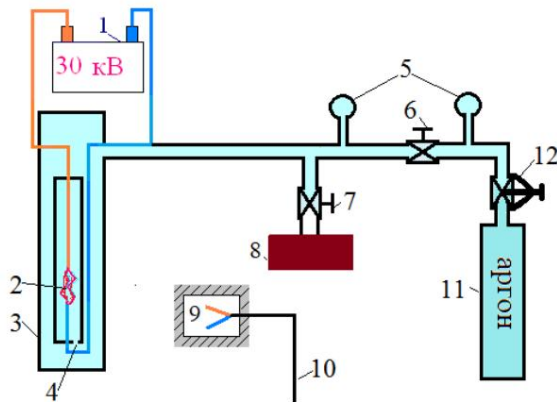


**Fig. 3.** Scheme of the experiment on discharge in argon. 1 - high-voltage source, 2 - spark gap and discharge gap, 3 - plastic volume enclosing the spark gap, 4 - hole in the spark gap, equalizing the pressure in the spark gap and the enclosing volume, 5 -

pressure gauges, 6 - valve, 7 - valve, 8 - vacuum pump, 9 - antenna in a lead box, 10 - cable to the amplitude analyzer and computer, 11 - argon cylinder, 12 - reducer.

A spark gap of the same type as shown in Fig. 1 was placed in an enclosing hermetic plastic volume with a nipple for pumping gases out of the volume and for feeding gases into the volume. The enclosing volume was used to create a reliable hermetic area filled with argon. A small hole (4) was made in the syringe barrel on the basis of which the spark gap was made, which allows equalizing the pressure and composition of the gases filling both the enclosing volume and the spark gap. In preparation for the discharge, air is pumped out of the enclosing volume (3) and the spark gap (2) by a pump (8) to a pressure of 10-3 atm. After this, the enclosing volume was filled with argon to a pressure of 1.5 atm. Through the hole (4), the argon pressure in the enclosing volume (3) and in the spark gap (2) is equalized to a pressure of 1.5 atm. After filling both the spark gap and the surrounding volume with argon, voltage from a 30 kV source is applied to the spark gap electrodes spaced 3 cm apart. An antenna (9) in a lead box is located 120 cm from the spark gap. Its signal is sent to the ADC (Theremino) via a cable (10) and then to the computer. Let me remind you that the

ADC registers only unipolar signals. In a spark gap filled with pure argon, when voltage is applied to the electrodes, a beautiful smooth (not curved) bright white spark discharge with a discharge voltage of 18 kV is formed. With such a beautiful discharge in pure argon, the ADC practically **does not register signals from the antenna**. In 308 seconds, the antenna registered only 56 pulses. Which is an average of 0.2 pulses per second.

In order to try to obtain signals registered by the antenna, we injected a small amount of water into the enclosing volume filled with argon. In this case, the argon pressure in the enclosing volume decreased to 1 atm. After a pause of 10 -15

minutes to evaporate the water in the enclosing volume, and to equalize the gas composition in the enclosing volume and in the spark gap, a voltage of 30 kV is applied to the spark gap. A spark discharge is ignited in a mixture of argon and water vapor, which does not look as powerful as a discharge in pure argon. The color of the discharge in a mixture of argon and water vapor is duller, compared to a discharge in pure argon, with a reddish tint. The shape of the discharge is curved, in the form of an arc. But unlike a discharge in pure argon, when discharging in a mixture of argon and water vapor, the ADC **registers a huge number of signals from the antenna**, which we call "special electromagnetic pulses." On average, 1067 pulses were registered per second. We emphasize once again that during quantity a spark discharge in pure argon in the absence of water vapor, the antenna does not register unipolar signals. A discharge in a mixture of argon and water vapor generates unipolar signals with a large number of pulses per second in the antenna.

### **3. Dependence of the spectrum recorded by the antenna on the distance between the antenna and the discharge**

This section presents an experiment that was conducted on the stand in Fig. 1. We checked the dependence of the signal spectrum recorded by the antenna during a spark discharge in air with a high concentration of water vapor on the distance L between the antenna (9) and the spark gap (2). Three antenna positions were considered: L = 60 cm, 90 cm and 120 cm. Before presenting the experimental results, let us try to imagine theoretically how the spectrum should change if the antenna recorded only electromagnetic oscillations.

From the solutions of Maxwell's equations for a spherical wave in free space it is known that the flux density of the Poynting vector  $\mathbf{P}$  changes as

$1/R^2$ , where R is the distance from the source [5]. It follows that the electric field in a spherical wave, which is proportional to  $(P)0.5$ , changes proportionally to  $1/R$ . Thus, if the antenna were to register the voltage generated by an electromagnetic wave, then with a 2-fold increase in distance, the voltage should decrease by 2 times. In the results presented in this section, we will see that with a 2-fold increase in distance, the voltage on the antenna decreases by 10 times or more. In addition, it should be borne in mind that the analog-to-digital converter registers only a unipolar signal, and an electromagnetic wave is an oscillatory, bipolar process. Obviously, in our experiment, the antenna equipped with an ADC does not register an electromagnetic wave. Thus, the term "special electromagnetic signal" introduced above in this article does not mean an electromagnetic wave, but rather a particle with electromagnetic properties that allow a signal to be generated in the antenna.

Fig. 4 shows an oscilloscope of a signal from a spark discharge in a water-air environment on an antenna placed in a lead box located at a distance of 60 cm from the spark gap.

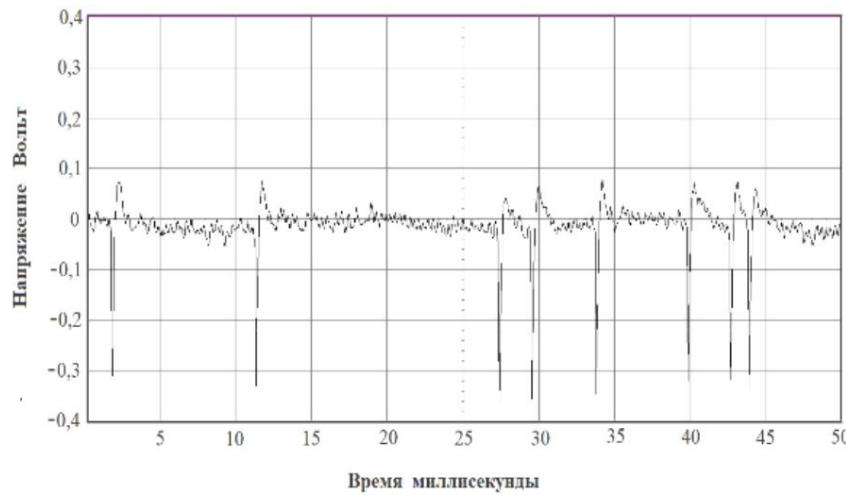


**Fig. 4.** Oscillogram of a spark discharge in a water-air medium. Sharp bursts on the oscillogram are particles generating unipolar signals on the antenna.

The oscillogram confirms that the antenna is not registering electromagnetic radiation wave, but a particle that forms a peak-shaped unipolar signal.

If we consider another version, that a spark discharge in a water-air mixture creates a spherically symmetrical flow of "unknown particles" that, flying through the antenna, generate an electric pulse in it, then the following characteristic features of such a pulse are obvious: the pulse energy should decrease with increasing distance R from the discharge; the number of pulses recorded in a certain time, which is equal to the number of particles that have flown through the antenna during this

time, should decrease as  $1/R^2$ . The pulses obtained from the spherically symmetric flow of "unknown particles" should shift to the left along the energy axis into the zone of lower energies, and the amplitude of the maximum should decrease.

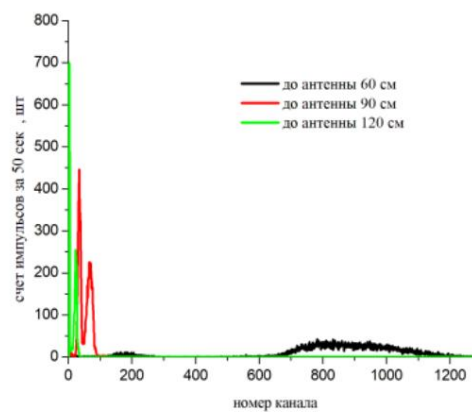


**Fig. 5.** Comparison of histograms of signals on the antenna (**without external voltage on the antenna**) for three distances R between the spark discharge and the antenna: black curve 60 cm, red 90 cm, green 120 cm. The antenna is located in a lead box. The abscissa axis shows the ADC channel number, which corresponds to the voltage on the antenna in relative units. The ordinate axis shows the number of registered pulses in 50 sec.

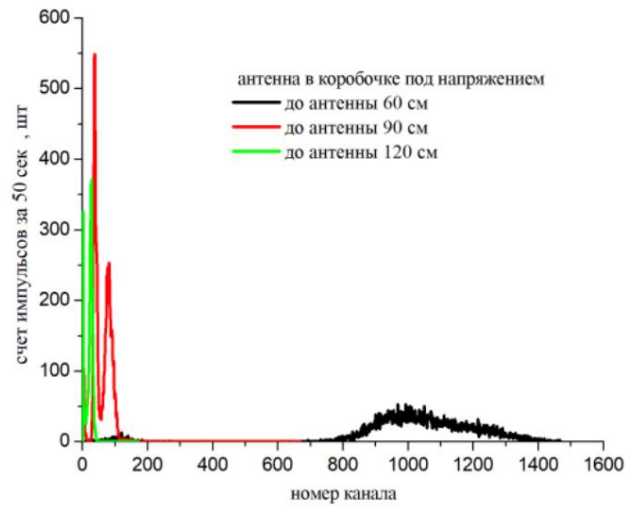
Fig. 5 shows a histogram of pulses on the antenna placed in a lead box, without applying external DC voltage. It follows from Fig. 5 that the pulse energy decreases with increasing distance R. When the distance is doubled, the position of the maximum shifts from channel #783 (black curve) to channel #3 (green curve). Such a shift of the maximum corresponds to a decrease in the pulse voltage on the antenna by  $783/3 = 261$  times. Such a change in voltage does not correspond at all to the model of propagation of a spherical electromagnetic wave in a space filled with air, in which the voltage should decrease only by half. As for the particle model, a decrease in voltage by 261 times does not contradict the particle model, since "unknown particles" can lose a lot of energy when interacting with air.

From the experimental data, on the basis of which the histogram in Fig. 5 was drawn, it follows that the total number of pulses S across the entire spectrum decreases with increasing distance R: for  $R = 60$  cm  $S = 11050$ , for  $90$  cm –  $9450$ , for  $120$  cm –  $3575$ . Dividing the total number of pulses S for  $R = 60$  cm by S for  $R = 120$  cm, we get  $3575/11050 = 3$ , i.e. the number of registered pulses decreases less than  $1/R^2 = 0.25$  with increasing distance R between the antenna and the discharge.

But the most striking consequence of Fig. 5 is that the half-width of the pulse (the pulse width at half-maximum) decreases significantly, while the pulse amplitude increases noticeably with increasing R. This completely contradicts the model of a spherically symmetric flow of particles of constant composition that diffuse through the air and are scattered upon interaction with

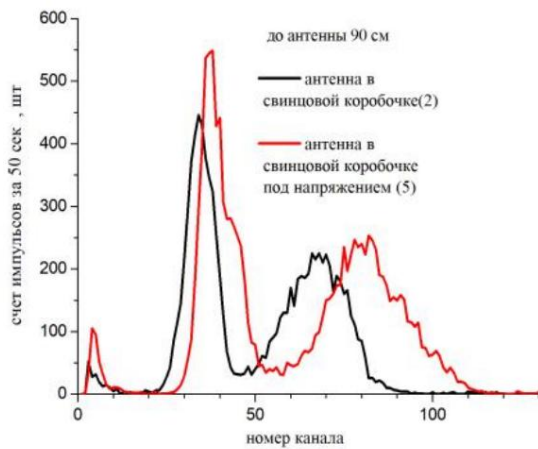
air atoms.

Fig. 6 shows a histogram of pulses on the antenna in a lead box, a constant voltage of 659 V is applied to the antenna. Comparison of Fig. 5 and Fig. 6 shows that that applying a constant voltage to the antenna leads to an increase in the voltage of the pulse recorded by the antenna. In particular, for a distance of  $R = 60$  cm between the antenna and the discharge (black curve), the peak of the histogram for conditions without external voltage (Fig. 5) is located on ADC channel No. 783, and the peak of the histogram with external voltage (Fig. 6) is located on channel No. 1011. Increasing the channel number means an increase in the registered voltage on the antenna.



**Fig. 6.** Comparison of histograms of signals on the antenna in a lead box (with an external constant voltage of 659 V on the antenna) for three distances  $R$  between the spark discharge and the antenna. The black curve is 60 cm, the red one is 90 cm, and the green one is 120 cm. The abscissa axis shows the ADC channel number, which corresponds to the voltage on the antenna in relative units. The ordinate axis shows the number of pulses registered in 50 sec.

The increase in the pulse amplitude when applying a constant voltage to the antenna is even more clearly seen in Fig. 7, which shows a comparison of the histogram of voltages on the antenna in the absence of a constant voltage (black curve), when applying a constant voltage of 659 V to the antenna <sup>and</sup> (red curve). The distance between the antenna and the discharge is 90 cm.



**Fig. 7.** Comparison of histograms of pulses on the antenna in the absence of a constant voltage on the antenna (black curve), and when a constant voltage of 659 V is supplied to the antenna (red curve).

**Conclusion:** An increase in the amplitude of the pulse recorded by the antenna when applying a constant voltage to the antenna may mean an increase in the energy of the recorded particle, i.e. the particle recorded by the antenna reacts to the external electric field.

#### **4. Some considerations about the mechanism of impulse excitation and about the transformation of energy in the antenna.**

As follows from the experiments presented in the previous section, the antenna most likely registers not an electromagnetic signal, but a particle capable of generating an electromagnetic pulse in the antenna. When generating a pulse in the antenna, the particle energy is converted into the energy of an electromagnetic pulse in the antenna. Based on the assumption that a particle is registered, we will estimate some parameters of such energy conversion.

Let us assume that the main negative peak of the pulse (oscillogram Fig. 4) corresponds to the particle entering the antenna. The characteristic voltage value of this peak is  $U_{\text{input}} = -0.3 \text{ V}$ . Immediately after the sharp negative voltage peak there follows a small positive voltage peak  $U_{\text{out}} = +0.06 \text{ V}$ . It can be assumed that the positive peak is generated when the particle exits the antenna. In further estimates we will neglect the energy that the particle carries away after passing through the antenna, since  $U_{\text{out}}^2 \ll U_{\text{input}}^2$ .

The pulsed electromagnetic energy generated in the antenna when a particle passes through it is transformed by two processes: (1) - radiation of an electromagnetic signal by the antenna into the surrounding space, (2) - generation of heat in the antenna's own resistance and other resistances in the antenna load. The antenna capacity  $C$  can be estimated as

$$C = 4\epsilon_0 l \sim 5 \cdot 10^{-12} \text{ F} \quad (1)$$

where  $\epsilon_0$  is the dielectric constant of vacuum and  $l = 0.05 \text{ m}$  is the length of the antenna wire.

To obtain voltage  $U_{\text{input}} = -0.3 \text{ V}$  on a capacitor with capacity  $C$ , it is necessary  $Q = 2.5 \cdot 10^{-13} \text{ C}$  electromagnetic energy  $W_{\text{cond}} = C U_{\text{input}}^2 \sim 1 \text{ MeV}$ . The charge spends the capacitor in such a process must be increased by  $q = C U_{\text{input}} = 1.5 \cdot 10^{-12} \text{ C}$ , which corresponds to 107 electron charges. If we take into account that when releasing energy in Since approximately half of the energy is radiated into space in the form of an electromagnetic wave, the total energy transferred to the antenna by the "unknown particle" during pulse generation is twice the energy of the current pulse  $W_{\text{cond}}$ , and the "unknown particle" must transfer energy to the antenna  $W_{\text{part}} = 2 * W_{\text{cond}} = 2 \text{ MeV}$ .

If we assume that the duration of the peak of the voltage pulse on the antenna corresponds to the time of passage of the particle through the antenna, then from the oscillogram of Fig. 4 it follows that the particle passes through the antenna wire in 0.5 ms. Assuming that the particle crosses the antenna wire, which has a diameter of 1 mm, we obtain that the speed of the "unknown particle"  $u = 10^{-3} \text{ m} / 0.5 \cdot 10^{-3} \text{ sec} = 20 \text{ m/s}$ . If we assume that the kinetic energy of the "unknown particle" is converted into an electromagnetic pulse in the antenna, then at a speed of 20 m/s its mass should be no less than 1013

a.m.u., which is unlikely. Thus, when the "unknown particle" passes through the antenna wire, a transformation of electromagnetic energy occurs.

Earlier, in the 90s of the 20th century, academician G.A. Mesyats [6] suggested that portions of electrons are formed during discharges, which he called "ectons". "Ectons" can consist of a huge number of electrons, and could play the role of an "unknown particle". But if we take into account that in our experiments "unknown particles" overcome a layer of dielectric, a 2 mm layer of lead, then a natural assumption arises that unknown particles are most likely electrically neutral. Ideas with the formation of particles called EVO and having a huge charge (trillions of electrons) were put forward at the beginning of the 21st century by K. Shoulders.

EVOs, it seems to us, can be rejected for the same reasons as the "ectons".

Note that the ideas of Mesyats and Shoulders about the huge charges of particles in their experiments are based on the concept of electrostatic energy to explain the transformations. Namely, the small energy, comparatively of electrons in the "unknown particle" ~~particle~~ ~~and energy mechanism~~ ~~strong interaction~~ ~~the voltage pulse~~ ~~is necessary~~ to place millions antenna can be proposed, based on the use of magnetic energy, which does not require the use of a huge number of electrons. In the "dark hydrogen" particle proposed by the

authors in [1], a pair of relativistic electrons that make up the nucleus of "dark hydrogen" creates a powerful magnetic field in the vicinity of "dark hydrogen". The "dark hydrogen" particle is electrically neutral, since it consists of two electrons and two protons. When it passes through the antenna wire, only one free electron of the wire can come close (at a distance of less than 10-12 m) to the free electron of the wire will be "dark hydrogen". At this distance, it is captured by magnetic interaction with the electron pair of "dark hydrogen". The magnetic energy of such interaction is sufficient to release 2 MeV in the form of a gamma quantum when a free electron approaches an electron pair of "dark hydrogen". The interaction of a 2 MeV gamma quantum with the wire substance will lead to a chain of high-energy processes: ionization of the wire substance, formation of electron-positron pairs.

A full calculation of such a high-energy process is beyond the scope of this paper. It is important that from the point of view of the law of conservation of energy, the magnetic interaction of just one electron and one particle of dark hydrogen is sufficient to form a voltage pulse on the antenna. Thus, it can be assumed that it is precisely the "dark hydrogen" that is the "unknown particle" that the antenna registers during a spark discharge in a water-air medium.

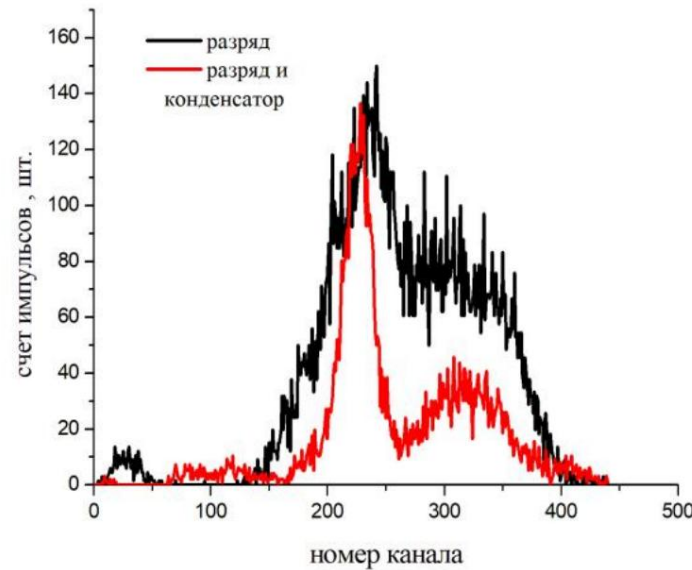
#### **The influence of an air capacitor located between the antenna and the discharge on the number of recorded pulses**

Fig. 1 shows an air capacitor (5) that can be charged by a high-voltage source (6) to a voltage of 30 kV. The results show that

shown above, no voltage was applied to the air capacitor. The idea behind using a capacitor is that it can be used again

confirm that the "unknown particle" reacts to an external electric field. Recall that it was shown above (Fig. 7) that applying voltage to the antenna increases the pulse voltage registered by the antenna. The air capacitor consists of two copper foils, 20\*10 cm in size, spaced at a distance of approximately 4 cm. Under

such conditions, at a voltage of 30 kV, the capacitor discharges weakly without breakdown. The air capacitor is installed on the path between the spark gap (2, Fig. 1) and the antenna (9, Fig. 1).



**Fig. 8.** The influence of an air capacitor on the spectrum of pulses recorded by the antenna.

In Fig. 8 the histograms obtained during a spark discharge in the arrester with no voltage on the capacitor (black curve) and when applying a voltage of 30 kV to the air capacitor (red curve) are compared. It is clearly seen that applying voltage to the air capacitor significantly reduces the total number of pulses on the antenna without changing the shape of the histogram. Such changes in the histogram can easily be explained by the model of electroactive particles that, moving from the arrester to the antenna, are partially intercepted by the electric field of the capacitor. Once again, we note that a dipole electrically neutral particle can interact with an external electric field

field.

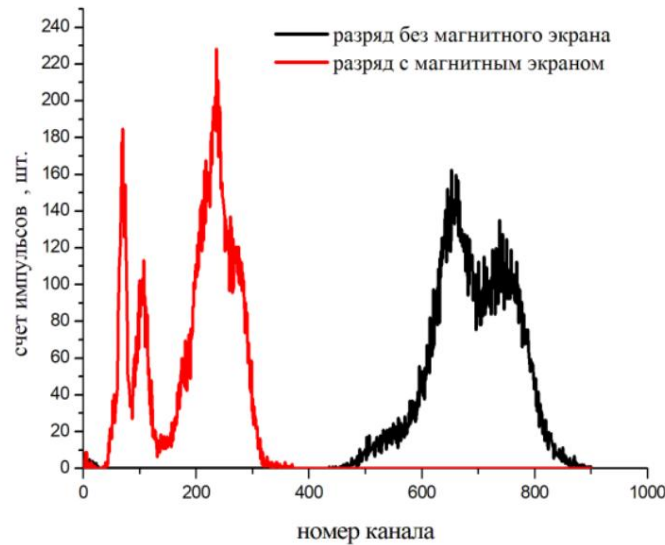
#### The influence of magnetic film on the spectrum of pulses recorded by the antenna

Fig. 1 shows the magnetic plastic film (8) which was used to wrap the antenna (9) in this experiment. The magnetic film acts as an additional screen to the lead box, protecting the antenna from radiation.

"unknown particles." Magnetic plastic film was used only in

this experiment. In the results presented above, the magnetic plastic film was not used.

Fig. 9 shows two histograms of the pulse spectra on the antenna (9, Fig. 1): the black curve means that magnetic film was not used, the red curve means that the lead box containing the antenna was wrapped in a layer of plastic magnetic film.



**Fig. 9.** Shielding the antenna with magnetic plastic film.

Fig. 9 shows that the use of magnetic plastic film leads to a decrease in the voltage on the antenna when using magnetic plastic film. Such changes in the histogram can be explained if we assume that the "unknown particles" have magnetic properties. The magnetic field of the film,

wrapped around a lead box will obviously have field gradients. Overcoming such a screen, which has magnetic field gradients, by particles with a magnetic moment will require the expenditure of particle energy, which is reflected in the histogram (red color, Fig. 9).

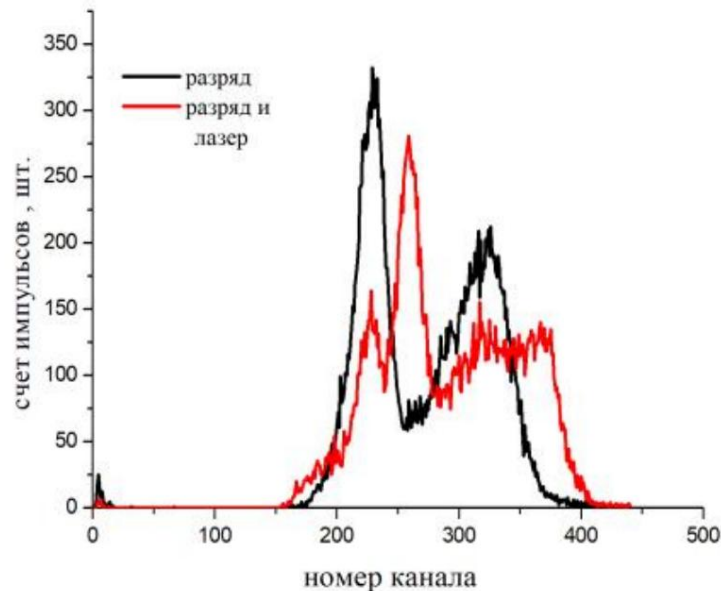
#### Irradiation of an antenna with a laser beam passing through an optical fiber wrapped in around the spark gap

Fig. 1 (4) shows an optical fiber wrapped around a spark gap (2). The laser experiment is carried out as follows. An optical fiber about 10 m long is pulled from the laser to the spark gap, wrapped around the spark gap several times, and then pulled to the antenna. The green laser beam of 532 nm emitted by the laser (7) enters the optical fiber at a distance of about 2 m from the discharge. Then the laser beam

transported via optical fiber, passes through optical fiber near the arrester,

comes out of the optical fiber at a distance of about 5 cm from the antenna and irradiates with laser light light antenna. Figure

10 compares the histograms of pulses on the antenna obtained during discharge operation but with the laser turned off (black curve) and the histogram of pulses on the antenna during discharge operation and laser irradiation of the antenna (red curve). It is evident that laser irradiation significantly affects the shape of the histogram.



**Fig. 10.** Change in the pulse spectrum when the antenna is irradiated with a laser beam that has passed through an optical fiber near the discharge.

In the work [7], it is shown that electrically neutral subatomic particles with a magnetic moment are moved by the radiation flow in a fiber optic line. The essence of the effect of moving subatomic magnetic particles by the radiation flow is that the magnetic moment of the particle, interacting with the magnetic field of the laser radiation, rotates in this field. As a result, during the first half-period of the oscillation of the magnetic field of the laser radiation, the magnetic moment of the particle is directed slightly differently than during the second half-period of the oscillation of the laser radiation. The change in the direction of the magnetic moment leads to the fact that the resulting force of interaction of the magnetic moment of the particle with the magnetic field of the laser radiation is not equal to zero. It is this resulting force that moves the dipole particle along the optical fiber.

"Dark hydrogen" [1] is a subatomic particle, i.e. a particle of a size significantly smaller than the size of an atom. In addition, "dark hydrogen" has

magnetic moment and is electrically neutral. If we assume that such a particle is formed in a discharge, then its properties allow us to explain the effect of irradiation by the laser beam of the antenna on the spectrum of pulses recorded by the antenna and shown in Fig. 10.

### Conclusions

1. A discharge in a water-air mixture generates not only an electromagnetic signal, but also "unknown particles." Such particles are not generated in dry air or argon. The movement of these "unknown particles" in the vicinity  
The discharge is registered by the antenna.
2. These "unknown particles" have the following properties:
  - at a distance of more than a meter from the source, the energy of interaction with the antenna decreases hundreds of times,
  - have high penetrating ability,
  - interact with the magnetic field,
  - interact with the electric field,
  - are transferred by a laser beam through optical fiber over a distance of about 10 m.
3. A mechanism for generating a pulse in an antenna based on magnetic interactions of "dark hydrogen" with free electrons of the wire antennas.

### Literature

1. Baranov D.S., Zatlepin V.N. Mechanism of formation and physicochemical properties Proceedings of "dark hydrogen". the 26th Russian Conference on Cold Transmutation of Nuclei of Chemical Elements and Ball Lightning, Moscow, September 28 – October 2, 2020, pp. 64 – 86.
2. Zeiner-Gundersen SA, Olafsson S. Nature of spontaneous signal and detection of radiation emitted from hydrogen Rydberg matter. *AIP Advances* 14, 055124 (2024)
3. Bromley D. Nuclear molecules. *Uspekhi Fizicheskikh Nauk.* Vol. 131. No. 4 (1980).
4. Baranov DS, Baranova OD Evidence of the Formation and Decay of Giant Long-lived Nuclear Molecules. INTERN. SYMP. ON EXOTIC NUCLEI (EXON2012). (October, 2012, Vladivostok) CONFERENCE PROCEEDINGS P 209-212. <http://exon2012.jinr.ru>
5. Rodos L.Ya. Electrodynamics and propagation of radio waves (propagation of radio waves) Study guide. St. Petersburg: Publishing house of SZTU, 2007. – 90 p.
6. Mesyats G.A. Ectons. In 3 parts. Moscow: Nauka, 1993, 1993, 1994.
7. Baranov D.S., Zatlepin V.N., Shishkin A.L. Experiments on the movement of "particles of unknown radiation" along a fiber optic cable when passing a laser beam. Proceedings of the 27th Russian Conference on Cold Transmutation of Nuclei of Chemical Elements and Ball Lightning. Moscow, October 3–7, 2022, pp. 65–75.

## **Investigation of a spark electric discharge in a water-air environment using an antenna. The effect of the electric field, laser, and magnetic field on the amplitude spectrum of pulses in the ant**

**D.S. Baranov<sup>1</sup>, VN Zatelepin<sup>1</sup>, AL Shishkin<sup>2</sup>**

<sup>1</sup> INLIS Laboratory, Moscow

<sup>2</sup> AVK BETA Laboratory, Dubna

A spark electric discharge in a closed volume with dielectric walls in two types of media was studied: dry air, air with high humidity (about 100%). To register the electromagnetic signal generated by the discharge, an antenna made of copper wires in the form of a Latin letter V with a characteristic size of 10 cm was located at various distances from the discharge. The signal from the antenna was fed to an analog-to-digital converter (ADC Theremino), which allocates and registers single-half-period signals taking into account the amplitude of the signal. The signal from the ADC was accumulated on the computer, which allows you to build a distribution of the number of registered signals depending on the amplitude of the signal (discharge spectrum). The effect of various devices located next to the antenna on the recorded discharge spectrum has been studied: high-voltage air capacitor; irradiation of the antenna with a laser beam that has passed near the discharge; magnet and magnetic film.

An analysis of the results obtained leads to the conclusion that a discharge in a water-air environment generates, in addition to an electromagnetic signal, unknown particles with electrical and magnetic properties. The passage of these particles near the antenna creates an additional signal to the electromagnetic wave from the discharge, which significantly changes the discharge spectrum. It can be assumed that the role of these unknown particles is played by the "dark hydrogen" introduced earlier by the authors. "Dark hydrogen" is created in a discharge in a water-air environment and has both electrical and magnetic properties.

# Properties of strange radiation tracks. An attempt at explanation

<sup>1</sup> Parkhomov A.G., <sup>2</sup>Zhilalov V.A.

<sup>1</sup> Experimental Design Laboratory "K.I.T." Moscow, Russian Federation,

<sup>2</sup> Kazakh National Research Technical University named after K. I. Satpayev. Alma-Ata, Republic of Kazakhstan

The discovered properties of tracks that appear near installations where LENR processes occur are described. The explanation of where the particles that "draw" tracks hypothesis, why the track patterns are unique, and why the intensity of track appearance is inconstant is presented. Experiments that confirm this hypothesis are described.

## 1. Introduction

The phenomenon, called "strange radiation tracks" (SRTs), was first described in detail in a paper on effects observed in electrical foil explosions [1], although such tracks were not observed by LENR researchers

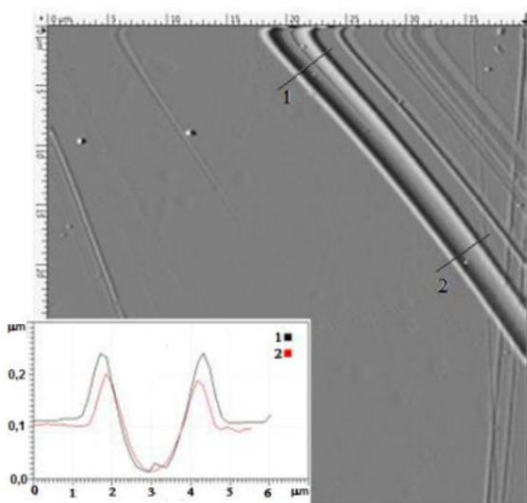
(low energy nuclear reaction - nuclear reactions at low energies) have been observed before [2,3,4]. In the study [1], photo emulsions were used as detectors. The detected traces were not similar to tracks formed by high-energy charged particles, especially those of very large length (up to several millimeters). The shape of the detected tracks is different: continuous straight or curved tracks, tracks with kinks, tracks with a complex periodically repeating pattern. All tracks are located strictly along the surface. An estimate of the energy release in the tracks gave a value of ~1000 MeV (particles arising in nuclear reactions have an energy of ~1 MeV). Note that the effects of strange radiation are not only extended tracks, but also microcraters [5].

In the experimental design laboratory of KIT, LENR reactors of different types (nickel-hydrogen, with incandescent lamps, with electrolysis and plasma electrolysis) were created in 2015-2022 [6-13]. Some of them operated continuously for a long time (up to 7 months). The duration and stability of the reactors' operation made it possible to conduct systematic studies of TSI, investigating not only the type of specific tracks, but also the rate of their appearance on the surface of the detectors, their dependence on distance and their dynamics over time.

Initially, detectors used in nuclear physics experiments to register high-energy charged particles were used to study TSI: photographic films, X-ray films and nuclear photoemulsions. But it was soon discovered that TSI also appears on smooth surfaces of almost any substance. In addition to photoemulsion detectors, glass, mica, metals, plastics and detectors made of a number of other materials were tested at OKL KIT. Most of the experiments were performed using CD and DVD discs (polycarbonate) as detectors. Fresh discs have a very smooth surface without scratches and are readily available in large quantities, which makes it possible to increase the statistical reliability of the results obtained. For

To study the shape of the tracks, methods of optical, scanning electron microscopy (SEM) and atomic force microscopy (AFM) were used.

This article does not aim to provide a detailed description of the methodology of the conducted studies and the array of data obtained, as they are presented in publications [14-19]. Here, only the most important results and main conclusions arising from the various studies conducted are presented. We will systematize the types of tracks, provide an analysis of the results obtained, and, based on the identified patterns, formulate a hypothesis explaining the main experimentally discovered properties of TSI.



## 2. Track types

### 2.1 Smooth Tracks

Smooth tracks are predominant in plastic, easily fusible materials (plastics, gelatin in photo emulsions). Such tracks look like grooves about 0.1  $\mu\text{m}$  deep and several  $\mu\text{m}$  wide. On the sides, protrusions are visible, approximately equal in height to the groove depth (probably extruded material).

**Fig. 1.** "Smooth" tracks on polycarbonate. Image obtained by atomic force microscopy (AFM) [18,19].

### 2.2. Tracks with a periodically repeating complex pattern

Tracks with a period of 44 to 200  $\mu\text{m}$  were found. Each track of this type has a unique pattern (Fig. 2). They occur in both plastic materials and moderately hard and heat-resistant ones (glass, metals). The cross-sectional profile of such tracks has a complex character (Fig. 3). Sometimes a smooth track can be observed to transition into a periodic one (Fig. 4).

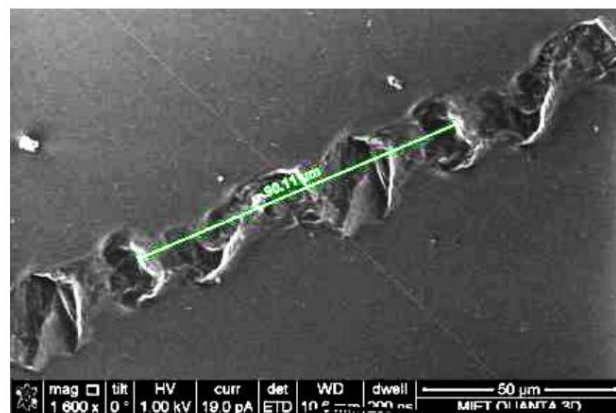


**Fig. 2.** Fragment of a typical track with a periodic pattern on the surface of polycarbonate (SEM). The period is about 90  $\mu\text{m}$  [18,19].

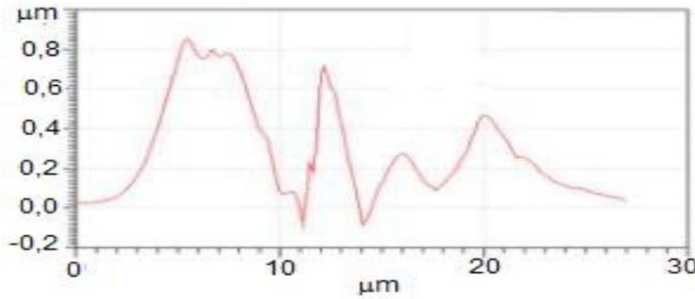


**Fig. 3.** Example of an AFM profilogram of the cross section of one of the sections of a periodic track on polycarbonate [18,19]



**Fig. 4.** Transition of a periodic track (period 45 μm) into a smooth one. Polycarbonate. Optical microscope [15]

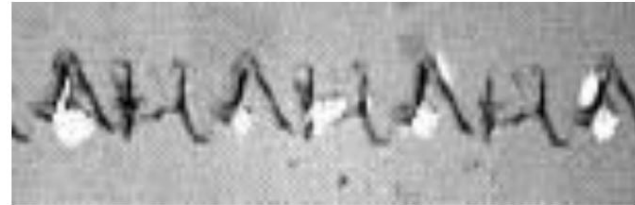


**Fig. 5.** Fragment of a track on glass. Optical microscope. The track pattern is repeated with a period of about 70 μm. Light areas are possibly cracks in the glass [22].

**2.3. Tracks along which cracking and scattering occurs.** Occurs in fragile heat-resistant materials (mica, glass, ceramics, etc.)

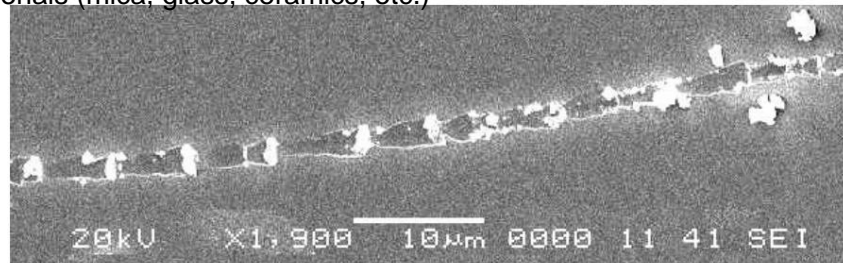


**Fig. 6.** Example of a track on mica (SEM) [15,17]. Tracks on mica are extended traces of surface destruction, as if the captured material is raked up and then periodically left behind on the further path. Small particles of mica are visible near the tracks on the mica surface, possibly ejected from the track.

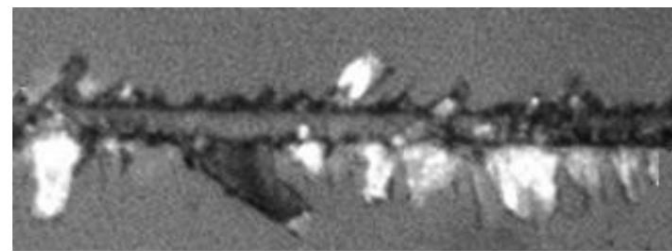


**Fig. 7.** Tracks on the surface of lithium niobate LiNbO<sub>3</sub> are accompanied by numerous cracks. Optical microscope [22].

#### 2.4. Tracks in the form of chains of round spots ("drop tracks")

Found near electrolysis plants

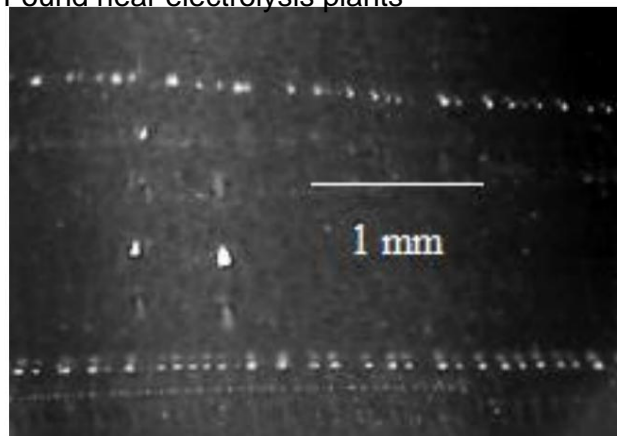


**Fig. 8.** "Drip" tracks on DVD discs near an H<sub>2</sub>SO<sub>4</sub> electrolytic cell with nickel electrodes [12].

#### 2.5. Microcraters

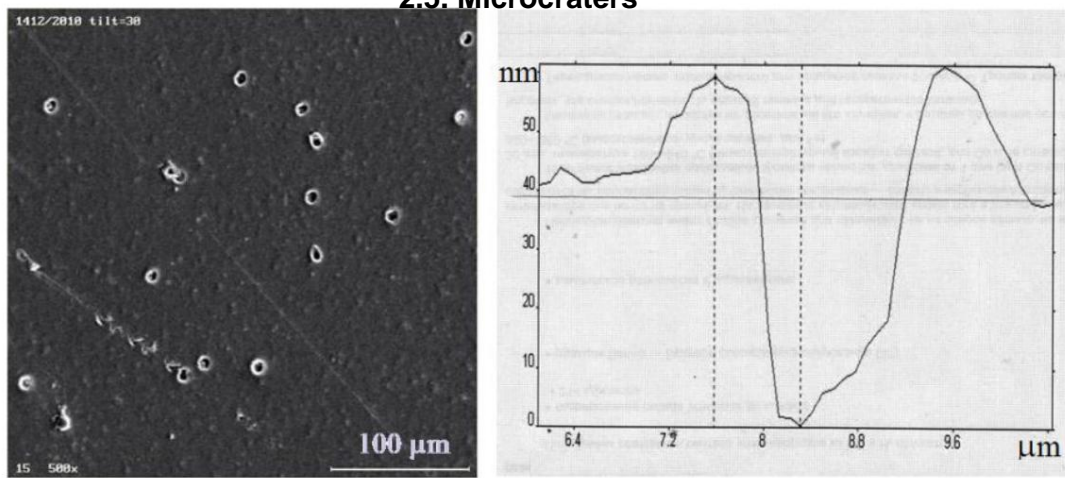


**Fig. 9.** Left: microcraters and tracks detected on the X-ray film located near the cavitation setup. Right: AFM profilogram of one of the microcraters. This microcrater has a diameter of about 1.1 μm and a depth, measured from the plane of the film, of 38 nm [5].

### 3. General properties of strange radiation tracks

#### 3.1. Intensity of track appearance depending on the distance to LENR reactors. Variability

For the numerical assessment of the intensity of track appearance, the method of calculating the total track length and comparing the obtained values of the test samples with the control was used [14-16]. The usual duration of each exposure is 1 week. Due to the fact that the sizes of the detectors are comparable with the size of the area in which the appearance of a sufficiently large number of tracks is observed, and, in addition, the intensity of track appearance is extremely unstable over time, the determination of the dependence on distance can only be estimated. Despite this, numerous long-term measurements allow us to conclude that the intensity of track appearance sharply decreases at a distance of more than 20 cm from the reactors. Thus, the average total track length on mica for 5 exposures for distances of 5 cm from the reactors (948 mm per sample) exceeds by more than an order of magnitude the average total length for 10 exposures for greater distances (37 mm per sample). A large spread of individual measurement values is characteristic.

The results on the DVD are similar to those obtained for mica: an average of 980 mm per sample for the zone closer than 20 cm from the reactors (49 exposures) and 54 mm per sample for the zone further than 20 cm (30 exposures). Here too there is a large scatter of values obtained in both the near and far zones (see Fig. 10).

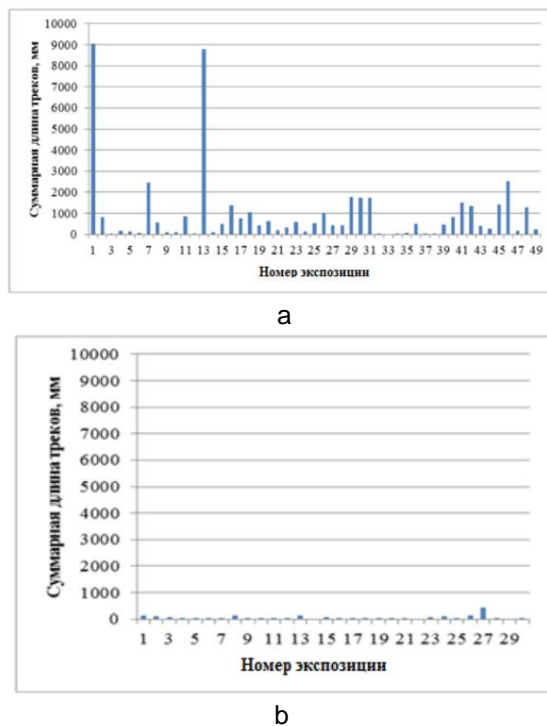


**Fig. 10.** Total track lengths on DVD by exposure: (a) for the near zone, (b) for the far zone [14,15].

Note that the appearance of tracks is a rather rare phenomenon. According to data [14,15], the average rate of track accumulation at a distance of 5-13 cm from a nickel-hydrogen reactor [7] is 0.027 mm per cm<sup>2</sup> per hour, i.e. the appearance of tracks with a total length of 1 mm on a square centimeter of the detector can be expected in about 37 hours.

**3.2. Intensity of track appearance depending on shielding and orientation of detectors** The following was found in the course of various experiments [16]. Disks tightly arranged in a stack protect each other (tracks appear mainly on the first disk). On disks arranged in a plastic box closed on all sides, few tracks appear.

In some of the exposures from the nickel-hydrogen reactor, a curtain of aluminum foil protected the DVD discs from thermal radiation. This curtain did not form a continuous shell around the disc, and was spaced several centimeters from the disc. In this case, the discs accumulated a significant number of tracks, unlike the control discs located at a distance from the reactor. Protection against the appearance of tracks apparently works only in the case of a screen tightly covering the detector from all sides.

*Patterns in the accumulation of tracks by discs depending on their orientation in were not observed in our experiments.*

### **3.3. Study of the elemental composition of matter in tracks**

One of the methods used to study the shape of the tracks was scanning electron microscopy (SEM). This method, along with obtaining high-resolution images, allows for the analysis of the elemental composition of the substance at specified points on the surface being studied. Analyses performed in the area of the tracks and at a distance from them did not reveal any significant differences.

## **4. Hypothesis about the nature of strange radiation tracks**

An overview of approaches to explaining TSI (hypothesis of magnetic monopoles, hypothesis of tachyons, hypothesis of magneto-torus-electron radiation, hypothesis of "dark" hydrogen, hypothesis of multiply charged clusters, etc.) can be found in the article [23]. None of these hypotheses can explain the complex of properties inherent in this amazing phenomenon. In particular, two most important properties are ignored, without an explanation of which it is impossible to do: a very complex, diverse, non-repeating pattern of periodic tracks, and strong unpredictable variability in the intensity of the appearance of tracks. The hypothesis presented below makes it possible to come closer to explaining not only one aspect of this phenomenon, but the entire set of experimentally discovered properties.

**4.1. Tracks with a periodically repeating complex pattern** can be formed as a result of rolling objects with sizes from 14 to 64  $\mu\text{m}$  [18,19]. The irregularities of these objects are imprinted on the surface of the detector, which ensures the repeatability of the pattern with detected periods from 44 to 200  $\mu\text{m}$ .

**4.2.** It is reasonable to assume that these objects are dust particles suspended in the air. The diversity of dust particle shapes explains the uniqueness of the patterns in different tracks (Fig. 11). The dustiness of the air, and therefore the intensity of the appearance of tracks, depends on many difficult-to-control circumstances. Dust particles, moved by air currents, can penetrate into any places that do not have reliable protection from air penetration.

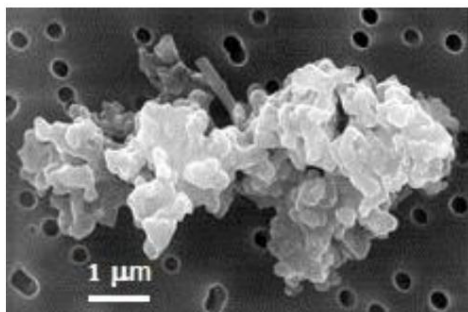


**Fig. 11.** Dust particle under a microscope [20]

**4.3.** In order for a speck of dust to leave an imprint, it must be harder compared to the detector material and pressed quite strongly against the surface  
detector. If count square contact of dust with the surface

detector  $1 \text{ } \mu\text{m}^2$  and a tensile strength of 50 MPa (polycarbonate), for irreversible deformation a force of  $f \sim 5 \cdot 10^{-5} \text{ N}$  is required.

**4.4.** Let us assume that the force is associated with the electric charge of the dust particle. Let us assume that the dust particle has the shape of a sphere with a diameter  $d = 20 \text{ } \mu\text{m}$ . To be attracted to a flat conductive surface with a force  $f = 5 \cdot 10^{-5} \text{ N}$ , a sphere with a diameter of  $20 \text{ } \mu\text{m}$  must have a charge  $q = 2d (\epsilon_0 f)^{1/2} = 1.5 \cdot 10^{-12} \text{ C}$  ( $9.3 \cdot 10^6$  electron charges). The force of attraction to a dielectric surface is of the same order of magnitude (depends on the permittivity). The electric capacitance of a sphere with a diameter of  $20 \text{ } \mu\text{m}$  is  $C = 2\pi\epsilon_0 d = 1.1 \cdot 10^{-15} \text{ F}$ , the potential is  $\phi = q/C = 1350 \text{ V}$ , the energy of the electric field is  $W = C\phi^2/2 = 1.0 \cdot 10^{-9} \text{ J} = 6300 \text{ MeV}$ , the electric field strength on the surface of the sphere  $E = q/\epsilon_0 d^2 = 1.3 \cdot 10^8 \text{ V/m}$ .

**4.5.** Such a charge can appear in a dust particle when it is near LENR reactor. Experiments show that the agent causing nuclear transmutations acts not only inside but also outside the reactor [9-11]. Discussion of the nature of this agent is beyond the scope of this article. It is this agent, which has a high penetrating ability, that is the "strange radiation". **4.6.** The electron shells of the atoms resulting from nuclear transmutations are in a highly excited state (this is evidenced by the soft X-ray radiation near LENR reactors) [21]. The excitation of the electron shells is removed not only by X-ray radiation, but also by the emission of electrons with energies of up to tens of keV. They are usually absorbed in nearby areas of the surrounding matter. But in the case of a small dust particle, they can escape. For example, the mean free path of an electron with an energy of 10 keV in a substance with a density of  $2 \cdot 10^3$

$\text{kg/m}^3$  (silicon dioxide) about  $5 \mu\text{m}$  [24]. As a result, the dust particle acquires a positive charge. Considering that each act of nuclear transmutation is accompanied by the loss of one electron, for the dust particle to acquire a charge of  $1.5 \cdot 10^{-12} \text{ C}$

<sup>12</sup> CI requires 9.3. 106 transmutations (approximately one transmutation per 108 atoms substance of the dust particle). 4.7. A high electric field strength near a charged dust particle (~108 V/m) would seem to lead to the ignition of a corona discharge and rapid draining of the electric charge. However, for electron avalanches to occur, not only a high field strength is needed, but also a sufficiently high potential difference [25]. A potential difference of about 1000 V is not enough for this. In addition, dielectric particles are charged volumetrically as a result of nuclear transmutations, which complicates the draining of charges that occurs with

surface. **4.8. A**

speck of dust attracted to the detector surface can either release the energy of an electric charge, forming a microcrater (6300 MeV is quite enough energy for this), or start moving if there is an electric field along the surface or the detector material is non-uniform (its relative permittivity is not constant). There may also be reasons not related to

electric field, for example, the movement of air along the surface of the detector. Moreover, the particle will predominantly not slide, but roll, since the coefficient of rolling friction is 2-4 orders of magnitude less than the coefficient of friction

sliding.

**4.9.** "Smooth" tracks are formed by particles up to 10 µm in size [18,19]. During the movement, heat is released as a result of deformation and destruction of the detector material and the dust particle. This can lead to melting of the material on which the tracks are formed and to smoothing out possible irregularities [18, 19]. It is clear why "smooth" tracks are especially numerous on low-melting materials (plastics).

**4.10.** Brittle materials with a high melting point (e.g. mica, glass) are destroyed by a moving particle not only by pressure, but also by a sharp temperature change. Particularly strong destruction occurs in materials with piezoelectric properties (e.g. lithium niobate) as a result of the action of a strong electric field. Approaching the surface

of a positively charged body causes polarization of the dielectric equivalent to the action of a negative charge of the same magnitude (in our example  $q=1.5 \cdot 10^{-12} C$ ). If the substance has piezoelectric properties with a typical piezoelectric modulus  $d \sim 10-11 C/N$ , it will be compressed with a force  $f=q/d \sim 0.1 N$ . This force acts on an area of about  $10 \text{ } \mu\text{m}^2$  ( $10-11 \text{ m}^2$ ), causing a pressure of  $1010 \text{ Pa}$ , which significantly exceeds the strength limits of conventional materials. **4.11.** "Droplet" tracks. During electrolysis, many droplets of electrolyte are formed in the form of an aerosol. Some of them, being in the area of action of the agent causing nuclear transmutations, acquire a positive electric charge. The properties of such droplets ("charged clusters") were studied in detail in 117

work [23]. They move, periodically approaching and moving away from the detector surface, dropping a cluster much smaller than the main one at the moment of approach. Chains of round traces appear on the detector.

**4.12.** The sharp decrease in the probability of track appearance at a distance of 20-30 cm from LENR reactors is possibly associated not only with the geometric weakening of intensity agent that activates dust particles, but also the limited retention time electrical charges on dust particles.

## 5. Experimental justifications

### 5.1. Modeling the process of track formation as a result of dust particles rolling on the detector surface [22]

#### 5.1.1. Tracks on DVD

- a) For two days, a clean DVD disc without scratches lay on the windowsill next to an open window, with the working surface facing up, collecting dust. Then the working surface of the dusty disc was rubbed against another disc with very light pressure. On the disc traces with periodic patterns appeared, as well as smooth single and double traces, very similar to the tracks of strange radiation (Fig. 12).

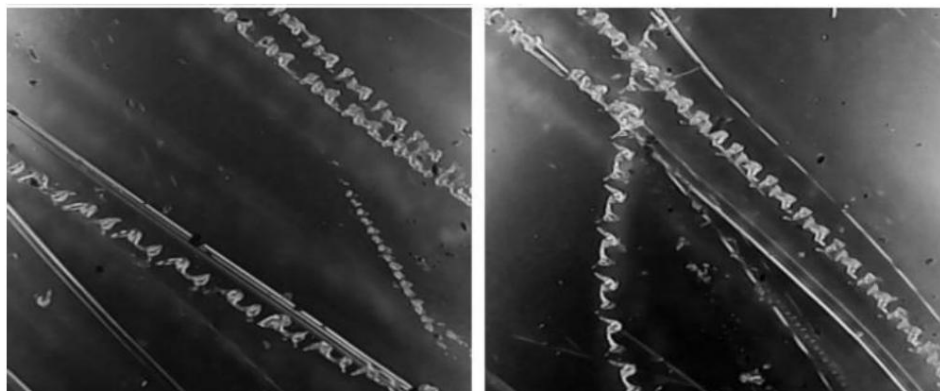


**Fig. 12.** Tracks formed on the surface of a DVD disc when dust particles roll (optical microscope).

- b) Several particles of carbonyl nickel, having a shape close to spherical and a size from 5 to 20  $\mu\text{m}$ , were applied to a fragment of a clean DVD, covered with another fragment of a clean DVD and the upper disk was moved by approximately 1 cm. Several parallel tracks with a width of  $\sim 10 \mu\text{m}$  appeared on the disks (Fig. 13).

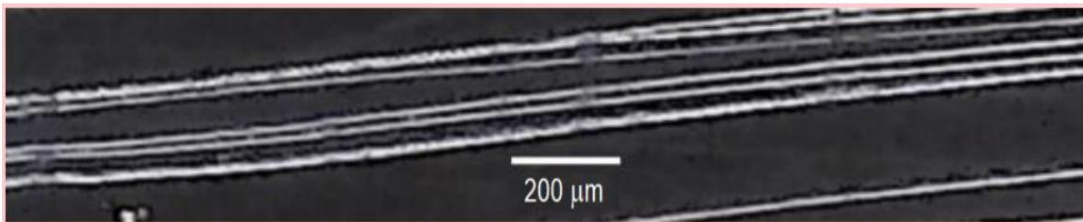


**Fig. 13.** Tracks formed on the surface of a DVD disc when carbonyl nickel particles rolled (optical microscope).



### 5.1.2. Tracks on glass

**Fig. 14.** Arrangement of microscope slides.

Between microscope slides

grains of quartz sand, corundum, carbonyl nickel were placed (Fig. 14).

The compression force of the plates was ~ 1 N (light finger pressure), the movement of the upper glass relative to the lower glass was about 1 cm. Fig. 15 shows one of the tracks that arose when using corundum grains of ~ 50  $\mu\text{m}$  in size. The chaotic nature of the track pattern may be due to the randomness of the process of crack formation in the glass, as well as the gradual destruction of the grain

corundum.

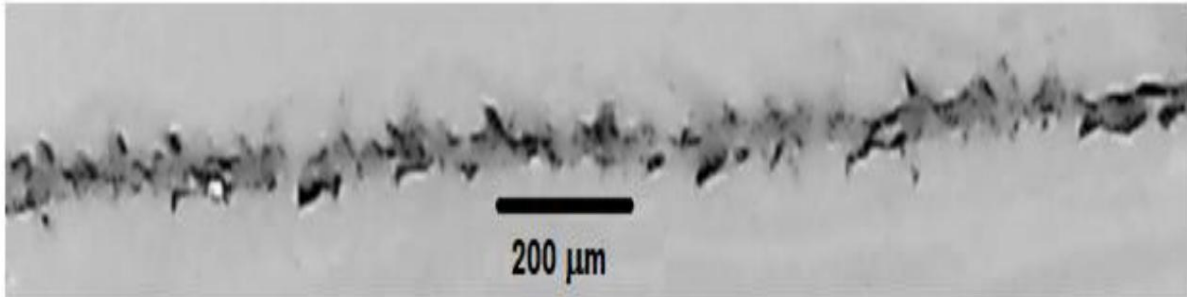


**Fig. 15.** Object glasses, corundum grains ~ 50  $\mu\text{m}$  in size (optical microscope).

When using quartz sand and carbonyl nickel grains, no tracks appeared on the glass (the hardness of these substances is lower than the hardness of glass).

### 5.1.3. Tracks on the photo emulsion

Several grains of quartz sand measuring 100-200  $\mu\text{m}$  were applied to an RM-1 X-ray film measuring 2x5 cm<sup>2</sup>, covered with the same film, and the upper film was moved approximately 1 cm with light pressure. Tracks with a clearly expressed periodicity of the pattern appeared on the films (Fig. 16).



**Fig. 16.** Track on X-ray film from a grain of quartz sand (optical microscope).

These experiments confirm the possibility of the appearance of traces similar to the tracks of strange radiation when various particles roll over the surface of various materials.

## 5.2. High intensity of track formation at high concentration of dust-like particles

A halogen incandescent lamp with a nominal power of 300 W at a supply voltage increased from 220 to 320 V is suspended inside a ceramic tube (Fig. 17). As experiments show, incandescent lamps operating in a forced mode are sources of an agent that causes nuclear transmutations [9-12]. When turned on, the lamp and ceramic tube heat up to a high temperature, which promotes air movement from the bottom up.

If powder, such as corundum, is poured at the bottom, small enough

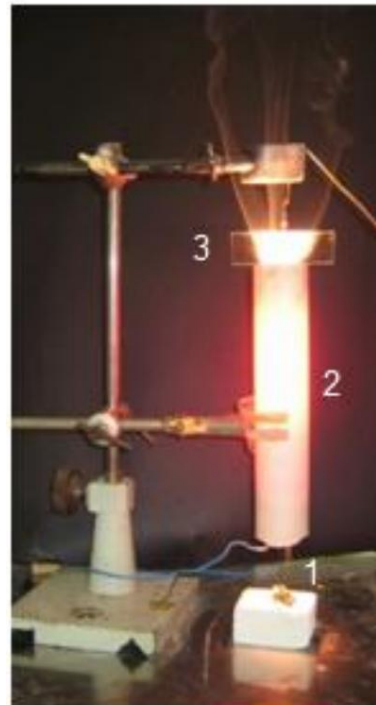
convection

particles are carried away by the rising air flow and pass near the lamp. On top of the pipe there is (for example, a plate) detector Air leaving the pipe with captured particles<sup>glass</sup>

washes the detector.

**Fig. 17.** Track "generator". 1 - aerosol source, 2 - ceramic tube with a halogen incandescent lamp located inside, 3 - detector.

To avoid overheating, the setup can only be turned on for 1 minute. But even this time is enough for tracks to appear on the detectors (examples in Fig. 18). This is a very high intensity. Let us recall that under normal conditions, the appearance of tracks on



square centimeter of the detector, tracks with a total length of 1 mm can be expected in about 37 hours (see section 3.1)

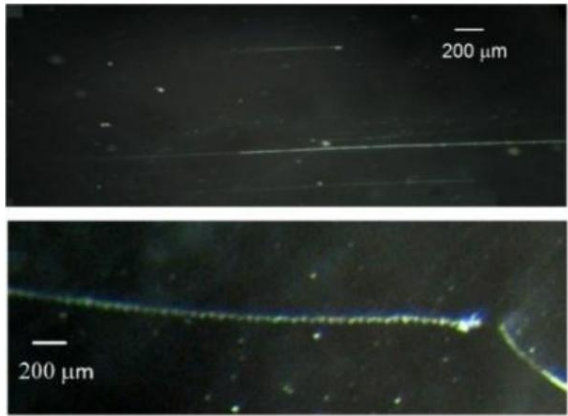


**Fig. 18.** Some of the tracks that appeared on the slides during 1 minute of operation of the "track generator" (optical microscope)

## Conclusion

The assumption that the tracks are formed by dust strange radiation particles suspended in the air or liquids that have acquired an electric droplets of nuclear charge as a result

transmutations allows us to explain many of the features of the phenomenon of strange radiation tracks, indicated at the beginning of the article. The proposed hypothesis answers the questions:

- *why do tracks only appear on the surface;*
- *where do the particles that form the tracks come from;*
- *why do they get an electric charge and what does LENR have to do with it;*
- *how tracks with unique periodic patterns, smooth tracks, cracked tracks and "drip" tracks are created;*
- *why the intensity of track appearance is not constant under seemingly identical conditions.*

The possibility of the appearance of tracks similar to TSI during the movement of dust and dust-like particles pressed to the surface of various detectors has been confirmed experimentally. Based on the proposed hypothesis, an experimental setup has been created in which the intensity of the appearance of tracks

significantly increased compared to the natural process. Thus, the proposed hypothesis allows us to explain a number of characteristic features of the phenomenon of strange radiation tracks that seemed mysterious. At the same time, there are still questions that require reflection and further research.

## LITERATURE

1. Urutskoev L.I., Liksonov V.I., Tsinoev V.G. Experimental detection of "strange" radiation and transformation of chemical elements. *Applied Physics*, 2000, 4:83-100, [http://www.urleon.ru/files/article\\_58.pdf](http://www.urleon.ru/files/article_58.pdf).
2. Matsumoto T., Kurokawa K.. Observation of Heavy Elements Produced During Explosive Cold Fusion. *FusionTechnology*, 1991, 20(3): 323-329.
3. Solin M.I. Experimental facts of spontaneous generation of soliton charge condensate with formation of nuclear fusion products in liquid zirconium. Part 1. *Physical Thought of Russia*, 2001, 1: 43–58, <http://www.invur.ru/print.php?page=proj&cat=neob&doc=solin1> .
4. Rodionov B.U., Savvatimova I.B. On the nature of strange tracks. *Materials 13 Russian Conference Cold Transmutation of Nuclei of Chemical Elements and Ball Lightning (CTNC&BL)*, 2005, 187-205.
5. Shishkin A.L., Tatur V.Yu. Assessment of the impact of strange radiation on biological objects. *Proceedings of the 25th Russian Conference of Chemistry and Nuclear Medicine*, 2018, 76-80.
6. Parkhomov A.G., Alabin K.A, Andreev S.N. etc. Nickel-hydrogen reactors: heat release, isotopic and elemental composition of fuel. *Radioelectronics. Nanosystems. Information technologies (RENSIT)*, 2017, 9(1): 74-93.
7. Alabin KA, Andreev SN, et al. Isotopic and Elemental Composition of Substance in Nickel-Hydrogen Heat Generators. *J. Condensed Matter Nucl. Sci.* 2018, 26: 32, [www.iscmns.org/CMNS/JCMNS-Vol26.pdf](http://www.iscmns.org/CMNS/JCMNS-Vol26.pdf).
8. Parkhomov A.G., Zhigalov V.A., Zabavin S.N., Sobolev A.G., Timerbulatov T.R. Nickel-hydrogen heat generator that operated continuously for 7 months. *Journal of Emerging Directions of Science (JFNS)*, 2019, 23-24(7): 57-63.
9. Parkhomov A.G., Karabanov R.V. Study of elemental and isotopic changes in substance near incandescent lamps. *J. Phys. Science*, 2021, 27(8): 116-119, <http://www.unconv-science.org/pdf/27/parkhomov2.pdf> .
10. Parkhomov A.G., Karabanov R.V. LENR as a manifestation of weak nuclear interactions. A new approach to creating LENR reactors. *RENSIT*, 2021, 13(1):45-58. [http://rensit.ru/vypuski/article/372/13\(1\)45-58.pdf](http://rensit.ru/vypuski/article/372/13(1)45-58.pdf)
11. Parkhomov AG, Karabanov RV, Belousova EO. Investigation of LENR Processes Near Incandescent Metals. *Proceedings of the 23rd International Conference on Condensed Matter Nuclear Science, Xiamen, China June 9–11, 2021. J. Condensed Matter Nucl. Sci.* 2022, 36: 362–376, <https://yadi.sk/d/sZOkktMQkxDjvg> .
12. Zhigalov V.A., Parkhomov A.G., Nevolin V.K. Study of strange tracks radiation near incandescent lamps and electrolytic cells. *RENSIT*, 2023, 15(1): 95-105.
13. Parkhomov A.G. Study of processes in a pulse plasma electrolysis unit. *Proceedings of the 20th Russian Conference of Chemical Technology and Chemical Materials*, 2013, 65-76. <http://www.unconv-science.org/n25/parkhomov>.
14. Parkhomov A.G., Zhigalov V.A., Zabavin S.N., Sobolev A.G., Timerbulatov T.R. Statistics of strange radiation tracks from two types of LENR reactors. *Proceedings of the 25th Russian Conference of Nuclear and Nuclear Mechanics*, 2018, 51-62.

15. Zhigalov V.A., Zabavin S.N., Parkhomov A.G., Sobolev A.G., Timerbulatov T.R. Statistics and structure of strange radiation tracks from two types of LENR reactors. *ZhFSN*, 2018, 21-22(6): 10-25, <http://www.unconv-science.org/pdf/21/zhilalov1.pdf>.
16. Zhigalov V.A. Strange radiation and LENR: what is the connection? *RENSIT*, 2021, 13(3): 329-348
17. Parkhomov A.G., Zhigalov V.A., Zabavin S.N., Sobolev A.G., Timerbulatov T.R. Structure of strange radiation tracks from two types of LENR reactors Proceedings of the 25th Russian Conference on Nuclear and Nuclear Problems, 2018, 63-75 .
18. Zhigalov V.A., Parkhomov A.G. Tracks of strange radiation – motion of solid particles along the surface. *Proceedings of the 27th Russian Conference of Chemistry and Nuclear Materials*, 2022, 51-64 .
19. Zhigalov VA, Parkhomov AG Strange radiation tracks - the movement of solid particles along the surface. *Preprint*. August 2023.  
<https://www.researchgate.net/publication/373257344>
20. <https://ru.wikipedia.org/wiki/%D0%BF%D0%BE%D0%BB%D0%BD%D0%BE%D0%BC%D0%BE%D0%BD%D0%BE%D0%BC>
21. Klimov A.I., Belov N.K., Tolkunov B.N. Measurement of neutron fluxes, soft X-ray radiation in heterogeneous nano-cluster plasma. *Proceedings of the 26th Russian Conference of Chemistry and Nuclear Medicine*, 2020, 29-36 .
22. Parkhomov A.G., Zhigalov V.A. A new approach to the study of strange tracks radiation. *Presentation of the report at the webinar by Klimov-Zatelepin on June 21, 2023* <http://lenr.seplm.ru/seminary>
23. Nikitin A.I., Nikitin V.A., Velichko A.M., Nikitina T.F. Strange traces of "strange" radiation. *RENSIT*, 2022, 14(3): 249-268.
24. Physical quantities. Handbook. Edited by Grigoriev I.S. and Meilikhov E.Z. M.: Energoatomizdat, 1991, p. 1170.
25. Raiser Yu.P. Physics of gas discharge. Moscow: Nauka, 1992, 536 p.

### **Properties of strange radiation tracks. An attempt at explanation**

<sup>1</sup>Parkhomov AG, Zhigalov VA

<sup>1</sup>KIT Experimental Design Laboratory Moscow, Russian Federation, Kazakh

<sup>2</sup>National Research Technical University named after KI Satpayev. Alma-Ata,  
Republic of Kazakhstan

Discovered properties of tracks that occur near installations in which LENR processes take place are described. A hypothesis is presented explaining where the particles that "draw" tracks come from, why the drawings of tracks are unique, why the intensity of the appearance of tracks is unstable. Experiments confirming this hypothesis are described.

# **Mass spectra of tungsten isotopes and their oxides and estimation of the number of massive electron pairs in modified tungsten atoms**

**M.P. Kashchenko<sup>1,2</sup>, M.A. Kovalenko<sup>1</sup> V.I. Pechorsky<sup>2</sup>, N.M. Kashchenko<sup>1</sup>**

<sup>1</sup>UrFU named after B.N. Yeltsin, [mpk46@mail.ru](mailto:mpk46@mail.ru)

<sup>2</sup>USFTU, [mpk46@mail.ru](mailto:mpk46@mail.ru)

The mass spectra of tungsten isotopes and their oxides of the *WOn* type ( $n=1, 2, 3, 4$ ) are presented, containing "spikes" of atoms and oxides with increased masses. These "spikes" are caused by modified tungsten and oxygen atoms, in the electron shells of which massive compact electron pairs are present. A comparison of the spectra allows us to state that in the analyzed cases the modified tungsten atoms contain no more than two electron pairs.

## **Introduction**

The conceptual solution to the problem of cold fusion of nuclei proposed in [1, 2] is based on a generalization of the known reaction of muon catalysis. In this case, the functions of the reaction catalyst are performed by KK activators, which are ring orbits on which compact massive electron (ee) pairs are located. The spins of the electrons in the pair are opposite. When the coupling is due to the magnetic dipole-dipole interaction (on the Compton scale), we will use the designation (ee) $\circlearrowright$ . If the coupling is realized due to the contact interaction [3] (on the hadron scale), we will use the designation (ee) for the pairs, as in cases where the nature of the coupling is not significant. It is clear that with a certain number of (ee) pairs between positive nuclei, the nuclei will begin to converge to critical distances of the order of the radius of the strong interaction. Thus, the main problem of overcoming the Coulomb barrier that exists between the "bare" nuclei is removed.

Such a simple explanation poses the problem of experimental confirmation existence of (ee) – pairs. One of the most important areas of research is mass spectroscopy. The fact is that the entry of a massive (ee) – pair into the electron shell of an atom (or even into its nucleus [4]) should be accompanied by the appearance of modified atoms with increased masses  $m^*$ , exceeding the masses  $m$  ordinary atoms. At present, such atoms have been discovered (see, for example, [5-7]). Therefore, the issues of determining the number of (ee)-pairs in modified atoms, assessing the width of the mass spectrum of an individual (ee)-pair and, in general, the need to take (ee) -pairs into account in physical materials science come to the fore [8-11].

As was shown in [12] using titanium as an example, the number of (ee) – pairs can be determined by comparing the mass spectra of isotopes of the initial element  $X$  and its oxides. In this case, the data on the electronic structure of the initial atom and the assumed electronic structure of the modified atom  $X^*$  are taken into account. In this work, we use the technique [12] of the spectra of isotopes of  $W$  and their oxides of the type *WOn* ( $n=1, 2, 3, 4$ ). 124

for mass analysis –

We will use the simplified binary gradation for the states of  $X^*$  atoms introduced in [12]. If (ee) - pairs occupy stationary deep orbitals near nuclei, then the states of the  $X^*$  atom are designated (index  $d$  from "down"), where  $n$  is

number of (ee) - pairs. In case  $n = 1$ , the value of  $n$  is not given, since the symbol (\*) already indicates the modification of the atom. If (ee) - pairs of atoms\* are in non-stationary states, trying to dive into deep orbitals and disturbing the states of ordinary electrons, then the states are designated (index  $u$  from "up"). Mixed  $du$  variants are also possible. For example, the designation corresponds to an atom\* with two (ee) - pairs, of which only one is in a stationary orbital.

Dipole-dipole interaction is capable of forming pairs at greater distances, compared to contact interaction. Smaller masses (ee) - steam should increase the time of their "immersion" from non-stationary u-states to  $d$  - states. This is especially true for elements with large charge numbers of nuclei Z (such as W-74), which have multilevel electron shells. Therefore, we will assume that (ee)- pairs in the shells of modified tungsten atoms\* are predominantly of the  $u$  -type, and for brevity, we will omit the  $u$  symbol. For example, for tungsten atoms\* with one (ee)- pair, we will use the designation .

### **Electron configurations of W and W\* atoms and structural schemes for tungsten oxides**

#### **The electron formula of the tungsten atom in the order of levels:**

$$1s2\ 2s2\ 2p6\ 3s2\ 3p6\ 3d10\ 4s2\ 4p6\ 4d10\ 4f14\ 5s2\ 5p6\ 5d4\ 6s2. \quad (1)$$

#### **The reduced electron configuration of W is:**

$$[Xe] 4f14 5d4 6s2 \quad (2)$$

Since not only the xenon shell  $[Xe]$ , but also the f-subshell are completely filled with electrons, the oxidation states (CO) are permissible for W atoms : + 2, +3, +4, +5, +6 (when giving up d- or s-electrons).

However, the electron formula of the tungsten atom, in order of increasing orbital energies, contains 6s states just above the  $[Xe]$  configuration:

$$[Xe] 6s^2 4f 14 5d4. \quad (3)$$

From (3) follows the possibility of tungsten behavior, first of all, as a tetravalent metal. Then CO + 2, + 3, + 4 correspond successively to the oxides  $WO$ ,  $W_2O_3$  and  $WO_2$  for ordinary atoms. It is obvious that in this case the tungsten atom gives up two, three or four electrons from the states  $5d4$ . Let us first discuss the variant when the modified  $W^*$  atoms are electrically neutral and form oxides with unmodified

atoms of the main oxygen isotope  $^{16}O$  (without taking into account possible covalent bonds of oxygen atoms).

Then, for example, the appearance of one (ee) - pair in the electron shells of  $W$  atoms leads to atoms accompanied by the loss of two ordinary electrons. The remaining two 5d2 electrons are capable of providing the formation of only the simplest oxide  $W^*O$ . In the mass spectrum of such oxides, one "peak" should be present. Obviously, at  $CO + 4$ ,  $W$  atoms , having received two (ee) - pairs in the electron shell, are not capable of forming oxides. In this become atoms case, "peaks" in  $W^*O_2$  oxides should be absent, as in titanium oxides, when tungsten isotopes capture two (ee) - pairs.

If there are "spikes" in the mass spectra of  $W^*O_2$  oxides , this indicates either  $CO + 4 W^*$  atoms or the formation of a covalent bond between oxygen atoms (at  $CO + 2$  atoms). These options are shown schematically in Fig. 1.

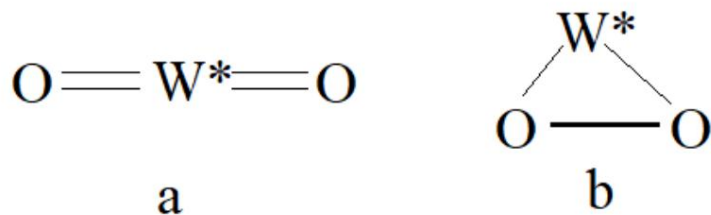


**Fig. 1.** Schematic structure of  $W^*O_2$  oxides with one (ee) - pair in the electron shell of neutral  $W^*$  atoms: a)  $CO + 4$ , b)  $CO + 2$  (the thick line corresponds to the covalent bond, in contrast to the thin lines corresponding to the ionic type of bond)

At the oxidation state of +6,  $WO_3$  oxides should be observed in the mass spectrum. The presence of  $W^*O_3$  oxides with increased mass at electroneutrality and  $CO + 4$  for  $W^*$  is possible when taking into account the covalent bond between a pair of oxygen atoms, as shown in Fig. 2 b.

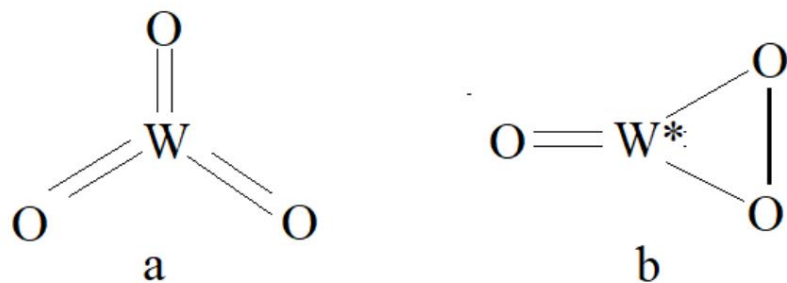


**Fig. 2.** Schematic structure of oxides:  $WO_3$  at  $CO + 6$  of the  $W$  atom (Fig. 2 a) and  $W^*O_3$   $CO + 4$  for the  $W^*$  atom with one (ee) - pair in the electron shell, taking into account the covalent bond between the oxygen atoms (Fig. 2 b)

Taking into account the covalent bond of oxygen atoms, it is easy to propose schemes oxides  $WO_4$  (Fig. 3 a, 3 b) and  $W^*O_4$  (Fig. 3 c)

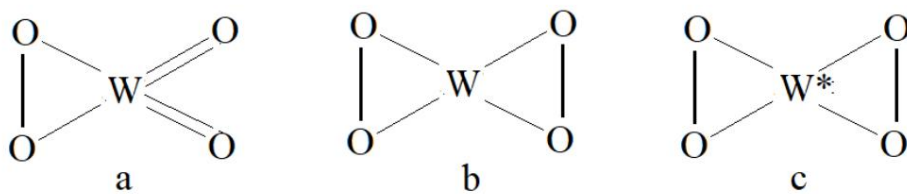


**Fig. 3.** Schematic structure of oxides:  $WO_4$  for the  $W$  atom at  $CO + 6$  (Fig. 3 a) and at  $CO + 4$  taking into account the covalent bonds of the  $O$  atoms (Fig. 3 b), as well as  $W^*O_4$  at  $CO + 4$  for the  $W^*$  atom with one ( $ee$ ) -pair in the electron shell taking into account the covalent bonds between the oxygen atoms (Fig. 3 c).

Formally, it is easy to continue such schemes, for example, for oxide complexes  $WO_5$ ,  $W^*O_5$  or  $WO_6$ ,  $W^*O_6$ . However, for comparison with the results of experimental mass spectra of oxides with one  $W$  atom and a relatively small number of oxygen atoms, it is more useful to supplement the analysis taking into account the modification of oxygen atoms. For certainty, we assume that the  $O^*$  atoms correspond to the capture of one (*its*) - pair of the main isotope  $8O16$ . Then, chemically, the  $O^*$  atoms will be close to carbon. We also assume that the  $O^*$  atoms, when interacting with  $W$  (or with each other due to covalent bonds), tend to fill *the 2p* - subshell, which has 4 vacant states. With these assumptions, the following variants are compared to the realizations of the simplest oxides:

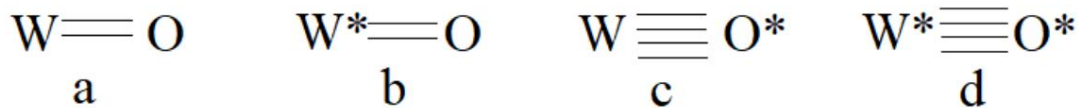


**Fig. 4.** Variants of tungsten oxide formation taking into account the possibility of modifying oxygen atoms.

It is obvious from Fig. 4 that the appearance of variants *c* and *d* should be accompanied by an increase in the intensity and width of the "peaks", and due to variant *d*, one can also expect a shift in the peak maximum toward larger masses of the average spectrum. In the limiting case of a large number of oxides of type *d*, additional "peaks" could also arise in the group of lines of the mass spectra of tungsten oxides with one oxygen atom.

But the actual formation of such complexes with a large number of oxygen atoms, although possible, is less probable than complexes with a smaller number of oxygen atoms. As a comparison of the mass spectra of titanium isotopes and their oxides shows, the constant "markers" of the presence of ( $ee$ ) -pairs in the electron shells are mainly single "peaks" to the right of the main peak. Therefore, the most probable anomalies in the mass spectra of tungsten oxides are expected as the presence of single "peaks", which does not exclude their superposition character associated with the contributions of modified oxygen atoms.

### Mass spectra of W , WO and WO<sub>2</sub>

Experiments with arc discharges were carried out in air using a tungsten cathode. Various metals (titanium, aluminum, iron, tin, lead, tantalum) were used as anodes. This paper focuses on the results obtained for tungsten atoms and tungsten oxides (with one W atom) using various anodes.

To determine the mass spectrum of the elements of the surface layers of the electrodes, as well as the surface of the copper substrate on which the atoms from the interelectrode plasma were deposited, a time-of-flight mass spectrometer of secondary ions was used: Phi Trift V nanoTOF with a sensitivity of up to 107 at/cm<sup>2</sup>. The composition of scrapings from the surfaces was analyzed at different durations of preliminary etching with an argon gun, including the initial (without etching) version. The results given below are practically independent of the etching time. The mass spectrum in Fig. 5 clearly demonstrates three groups of peaks, comparable to tungsten WO<sub>2</sub>.

isotopes And their oxides WO,

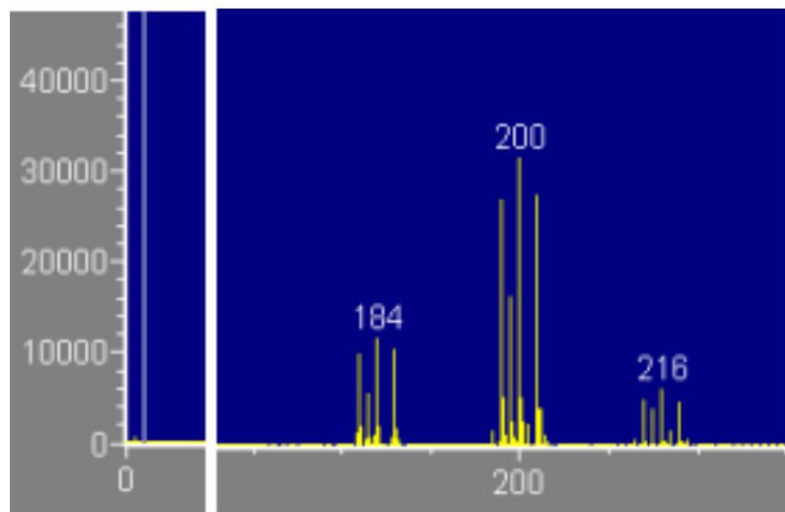


**Fig. 5.** Part of the mass spectrum (in amu units) of a scraping from a tungsten cathode, including three groups of lines of W isotopes and WO, WO<sub>2</sub> oxides.

Groups of lines for the oxides WO<sub>3</sub> and WO<sub>4</sub> having lower intensity will be given below.

The tungsten spectra in Fig. 6 show clearly defined “peaks” to the right (W\* atoms with masses m\*) of the main peaks (W, m) and significant broadenings to the left from the main peaks.

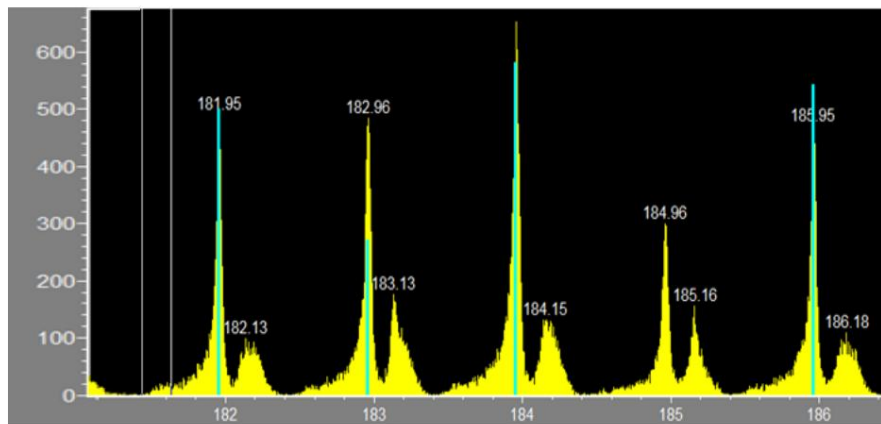


**Fig. 6.** Mass spectrum (in amu units) of four tungsten isotopes: main peaks (blue) with obvious "spikes" on the right and anomalous broadening on the left

The nature of the anomalous broadening to the left of the main peaks is due, according to [12], to small changes in the ion velocities that occur during the process of electrons escaping from the atomic shell during the formation of a massive (ee) - pair in the shell. That is, this fact also indirectly testifies in favor of the existence of (ee) - pairs.

Fig. 7 shows the mass spectra of the simplest tungsten oxides.

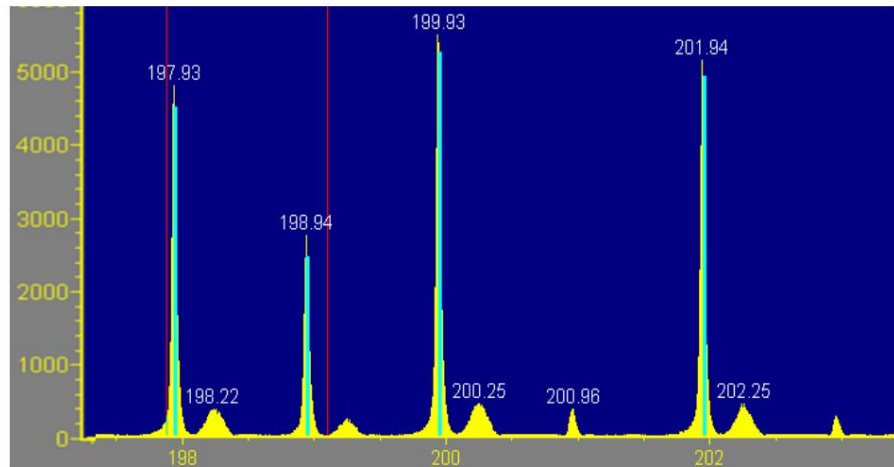


**Fig. 7.** Mass spectra (in amu units) of oxides of tungsten isotopes.

Firstly, a noticeable decrease in the broadening on the left of the main peaks compared to the spectrum of tungsten isotopes is visible. This is consistent with the conclusion that the broadened regions corresponded to W\* atoms with several (ee) - pairs, incapable of forming oxides. Secondly, the "peaks" to the right of the main peaks are shifted relative to the WO peaks by one and a half times more than in W\* atoms. This most likely indicates contributions from oxides, in which tungsten atoms, having the initial CO + 6, can contain either two bound electron pairs ( or ), or one (ee)

-pair, but the modified atom  $W^*$  is linked to the modified oxygen atom  $O^*$  (case d in Fig. 4).

Fig. 8 and Fig. 9 show the mass spectra of tungsten dioxides.

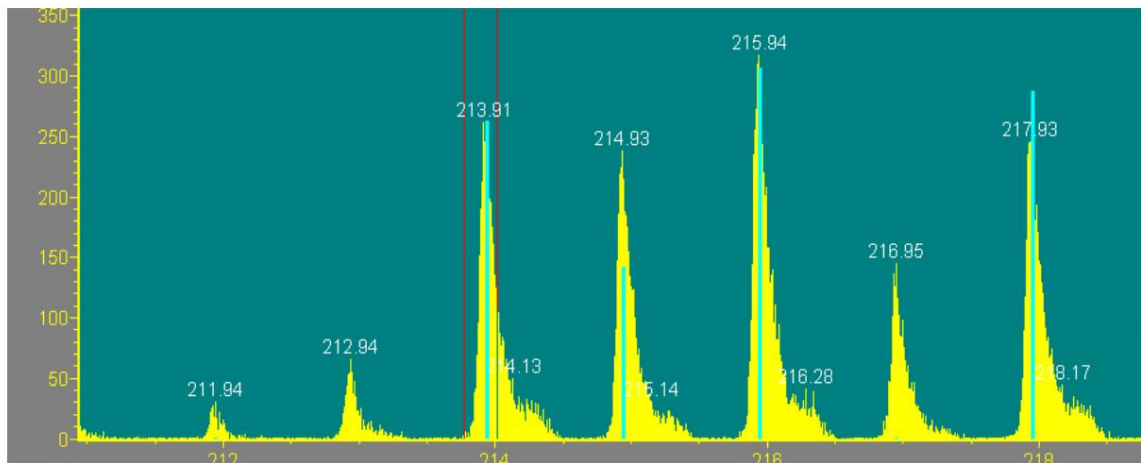


**Fig. 8.** Mass spectra (in amu units) of tungsten dioxides (without clearly defined “peaks”).

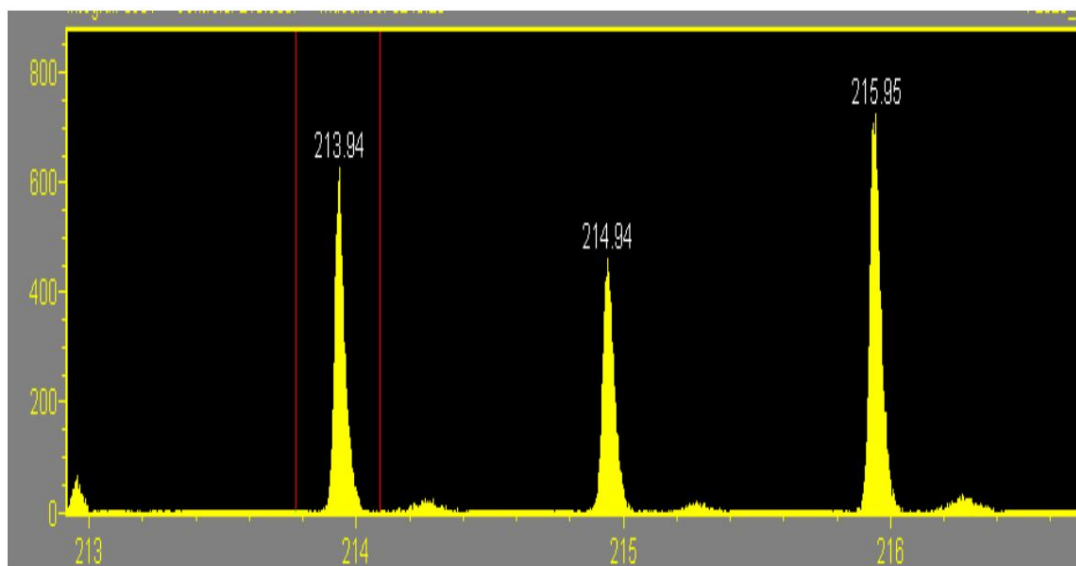


**Fig. 9.** Mass spectra (in amu units) of tungsten dioxides (with clearly defined “peaks”).

The difference between Fig. 8 and Fig. 9 can be interpreted, similarly to [12], as exclusion from the spectrum of tungsten dioxides in Fig. 8 of dioxides containing tungsten atoms with  $(ee)\mu$  pairs.

### Mass spectra of $WO_3$ and $WO_4$

Figures 10-12 refer to the mass spectra of  $WO_3$  and  $WO_4$  oxides, including, apparently, variants with modified  $W^*$  and  $O^*$  atoms.

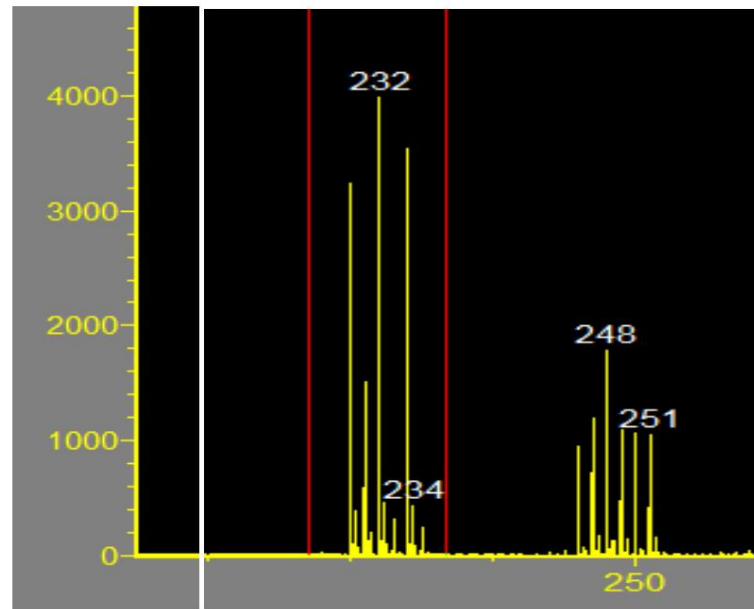


**Fig.10.** Mass spectra (in amu units) of tungsten oxides  $WO_3$  and  $WO_4$  (lines 249 and 251 do not apply to  $WO_4$ )

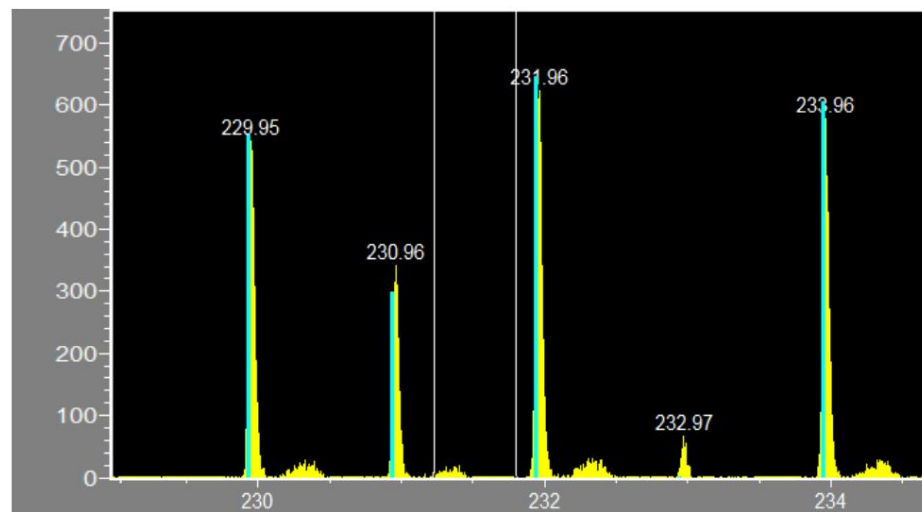


**Fig.11.** Mass spectra (in amu units) of tungsten oxides  $WO_3$  (with clearly defined "peaks").

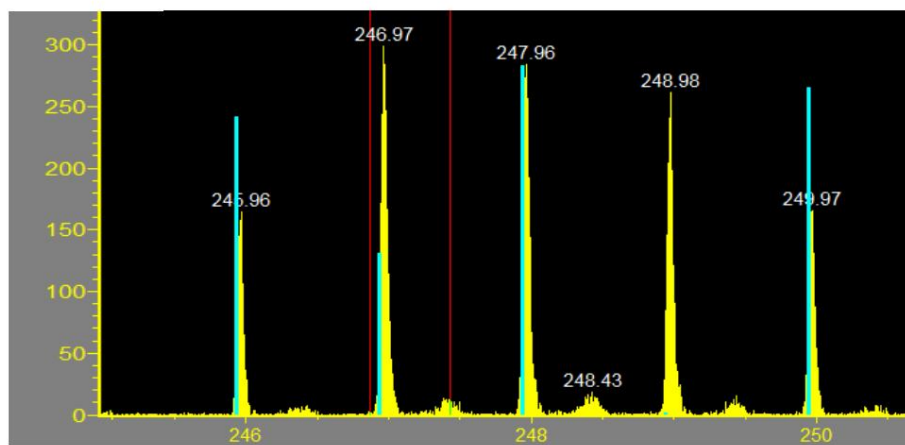


**Fig. 12.** Mass spectra (in amu units) of tungsten oxides  $WO_4$  (with clearly defined "peaks").

### Discussion of results

Comparison of the mass spectra of tungsten and its oxides  $WOn$  ( $n=1, \dots, 4$ ) demonstrates the following patterns.

1. In the spectrum of oxides of all isotopes of tungsten are present, as in the spectrum tungsten isotopes, "spikes" to the right of the main peaks.
2. The shift of the maxima of the "peaks" in oxides in relation to the main peaks is somewhat greater than the similar shift of the "peaks" for tungsten, and the displacements increase with increasing  $n$ , so that the displacements of the right boundaries of the "peaks" reach and even slightly exceed (at  $n = 4$ ) 0.5 amu.
3. As  $n$  increases, the broadening on the left of the main peaks decreases noticeably compared to the left broadening for the tungsten peaks. This supports the already presented ideas that link this type of broadening of the mass spectrum with modified atoms that reach the detector faster due to the additional momentum during the formation of (ee)- in the electron shell.  
steam.

It is clear that if the  $[Xe] 4f14$  configuration is preserved and there are three (ee)-pairs in the electron shell, the modified tungsten atoms cannot form oxides. So the absence of "spikes" in the spectra of tungsten oxides (with the presence of "spikes" in the spectrum of tungsten) would indicate three (ee)-pairs in the  $W^*$  atoms. Since "spikes" are present in the spectra of oxides, it can be stated that the modified tungsten atoms contain one or two (ee)-pairs.

"Spikes" in the mass spectra of tungsten oxides are most likely of a superposition nature, reflecting variants of compositions including modified tungsten atoms with one or two (ee)- pairs in combination with ordinary O and modified  $O^*$  oxygen atoms. The number of combinations increases with increasing  $n$  and the oxidation state of tungsten. To illustrate this, Fig. 13 shows structural diagrams of oxide molecules in

on the assumption that the  $W^*$  and  $O^*$  atoms contain one (ee)-pair each, and the oxidation state of  $W$  takes the values +2, +4. When constructing the diagrams, it is assumed that  $W$  has 4 electrons for the bond, and  $W^*$  only +2.

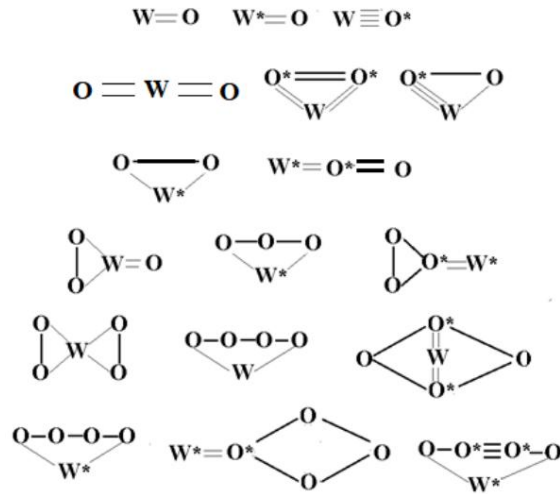


**Fig.13.** Part of the variants of structural schemes for oxide molecules

It is clear from the given schemes that as  $n$  increases, the number of components of the "spike" with different masses increases. However, such a detailed specification of the mass spectrum is beyond the scope of this work.

## Conclusion

The mass spectra of tungsten and its oxides of the  $WO_n$  type contain "peaks" corresponding to increased masses, and the mass shifts for the oxides exceed the shifts for tungsten, reaching 0.5 amu. The comparison of the mass spectra allows us to state that in the observed spectra the atoms of modified tungsten contain no more than two bound massive electron pairs.

The authors are grateful to the participants of the conference RKHTYA and SM-28 for the discussion results of the work and useful comments.

## Literature

1. Kashchenko M.P., Balakirev V.F. Model of intermediate quasi-molecular state and variants of synthesis of chemical elements. // Letters on materials. 2018. **8** (2). P. 152 – 156.  
DOI: 10.22226/2410-3535-2018-2-152-157 2.
2. Kashchenko M.P., Kashchenko N.M. Low-temperature nuclear fusion: introduction to the problem and its conceptual solution. Ekaterinburg: USLTU, 2022. - 180 p.
3. Santilli. R. M. Foundations of Hadronic Chemistry. With Applications to New Clean Energies and Fuels. Boston - Dordrecht - London: Kluwer Academic Publishers, 2001. – 544 p.

4. Santilli R. M. Apparent Experimental of Pseudoprotons Confirmation  
and Their Application to New Clean Nuclear Energies // International Journal of Applied Physics and Mathematics. 2019.  
Vol. 9, No. 2. P. 72 – 100.
5. Kashchenko M.P., Kovalenko M.A., Pechorsky V.I., Kupryazhkin A.Ya., Kashchenko N.M. // "Registration of titanium atoms with increased mass as a consequence of the capture of massive electron pairs". Mat. RKHTYA-27. Moscow, 2023. Pp. 159 - 165.
6. Kashchenko M., Kovalenko M., Pechorsky V., Kupryazhkin A., Kashchenko N. Mass spectroscopic registration of modified tungsten isotopes with increased masses. Abstracts of the 15th International Ural Seminar "Radiation Physics of Metals and Alloys", published by IPM Ural Branch of the Russian Academy of Sciences, Yekaterinburg, abstracts, 2024.  
P. 30-31 https://radiation.imp.uran.ru/Eng/AbstractBook\_15.pdf DOI: 10.13140/RG.2.2.17245.83682
7. Kashchenko M., Kovalenko M., Pechorsky V., Kashchenko N. Mass spectra of modified tungsten isotopes. Preprint. October 2024. <https://www.researchgate.net/publication/385193135>.  
DOI: 10.13140/RG.2.2.22037.95206.
8. Kashchenko M.P., Kashchenko N.M. Massive electron pairs as possible initiators of the electroplastic effect / Current issues of strength: Collection of abstracts LXVII  
International Conference (Ekaterinburg, April 2, 2024) / editor-in-chief D.V. Zaitsev. Ekaterinburg: UGMU Publishing House, 2024. Pp. 41 - 42.
9. Kashchenko M.P., Kashchenko N.M. Synthesis of elements during ultra-deep penetration of particles using the example of silicon carbide penetration into aluminum / In the collection: Physics and Technology of Advanced Materials - 2023.  
Collection of Proceedings of the International Conference. Ufa, 2023. pp. 147-148.
10. Kashchenko M.P., Kashchenko N.M. Massive electron pairs as an object of radiation materials science / In the collection:  
Interaction of radiation with a solid body. Proceedings of the 15th International Conference. Minsk, 2023. P. 164 - 167.
11. Kashchenko M.P., Kashchenko N.M. Nanopowders as a promising material for obtaining chemically modified atoms / In the collection: Ultrafine-grained and nanostructured materials / ed. A.A. Nazarov. - Ufa: RIC UUNIT, 2024. Pp. 103 - 104.
12. Kashchenko M., Kovalenko M., Pechorsky V., Kashchenko N. Mass spectra of titanium isotopes  
and their oxides and estimation of the number of massive electron pairs in modified titanium  
atoms. Preprint. May 2024.  
<https://www.researchgate.net/publication/380324916>. DOI: 10.13140/RG.2.2.36243.08488.

## Mass spectra of tungsten isotopes and their oxides and estimation of the number of massive electron pairs in modified tungsten atoms

M. P. Kashchenko<sup>1,2</sup>, M.A. Kovalenko<sup>1</sup> VI Pechorsky<sup>2</sup> , NM Kashchenko<sup>1</sup>

<sup>1</sup> UrFU named after BN Yeltsin, [mpk46@mail.ru](mailto:mpk46@mail.ru)  
USFEU , [mpk46@mail.ru](mailto:mpk46@mail.ru)

The mass spectra of tungsten isotopes and their oxides of the WOn type ( $n = 1, 2, 3, 4$ ) are presented, containing "spikes" of atoms and oxides with increased masses. These "spikes" are caused by modified tungsten and oxygen atoms, in the electron shells of which massive compact electron pairs are present. A comparison of the spectra allows us to state that in the analyzed cases the modified tungsten atoms contain no more than two electron pairs.

## **Lightning-like erosion structures of the activating effect of light, magnetic field and magnetorheological fluid on the remaining magnetic charges in solid zirconium after their generation in nuclear transformations in electron melting**

**Solin M.I.**

Microenterprise "IP Solin I.M."  
solmiv@mail.ru

It was previously established experimentally that in the experiments conducted in 1976-78 under conditions of industrial electron melting of zirconium, when the critical mass of the melt was reached, anomalous nuclear structural-phase transformations were spontaneously initiated in it. These processes proceed with the transformation of nuclear energy into electromagnetic energy due to the generation of magnetic charges under these conditions. The mass of liquid zirconium was 250-350 kg, the accelerating voltage of the electron beam was 30 kV, the current of the electron beam was 26-30 A.

The obtained results of the experimental studies were published in the journals Physical Thought of Russia (2001), Proceedings of the Russian Chemical Society and the Russian Chemical Society (2004, 2009), in patents of Russia (No. 2087951, 1992-97, 2173894, 2001), Kazakhstan (No. 14139, 2004), Belarus (No. 8353, 2006) for pioneering inventions in the development of an environmentally friendly new energy source - a quantum nuclear reactor with control elements. Based on the study of numerous interrelated experimental data, it was found that magnetic charges have the property of strongly destroying the

structure of zirconium both under conditions of extreme electron melting and after switching off the electron beam. In this regard, the task was set: to find out whether magnetic charges are preserved in statics in solidified zirconium. Therefore, after the completion of metallographic studies in February - March 1990, long-term observations were carried out on the state of the surfaces of samples cut from a zirconium ingot obtained in 1976. The first results confirming the existence of magnetic charges in statics were obtained in June 2001, and subsequently in April 2009. In the latter case, this fact manifested itself in the form of erosion of brightly glowing round formations symmetrically lined up on the surface of one of the samples. Their number increased sharply when it was illuminated by an incandescent lamp with a power of 40 W, resulting in the formation of a permanently preserved extended track. Tracks of the same type were formed when the samples were located between two permanent magnets with different polarity with a magnetic induction of 2.3 T. Under the influence of the magnetic field of electromagnetic windings extracted from the housings of electric motors with a power of 300 and 600 W and connected to a 220 V electrical network, they arose in a shorter time (during the experiment). After applying a magnetorheological fluid to the surface of a zirconium sample (April 2021), a hydrodynamic pattern of movement arose

migrating white glare after a moment of appearance and disappearance of round brightly glowing point objects in it, which occurs with subsequent volumetric destruction of the structure of its solidifying layer. It is caused by the effect of the emitted spherical magnetic field of magnetic charges in solid zirconium. In its magnetized liquid layer, the said objects are

magnetic domains exploded.

The resulting tracks display the nature of the impact of a highly disturbed, explosively acting energy source in the form of small-sized lightning radiation in the surface layers of the samples and magnetorheological fluid. It is concluded that continuous transformations occur in the mass (structure) of magnetic monopoles that are static - discharges with very low intensity, which manifest themselves after many years due to their destructive effect on the zirconium structure. The detected effects are clearly manifested in the zones of concentrated accumulation (spherical magnetic domains) of these particles.

Light, constant, alternating magnetic field and magnetorheological liquids have an activating effect on these processes.

The electron beam exerts an even stronger activating effect on magnetic charges, leading to the emergence of magnetic lightning - alternating magnetic currents under conditions of extreme electron melting. This conclusion is consistent with the data obtained and the characteristic features of the discovered phenomena described in the above-mentioned works.

## **Lightning-like erosive structures of the activating effect of light, magnetic field and magnetorheological fluid on preserved magnetic charges in solid zirconium after their nucleation in nuclear transformations in electronic melting**

**Solin MI**

[solmiv@mail.ru](mailto:solmiv@mail.ru)

Previously, it was experimentally established that in the 1976-78 years under the conditions of industrial electronic melting of zirconium, when the critical mass of the melt is reached, abnormal nuclear structural and phase transformations are spontaneously initiated in it. These processes occur with the transformation of nuclear energy into electromagnetic energy due to the generation of magnetic charges under these conditions. The mass of liquid zirconium was 250-350 kg, the accelerating voltage of the electron beam was 30 kV, the current of the electron beam was 26-30 A. The obtained results of experimental studies have been published in the journals of Physical Thought of Russia (2001), materials of the RCCTE (2004, 2009), in patents of Russia (No. 2087951, 1992-97, 2173894, 2001), Kazakhstan (No. 14139, 2004), Belarus (No. 8353, 2006 G.) on pioneering inventions for the development of an environmentally safe new energy source – a quantum nuclear reactor with regulatory elements.

Based on the study of numerous interrelated experimental data, it has been established that magnetic charges have the property of strongly destroying the structure of zirconium

both under conditions of extreme electron melting and after switching off the electron beam. In this regard, the task was set: to find out whether magnetic charges remain static in solidified zirconium. Therefore, after the completion of metallographic studies in February - March 1990, long-term observations were carried out on the condition of the surfaces of samples cut from a zirconium ingot obtained in 1976.

The first results confirming the existence of magnetic charges in statics were obtained in June 2001, and subsequently in April 2009. In the latter case, this fact manifested itself in the form of an erosive formation of brightly glowing round formations symmetrically lined up on the surface of one of the samples. Their number increased dramatically when illuminated by an incandescent bulb with a power of 40 watts, as a result, a permanently preserved extended track was formed, the same type of tracks were formed when the samples were placed between two permanent magnets with different polarities with a magnetic induction of 2.3 Tl. Under the influence of the magnetic field of the electromagnetic windings extracted from the housings of electric motors with a power of 300 and 600 watts and connected to the electrical network (220 V), they arose in a shorter time (during the experiment).

After applying a magnetorheological liquid to the surface of a zirconium sample (April 2021), a hydrodynamic pattern of the movement of migrating white glare appeared after the instant of the appearance and disappearance of round brightly glowing point objects in it, followed by a volumetric destruction of the structure of its solidifying layer. It is caused by the action of the radiated spherical magnetic field of magnetic charges in solid zirconium on it. In its magnetized liquid layer, these objects – magnetic domains - exploded. Problems that have arisen The resulting tracks reflect the nature of the impact of a highly disturbed, explosively acting energy source in the form of small-sized lightning radiation in the surface layers of samples and magnetorheological fluid.

It is concluded that in the mass (in the structure) of magnetic monopoles in static, continuous transformations occur - discharges with very low intensity, which manifest themselves after long years due to their destructive effect on the zirconium structure. The detected effects are clearly manifested in the zones of concentrated accumulation (spherical magnetic domains) of these particles. Light, a constant, alternating magnetic field and a magnetorheological fluid have an activating effect on these processes. The electron beam has an even stronger activating effect on magnetic charges, leading to the appearance of magnetic lightning – alternating magnetic currents in conditions of extreme electronic melting. This conclusion is consistent with the results obtained in the above mentioned works.

## **Experiments with torsinds or the effect of accelerated rotation of a body on another stationary body. Hypothesis of gravity.**

V.A. Chizhov Chijov\_va@bk.ru

I.N. Stepanov stepanovigorn@gmail.com

The work shows that accelerated rotation of a gyroscope with constant acceleration ( $\ddot{\gamma} = \sim 25 \text{ rad/s}^2$ ) or accelerated rotation of a disk of  $150 - 200 \text{ mm}$

(corundum or metal) affects sensors isolated from these objects, which are called *torsinds*,  $74 \text{ mm}$  in diameter, weighing less than  $0.4 \text{ g}$ . The artifact was that when the body (gyroscope or disk) was acceleratedly rotating, isolated from the torsind (the torsind is placed in a sealed glass flask), it began to slowly rotate in the opposite direction, i.e., if the body rotated clockwise, the torsind rotated counterclockwise and vice versa. Torsinds rotate like gears when the body of rotation and the torsind come into contact (the torsind rotates very slowly), but there is no contact of the rotating body with the torsind in this process. It was this fact that attracted the study and an attempt to understand it. To explain this artifact, a hypothesis was introduced about the existence and violation of the diffusion gradient layer of ether at the surface of the accelerated rotating body. An assessment was made of the coefficient of transfer of accelerated rotation of the gyroscope to torsinds made of aluminum and mica, which are isolated in a separate environment. It was these experiments with torsinds that led to the hypothesis of gravitational action being proposed as a new view of gravity.

### **Experiment**

The experiments were conducted with disks of aluminum foil, mica, and paper sheet. The diameter of the torsinds was  $74 \text{ mm}$ ; the weight of the disks did not exceed  $0.4 \text{ g}$ . Each of the torsinds was placed in a chemical beaker  $80 \times 200 \text{ mm}$  (manufactured in Belarus), the torsind was centered, and the flask (chemical beaker) was hermetically sealed.

Various actions on these sensors were tested:

1. Magnetic field of  $2800 \text{ G}$  does not work;
2. The electrostatic field has a significant effect on all torsinds. Plastic rubbed against wool sets disks of aluminum, mica, paper in motion: they move after the electrified object.
3. The luminous flux of  $360 \text{ lm } 5 \text{ W}$  (white flashlight) has an effect on all torsins, but the strongest effect on the torsin with an aluminum disk. Focusing a light spot of  $2 - 2.5 \text{ cm}^2$  on the left side of the torsin surface at an angle of about  $30$  degrees after some time causes rotation in the direction of the beam. When the beam is transferred to the other side of the disk, it rotates in the opposite direction.

### The effect of the gyroscope on the torsinds

**torsinds** Electrostatics were removed from the glass by wiping with wet hands, which allowed to get rid of the influence of electrification. Only after this check were experiments conducted with the gyroscope gaining rotation.

**Gyroscope.** A three-phase gyroscope from a German aircraft (1942) by Henkel (Germany) was used in the experiments:

1. Maximum speed *40,000 rpm*;
2. Acceleration time to maximum speed *3.5 min*;
3. Gyroscope dimensions: diameter *53 mm*, height *32 mm*;
4. Gyroscope weight *280 g*;
5. Weight of active rotating part *50 g*.

It should be noted that this experiment with torsinds should be classified as high-precision (very sensitive to external influences). For example, when trying to take a picture on a sunny summer day on an outdoor table, the torsinds began to rotate chaotically. Therefore, all experiments with torsinds were conducted in a darkened room. If the technical accuracy of the experiment preparation is observed, the process is reproducible.

"Bulgarian" - a motor with a *200 mm* disk (corundum or metal) develops clockwise rotation speed, and the torsind begins to slowly rotate counterclockwise, like a gear, but there is no contact (Fig. 1, 2). The disk acceleration time to *9000 - 11000 rpm* is *3 - 5 sec*. The torsind begins to rotate like a "gear" after *10 - 15 accelerations*.

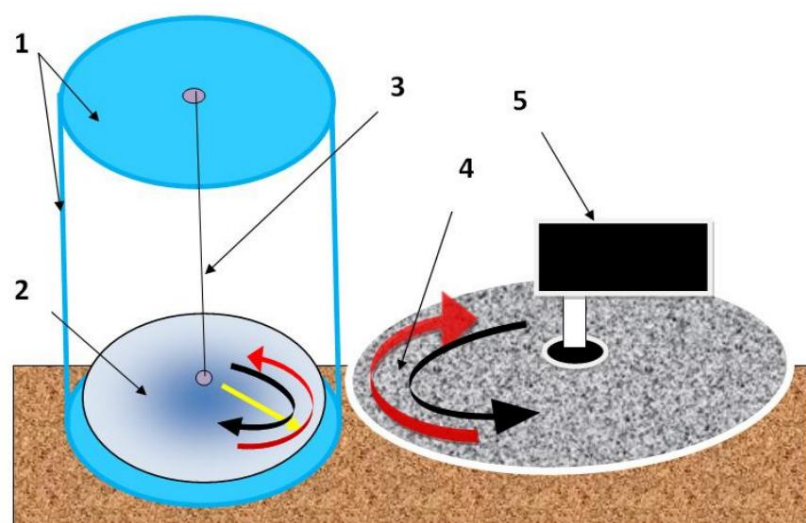


**Fig. 1.** Experimental scheme: 1 - sealed glass flask; 2 - torsion bar made of  $14 \mu\text{m}$  thick Al foil with a diameter of *74 mm* or *15 \mu\text{m}* thick mica of the same diameter; 3 - spider web; 4 - disc with a diameter of *200 mm*, corundum or metal; 5 - motor *350 W 11,000 rpm*.



**Fig. 2.** Photo of the experiment with a torsind according to the scheme in Fig. 1.

In other experiments, due to the lack of a spider thread, a Henkel gyroscope and H-shaped torsions for aluminum and U-shaped torsions with mica and paper disks were used.



**Fig. 3.** From left to right: "U-shaped" torsion bar with a mica disk (0.38 g); "Henkel" gyroscope; stopwatch; "U-shaped" torsion bar with a paper disk (0.18 g) and "H-shaped" torsion bar with an aluminum disk (0.36 g). The disks are suspended on a very thin (15-20  $\mu\text{m}$ ) synthetic thread.

The rotation of the torsions begins after 70 - 90 s, when the gyroscope reaches 10,000 - 12,000 rpm. The rotation intensifies when the maximum rotation speed is reached – 40,000 rpm. At a constant rotation speed, the torsinds sharply slow down or stop.

When the gyroscope reverser is turned on, if the torsinds are suspended on a synthetic thread with a diameter of 15-20 microns, the time it takes for the entire torsind system to settle is more than 5 minutes. After the entire system has settled and the reverser is turned on, the disks begin to slowly rotate in reverse, like gears when they touch. But in our experiments, there is no contact.

Thus, the entire effect of the action on the torsion occurs when the gyroscope accelerates, when the gyroscope picks up speed.

It should be noted that working with a gyroscope, in contrast to a high-speed motor (grinder 11,000 rpm), is more preferable, since when gaining speed there is a constant angular acceleration (25 rad/s<sup>2</sup>), which made it possible to estimate the coefficient of "transfer" or action ( $\hat{y}$ ) of the gyroscope on the torsion bars (see below).

### **How can we explain exactly this reaction of torsinds to the accelerated rotation of a disk or gyroscope?**

The experiments conducted are similar to the experiments of Henry Cavendish in 1798, who determined the gravitational constant G. But in our case, it is rotation, and not just rotation, but accelerated rotation of a volumetric body (grinder disk or gyroscope rotor) on an isolated sensitive sensor - torsind. The gyroscope or volumetric disk, when rotating at an accelerated rate, acts on the torsind like the rotation of contacting gears, but there is no direct contact between them. The torsind disk is in a hermetically sealed flask (chemical beaker), and the accelerated rotating body is behind the flask.

It should be noted that V.N. Zatelepin and D.S. Baranov back in 2018 drew attention to the addition of a correction to the formula of universal gravitation - accelerated rotation of the body (reports at the seminar of the Physics Department of Moscow State University and at the conference of the Russian Chemical Society and the Russian Academy of Sciences - 25) [1].

### **Hypothesis. An attempt to explain the results of experiments with torsinds by the action of gravity**

Existing theories of elementary particles emphasize their vortex stable formations, but any vortex structure needs an energy supply, or should we recognize elementary particles (e) and (p) as perpetual motion machines?

Let us assume that in order to maintain their properties (we will consider only the masses, and leave the charges alone) these elementary particles absorb (draw or replenish) something, replenishing their energy from the ether – the substance of the Universe, which ensures the infinite stability of their masses and their properties in time. Thus, the paradox of their perpetual motion machines is removed. This assumption can be presented in the form of a formula:

$$\text{MASS} + (\text{ether}) f(t) = \text{const } m.$$

This assumption can be justified by the fact that it is impossible to cool a substance to absolute zero temperature (0K). There always remain ZERO-DIMENSIONAL oscillations, which can be associated with the parameter of ether suction to maintain the vortex structure of an elementary particle. (e) and (p)+ (ETHER)  $f(t)$ .

The introduction of this postulate is apparently justified, since the paradox of the PERPETUAL MOTOR for the "elementary" particles that make up a body with a certain mass is physically eliminated.

Any body consists of "elementary particles". Then the ETHER will be "sucked in" by the body through its surface, as shown in Fig. 4.

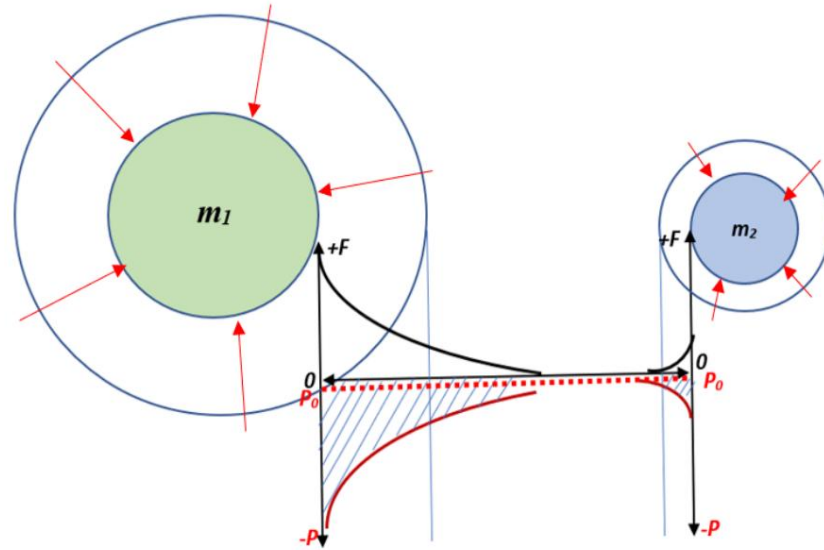


**Fig. 4.** Gravitational interaction diagram of two bodies. "+F" is the ordinate of the force of gravitational attraction; " $P_0$ " is the state of ether remote from the surface of the body; "-P" is the rarefied state of ether at the surface of the bodies or the gradient (*grad*) of the ether flow.

Consequently, at the surface of any body a diffusion layer of ether with its own gradient is created, which determines the attraction or *gravitational action (gravity)*. We believe that the powerful accelerated rotation of a body changes the diffusion layer or

gradient of the ether medium at the surface of a body rotating with acceleration, as shown in Fig. 5. Then, having learned to change the diffusion gradient of ether at the surface of a body, we can change the attraction - GRAVITY - of this body, and it will interact with a stationary body differently than in a conditionally stable state.

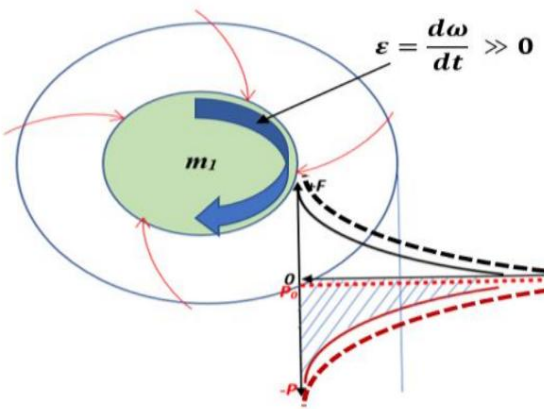


**Fig. 5.** Scheme of change of diffusion layer of ether suction into the body during strong accelerated rotation of the body. Dotted lines show increase of gradient of ether medium at the surface of the body due to accelerated rotation of the body.

A powerful acceleration of the rotation of a body changes the diffusion layer or gradient of the etheric medium at the surface of this body, as shown in Fig. 5, 6. This leads to an effect on the body that was in a state of rest, Fig. 6.

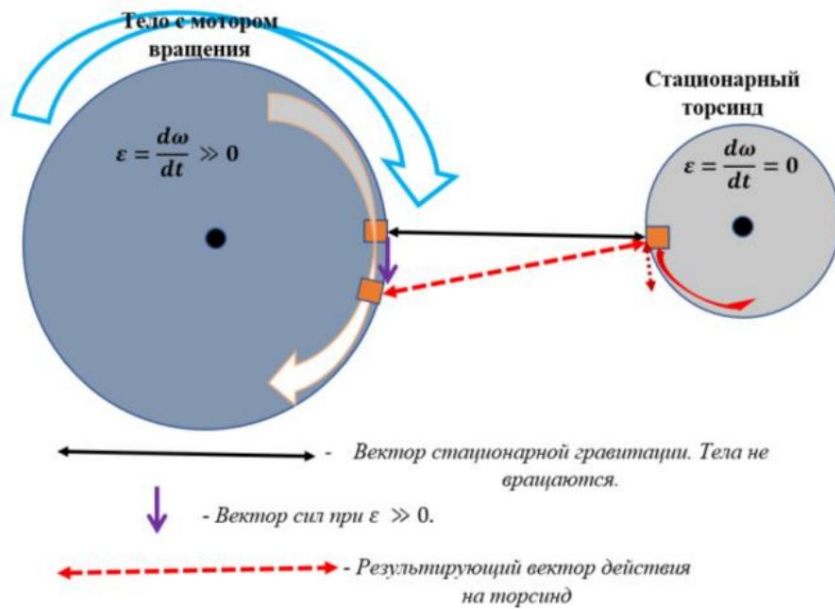


**Fig. 6.** Scheme of the action of bodies during accelerated rotation of one of them.

An assessment was made of the transfer coefficient (impact) during accelerated rotation of the gyroscope on a torsion bar with an H-shaped aluminum body (Fig. 7) and a torsion bar with a U-shaped mica body suspended on a thin synthetic thread with a diameter of 10-15  $\mu\text{m}$ .



**Fig. 7.** Photo of the “H-shaped” aluminum torsion bar and rotating gyroscope.

The coefficient of transfer ( $\ddot{\gamma}$ ) of the moment of force from the gyroscope to the torsion bar with accelerated rotation of the gyroscope ( $\ddot{\gamma}\dot{\gamma} = \sim 25 \text{ rad/s}^2$ )

$\ddot{\gamma} = \ddot{\gamma}\dot{\gamma}/\dot{\gamma}\dot{\gamma}$ . For a torsion bar with an aluminum body weighing 0.36 g at  $L = 10 - 12 \text{ cm}$  (distance edge of the gyroscope to the center of the torsion bar)  $\ddot{\gamma} = MT/MG = 10^{-5}$ , where:  $MT = J\ddot{\gamma}T = \sim 10^{-9} \text{ Nm} \cdot \text{s}$  – force from the action of the gyroscope for 120 s;  $MG = J\ddot{\gamma}G = \sim 10^{-4} \text{ Nm}$  is the moment of gyroscope for 120 s.

For a torsion beam with a mica body weighing 0.38 g,  $\ddot{\gamma} = MT/MG = \sim 10^{-6}$

From the above it follows that when an accelerated rotating body moves, it is necessary to introduce a correction into the gravitational action of this body, for example, when a rocket rotates rapidly during its movement (Fig. 9).

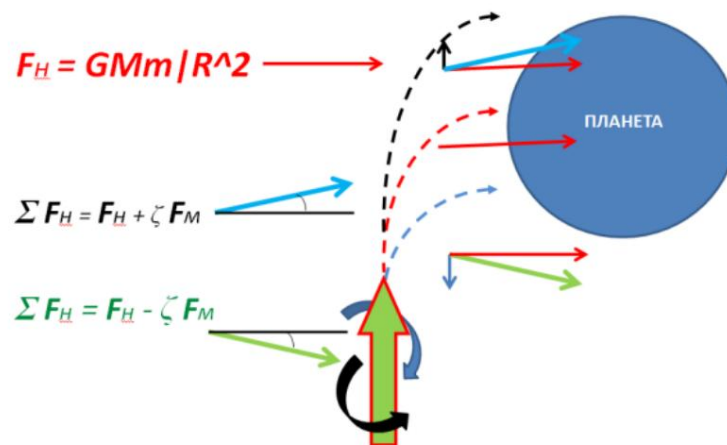


**Fig. 9.** Diagram of the change in the rocket trajectory during its accelerated rotation.

$F_H$  – Newtonian gravitational force;  $\dot{\gamma}F$  – force from the moment of accelerated rotation;  $\ddot{\gamma}F$  – total force during accelerated rotation of the rocket. The total vector  $\ddot{\gamma}F$  depends on the direction of accelerated rotation of the rocket and the moment of force

Experiments with torsinds are ongoing. At this stage, in our experiments with torsinds, we note the theoretical work [1].

## Literature

1. Baranov D.S., Zatelepin V.N. On the weight of rotating bodies. Collection of works of RKHTYAiShM-25. Sochi-Adler. P. 221-237. 2018. "MIS-RT"-2021 Collection No. 76-1-1 <http://ikar.udm.ru/mis-rt.htm>.

### **Experiments with torsinds or the effect of accelerated rotation of a body on another stationary body. The hypothesis of gravity.**

VAChizhov Chijov\_va@bk.ru  
IN Stepanov stepanovigorn@gmail.com

The paper shows that accelerated rotation of a gyroscope with constant acceleration ( $eG = \sim 25 \text{ rad/s}^2$ ) or accelerated rotation of a disk of 150-200 mm (corundum or metal) affects sensors isolated from these objects, which are called torsinds, with a diameter of 74 mm, weighing less than 0.4 g. . The artifact was that with accelerated rotation of the body (gyroscope or disk) isolated from the TORSINDE (the torsinde is placed in a sealed glass flask), it began a slow rotation in the opposite direction, ie, if the body rotated clockwise, then the TORSINDE rotated counterclockwise and vice versa. The torsins rotate like gears when the rotating body and the torsind come into contact (the torsind rotates very slowly), but there is no contact of the rotating body with the torsind in this process. It was this fact that attracted me to research and try to understand it. To explain this artifact, the hypothesis of the existence and violation of the diffusion gradient layer of ETHER at the surface of an accelerated rotating body is introduced. The transfer coefficient of the accelerated gyroscope rotation to aluminum and mica torsodes, which are isolated in a separate medium, is estimated. It was these experiments with torsinds that led to the proposed hypothesis of gravitational action, as a new look at GRAVITY.

## **Theoretical models**

---

## **Theoretical Models**

# An approach to understanding the mechanism of low-energy nuclear transformations based on experimental assumptions

A.G. Parkhomov  
alexparh@mail.ru

The hypothesis that in hot matter, especially matter containing many free electrons (for example, in metals), neutrino-antineutrino pairs are formed that are capable of carrying out nuclear transformations via the weak nuclear interaction channel, as well as the use of statistical physics, make it possible to explain not only the fundamental possibility of low-energy nuclear transformations, but also the experimentally discovered properties of this phenomenon: the formation of many different nuclides, the emission of soft X-rays instead of the hard gamma radiation usual for nuclear reactions, the low probability of the formation of radioactive nuclides, the appearance of new nuclides and other changes **outside** the active zone of reactors (including the appearance of tracks on smooth surfaces), and the long-term continuation of changes at the nuclear level after the substance has been in and around LENR reactors.

An analysis of the results of numerous diverse experiments [1] shows that when creating a theory of cold nuclear transformations, one must proceed from the fact that this is the work of weak nuclear interactions, which can affect not only one atom, but also several atoms. Moreover, the participation of hydrogen in this process is not necessary. The theory must explain not only the fundamental possibility of low-energy nuclear transformations, but also a number of experimentally discovered properties of this phenomenon. Such as: a huge variety of emerging nuclides; the possibility of LENR occurring both in solids and in liquid media and in dense low-temperature plasma; the emission of soft X-rays instead of hard gamma, which is usual for nuclear reactions; a low probability of the formation of radioactive nuclides; the formation of new nuclides and other changes **outside** the active zone of reactors (including the appearance of "tracks" on smooth surfaces); a long continuation of changes at the nuclear level and the emission of soft X-rays **after** the substance has been in LENR reactors.

and around them.

## Hot matter and light produce intense streams of neutrinos and antineutrinos

Let's start with the question: why do we *usually* not see any manifestations of weak interactions other than beta decays, but in LENR reactors they are observed? Let's consider, for example, nickel-hydrogen reactors, many of which we have manufactured and tested in our laboratory. In principle, they are very simple: nickel powder, in which hydrogen is dissolved (what we called "fuel"), is heated by a tungsten coil [2]. The power consumed by the electric heater and the heat output are measured.

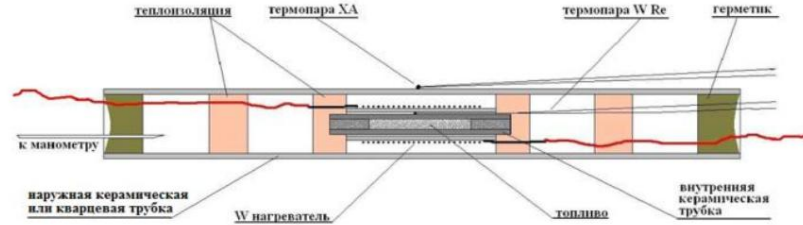


**Fig. 1.** Typical design of nickel-hydrogen reactors [2]

At low temperatures, the power consumed exactly matches the heat output. When the "fuel" is heated to 1100-1200 ° C, the heat output begins to exceed the power consumed by the electric heater, and the difference becomes greater at higher temperatures. Excess heat, much greater than the capabilities of chemical reactions, is an indicator that low-energy nuclear reactions are occurring. Experiments in reactors show that LENR requires heating above a certain temperature. And LENR

is the result of the work of weak nuclear interactions. The keys that trigger the reactions of weak interactions are neutrinos and antineutrinos. Therefore, heating to a temperature of about 1000 ° C and above creates conditions for the generation of neutrinos and antineutrinos.

How can this happen? A well-known method for producing particles in pairs with antiparticles is to bombard targets with protons, electrons or other particles. This occurs under the condition that the bombarding particle can contribute energy exceeding the rest energies of the particle and antiparticle. In this way, electron-positron, proton-antiproton and many other particles, including neutrino-antineutrino pairs, are produced at accelerators. The same mechanism works in the collision of molecules, atoms, ions and electrons during their thermal motion in matter. For example, photons emitted by heated matter (and at temperatures above 600 ° C we see them with our eyes) are precisely the result of collisions of matter particles. At such a temperature, some of the collisions occur with an energy of about 1 eV, which is sufficient to form photons of visible light.

range.

Nothing prevents the formation of neutrino and antineutrino pairs in the collision of particles of matter, in addition to photons. Since the mass of neutrinos is no more than tenths of an eV, some of the colliding particles have enough energy to form them. Fig. 2 shows the fraction of particles of matter with a thermal motion energy greater than 0.5 eV, sufficient to produce neutrino-antineutrino pairs. At room temperature, the fraction of such particles is 10-8

. A noticeable proportion of particles with energy above 0.5 eV appears only at a temperature of about 1000° C. At a temperature of 1600° C there are already 10% of such particles, and at a temperature of 4500 ° C - 50%. Thus, the threshold for thermal generation of neutrino-antineutrino pairs is about 1000 ° C, which is quite consistent with the threshold for the onset of low-energy nuclear processes in nickel-hydrogen reactors.

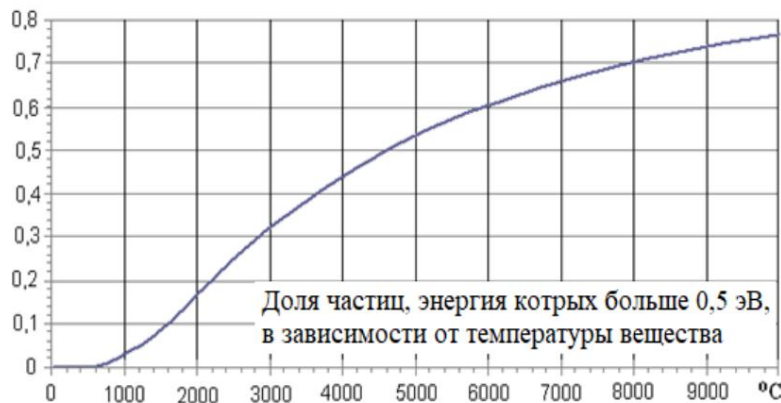


Fig. 2 [3, 4]

We do not yet know the probability of the formation of neutrino-antineutrino pairs in thermal collisions. Apparently, the probability is small. The small probability can be compensated by a large number of collisions.

An electron experiences about  $10^{13}$  during its thermal motion in metals. collisions per second [3]. Considering that the number of free electrons in  $1 \text{ cm}^3$  metal of the order of  $10^{23}$ , we find the number of collisions per second in  $1 \text{ cm}^3$  of metal:  $10^{36}$ . Such a huge number of collisions allows us to assume that in hot metals neutrinos and antineutrinos arise with an intensity sufficient to initiate nuclear transformations that yield significant energy release even with very low probabilities of neutrino-related processes. Let us assume that only one out of  $10^{20}$  collisions generates a neutrino-antineutrino pair that causes a nuclear transformation. Even with such negligible probabilities,  $1 \text{ cm}^3$  of hot metal produces  $10^{16}$  nuclear transformations per second. Considering that in each act of such transformations about 1 MeV is released, we obtain a power of released energy of approximately 1 kW.

Unlike metals, the distances between molecules in gases are much greater, and there are very few free electrons. In gases, the speed of molecules in thermal motion is much less than the speed of electrons. Therefore, the frequency of collisions in gases during thermal motion is many orders of magnitude less than in metals or plasma. Thermal generation of neutrinos and antineutrinos, although possible, occurs with very low intensity. Intensive generation requires a hot, dense medium with a high content of free electrons. In addition to metals, such a medium is high-density plasma, which briefly occurs, for example, during explosions of metal conductors, in cavitation, or with a sufficiently strong pulsed energy release in liquids, for example, in plasma electrolysis units. Another method of generating neutrino-antineutrino pairs is also possible. The energy of optical photons (about 1 eV) is quite sufficient for transformations of the type photon  $\gamma + \gamma \rightarrow \nu + \bar{\nu}$ . It is reasonable to assume that it is precisely with the transformation of photons into neutrinos and antineutrinos of ultra-low energies that the appearance of new nuclides is associated under the action of radiation from LEDs or lasers

in the experiments of Yu. N. Bazhutov et al. [5,6],

U. Mastromatteo [7], J.-P Biberian [8], as well as in experiments with a laser by D.S. Baranov, V.N. Zatelepin and others [9].

Thus, the proposed mechanism of low-energy nuclear transformations points to precisely those methods of LENR excitation that were discovered empirically.

### **Ultra-low energy neutrinos and antineutrinos cause nuclear transformations of many atoms into many other atoms**

The size of the interaction region of objects in the microworld is approximately equal to the de Broglie wavelength. For neutrinos and antineutrinos that arise during thermal collisions, it is about 1 micron. Fig. 3 shows the dependence of the de Broglie wavelength on the energy of a neutrino or antineutrino. It is evident that at energies of about 10 keV and higher, the interaction can involve only one atom. At energies of several keV, the interaction already involves several atoms. And neutrinos and antineutrinos with energies less than 1 eV involve many billions of atoms in their interaction. This is exactly what is required for transformations involving many atoms and nuclei and the formation of many different nuclides.

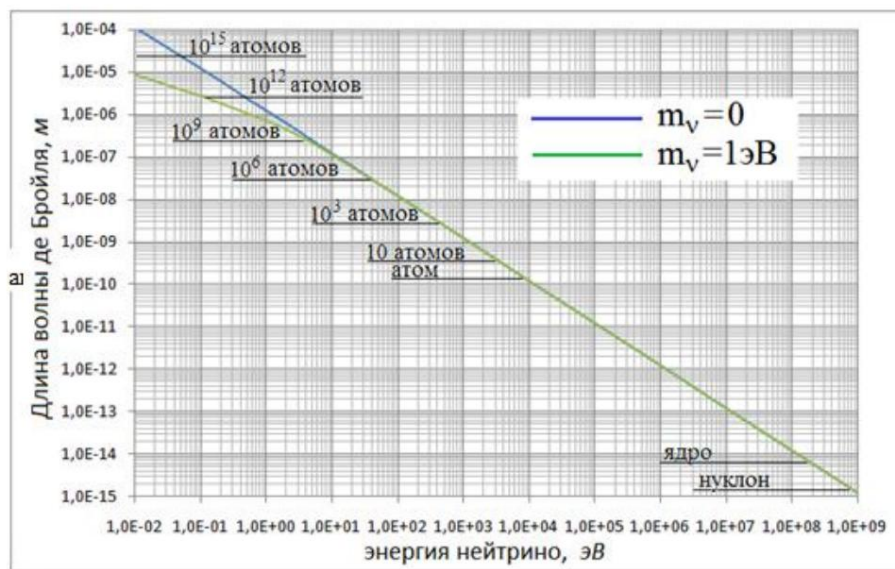


**Fig. 3.** Dependence of the de Broglie wavelength of a neutrino or antineutrino (size of the interaction region) on the neutrino energy. The number of atoms of solid or liquid matter in the interaction region is indicated [10]

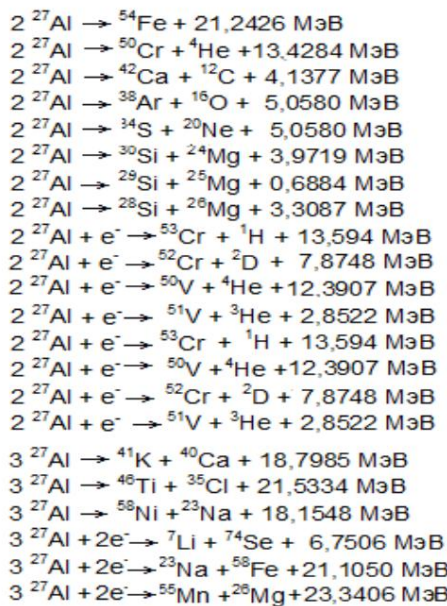
Here we enter an area that has hardly been touched upon by physical research. What properties do ultra-low energy neutrinos and antineutrinos have at their high density? It is clear that this is degenerate matter, i.e. a substance whose properties are significantly affected by quantum effects arising from the identity of the particles. Degeneracy occurs under conditions where the distances between the particles become commensurate with the de Broglie wavelength [11] (this condition is satisfied in our case).

Depending on the spin of the particles, two types of degenerate substances are distinguished: those formed by fermions (particles with half-integer spin) and those formed by bosons (particles with integer spin).

What type does a degenerate substance of neutrinos and antineutrinos have? On the one hand, they are fermions, then this is a Fermi gas, in which a high concentration of particles can be achieved only as a result of high pressure. However, it is very difficult to exert pressure on a weakly interacting substance, so there cannot be a high density of particles. Neutrinos and antineutrinos are born and immediately "run away", which greatly complicates interaction with matter. On the other hand, if neutrinos and antineutrinos are able to create complexes with an integer spin, then they can form a Bose condensate and accumulate to high concentrations, just as a Bose

condensate can, under certain conditions, form pairs of electrons, also fermions. If this happens, the substance turns out to be saturated with a neutrino-antineutrino substance. And neutrinos and antineutrinos are exactly what triggers nuclear reactions of weak interaction. When the interaction covers many atoms, nuclear transformations of many atoms into many other atoms become possible. If this substance can be retained in matter for a long time, this would explain the experimentally detected long-term transformations in matter that has been in the LENR reactor (changes in elemental and isotopic composition, soft X-ray radiation).

### Why LENR does not produce hard gamma radiation and radioactive nuclides



The article [1] provides examples of real nuclear reactions in which the resulting nuclides receive energy insufficient to excite even the very first level. Such nuclei cannot emit gamma quanta. But the question arises: why shouldn't nuclei with energy sufficiently high for their excitation also appear in other reactions? The answer may be as follows. Any substance is not simply a system of a large number of particles, but a system of particles in which there is a potential for a large release of energy as a result of nuclear transformations.

**Fig. 4.** Examples of potential nuclear transformations in aluminum [12]

As an example, Fig. 4 shows some of the potential nuclear transformations in aluminum, the reality of which was confirmed by long-term irradiation in a LENR reactor and comparison of the content of various elements before and after irradiation [14]. Even in monoisotopic aluminum there are many opportunities for energetically favorable nuclear transformations. Usually, transformations at the nuclear level are prohibited by the Coulomb barrier. But such a possibility appears as a result of weak nuclear interaction. The initiators of weak interaction are neutrinos and antineutrinos. At sufficiently low energies, the interaction involves many atoms or molecules of matter at once. And if the interaction involves many particles, their behavior cannot be considered in isolation.

The consideration of systems in which nuclear transmutations occur not from the standpoint of interaction of individual particles, but as a set of a large number of particles, is the subject of statistical physics [11]. Any system of many particles tends to a state of equilibrium, to minimum energy. If there is a possibility of releasing energy, it is released. In the presence of neutrinos and antineutrinos, such a possibility, even if unlikely, appears. And for the release of noticeable energy, a high probability is not required. Even rare but high-energy events of nuclear transformations ultimately yield significant energy release. In a system of a large number of interacting atoms (molecules), there are many options for the formation of products with stable and unstable isotopes, with excited and unexcited nuclei. In accordance with Ziegler's principle [13], a nonequilibrium system develops in such a way as to maximize the production of entropy. The entropy production during the formation of stable and unexcited nuclides is higher than during the formation of unstable and excited ones, so the formation of stable unexcited nuclides occurs with a higher probability. Thus, the use of statistical physics allows us to explain the most intriguing feature of LENR - a very low level of hard radiation. Moreover, this does not even require delving into the features of the nuclear transformations themselves. It is enough to assume that the process involves a system of a large number of particles.

***So, in essence, LENR is the pursuit of equilibrium of a non-equilibrium substance in the nuclear sense. The task of LENR reactors is to create suitable conditions for this.***

Now about the appearance of soft X-ray radiation. The newly formed atoms do not have a formed electron shell. Its formation is inevitably associated with the emission of photons of different energies, including X-rays, as well as Auger electrons. Since nuclear transmutations occur not only inside but also outside the reactors, it is not surprising that soft X-ray radiation, which, it would seem, cannot go outside, is registered near the surface of the reactors and near nearby objects.

## A New Approach to Designing Cold Nuclear Reformation Reactors

Thus, a hot substance containing many free electrons generates neutrinos and antineutrinos — an agent that can cause nuclear transformations not only in the substance itself, but also in the surrounding environment. Consequently, the source of neutrinos-antineutrinos (hot metal or dense plasma) can be separated from the "fuel" — the substance where nuclear transformations occur. This opens up the possibility of new approaches to the design of LENR reactors. The "source" can be placed inside the reactor and create conditions for heating with minimal losses, and the "fuel" - on the periphery, where it is easy to ensure effective heat removal.

The simplest way to implement this idea is in reactors using incandescent lamps, in which the tungsten filament is heated to a temperature of over 2500 °C. Several experimental setups have been created based on incandescent lamps. Excess heat and the appearance of new nuclides in reactors with incandescent lamps confirm the correctness of the idea of hot matter as a source of neutrinos and antineutrinos, agents that cause nuclear transformations. In addition to reactors with incandescent lamps, reactors with hot iron and tungsten cores [4] and with molten aluminum have been tested.



**Fig. 5.** One of the reactors with an incandescent lamp [4]

### Conclusion

A hypothesis has been put forward that in hot matter, especially in matter containing many free electrons, such as metals, neutrino-antineutrino pairs are formed that are capable of carrying out nuclear transformations. This hypothesis, as well as the use of statistical physics, make it possible to explain not only the fundamental possibility of low-energy nuclear transformations, but also the experimentally discovered properties of this phenomenon: • the formation of many different nuclides,

- soft X-ray radiation instead of the hard gamma radiation usual for nuclear reactions and a low probability of the formation of radioactive nuclides,
- the need for hot dense media containing many free electrons for LENR to occur, • the appearance of new nuclides and other changes **outside** the active zone reactors, including the appearance of "tracks" on smooth surfaces.
- long-term continuation of changes at the nuclear level after the stay substances near operating LENR reactors.

The topic of "strange radiation tracks" is not touched upon in this article. This collection and the RENSIT journal contain articles with a detailed description of the properties of this phenomenon and with a hypothesis explaining the discovered properties [14,15]. The hypothesis put forward was confirmed in specially conducted experiments. It is in good agreement with the ideas presented in this article.

## LITERATURE

1. Parkhomov A.G. Experimental prerequisites for the theory of cold nuclear transformations. *In this collection*
2. Parkhomov A.G., Alabin K.A., Andreev S.N. etc. Nickel-hydrogen reactors: heat release, isotopic and elemental composition of fuel. *RENSIT*, 2017, 9 (1): 74-93.
3. Parkhomov A.G. LENR as a manifestation of weak nuclear interactions. *J. Phys. Sci.*, 2019, 23-24(7):6-8, <http://www.unconv-science.org/pdf/23/parkhomov1.pdf>
4. Parkhomov A.G., Karabanov R.V. LENR as a manifestation of weak nuclear interactions. A new approach to creating LENR reactors. *RENSIT: Radioelectronics. Nanosystems. Information technologies*, 2021, 13 (1): 45-58.
5. Bazhutov Yu.N., Gerasimova A.I., Koretsky V.P., Evmenenko V.V., Parkhomov A.G., Sapozhnikov Yu.A. Calorimetric and neutron diagnostics of aqueous solutions under intense light irradiation. *Proceedings of RKHTYAi SHM-20*, 2013, 55-64.
6. Bazhutov Yu.N., Gerasimova AI, Evmenenko VV, Koretskiy VP, Parkhomov AG and Sapozhnikov Yu.A. Calorimetric and Radiation Diagnostics of Water Solutions Under Intense Light Irradiation. *J. Condensed Matter Nucl. Sci.* 2016,19:10-17.
7. Mastromatteo U. LENR Anomalies in Pd–H<sub>2</sub> Systems Submitted to Laser Stimulation. *J. Condensed Matter Nucl. Sci.* 2016, 19:173–182.
8. Biberian JP. Transmutation induced by laser irradiation. *Le colloque RNBE 2020*. 9. Baranov DS, Zatelepin VN, Shishkin AL et al. Powerful effect of laser beam, passed through the fiber optic line in the vicinity of the electric discharge, onto the surface of the CD-disk. *Proc. RKHTYAiShM-27*, 2022, 65-73.
10. Parkhomov A.G. Nuclear reactions at low energies: experiments, strange results and attempts at explanations. *Presentation of the report made in March*

2021 at the seminar named after A.P. Levich (Moscow State University) <https://cloud.mail.ru/public/aHov/tSlVJmuAt>

11. Landau L.D., Lifshitz E.M. Theoretical Physics, v.5: Statistical Physics. Part 1. 5th ed., Moscow: FIZMATLIT, 2002. 616 p.
12. Parkhomov A.G. Nuclear transmutations and excess heat in reactors with lamps incandescent. *Proceedings of RKHTYAiShM* -27, 2022, 25-34.
13. Martyushev L.M., Seleznev V.D. The principle of maximum entropy production in physics and related fields. *Ekaterinburg: State Educational Institution of Higher Professional Education USTU-UPI*, 2006. 83 p.
14. Parkhomov A.G., Zhigalov V.A., Nevolin V.K. Tracks of strange radiation. Their properties. An attempt at explanation. *RENSIT*, 2024, 16(1):79-88.
15. Parkhomov A.G., Zhigalov V.A. Properties of strange radiation tracks. An attempt explanations. In this collection, pp. 110-123.

### **Approach to understanding the mechanism of low-energy nuclear transformations based on experiments**

**AGParkhomov**

[alexparh@mail.ru](mailto:alexparh@mail.ru)

The hypothesis that in a hot substance, especially a substance containing many free electrons, for example in metals, neutrino-antineutrino pairs are formed neutrino-antineutrino pairs capable of carrying out nuclear transformations through the channel of weak nuclear interactions, as well as the involvement of statistical physics, allow us to explain not only the fundamental possibility of low-energy nuclear transformations, but also the experimentally discovered properties of this phenomenon: formation of many different nuclides, emission of soft X-rays instead of the hard gamma radiation usual for nuclear reactions, low probability of the formation of radioactive nuclides, appearance of new nuclides and other changes outside the reactor core, including the appearance of tracks on smooth surfaces, prolonged continuation of changes at the nuclear level and soft X-ray radiation after the substance was in and around LENR reactors.

## Four Steps of LENR Reactions (multi-electron reaction model)

V.F. Chibisov

st.4p@mail.ru

The article attempts to clarify the physics of LENR processes taking into account the quark (Standard Model) and preon (Corpuscular-Symple Theory) structure of nucleons and electrons. In this case, the consideration of LENR reactions is structured into four stages (steps):

- Step 1 - formation of pairs of electrons and multi-electrons.
- Step 2 - initiation of fission reactions by electron pairs.
- Step 3 - initiation of multi-electron fusion reactions.
- Step 4 - formation of particles of strange radiation.

### Introduction

Different researchers propose different models of LENR reactions. Quite often, pairs of electrons, multi-electrons, and heavy electrons are considered as catalysts for low-energy nuclear fission and fusion reactions (Baranov and Zatelepin [1], Kashchenko [2], Andras Kovacs [3], etc.). Usually, these are EPN models - based on electrons, protons, and neutrons. But it has been known for more than half a century that, according to the

Standard Model (SM), protons and neutrons consist of a triad of valence quarks and a sea of quark-antiquark pairs. Both models have problems, since the descriptions of the  $\gamma+$  decay reaction have the following

view:

in EPN:  $p \gamma n + e+ + \bar{e}$ , in SM:  $u+2/3 \gamma d-1/3 + e+ + \bar{e}$ .

In both cases the masses do not converge (from less comes more).

In the 1970s, the Preon theory appeared, according to which all quarks and leptons consist of single proto-particles – preons. Within the framework of this theory, in all nuclear reactions, there is no transformation of particles into each other, but rather the defragmentation of some particles into preons, and the formation of other particles from these preons.

In the 80s, String Theory appeared, it pushed aside Preon Theory. In the 90s, the first crisis of String Theory occurred, and Preon theories began be reborn again.

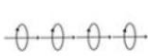
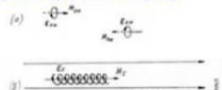
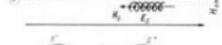
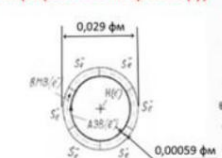
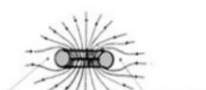
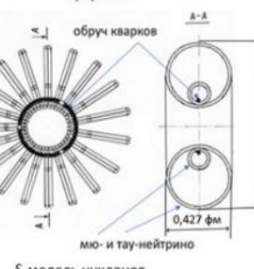
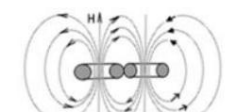
In 1998, the Preon Trinity theory [4] appeared, according to which all elementary particles with mass consist of 3 types of preons. In 2022, at the

27th conference of the Russian Society of Physics and Mathematics (RKHTYalISM-27), I reported on the Corpuscular-Simple Theory (CST) [5-10], which belongs to the class of Preon theories. According to the CST, matter consists of 6 preons of a single nature, with different masses, corresponding to 6 stable particles of the SM.

Tab 1 shows the basic models of the QST and their analogs in the SM. I draw attention to the structural similarity of the nucleon models, consisting of a triad of valence quarks and a certain set of additional components with opposite charges.

Of particular interest is the model of formation of lines of force (LL) of the electric field of preons-simples (including electrons), as a result of the interaction of toroidal and azimuthal electric vortices. This model creates a screen, a zone around the electron torus, in which Coulomb's law does not apply, which contributes to the formation of electron pairs.

**Tab 1.** Basic models in KST and their analogues in SM

<b>Модели эфира и вещества в КСТ (см. моя статья в сборнике РХХТЯиШМ-27)</b>			
<b>КТ:</b>			1. виртуальный фотон 2. силовые линии эл. и магн. полей 3. связанные Е- и Н-вихри ЭМИ 4. преоны (симплы)
	квант ПВ, ФВ, эфира связанные элем. Е- и Н-вихри (закрытые струны)	корпускулярное пространство аналог эфира Лоренца (стационарность, $\beta$ -фактор, электрографитика по Цельнеру)	образование Е- и Н-дипольных цепочек – главное свойство эфира КСТ
<b>СТ (класс Преонных теорий):</b>	(a)  (b)  (c) 	 модель образования симплов S(-) и S(+) (вещество Вселенной)	4-е базовых элемента из дипольных цепочек (материя Вс.)
<b>Образование пар-электронов в КСТ:</b>			 аналог в СМ →
	образование СЛ эл. заряда e-	образование экран. зон в ЭП у e-	кварковая модель нуклонов (СМ)
			аналог в СМ
		пересоединение СЛ-МП 2e ( $\uparrow\downarrow$ )	спиновая пара (ee)
		→	
		скатие СЛ-МП 2e в КСТ (магнит Николаева)	

## Pair-electron and multi-electron models in SP and LENR

Ginzburg in his work "Superconductivity: the day before yesterday, yesterday, today, tomorrow. Uspekhi Fizicheskikh Nauk, 2000" [11] writes: "In real matter, there exists simultaneously electron-phonon (BShK model), spin, and electron-electron interactions with the formation of pairs of electrons with a charge of 2e and their collectivization."

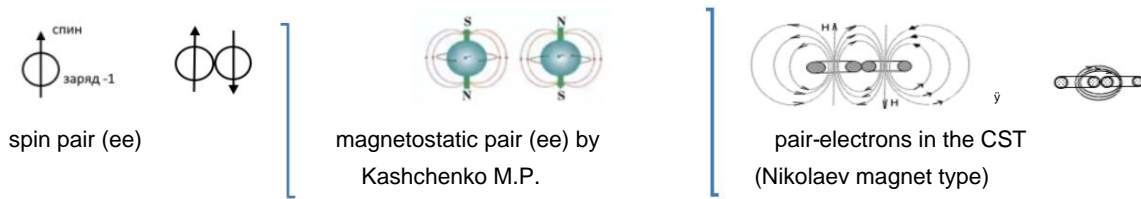


**Fig. 1.** Single electron pairs in different theories

As we can see, at the level of single electron pairs (ee), their models in different theories are very similar. At present, studies have already been conducted on the breakup of Cooper pairs of electrons in superconductors into individual electrons by a powerful magnetic field – see "The Quantum Secret to Superconductivity" (Quantum Secret

superconductivity) [12]. This indirectly proves that the electrons in Cooper pairs are linked by magnetic interaction with mutually inverted magnetic poles, as in the Nikolaev magnet.

In the paper "High-Temperature Superconductivity Understood at Last" [13] it is said – "Many Cooper pairs come together and merge into a single quantum mechanical state." In 2016, the first experimental detection of a cluster of Cooper pairs of electrons in cuprates (I call them multi-electrons) was made.

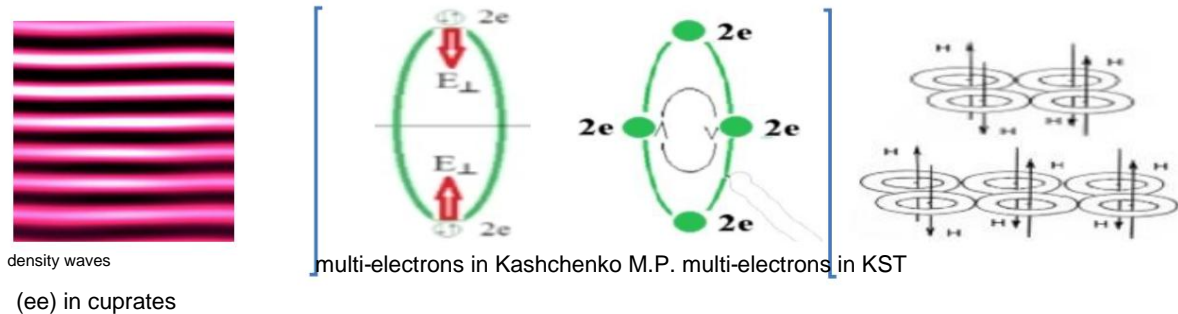


**Fig. 2.** Multi-electron models in different theories

As we see, at the level of collectivization of pair-electrons into multi-electrons  
The models of different authors differ significantly.

### Step 1: Formation of pair- and multi-electron electrons in CST

The reason for the pairing of electrons is probably the "shaking" of the electron shells of atoms in LENR reactors due to external influences (discharge, heating, vibration, ultrasound, particle impact, cavitation, etc.). Different orbitals contain different numbers of 1, 3, 5, 7 pairs of electrons with opposite spins.

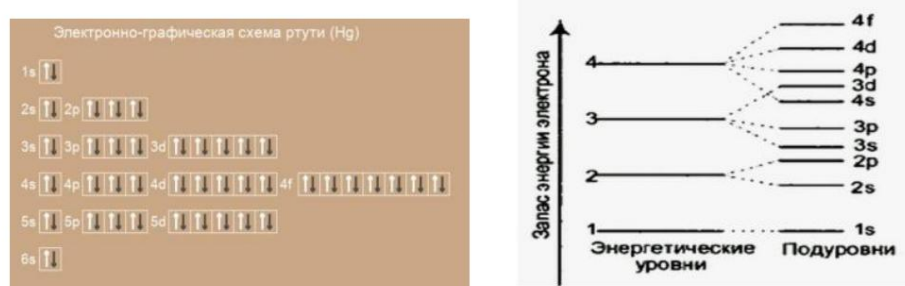


**Fig. 3.** Electron orbitals

Accordingly, when electron shells are "shaken", multi-electrons with charges of para-electrons (-2), hexo-electron (-6), deca-electron (-10), tetracosa-electron (-14) can be formed. Considering that the sublevels of electron orbitals are located very close or overlap, when they are "shaken", multi-electrons with an even number of pairs can also be formed.

electrons. Below are models of pair-electrons and some multi-electrons:

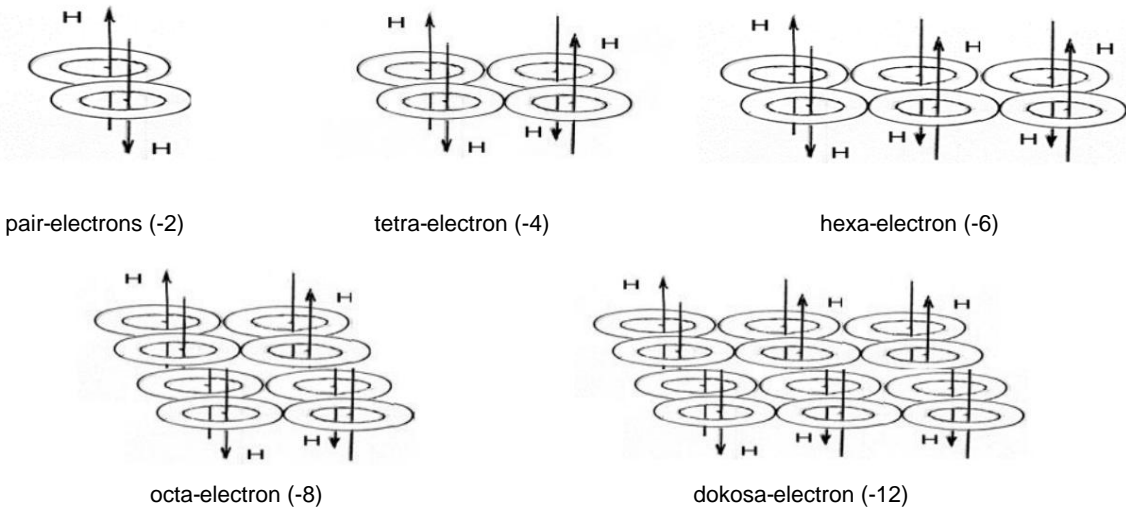
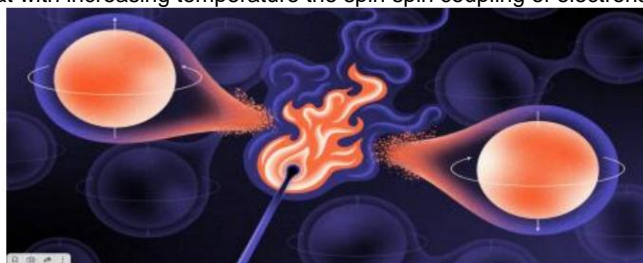


Fig. 4. Models of multi-electrons with different charges

### Mechanism of superconductivity according to KST

The magnetic field of para- and multi-electrons resembles the Nikolaev magnet, which has no magnetic field at macro-distances. Such para- and multi-electrons, if they are formed in the outer orbital, can break away from their atoms (by analogy with free electrons). Free para- and multi-electrons, moving along the channel between the nuclei of the crystal lattice, do not experience magnetic interaction with the magnetic moments of the nuclei and the orbital magnetic moments of the electrons, which stimulates the transition of materials to the superconductivity mode.

In August of this year, an article was published titled "Computer Scientists Prove That Heat Destroys Quantum Entanglement" (Heat destroys quantum entanglement) [14], in which it is proven at the mathematical level that with increasing temperature the spin-spin coupling of electrons into pairs (entanglement), which determines superconductivity, is DESTROYED.



**Fig. 5.** Illustration of the destruction of electron bonds

This may mean that pair- and multi-electrons at normal and especially elevated temperatures are unstable objects (opposite forces of attraction and repulsion constantly fight in them). That is why SP is observed in the low temperature range, and in the temperature range of LENR reactions, SP is absent, since it requires the presence of stable pair-electrons. But

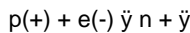
for the LENR reactions to occur, the lifetime of para- and multi-electrons at these temperatures is sufficient. This is indirectly confirmed by the fact that LENR reactions, as a rule, are not avalanche-like, but individual in nature, and the rate of their occurrence is completely determined by the rate of external influences stimulating the formation of new para- and multi-electrons.

The question of the absence of LENR reactions at low temperatures in superconductors remains open. Probably, low temperatures somehow "quench" the implementation of LENR reactions.

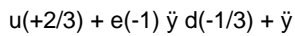
## **Step 2: LENR fission reactions at the quark structure level**

### **nucleons**

Pairs of electrons formed in the lower orbitals leave their orbitals and are captured by the nuclei of atoms by the forces of Coulomb attraction (similar to the capture of single electrons in E-capture reactions). The reaction equation for a single E-capture reaction is:



At the quark level, this reaction looks like this:



Thus, the triad of valence quarks of the proton ( $u+u+d$ ) is transformed into a triad valence quarks of the neutron ( $u+d+d$ ). The atom shifts by 1 position.

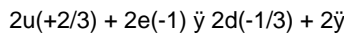
Sometimes a double E-capture (of two single electrons) occurs. In this case, two intranuclear protons are converted into two intranuclear neutrons, and the atom in the table of elements shifts by two positions.

Please note that the SM does not explain the mechanism of particle transformation.

In our case, we are not talking about the capture of two single electrons, but about the capture of a pair of electrons (a single block of two electrons). Such a single block of electrons cannot be captured by two protons, it can only react with

one proton, or more precisely with two u-quarks of this proton. Let us formulate

the equation of the capture of a pair of electrons by a proton:



That is, the triad of valence quarks of the proton ( $u+u+d$ ) is transformed into a triad of quarks ( $d+d+d$ ) of a new unknown nucleon. In modern physics, such nucleons are not known, which means that they cannot exist and must decay. This conclusion will be further analyzed by us when analyzing this reaction at the preon (simple) level. And now we only state that when an intranuclear proton captures a pair of electrons, this proton must decay, and the total number of nucleons in the nuclide as a result of this reaction must

decrease by one proton.

Let us note right away that the proposed model is absent from all other researchers.

### Step 2: LENR fission reactions at the preon structure level

#### nucleons At

the preon level, the reason for the "disappearance" of the proton is the shorter length of the d-quarks compared to the u-quarks, as a result of which the gaps in the hoop of the valence quark triad increase, into which the mu-neutrinos fall, and their mutual annihilation with the d-quarks occurs. The hoop of valence quarks disappears in the nucleon, pulling the entire block of nucleon simplons into a toroidal aggregate. All that remains of the proton is a neutron-like block of 60 tau-neutrinos, which make up 99% of the mass of the nucleons. This block of tau-neutrinos straightens out, but does not disintegrate into individual tau-neutrinos, and under the action of the dipole-dipole magnetic interaction of the magnetic moments, the tau-neutrino retains its

unity.

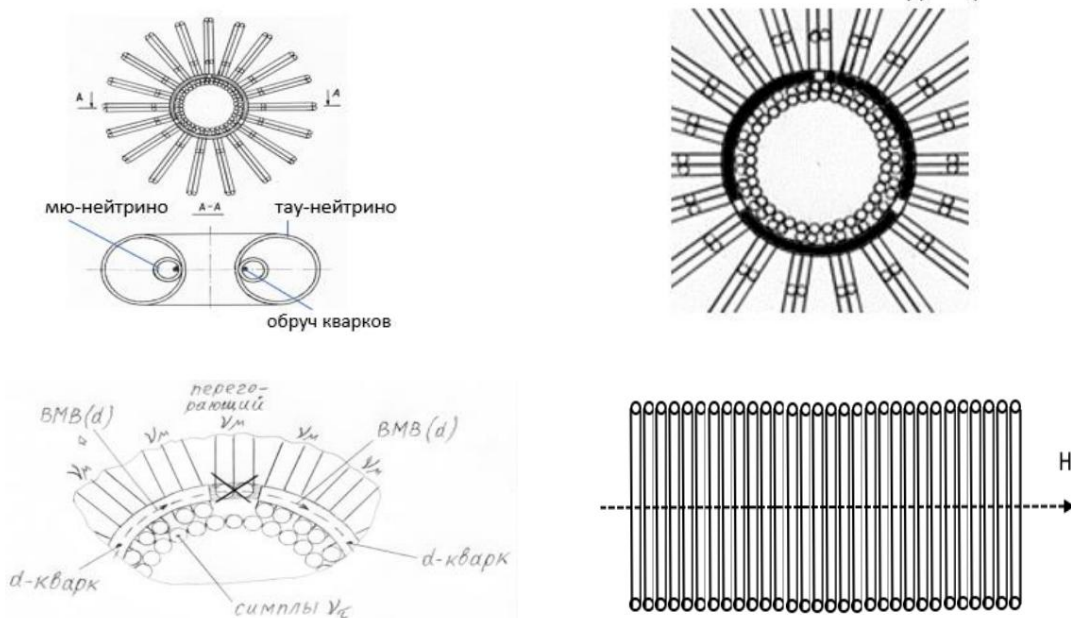


**Fig. 6.** The structure of the ddd nucleon and the process of its destruction

Given the neutral charge of this block, its subnuclear dimensions (diameter 0.43 fm, length 0.07 fm), and the absence of quarks in its composition, which are responsible for nuclear interaction, this block freely leaves the nucleus of the atom, leaving a "hole" in it, which leads to the division of the nucleus into two parts. Next, we will give the S-formula of this fission reaction, in which we will use data on the composition

elementary particles from simplists: tau-

neutrino =  $S\bar{y}^- + S\bar{y}^+$ ; mu-neutrino =  $S\bar{y}^- + S\bar{y}^+$ ; d-quark =  $2Sd^-$ ; u-quark =  $4Su^+$ .      electron =  $6Se^-$ ;

Symbol designation	Sy-, Sy+	Sy-, Sy+	Se-, Se+	Sd-, Sd+	Su+
Simple form	bagel	donut	spiral	spiral	spiral
Mass of the sample (MeV/c <sup>2</sup> )	7.733128152	0.092914675	0.085166485	0.07233125	0.037926625
El. charge of the simple	-/+ 1/6	-/+ 1/6	-/+ 1/6	-/+ 1/6	+ 1/6
Length of the simple (fm)	1.340978222	0.016112051	0.014768461	0.012508386	0.006576741
Sample diameter (fm)	0.427435833	0.005717825	Density in (g/cm <sup>3</sup> )	3.77*10 <sup>19</sup>	3.77*10 <sup>19</sup>
Body diameter S (fm)	0.0005892	0.0005892	0.0005892	0.0005892	0.0005892

## Experimental materials used to verify calculations

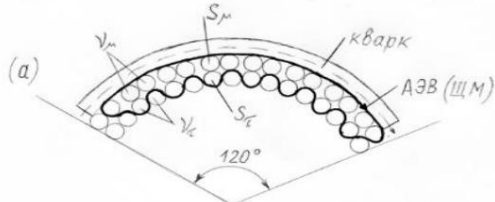
Before moving on to the formulas and calculations, we note that to compare their results with experimental data, experimental materials from the work of Parkhomov A.G., "Nuclear transmutations and excess heat in reactors with incandescent lamps", collection of materials of the RKHTYAiShM-27 [15] are used.

El.	To	After	Difference + numbers of atoms
Li	0.6	4.5	3.9 3.35E+17
Na	<0.42	45.7	45.3 1.19E+18
Mg	6.4	37.4	31 7.68E+17
Al	source material	12.5 67.5	sample
K	1.3 10.2 161 203		55 8.47E+17
Ca			8.9 1.34E+17
Y <sub>ou</sub>			41.9 5.27E+17
V	208	232	24.5 2.90E+17
Cr	8.8	11.3	2.5 2.89E+16
Mn	37.5	43.7	6.2 6.79E+16
Fe	6549	7124	574.8 6.20E+18
Ni	44.8	71.5	26.7 2.74E+17
Cu	48.1	56.5	8.4 7.96E+16
Zn	21	36.8	15.9 1.46E+17
Ga	77	86.2	9.2 7.94E+16
Zr	6.7	7.5	0.9 6.18E+15
Cd	<0.0001	0.4	0.4 2.14E+15
Sn	90	122	32.7 1.66E+17
Sb	0.1	0.7	0.6 2.97E+15
La	2.4	3.1	0.6 2.60E+15
Ce	1.9	2.1	0.2 8.59E+14
Pb	21.3	38.8	17.5 5.08E+16
Bi	30.2	68.5	38.3 1,10E+17

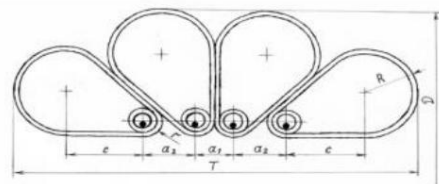
As we can see, LENR reactions produce chemical elements both heavier and lighter than the material of the initial sample in the reactor. Our task is to find out the mechanisms of intranuclear processes, how this happens.

### Calculation of fission reactions at the level of the preon structure of nucleons according to the KST

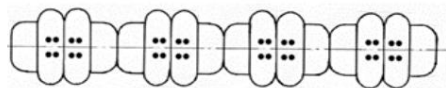
According to the KST, the nuclei of atoms are chains of nucleons [16], contracted MM quarks and twisted into a ball.



model of MM quark formation



MM-quark nucleon contraction model



chain of nucleons of the O-16 nucleus according to the CST result of rapid rotation simulation  
O-16 nuclei by physicists at Kyoto University

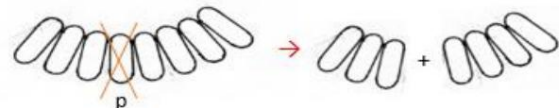
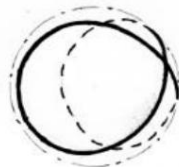


**Fig. 7.** The mechanism of formation of nuclei in the form of chains of nucleons, twisting of these chains into a ball, and their rupture when a proton is destroyed

#### S-formula of absorption of a pair of electrons and "disappearance" of a proton

1st stage - interaction of 2 u-quarks and 2 electrons:

$$2(u) + 2(e^-) = 8(Su^{+*}) + 12(Se^{-*}) \xrightarrow{\text{annihilation}} [8(Su^{+*}) + 8(Se^{-*})] + 4(Se^{-*}) \xrightarrow{\text{ann.}} 2(d) + 1.03 \text{ MeV}$$

Stage 2 – annihilation of 3 d-quarks and 9 mu-neutrinos that fell into the gaps:

$$3(d) + 9(\bar{\nu}_\mu) = 6(Sd^{-*}) + 9(S\bar{y}^{-*}) + 9(S\bar{y}^{+*}) \xrightarrow{\text{ann.}} [6(Sd^{-*}) + 3(S\bar{y}^{-*}) + 9(S\bar{y}^{+*})] + 6(S\bar{y}^{-*}) \xrightarrow{\text{ann.}} 1(e^-) + 1.54 \text{ MeV} + 1(\tau\text{ neutrino block})$$

**P.S.:** The energy of annihilation is carried away by photons and neutrinos. We cannot measure the energy of neutrinos so easily. The energy of photons is much less, it is converted into heat Q.

The total parameters of the reaction are as follows:

$$A_1 + A_2 = A_0 - 1; Z_1 + Z_2 = Z_0 - 1; N_1 + N_2 = N_0; +(e^-); + \tau\text{-neutrino block}$$

The calculation of the susceptibility of 256 natural nuclides of the stability valley to fission reactions during the capture of a pair of electrons was performed using these formulas. The calculation result shows that only heavy nuclides starting with 93Nb (it has 3 fission variants) are susceptible to this type of reaction. The next nuclide 94Mo gives 6-

t fission variants. The maximum number of fission variants 658 gives nuclide

192Pt. The nuclide 235U gives 521 fission variants, which means that the fission of the nuclide 235U possible not only by capturing a neutron, but also by capturing a pair of electrons.

#### Conclusions:

1. L-fission reactions with the capture of a pair of electrons are possible, but only for heavy elements, starting with 93Nb.
2. Nuclides 27Al cannot decay according to this scheme.

### Step 3: Multi-Electron-Fueled LENR Fusion Reactions

Pair and multi-electrons from the upper orbitals "leave" their orbitals and are located in the spaces between the nuclei of atoms, screening their charge, which initiates fusion reactions (the approach and fusion of nuclei).

According to M.P. Kashchenko's calculations, in order to bring together and merge aluminum nuclei with charges of +13, it is sufficient to place a tetra-electron with a charge of -4 ( $q/4$ ) between them. In this case, according to Kashchenko, the tetra-electron is an orbit with two pairs of electrons, and the union of aluminum nuclei occurs in the center of this orbit, and the tetra-electron itself remains outside the merged nucleus, as if out of work.

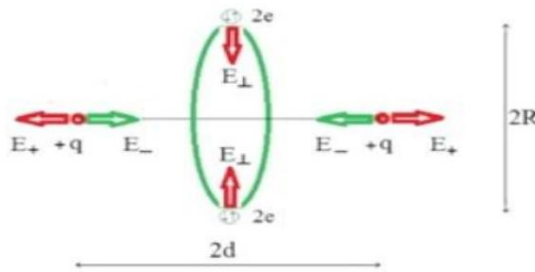


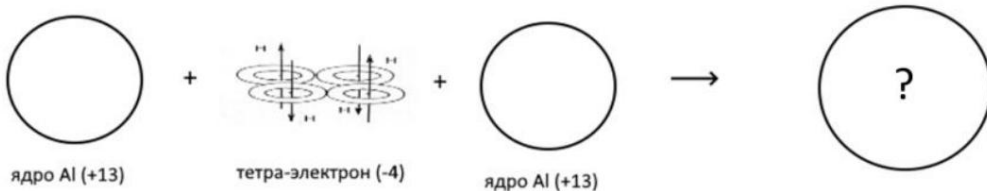
**Fig. 8.** Scheme of synthesis reactions according to M.P. Kashchenko.

The result of the reaction looks like the addition of the number of protons and neutrons:

$$A_3 = A_1 + A_2; Z_3 = Z_1 + Z_2; N_3 = N_1 + N_2.$$

In the CST, all electrons in para- and multi-electrons are closely adjacent to each other, and form a single block without "voids" between electrons. This block of electrons is located on the line of convergence of nuclei, and it cannot "slip out" somewhere to the side, and **must take part in the fusion reaction of nuclei**. In this case, the result of the reaction in the form of addition of the number of protons and neutrons is not obvious and

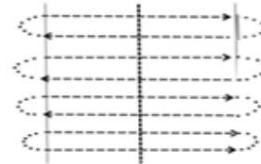
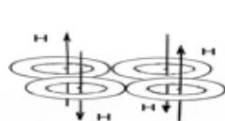
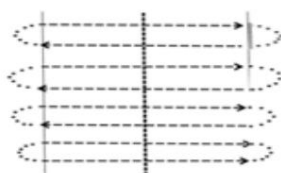
should look somehow different.



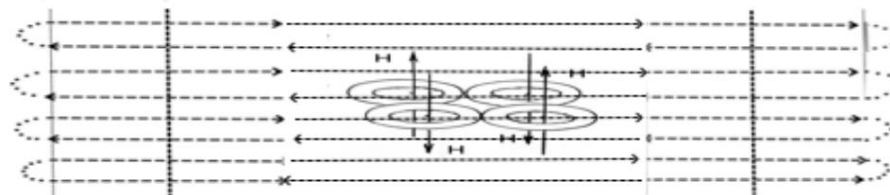
**Rice. 9.** Scheme of the synthesis reaction according to KST

It has already been noted that the attraction of nucleons into a nucleus is carried out by the magnetic moments (MM) of quarks, the distance between the axes of which is

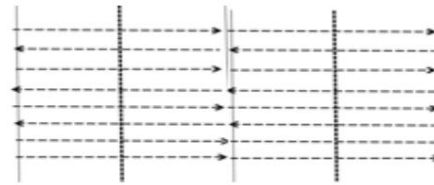
0.0005892 fm. These MM have opposite directions in pairs. At a great distance between nucleons, the lines of force of these MM of each nucleon reconnect to each other in pairs (there is no nuclear interaction between the nucleons). But when nucleons approach each other, the lines of force of MM quarks of different nucleons reconnect and pull the nucleons to each other. This mechanism of nuclear interaction fully corresponds to the mechanism of interaction by means of elementary particles - gluons, which are actually quasiparticles consisting of impulses of interaction of MM quarks.



reconnection of the field lines of MM quarks of two nucleons  
at a great distance from each other



reconnection of the field lines of MM quarks of two approaching nucleons



пересоединение ММ кварков двух нуклонов в ядре  
на близком расстоянии друг от друга

**Fig. 10.** Scheme of reconnection of MM quark field lines

Accordingly, our tetra-electron, which facilitates the convergence of two aluminum nuclei, will at some point find itself in a strong magnetic field of the reconnected  $126+126=252$  MM two nucleons. According to the previously mentioned article [14], this strong magnetic field will tear the tetra-electron into individual electrons, and under the influence of Coulomb electrostatic repulsion, all four electrons will fly apart from each other and "slip out" of the region of contraction of the two nuclei. These four electrons can leave the nucleus, but the positive charge of the nuclei will slow down these electrons, and some of them from 0 to 4 can be captured by intranuclear protons, and up to 4 reactions of single E-

captures, as a result of which these intranuclear protons will turn into intranuclear neutrons. The result of the LENR fusion reaction will look like this: A3 = A1 + A2; Z3 = Z1 + Z2 - K; N3 = N1 + N2 + K, where K = from 0 to 4

In relation to the fusion of two  $^{27}\text{Al}$  nuclei, taking into account possible reactions of proton capture of single electrons, 5 nuclides can be formed:  $^{54}\text{Fe}$ ,  $^{54}\text{Mn}$ ,  $^{54}\text{Cr}$ ,  $^{54}\text{V}$ ,  $^{54}\text{Ti}$ .

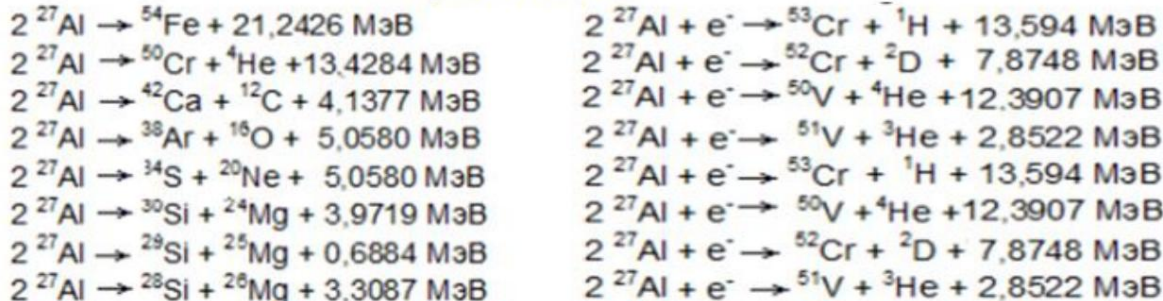
#### Conclusions:

1. Calculation shows that L-fusion reactions initiated by multi-electrons are accessible only to light nuclides up to krypton-69.
2.  $^{27}\text{Al}$  nuclides are susceptible to such reactions, but cannot produce nuclides lighter than  $^{27}\text{Al}$  (and they are formed in the A.G. Parkhomov reactor).

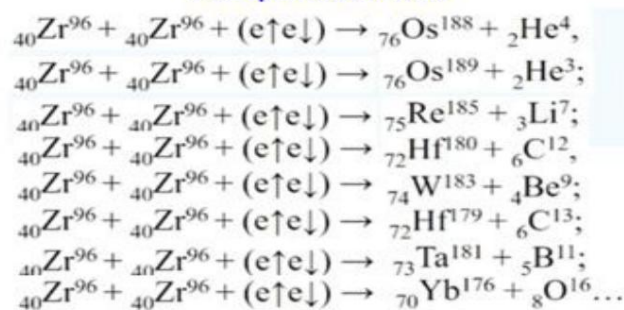
#### Compound LENR reactions according to the scheme 2

ÿ 2. In real LENR reactors, the set of nuclides formed at the output is much wider, and both lighter and heavier elements are formed. Solving this "puzzle", a number of researchers came to the conclusion about the existence of LENR reactions according to the scheme 2 ÿ 2, when two, for example, identical nuclides are transformed into two different nuclides with conservation of mass number (number of nucleons). Below are the equations of such theoretically predicted reactions by two authors:

#### Пархомов А.Г.



#### Кашченко М.П.



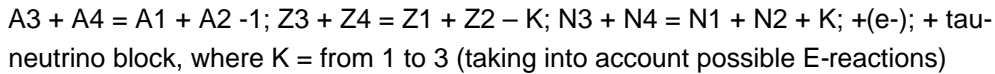
According to A.G. Parkhomov, the process of such reactions is controlled by a neutrino medium. According to Kashchenko, it is controlled by one or several pairs of electrons. For both authors, the main arguments in favor of such reactions are the laws of conservation of mass-energy and charge balances, but the mechanism of such reactions itself is not

is revealed. From a purely "external" point of view, these reactions look like "jumping" of protons and neutrons from one nuclide to another, which is impossible to explain purely physically. And there is no experimental confirmation of exactly this set of I did not find any reaction products in the authors' works, with an equal number of pairs of nuclides being formed.

Without denying the presence of  $2\bar{\gamma}2$  reactions in LENR reactors, it seems to me that Their actual physical mechanism includes two stages:

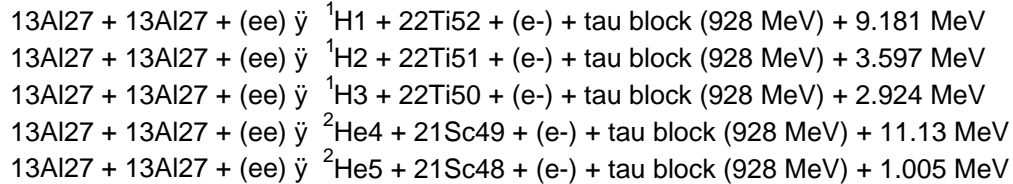
Stage 1 - the fusion of two nuclides with the participation of a multi-electron with the formation of an excited intermediate third nuclide, and stage 2 - the division of this intermediate nuclide into two new nuclides with the participation of pair-electrons.

The only additional condition for the implementation of such a reaction mechanism must be the breakup of a multi-electron by a strong magnetic field into single electrons and one pair of electrons, which immediately triggers the fission reaction of the intermediate nuclide. Generalized formulas for the  $2\bar{\gamma}2$  reaction involving a tetra-electron take the following form:



**PS:** An essential feature of  $2\bar{\gamma}2$  reactions is that it is not the "typical" reference nuclide that is divided, but the excited intermediate nuclide, the mass of which is equal to the sum of the masses of the two initial nuclides, and therefore such reactions can occur, despite the fact that for a similar reference nuclide they are not

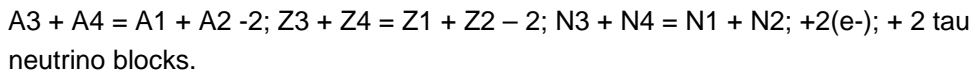
are available. Thus, for two initial nuclides  $^{27}\text{Al}$ , 5 reaction variants according to the scheme  $2\bar{\gamma}2$  are available:



Taking into account additional reactions of capture of two single electrons the total number of reaction options can reach 10.

#### Composite reactions of two nuclides $^{27}\text{Al}$ according to the scheme $2\bar{\gamma}2$

3 The tetra-electron can be broken by a magnetic field into two pairs of electrons, which will lead to the breaking of the chain of nucleons of the intermediate nuclide in two places into three fragments. Generalized formulas of the reaction  $2\bar{\gamma}3$  take the form:



Calculation of variants for  $^{27}\text{Al}$  nuclides according to this scheme gives 3 more variants of  $^{13}\text{Al}^{27} + ^{13}\text{Al}^{27} + (\text{ee}) \xrightarrow{\gamma} ^1\text{H}_1 + ^{22}\text{Ti}^{50} + 2(\text{e}^-) + 2(\text{bl. tau-neutrino}) + 5.25 \text{ MeV}$   $^{13}\text{Al}^{27} + ^{13}\text{Al}^{27} + (\text{ee}) \xrightarrow{\gamma} ^1\text{H}_1 + ^{22}\text{Ti}^{51} + 2(\text{e}^-) + 2(\text{bl. tau-neutrino}) + 3 \text{ MeV}$   $^{13}\text{Al}^{27} + ^{13}\text{Al}^{27} + (\text{ee}) \xrightarrow{\gamma} ^1\text{H}_3 + ^{22}\text{Ti}^{52} + 2(\text{e}^-) + 2(\text{bl. tau-neutrino}) + 5 \text{ MeV}$

+ No single electrons are formed in this decay of the tetra-electron, therefore, there will be no additional reaction options associated with E-capture.

**Composite reactions of two nuclides  $^{27}\text{Al}$  according to the scheme  $2 \bar{\gamma}$** **4** Electron shell of  $^{27}\text{Al}$  in the orbital $^2\text{p}$  contains three pairs of electrons, so there is a

probability of the formation of a hexa-electron, which decays into three pairs of electrons, and the rupture of the chain of nucleons of the intermediate nuclide in three places into four fragments. The generalized formulas for the reaction  $2 \bar{\gamma} 4$  in this case take the form:

$\text{A}_3 + \text{A}_4 = \text{A}_1 + \text{A}_2 - 3; \text{Z}_3 + \text{Z}_4 = \text{Z}_1 + \text{Z}_2 - 3; \text{N}_3 + \text{N}_4 = \text{N}_1 + \text{N}_2; +3(\text{e}^-); + 3 \text{ tau-neutrino blocks.}$

Calculation of reaction variants for two nuclides  $^{27}\text{Al}$  according to this scheme did not yield positive results.

**Proton "disappearance" in LENR fission reactions. Test scheme**

In fission reactions in different variants ( $1\bar{\gamma}2$ ,  $2\bar{\gamma}2$ ,  $2\bar{\gamma}3$ ), the number of atoms of the resulting fragments must coincide with each other. The equality of the number of nuclides-fragments was checked based on the experimental data of A.G. Parkhomov, given in his work [15]. The equality of the number of nuclides-fragments was not confirmed. And the set of nuclides-fragments itself corresponds to the calculations performed (and the calculations of the author himself) with a big stretch. There may be many reasons for this. A.G. Parkhomov himself writes on this topic - "In the reactors that we tested, mainly too many nuclides are formed from a multitude of initial ones to understand in which nuclear reactions they are formed. One can only guess."

This means that it is PROBLEMATICAL to test one or another theory (model) of LENR reactions based on the nomenclature of the formed nuclides and their quantity. However, our conclusion about the destruction of the intranuclear proton during LENR fission reactions and the disappearance of the entire mass of the nuclide is too radical, and it cannot but be reflected in the experimental results. After all, the magnitude of the mass reduction for one LENR fission reaction should be 100% of the mass of one proton and one electron, and not about 1% of the nucleon mass, as in other nuclear reactions. Such a result should be reflected in the aggregate data of all nuclides in the form of a corresponding reduction in the mass of the test sample. This reduction in mass should depend on the number of LENR fission reactions, i.e. on the duration of the operation time.

reactor. With a long period of reactor operation, a decrease in the mass of the sample should accumulate, which can be measured instrumentally.

**Step 4: Formation of strange radiation particles (SRP)**

The neutron-like block of 60 tau neutrinos formed in LENR fission reactions has its own dipole magnetic moment. After leaving the prototype and the reactor volume, the tau neutrino block enters the environment filled with gas of different atoms, molecules, and dust particles that have their own dipole magnetic moments. Dipole-dipole magnetic interaction comes into force, which attracts all these particles to the tau neutrino block. As a result, macro-objects up to several tens of nanometers in size are formed, leaving tracks and craters on the surrounding surfaces.

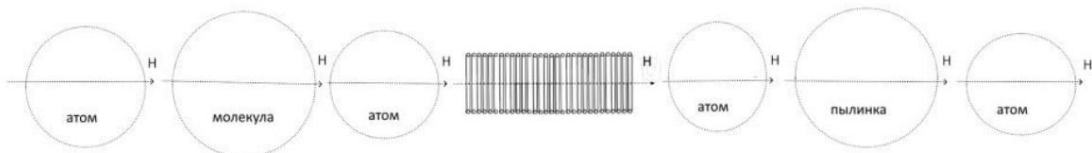


**Fig. 11.** Model of magnetic dipole-dipole formation of SI particles

**P.S.**: An example of such magnetic matter contraction is the process of planet formation. In the article "Astronomers Find Secret Planet-Making Ingredient: Magnetic Field" [17], the authors show that the Earth could not have formed from a protoplanetary cloud using gravity alone in 4.5 billion years. For the formation of the Earth to fit into such a time frame, an additional ingredient is needed –

local source of magnetic field.

According to the theory of Novosibirsk physicist, Doctor of Physics and Medicine Belozerov I.M., such local sources of magnetic field during the formation of planets (and stars, and asteroids too) are embryos of neutron matter [18], which have a strong magnetic field and impart a primary magnetic field to the formed astronomical objects. If we recall the reversals of the magnetic field of planets and stars, the fact that Uranus's axis of magnetic field is shifted from the center of Uranus by 1/3 of the radius and rotated relative to the axis of rotation of Uranus by 60 degrees, it becomes clear that no magneto-dynamo is capable of generating such a magnetic field of the planet. Seismic sounding of the Earth's core during earthquakes inside the iron-nickel core of the Earth revealed a smaller "nucleus" of greater density [19]. According to Belozerov's theory, this "nucleus" consists of neutron matter. Neutrons, separating into a free state from these neutron embryos located in the center of the planets, disintegrate into a proton and an electron, which form a hydrogen atom with an increase in the volume of matter by 10<sup>16</sup> times, which leads to the "inflation" of the Earth, and launches a series of LENR reactions inside the Earth according to the scheme of hydrogenation of elements (addition of protons). These reactions are not considered here, but they also cannot do without the participation of pairs of electrons.

## How to test preon theory (PT) as a basis for LENR reactions

The mass defect of nuclei in all nuclear reactions (NR) always increases and never decreases. All this is well explained in the concept of the preon structure of nucleons by the fact that under external or internal influences on the nucleus, a part of the mu-neutrino toroids and individual valence quarks are destroyed into preons, from which new particles are formed that leave the nucleus. This is what leads to a decrease in the mass of nucleons participating in NR, and to the mass defect of the nucleus as a whole.

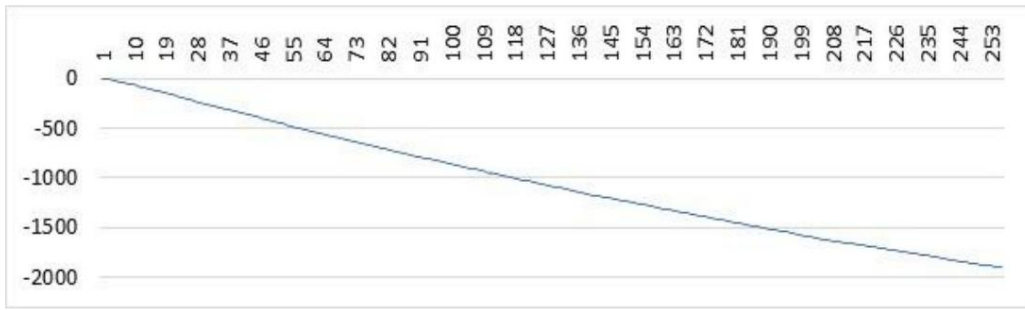


Fig. 12. Growth of mass defect with increasing number of nucleons in nuclei

This can be verified by "weighing" the protons and  $\gamma$ -particles emitted from unstable heavy isotopes during their spontaneous reactions of beta-decay and  $\gamma$ -decay. According to calculations, their mass should be less than the reference masses by up to 1%.

#### Relic Neutron. Revival of Nucleosynthesis According to Gamow's Scheme

This mass defect mechanism, if applied to all NRs retrospectively to the early cosmological epoch, means that the first nucleons in the Universe were not reference protons and neutrons, but relic neutrons of increased mass with 61 mu neutrinos.

Then the decay of some of these relic neutrons led to the formation of protons and electrons in equal quantities.

Another consequence of this scheme is the conclusion that the primary nucleosynthesis of all isotopes proceeded in a single cycle according to the Gamow scheme, by means of the sequential addition of relic neutrons.

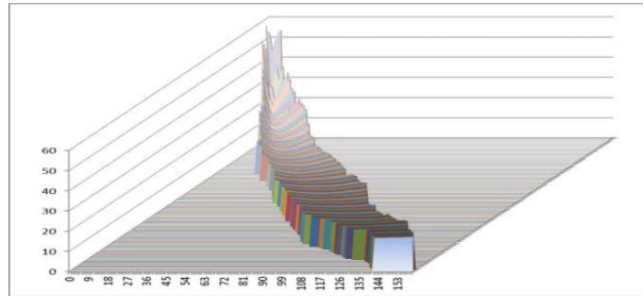
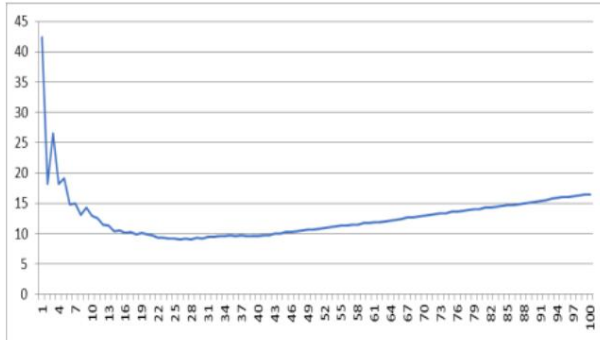


Fig. 13. Results of calculation of primary nucleosynthesis of the entire cloud of isotopes according to the Gamov scheme from relic neutrons

If the James Webb Space Telescope (JWST) interferometer MIRI did not lose its design parameters as a result of micrometeorite impacts, so MIRI should have detected heavy metals in the first galaxies even before the first supernovae exploded in them.

More details about these findings of the CST can be found in the article [20].

#### PS: Stability, instability, and mass spikes of LENR reaction products



According to the KST, all the original natural nuclides were formed in during primary nucleosynthesis according to the Gamow scheme, and represent chains of nucleons (twisted into a ball) with a very specific sequence of protons and neutrons, and having a very definite remainder of whole mu-neutrinos. The division of such a chain of nucleons into two parts leads to the formation of one natural nuclide (a fragment of the initial part of the chain), and one false nuclide (a term of A.I. Klimov). False nuclides have a very definite total number of protons and neutrons, formally corresponding to some

natural nuclide, but their sequence in the second fragment of the nucleon chain has a different sequence than in natural nuclides (and therefore a different "stability"), as well as a different total remainder of whole mu-neutrinos, which leads to a slight difference in their mass – shifted peaks on the spectrograms given in the works of M.P. Kashchenko.

#### Analysis of the energy results of LENR reactions

As already noted, the cause of LENR reactions are para- and multi-electrons formed as a result of external influences. Some external energy is spent on these external influences. Accordingly, the efficiency of devices implementing LENR reactions is measured by the ratio of the utilized released reaction energy to the spent external energy (COP). It should be noted that the maximum released energy of any nuclear reactions is equal to the annihilation energy of the destroyed mu-neutrinos and quarks, which is approximately 1% of the mass of nucleons participating in the reaction. There are nuclear reactions (for example, fission reactions caused by neutron absorption) that practically do not require external energy. Accordingly, the COP of such reactions is formally higher.

Another significant difference between various nuclear reactions is the possibility of autogeneration of individual reaction events (for example, nuclear decays with the absorption of neutrons, with the emission of new free neutrons). This leads to an avalanche-like scenario of multiplication of the number of reactions, which can (or cannot) be controlled.

With regard to LENR reactions, the question of the transition of these reactions to the autogeneration mode is probably possible (for example, the released energy leads to an additional shake-up of orbitals and the formation of more and more new para- and multi-electrons, stimulating more and more new acts of LENR reactions). In this 171

In this case, the source of external energy can be switched off, but the reactions will continue, and it is possible that with increasing energy. The issue of controlling these reactions at the stage of autogeneration requires additional theoretical and experimental research. At present, it has not been studied sufficiently, which can lead to emergency situations.

### **Accidents at industrial installations**

Here are the messages from just this year 2024:

PARIS, 10 Feb 2024 — RIA Novosti: "A fire broke out at a nuclear power plant in France.

Two reactors at the Chinon nuclear power plant in France were shut down due to a fire. Currently The cause of the fire remains unknown and an investigation is ongoing."

TOKYO, May 1, 2024 — RIA Novosti: "A fire broke out in Japan

the turbine hall of the second power unit of the Shimane NPP. The cause has not yet been determined."

Rostov NPP: There were two reactor shutdowns by the protection system this summer due to an overload of the power consumption system.

### **Possible cause of accidents**

Under intense external influence (vibrations) in the materials of the reactor, cooling system, energy removal system, para- and multi-electrons can be formed, leading to nuclear reactions LENR, which can lead to catastrophic accidents (Chernobyl Nuclear Power Plant, Fukushima, Sayano-Shushenskaya HPP, etc.). In the case of the Sayano-Shushenskaya HPP, LENR reactions probably led to the "transformation" of iron atoms of the fastening studs into atoms of other elements, which led to the accumulation of defects in the crystal lattice and the rupture of the studs.

In April I wrote a letter to ROSATOM with a proposal to check preon structure of nucleons by measuring the decrease in the mass of protons emitted in p-decay reactions. Confirmation of this fact would indicate the preon structure of nucleons and the possibility of fission reactions by the capture of pairs of electrons. The answer received states:

*"The subcriticality of the stopped reactor [in cold shutdown mode] and the nuclear safety of the reactor installation are ensured by increasing the concentration of the neutron absorber (boric acid) introduced into the coolant circuit. This completely eliminates the possibility of starting nuclear reactions, including those you mentioned."*

In my opinion, the authors of the answer do not distinguish between fission reactions initiated by neutrons and fission reactions LENR initiated by pairs-electrons.

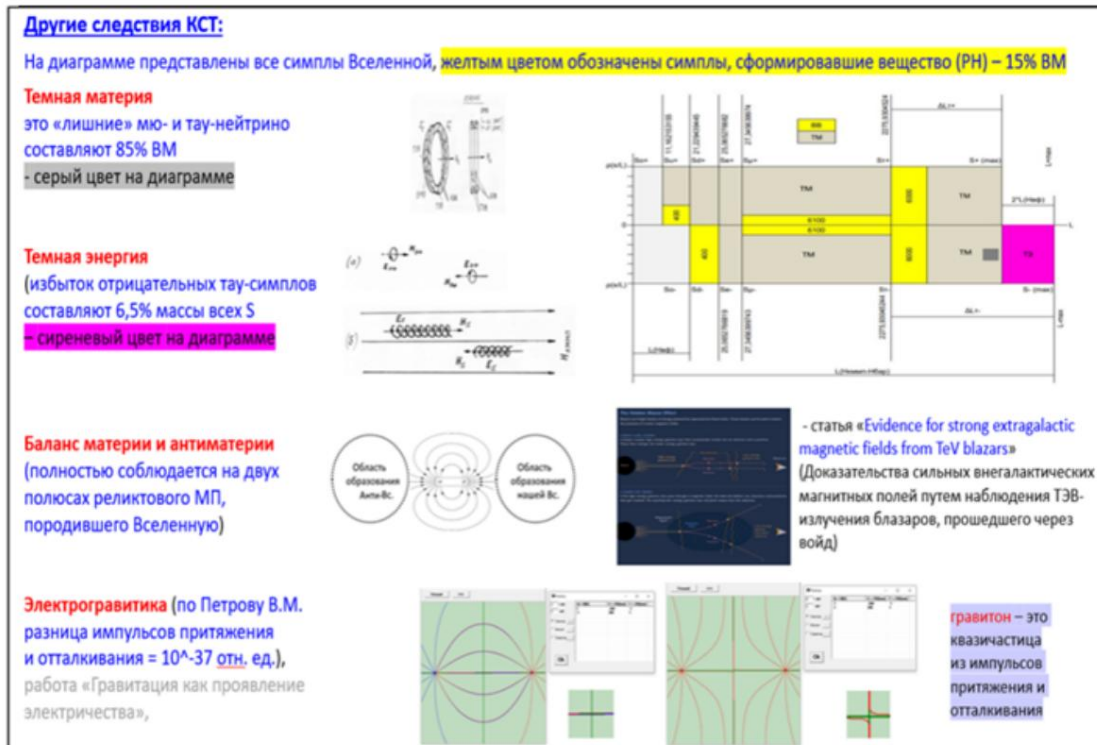
### **Cosmological consequences of CST**

Tab 2 presents the general provisions of the solution in the KST of the issues of Dark Matter, Dark Energy, the balance of matter and antimatter, and the physical model 172

"curvature of space" that generates gravity, based on electrogravitics according to Zollner [8, 21, 22].

The data of the CST consequence indicate that the Big Bang was not kinetic (hot), but polarization (electrodynamic - cold), as a result of which a cold Universe was initially formed from relic neutrons and Dark matter (tau-neutrinos). And only the annihilation of a part of short simplices (2% of the total number of simplices) heated the baryonic matter of the Universe to a temperature significantly lower than that stated by the Standard Cosmological Model. At the same time, Dark matter, not interacting with annihilation photons, remained cold.

**Tab 2. Cosmological consequences of the CST**



**PS:** James Peebles, for his contributions to cosmology and his decisive participation in the development of the Standard Cosmological Model ёCMD, received the Nobel Prize in Physics in 2019.

In December 2019, I plucked up the courage to write him a letter congratulating him on the prize and outlining my main points about the CST and its cosmological implications. James Peebles did not respond. But in June 2020, J. Peebles' article was published -

"Why the universe I invented is right – but still not the final answer"

which I invented is correct - but still not the final answer) [23]. "It is only an approximation to a deeper truth," he says in his article.

### **Appeal to LENR Experimenters**

I suggest you carry out the proposed experiments to check:

1. Reducing the mass of test material samples in LENR reactors.
2. Reduction of the mass of protons and  $\gamma$ -particles in the reactions of beta-decay and  $\gamma$ -decay to 1% compared to their reference mass.
3. Testing the formation of ball lightning by passing a strong current pulse through a conducting spiral (like a wet liana), which will cause it to "burn out" and turn into a plasma spiral, which, under the influence of the internal magnetic moment, will curl up into a glowing donut of BL (quasi-simple).

### **Conclusions**

1. Based on the preon structure of material matter, a model of the formation of pair-electrons and multi-electrons and their initiation of LENR fission and nuclear fusion reactions is proposed. As a result, a conclusion is made about the "disappearance" of protons in LENR fission reactions, which can be verified experimentally in the form of a corresponding decrease in the mass of the test samples of materials in LENR reactors.
2. An essential conclusion of the proposed model is the explanation that the "disappearing" proton is transformed into a neutron-like block of tau-neutrinos, which freely leaves the test sample and the LENR reactor region, and with its magnetic moment attracts atoms, molecules, and dust particles of the surrounding environment into macro-particles, leaving tracks and craters on the surrounding surfaces.
3. The preon structure of material matter is currently of a hypothetical theoretical nature, but can be verified experimentally by measuring the mass of protons and  $\gamma$ -particles emitted from unstable heavy isotopes during their spontaneous reactions of beta-decay and  $\gamma$ -decay. According to calculations, their mass should be less than the reference masses by up to 1%.
4. Experimental verification of the findings is important for more focused research and deeper understanding of LENR reactions.  
and preventing their possible negative consequences (accidents).
5. There are some prerequisites to believe that the phenomenon of Superconductivity and LENR reactions are based on para- and multi-electrons, and the phenomenon of Strange LENR radiation and Dark matter are based on tau-neutrinos. It is necessary to take a closer look at the methods and results of research in these seemingly different areas of physics.

## Literature

1. Zatelepin V.N. "Dark Hydrogen" ѕ2. Electromagnetic and chemical properties". "MIS-RT"-2021 Collection No. 76-1-16-6 <http://ikar.udm.ru/mis-rt.htm>
2. Kashchenko M.P. and Kashchenko N.M. Low-temperature nuclear reactions (course lectures), 2023 <http://lenr.seplm.ru/novosti/kurs-lektsii-lenr-kashchenko-mikhaila-petrovicha>, <https://disk.yandex.ru/d/5MjuHD1KTGQFxg>
3. Kovacs A., Zatelepin V., Baranov D., Signatures of 1.5 MeV Leptons in Nuclear Transmutations. Proceedings of the XXVII Russian Conference on Cold Transmutation of Nuclei of Chemical Elements and Ball Lightning, pp. 268-294.
4. Dugne J.-J., Fredriksson S., Hansson J.. Preon Trinity. A Schematic Model of Leptons, Quarks and Heavy Vector Bosons / Europhysics Letter, 2002, T. 60. arXiv:hep-ph/ 0208135 5.  
Chibisov V., S\_theory (electromagnetic model of the universe).
5. Chibisov V.F. "Corpuscular-Symbol Theory of Everything". Materials XXVII Russian Conference on Cold Transmutation of Nuclei of Chemical Elements and Ball Lightning, pp. 413-435. viXra:1802.0218,
6. Lorentz HA "AETHER THEORIES AND AETHER MODELS", (1901-1902), [https://retrolib.pdp-11.ru/books30/1936\\_lorentz.pdf](https://retrolib.pdp-11.ru/books30/1936_lorentz.pdf)
7. Zöllner Johann Karl Fridreich. Grundzüge einer allgemeinen Photometrie des Himmels. Leipzig 1861 (The Electrical Nature of Gravity), [https://openlibrary.org/books/OL8939339M/Grundz%C3%BCge\\_einer\\_allgemeinen\\_Photometrie\\_des\\_Himmels](https://openlibrary.org/books/OL8939339M/Grundz%C3%BCge_einer_allgemeinen_Photometrie_des_Himmels)
8. Zel'dovich, Ya. B. "Electromagnetic interaction with parity violation." Zh. Exp. Teor. Fiz. 33, 1531 (1957) [JETP 6, 1184 (1957)], [http://jetp.ras.ru/cgi-bin/dn/e\\_006\\_06\\_1184.pdf](http://jetp.ras.ru/cgi-bin/dn/e_006_06_1184.pdf)
9. Mende F.F. New ideas in modern electrodynamics. Kharkov 2012, UDC 537.812+537.312.62+621.372.834.
10. Ginzburg V. Superconductivity: the day before yesterday, yesterday, today, tomorrow. UFN, 2000, <https://ufn.ru/ru/articles/2000/6/b> DOI: 10.3367/UFNr.0170.200006b.0619 12. "The Quantum Secret to Superconductivity", <https://www.quantamagazine.org/medieval-magnet-reveals-superconductor-secret-20160222/>
11. "High-Temperature Superconductivity Understood at Last"  
<https://www.quantamagazine.org/high-temperature-superconductivity-understood-at-last-20220921/>
12. "Computer Scientists Prove That Heat Destroys Quantum Entanglement"  
<https://www.quantamagazine.org/computer-scientists-prove-that-heat-destroys-entanglement-20240828/>
13. Parkhomov A.G. Nuclear transmutations and excess heat in reactors with incandescent lamps. Proceedings of the XXVII Russian Conference on Cold Transmutation of Nuclei of Chemical Elements and Ball Lightning, pp. 25-34.
14. Science. Science and technology news. Breaking stereotypes: rod-shaped nuclei of atoms. Works of scientists from Kyoto University (Japan) on modeling

rotating nuclei of oxygen-16 atoms using the Hartree-Fock method. <http://sci-lib.com/article1246.html>

17. "Astronomers Find Secret Planet-Making Ingredient: Magnetic Field",  
<https://www.quantamagazine.org/simulation-reveals-how-magnetism-helps-form-planets-20210607/>
18. *Belozerov I.M.* Nature through the eyes of a physicist. <https://cyberleninka.ru/article/n/priroda-glazami-physics>
19. Evidence for the Innermost Inner Core: Robust Parameter Search for Radially Varying Anisotropy Using the Neighborhood Algorithm.  
[https://colab.w3/articles/10\\_1029%2F2020jb020545](https://colab.w3/articles/10_1029%2F2020jb020545)
20. *Chibisov V.* Exploration of Mass Defect, Preons and Relic Neutron. . viXra:  
2402.0055v1
21. Evidence for strong extragalactic magnetic fields from TeV blazars. arXiv:1006.3504
22. *Petrov V.M.* Gravity as a manifestation of electricity. "Engineer" No. 10, 2006.
23. *Peebles J.* Why the universe I invented is right – but still not the final answer  
<https://www.newscientist.com/article/mg24632851-400-why-the-universe-i-invented-is-right-but-still-not-the-final-answer/>

### **Four steps of LENR reactions (multi-electronic reaction model)**

**VF Chibisov**

[st.4p@mail.ru](mailto:st.4p@mail.ru)

The article attempts to clarify the physics of LENR processes taking into account the quark (Standard Model) and preonic (Corpuscular-Simple Theory) structures of nucleons and electrons. At the same time, the consideration of LENR reactions is structured into four stages (steps):

Step 1 is the formation of electron pairs and multi-electrons.

Step 2 is the initiation of fission reactions by electron pairs.

Step 3 - initiation of synthesis reactions by multi-electrons.

Step 4 - the formation of particles of strange radiation.

## **Geometrical theory of nuclear interactions and its practical consequences**

**E.A. Gubarev1 , A.N. Sidorov**

<sup>1</sup>Foundation for Assistance to Innovative Development of the State, Moscow

National Research Center of the Russian Academy of Sciences named after V.I.Shplilman, Tyumen

e.gubarev.21@gmail.com  
andrey.sidorov21@gmail.com

The geometric paradigm is based on the thesis that any interaction curves the space of events. For laboratory macroscopic fields, the perturbation of the metric is small and can be reduced to classical potentials on the background of a flat space. In the microworld, the magnitude of nuclear forces is significant, so they cannot be reduced to the classics and must be described by an effective Riemannian space. In accordance with the main features of electronuclear interaction (charge independence and short-range nuclear potential), the Newman-Unti-Tamburino (NUT) space is chosen as such a space, while the effective potentials of this space have the form of classical electronuclear potentials.

### **1. Phenomenological theories of nuclear forces**

The scientific community's attempts to construct a universal nuclear interaction potential and, on its basis, to construct a fundamental theory of nuclear forces have so far ended in failure. And at present, researchers have to describe nuclear forces phenomenologically, using nuclear potentials "introduced by hand" rather than those obtained from a hierarchically higher theory.

The parameters included in the phenomenological potentials are determined by fitting to experimental data. These parameters, as a rule, are not universal constants, but vary depending on external conditions (energy of scattered particles, charge and mass numbers of nuclei, etc.)

Since the beginning of the 1930s, under the pressure of experimental facts, such phenomenological theories as the theory of nuclear forces, the theory of electromagnetic form factors, theories of electrostrong and electroweak interactions, and various theories of elementary particles have developed at a rapid pace.

Let us cite the opinion of Werner Heisenberg, one of the founders of quantum mechanics: "By "phenomenological" theory we mean such a formulation of regularities in the field of observable physical phenomena, in which no attempt is made to reduce the described connections to the underlying general laws of nature, through which they could be understood" [1]. Thus, **phenomenological theories are**

**engaged in the classification of phenomena in their fields, but are essentially meaningless, since they do not reveal the true nature of the phenomenon being studied.**

## 2. Selecting the event space

The geometric paradigm is based on the thesis that any interaction curves the space of events. For laboratory macroscopic fields, the perturbation of the metric is small and can be reduced to classical potentials on the background of flat space. In the microworld, the magnitude of nuclear forces is significant, so they cannot be reduced to the classics and must be described by an effective Riemannian space.

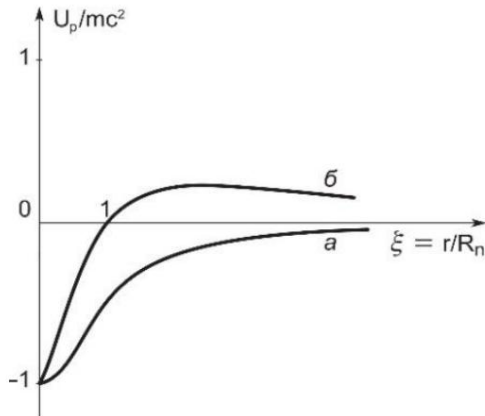


**Fig. 1.** Effective potential energy in the NUT space: a)  $R_e=0, R_n \neq 0$ , b)  $R_e \neq 0, R_n \neq 0, R_e/R_n = -2$

The choice of the event space for the purpose of describing the corresponding interaction is conveniently carried out by the effective potential. In the case of a weak field and non-relativistic velocity of the test particle of the component  $g_{00}$

The Riemannian metric is related to the potential  $\ddot{y}$ , which effectively describes the interaction field against the

background of a flat event space, as follows [2]:

$$2\ddot{y}/c^2. \quad (1)$$

Therefore, the effective potential is equal to  $-1/c^2/2$ . In accordance with the main features of electronuclear interaction (charge independence and short-range nuclear potential), the Newman-Unti-Tamburino (NUT) space was chosen as such a space [3]. The effective potentials of the NUT space have the form of classical electronuclear

potentials (Fig. 1). Two independent parameters of the NUT take the meaning of the electromagnetic and strong charge radii ( $R_e$  and  $R_n$ , respectively). The curves  $U_p(r)$  resemble the electronuclear potentials of classical nuclear physics, in which the region of action of short-range nuclear forces begins behind the Coulomb barrier. The Riemannian metric of the NUT space in spherical coordinates with respect to

the remote observer has the form

$$ds^2 = -(c dt + 4Rn \sin^2(\dot{\varphi}/2) d\theta^2)^2 + dr^2/U - (r^2 + Rn^2)(d\dot{\varphi}^2 + \sin^2\dot{\varphi} d\dot{\theta}^2), \quad (2)$$

where  $U = -1 + (rR_e + 2Rn)/(\dot{r}^2 + Rn^2)$  (3)

To solve the problem of the correspondence of the NUT space to electronuclear interactions, the following were developed: – the theory of classical scattering of particles (scattering of geodesics) in space NUT [4, 5]; – the theory of quantum scattering of particles in NUT space [5, 6, 7].

### 3. Scattering of geodesics

Let us present the main results of calculations of motion and scattering of spinless particles in the NUT space, two free parameters of which are given the meaning of electromagnetic  $R_e$  and strong charge  $R_n$  radii. At  $R_n=0$ , the NUT space passes into a space with a metric of the Schwarzschild type with a single free parameter  $R_e$ , i.e. it becomes the space of events of general relativistic electrodynamics [8]. Fig. 2 shows a graph of the numerical calculation of geodesics in the NUT space with  $R_e=0$ , which corresponds to the interaction of a scattered electrically neutral particle (neutron) and a nucleus.

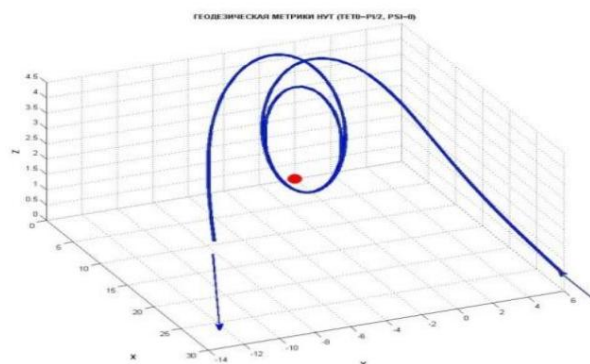
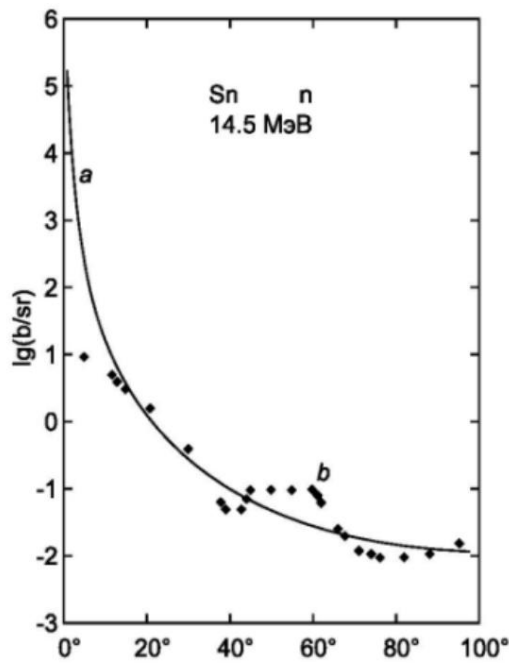


**Fig.2.** Numerical calculation  
geodesics in the NUT space with  $R_e=0$ ,  
 $R_n \neq 0$ . The parameters of entry and  
exit are clearly visible.  
particle flight, as well as double  
flight around the center of the field



The differential cross section for scattering of  
electroneutrals in the NUT field in the small-angle  
approximation is equal to [5]

$$\text{---} \quad \text{---} , \quad (4)$$

where  $\gamma_0 = v_0/c$  is the reduced velocity of the particle at  
infinity,  $\gamma$  is the angle of deviation of the particles from the  
straight trajectory.

**Fig. 3.** Differential cross-section of elastic scattering:  
electrically neutral particles with a  
rest energy of 939.6 MeV and a kinetic energy of 14.5  
MeV at  $R_n \approx 10-15$  cm; b – 14.5 MeV neutrons on tin  
nuclei [9]

#### 4. Quantum scattering theory

Based on the Klein-Gordon-Fock equation, a NUT space was constructed quantum theory of scattering of charged and neutral particles [5, 6, 7]:

$$\text{---} \quad \text{---} \quad \text{---} \quad \text{---} \quad \text{---} \quad (5)$$

Here  $\gamma$  is the mass of the particle.

The values of  $Rn$  determined from a comparison of the scattering of geodesics with experimental data were used in the theory of scattering of a quantum particle interacting with a field source in an electronuclear manner ( $Re \neq 0$ ,  $Rn \neq 0$ ). The values of  $Re$  were determined from the formula for the electromagnetic radius [8], which for scattered protons takes the form

$$Re = -2Z\gamma \gamma / \gamma pc, \quad (6)$$

where  $\gamma$  is the fine structure parameter,  $Z$  is the charge number of the nucleus,  $\gamma p$  is the proton mass.

Fig. 4 shows: theoretical calculation (a) and experimental data of elastic scattering of protons with kinetic energy of 17 MeV on copper nuclei,  $Rn = 3.15 \times 10^{-15}$  cm,  $Re = -8.9 \times 10^{-15}$  cm.

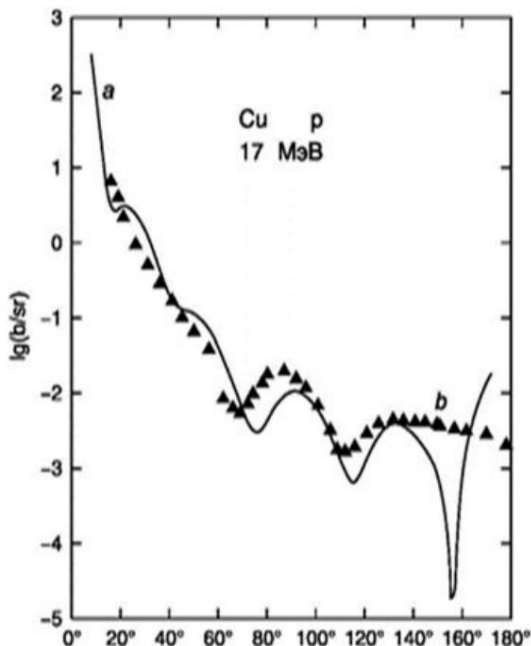


**Fig. 4.** Differential scattering cross-section: a – theoretical calculation at  $\gamma^2 = 938.5$  MeV,  $T = 17$  MeV,  $Rn = 3.15 \times 10^{-15}$  cm,  $Re = -8.9 \times 10^{-15}$  cm (solid curve); b – elastic scattering of 17 MeV protons on copper nuclei (experimental points)

Numerical calculations have shown that the scattering cross differential theoretical sections of quantum particles interacting with a strong field source are in good agreement with the experimental data on the scattering of neutrons and protons on nuclei, while the value of  $Rn$  found from theoretical calculations for various target nuclei is consistent with the experimental law of action

nuclear forces:  $Rn \sim A^{1/3}$ , where  $A$  is the mass number of the nucleus.

Some experimental effects in high-energy spin physics that seem anomalous from the point of view of modern theories can be explained within the framework of the geometric model of strong interaction. Consider, for example,

left-right asymmetry in the scattering of an unpolarized proton beam of ultrarelativistic energy by a polarized proton target [10]. At an incident beam energy of 28 GeV, the number of protons scattered to the left at an angle of 90° exceeded by 2/3 the number of protons scattered to the right at the same angle (Fig. 5, left). This effect poses a serious difficulty for quantum chromodynamics, according to which spin effects should decrease with increasing energy.

In the geometric model of strong interaction, this effect can be qualitatively explained by introducing an independent parameter characterizing the polarization (spin) properties of the target nuclei – the Kerr parameter  $R_s$ . The model will thus involve three parameters –  $R_e$ ,  $R_n$  and  $R_s$ , and the event space will be described by solving the vacuum equations with a metric of the Kerr–NUT type [8]. The introduction of the spin parameter  $R_s$  will lead to the well-known particle drag effect [11], which is significant both in the region of low and in the region of ultrarelativistic energies. Particle drag generates left-right asymmetry in the particle scattering cross section and, especially, in the particle capture cross section (Fig. 5, on the right).

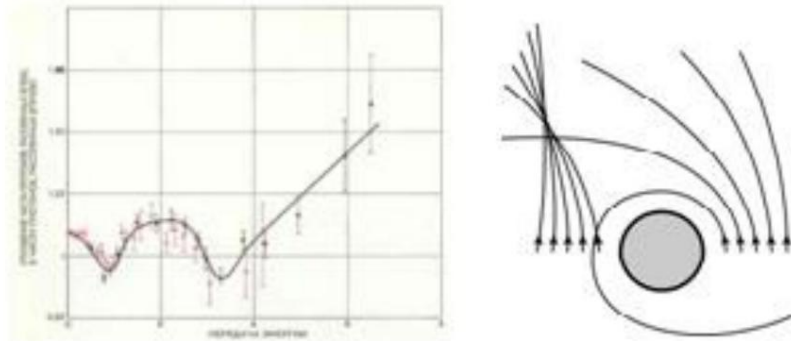


**Fig. 5.** Left: Scattering of an unpolarized 28 GeV proton beam on a polarized proton target. The vertical axis is the ratio of the number of protons scattered to the left at an angle of 90° to the number of protons scattered to the right at an angle of 90°, and the horizontal axis is the energy transfer in GeV [10]. Right: Illustration of the particle drag effect in the Kerr–NUT space.

## 5. Conclusion

The calculations performed allow us to state that the chosen solution of Einstein's vacuum equations with the NUT-type metric provides a fundamental description of nuclear interaction. At the geometric level, this interaction is generated by a strong charge radius. This is equivalent to the existence of a strong charge, which is the source of a strong field.

## LITERATURE

1. Heisenberg W. The role of phenomenological theories in the system of theoretical physics // Advances in Physical Sciences, Vol. 91, No. 4, 1967. Pp. 731–733.
2. Landau L.D., Lifshits E.M. Field theory. 7th ed., rev. M.: Nauka, 1988.
3. Newman E.T., Tamburino L., Unti T. Empty-Space Generalization of the Schwarzschild Metric // J. Math. Phys. 1963. V.4. No.7. P. 915–923.
4. Gubarev E.A., Sidorov A.N. Scattering of neutrons in the field of nonlinear electromesodynamics // Gravity and fundamental interactions: Collection of scientific papers edited by Ya.P. Terletsky. Moscow: Publishing house of UDN, 1988. P. 92.
5. Gubarev E.A., Sidorov A.N. Scattering of geodesics in the geometry of NUT. Geometric strong interaction model. Moscow: New Center, 2008.
6. Gubarev E.A., Sidorov A.N. Vacuum model of strong interaction // Theoretical and experimental problems of gravitation. Abstracts of reports of the 8th Russian gravitational conference. Moscow: 1993. P. 251.
7. Gubarev E.A., Sidorov A.N. Vacuum model of strong interaction. New results // Proceedings of the VI Seminar "Gravitational Energy and Gravitational Waves". Dubna, Publishing House of the Joint Institute for Nuclear Research, 1994. P. 146–152.
8. Shipov G.I. Theory of physical vacuum. Moscow: NT-Center, 1993.
9. Valentin L. Subatomic Physics: Nuclei and Particles: In 2 volumes. Moscow: Mir, 1986.
10. Krish A. Collisions of rotating protons // In the world of science, 1987, No. 10, pp. 12–18.
11. Dymnikova I.G. Motion of particles and photons in the gravitational field of a rotating body // Uspekhi fizicheskikh nauk, v.148, no.3, 1986. pp.393–432.

## Geometric theory for the nuclear interaction and its practical consequences

EAGubarev1 , ANSidorov2

<sup>1</sup> Assistance Fund to Innovative Development of the State  
<sup>2</sup> National Center for Subsurface Use named after VISHpilman  
[e.gubarev.21@gmail.com](mailto:e.gubarev.21@gmail.com)  
[andrey.sidorov21@gmail.com](mailto:andrey.sidorov21@gmail.com)

The thesis of any interaction curving the event space is basic for the geometric paradigm. The perturbation of the metric being small for the laboratory macroscopic field, it can be reduced to classical potential on the background of the flat space. As the magnitudes of nuclear forces are significant in the microworld, they cannot be reduced there to the classics and should be described by the effective Riemannian spaces. As such a space, the Newman-Unti-Tamburino (NUT) space is chosen according to the main features of the electro-nuclear interaction (the charge independence and the short-range nuclear potential). The effective potentials of this space take the form of classical electronuclear potentials.

# The Problem of Inertia and Rotation of Matter. Nonholonomic Mechanics

G.I. Shipov

Institute of Vacuum Physics, Moscow

[warpdrive09@gmail.com](mailto:warpdrive09@gmail.com)

For a complete description of the rotational motion of extended bodies, forces and inertial fields, the geometry of absolute parallelism is used, constructed on a 10-dimensional coordinate manifold of four holonomic translation coordinates and six of motion found for nonholonomic rotational coordinates. The equations in such nonholonomic mechanics take into account the forces and fields of inertia. Conservation laws are obtained that generalize the laws of Newtonian mechanics. Within the framework of the new mechanics, a theoretical description of the motion of the Tolchin inertial body and its more advanced model, the 4D gyroscope, is given. It has been experimentally proven that the generalized Tsiolkovsky equation allows for the creation of a fundamentally new means of transport for movement in space without the use of traditional jet propulsion.

engine.

In 1936, Vladimir Nikolaevich Tolchin, an engineer from Perm, accidentally discovered a phenomenon that led him to create a device that violated Newton's third law of mechanics. He called this device "inertsoid", created a number of different versions of the inertsoid, and conducted many experiments, proving to opponents that the cause of the inertsoid's movement was not friction, as famous mechanics claimed, but internal inertial forces. Tolchin's numerous applications for registration of the invention were rejected. In 1977, V.N. Tolchin published the book "Inertsoid. Inertial Forces as a Source of Motion [1]", but his discovery of a new phenomenon was never recognized by the scientific community. As will be shown below, V.N. Tolchin was right.

## Symmetrical vibrator

Tolchin's invention is based on symmetrical vibrator (Fig. 1), consisting of three masses: a central mass and two masses freely rotating in different directions on rods of length around the axis. If you twist the rods, the central mass will vibrate

along the axis , and the masses rotate synchronously around the axis . Writing the Lagrange function for a symmetrical vibrator and using the Lagrange equations, we obtain its equations of motion [10]

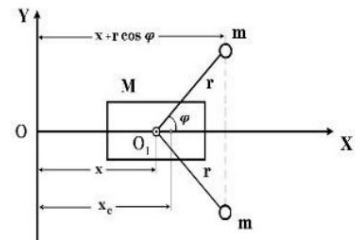


Рис.1

By integrating equations (1) and (2), we obtain their solution in the form

where is the initial coordinate, is the initial velocity of the central body, is the velocity of the center of mass, is the initial angle, is the initial angular velocity and -

elliptic integral of the second kind. From the equations of motion (1) and (2) it follows that the center of mass of a symmetrical vibrator is either at rest or moves with an initial speed , while the angle in the general case depends nonlinearly on . Equation (1), rewritten as , shows that three inertial forces act on the center of mass: 1) ; 2) the projection of the centrifugal force 3) the symmetrical vibrator along the axis translational inertial force ; compensates for force 1). As a result, the center of mass is at rest or moves rectilinearly and uniformly, which is what experiments have shown.

Experimental

The verification of equations (1) and (2) was carried out in 2000 in Thailand (Bangkok), where there was a laboratory created with the necessary equipped scientific equipment (Fig. 2). The symmetrical vibrator was mounted on 4 freely rotating wheels that moved along horizontal rails. The rotation angle sensors were fixed to the body



Рис. 2

the computer case. If we act , the readings of which were transmitted via a flexible cable to the coordinates of on a symmetrical vibrator (on the mass with a force acting along the axis (Fig. 1), the equation will be written as ,

It is known that inertial forces 1) and 2) have potential energy

— [2], therefore the work of the external force is spent both on increasing the kinetic energy of the center of mass and on increasing the internal rotational potential energy depending on the initial angle. This theoretical conclusion was tested experimentally in 2000 in Thailand. In particular, an absolutely elastic impact of a symmetrical vibrator on a wall was investigated, in which the phenomenon of the transition of the kinetic energy of the center of mass of a symmetrical vibrator into the internal rotational energy of the masses (Fig. 3) and vice versa (Fig. 4) was discovered [3].

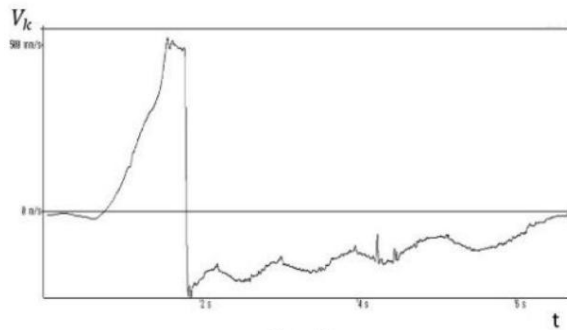


Рис. 3

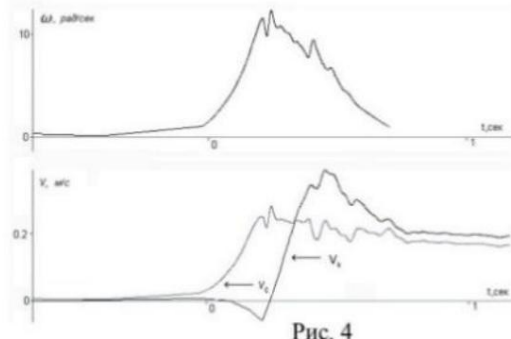


Рис. 4

Figure 3 shows a graph of a perfectly elastic impact of a symmetrical vibrator against a wall. Before the impact, to the left of the vertical line, the internal rotational energy of the loads is zero (the loads do not rotate) and the velocity of the housing is . During the impact, forces of the velocity of the center of mass of inertia appear inside the housing energy, which, due to the law in accordance with equation (5), and the energy is internal rotational of conservation of energy, takes away part of the initial kinetic energy. After the impact, to the right of the vertical line in Figure 3, the vibrator moves away from the wall with less energy of the center of mass (with a lower constant velocity of the center of mass), and the housing, moving away from the wall, vibrates relative to the center of mass. Thus, during a perfectly elastic impact of a symmetrical vibrator, the law of conservation of energy is satisfied, and the law of conservation of translational momentum is violated, since part of the translational momentum before the impact is converted into rotational momentum, causing rotation of the loads. Taking into account , the law of conservation of translational + rotational momentum of the loads , rotational momentum is satisfied. As a consequence of this phenomenon, with an absolutely elastic impact, double, triple, etc. impacts were observed, up to six impacts, before the symmetrical vibrator finally moved away from the wall.

Note that during an absolutely elastic impact of a symmetrical vibrator, a violation of Newton's third law of mechanics is observed, since the translational momentum of its center of mass before the impact is not equal in absolute value to the translational momentum after the impact due to the action of internal inertial forces. And, as is known, inertial forces do not satisfy Newton's third law of mechanics.

Of even greater interest is the internal shock in a symmetrical vibrator, which is described by the equation

Where moment of force acting on the axis of rotation equation (6), a spring (energy source) was installed inside the symmetrical vibrator, the purpose of which was to create a moment changing the angular velocity of rotation of the loads. In addition, a mechanism was installed that played the role of a motor-brake, which, using the energy of the spring, increased from 0 to 15 rad/sec in 0.3 sec and then decreased from 15 rad/sec to 0 in 0.6 sec. As the experiment showed (Fig. 4), during an internal impact in a symmetrical vibrator, the rotational energy of the loads is converted into translational kinetic energy due to the interaction energy of the center

In Fig. 4, the symmetrical vibrator is in place between and . Then a spring is triggered inside the vibrator and, in accordance with equation (6), angular velocity and rotational energy appear. Differentiating solution (3) with respect to time, we find Since at the initial moment, the velocity of

the center of mass appears ~~firstly~~ <sup>in the center</sup> see in Fig. 4, and then the velocity of the center of mass body increases

And the angular velocity changes.

, what are we

. Note that the speed

, i.e.,

When

### Tolchin's inertial system

After of what was said higher it becomes clear why Tolchin's inertia-control device contains two additional elements: a spring as a source of rotational energy (springs 6, 7 in Fig. 3) and a motor-brake consisting of a cam 8, a spring 9 and a bar 10. The task of the motor-brake is to perform two internal impacts in one cycle that change the speed of the center of mass, namely, to increase the speed of rotation of small masses in the sector of angles of 330-0 degrees (increase the speed of the center of mass) and decrease it in the sector of angles of 150-180 degrees (decrease the speed of the center of mass).

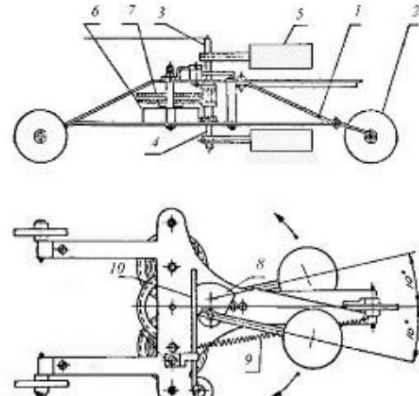


Рис. 5

It should be noted that none of V.N. Tolchin's opponents, who all claimed that the center of mass of the inertoid moves under the action of friction forces, took into account in their works the source of energy - the spring and the work of the motor-brake. Such famous mechanics as N.V. Gulia, E.L. Tarunin (professor of the Perm State

University, Honored Worker of the Russian Federation), E.R. Golnik (Patent Institute, Voronezh) were engaged in falsifying the inertiod, ignoring equations (1) and (2) and using fictitious, non-inertiod mechanical devices to describe the inertiod motion [4]. Violating the professional ethics corresponding to the scheme, these and many other scientists turned a blind eye to the numerous a decisive role in constructing a theory. experiments of V.N. Tolchin, forgetting that in physics it is the experiment that plays Trying to theoretically describe the motion of the inertiod using equations (1) and (2), I substituted the moment created on the axis of rotation of the loads by the motor-brake into the right-hand side of equation (6). As followed from theoretical calculations, this technique did not affect the acceleration of the center of mass in any way, i.e. the center of mass in the theoretical model continued to move rectilinearly and uniformly or was at rest. However, in the experiment, as was shown above, a completely different phenomenon is observed. *It was possible to reconcile theory and experiment after non-holonomic mechanics with a non-holonomic constraint was used to describe the motion of the inertiod instead of Newtonian mechanics.*

*between the holonomic coordinate of the center of mass and the non-holonomic rotational coordinate* In 1983, a group of scientists from Moscow State

University succeeded in one of the enterprises associated with space research, to make an inertial device (Fig. 6) according to the drawings from the book by V.N. Tolchin [1] and conduct scientific experiments with it, and not just demonstrate its movement. The data presented in Fig. 7 were obtained in the experiment, using the following technique. A ruler with a division value of 1 mm was attached to the horizontal smooth surface of the table. A movie camera was mounted on a special rail parallel to the table from above, filming the movement of the inertial device. Experiments on filming the movement of the inertial device were conducted by A.P. Gladchenko (a rocket technology specialist). After processing the film, the following dynamic parameters were removed from it: the coordinate of the loads, the coordinate of the body  $x(t)$ . Based on this data, using the well-known formula



Рис. 6

At first, the inertia-controller stands motionless on the table ( , while degrees. When the springs are wound up, it starts with a slight nudge

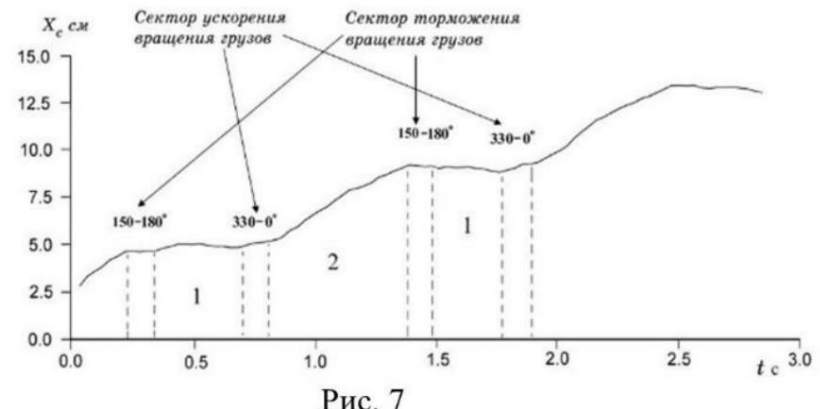


Рис. 7

one of the weights which overcomes the action of the bar 10 on the cam 8, which ensures further rotation of the weights. The weights begin to rotate, the center of mass remains in place until the weights approach the 330-360 degree sector (the first impact). Starting from 330 degrees, the bar 10, acting on the cam 8, creates a moment on the axis (the spring 9 is released (Fig. 5)), increasing the rotation speed of the weights in the 330-360 degree sector. This increase lasts for 0.1 sec, after which the weights rotate freely in the symmetrical vibrator mode with a constant speed. At the moment of increasing the angular velocity in the 330-360 degree sector, the speed of the center increases from sector, 0 to 6 cm/sec (Fig. 7) and this movement lasts for 0.7 sec. When the loads reach the 150-180 degree cam 8 runs onto bar 10, which causes a moment (second impact), while the speed of the center of mass decreases from 6 cm/sec to zero. The coordinate of the center of mass was calculated using the formula As a result, a curve was obtained describing the dynamics of the center of mass (Fig. 7). From the graph in Fig. 7 it is evident that initially on the axis (spring 9 is compressed), reducing the speed of rotation of the loads to the initial value within 0.1 sec. During this time, the speed of the center of mass decreases from 6 cm/sec to 0 and the rest of the center of mass lasts for 0.4 sec. This cycle continues periodically until the winding of springs 6 and 7 (Fig. 5), supporting the rotation of the loads, is completed.

In order to check the influence of friction forces on the inertzoid's motion, we launched it on a horizontal glass surface lubricated with oil. The inertzoid moved along such a surface just as confidently, but with a slightly higher speed. Therefore, it was concluded that the cause of the Tolchin inertzoid's motion is not friction forces, but the motor-brake, and springs 6, 7 and the motor-brake 8, 9, 10. It is enough to turn off the motor-brake with springs 6, 7 wound up, as the inertzoid began to work in the symmetrical vibrator mode, remaining in place. In 1983, a situation arose in which, on the one hand, experiments showed the possibility of controlling the motion of the center of mass of an isolated mechanical system using controlled inertial forces,

and on the other hand, there were no equations describing the phenomenon observed in the experiment.

## **Change in the geometry of space during rotation of matter**

The only theoretical clue that fundamentally changed Newtonian mechanics was E. Cartan's 1922 article [5], in which he argued that the rotation of matter changes the geometry of space, generating torsion

space. At the same time, E. Cartan in his work [5] does not provide any specific formulas that would accurately indicate the connection between the torsion of space and the rotation of matter. Nevertheless, he turned out to be right.

It is known that the mechanics of rotational motion was created by L. Euler, who in 1750 published the work "Discovery of a New Principle of Mechanics [6]". The novelty consisted in the fact that L. Euler introduced (in addition to the three holonomic translational coordinates) three – Euler angles – to describe rotational motion. These dimensionless non-holonomic coordinates are defined as

through the components of the nonholonomic Euler triad, the unit orthogonal nonholonomic vectors of which form a nonholonomic object [7]

---

Here the indices are coordinate indices, and the indices number the vectors of the nonholonomic triad. In addition, L. Euler introduces an infinitesimal rotation of the nonholonomic triad, which is written in tensor indices as [8] [2],

By squaring the relation (8), we obtain the rotational metric

defined on a set of nonholonomic rotational coordinates Size  
in mathematics it is called the Ricci rotation coefficients [9]

Angular velocity of rotation of matter

---

is introduced by dividing the infinitesimal rotation (8) by the arc element that follows or - length from the translation metric [8]

Following E. Cartan, we will look for a geometry in which the object of non-holonomicity (7) enters into the connection in the role of torsion. Such a simplest geometry, in the case under consideration, is the geometry of absolute parallelism, which is based on a six-dimensional manifold consisting of three holonomic translational coordinates and three non-holonomic rotational coordinates. This space is described by relations (7) - (12) and has

connectivity

Where Christoffel symbols defined through the metric (12) by the standard . Taking into account (10) and (7),  
image of - we find  
torsion of space with connection (13)

So, if matter rotates, then to fully describe non-relativistic rotation we must use the space of absolute parallelism and not Euclidean geometry, as physicists have done up to now.

Geometry belongs to the class of non-holonomic geometries, since, firstly, it contains non-holonomic coordinates in its structure differentials of which are non-holonomically related to the differentials (relation (8)). rotation (11) is determined through Secondly, the angular velocity of the holonomic coordinates of matter the non-holonomic object (7) via relation (10). Geodesic Motion of the center of mass of an arbitrary mass in geometry is described by equation [8]

which is found from the generalized Lagrange equation [7]

Equation (15) differs from the equations of Einstein's theory of gravity in that contains explicitly the inertial forces, which are fundamentally absent in Einstein's theory due to the absence of a non-holonomic object (7) Equation (15) describes the motion of the origin o and non-holonomic coordinates of the non-holonomic Euler triad . To describe the rotation of the triad vectors the equation is used

Here, the absolute differential with respect to the connection (13) is denoted by . It is precisely equations (15) and (17) that were used for the theoretical description of the motion of the Tolchin inertiaoid.

### Tolchin's Inertiaoid as a 4D Gyroscope

It is known that in mechanics there are 4 types of inertial forces [2]

- 1) - the force of translational acceleration: 2) - the  
 Coriolis force: 4) forces 2), — - the force caused by accelerated rotation.  
 3) and 4) are generated by the rotation of matter in the Euler spatial angles. From the point of view of the special theory of relativity, force 1) is also generated by rotation, but not in spatial angles, but in spatial-In Fig. 8 the angle is shown – the angle in the plane (- time angles  $x$ ), which in the non-relativistic approximation — allows you to record acceleration in the force of inertia 1) as

where is the speed of light.

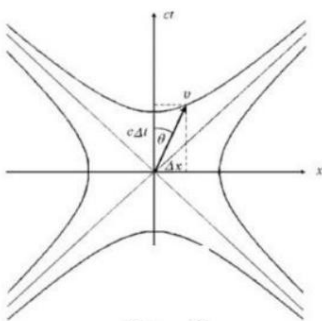


Рис. 8

From this record it is clear that a free symmetrical vibrator rotates along one spatial angle when the masses that comprise it move.

and one space-time angle. That is why I called it a 4D gyroscope [3, 10]. To describe the dynamics of non-holonomic mechanical systems, in which the main role is played by forces and inertial fields, it was proposed to use the geometry of absolute parallelism, built on a 10-dimensional coordinate manifold of four holonomic translational and six non-holonomic rotational coordinates.

coordinates

[8]

To describe the dynamics of nonholonomic systems, Cartan's structural equations are used, written in the form of an extended fully geometrized system of Einstein-Yang-Mills equations [8]

where equations (A) define the torsion

equations (B.2) , equations (B.1) turn out to be completely geometrized Einstein equations, and turn out to be completely geometrized Yang-Mills equations. In equations (B.1), the mass

is defined through the inertial field as

Where - the inertial field defining the 4D angular velocity as – volume, - the determinant of the metric tensor - the multiplier determined by the conditions of the problem, , , - speed - light,  $\dot{\gamma}$  equal to covariant derivative .Current tensor

is also defined through the inertial field , which must be considered as a matter field. Equations (A), (B) do not contain any physical constants, representing a matrix of possible physical objects born from the Vacuum. Their solutions contain constants and functions, the values of which are established using the correspondence with the solutions of known fundamental equations of theoretical physics. As unknown independent functions in equations (A), (B)

components of the Riemann tensor (or field) appear. Solution methods tension components physically and components of the nonholonomic tetrad of inertia, some important solutions are given in the work [8].

### **Generalized Tsiolkovsky equation and experimental Confirmation of non-holonomic mechanics of 4D gyroscope**

From the definition of mass (22) it follows that by changing the rotation of the elements that create it, it is possible to change the total mass of a mechanical system isolated from external forces. In this case, the equation for conservation of momentum is written as

The analogue of equation (24) is the law of conservation of rotational momentum

Where – variable moment of inertia. In nonholonomic mechanics, equation (24) can be called the generalized Tsiolkovsky equation, since it describes the motion of a vehicle in space without using a traditional jet engine.

In 2000, in Thailand, a group of Russian scientists conducted research on a 4D gyroscope, in which the motor-brake was replaced by a servomotor (Fig. 9) and which was controlled by a specially developed computer program. The program slowed down and accelerated the rotation of the weights in certain angular sectors,

In this case, the 4D gyroscope moved only forward (see Fig. 11), refuting the objections of opponents who claimed that the cause of the movement was the friction forces between the wheels of the supporting carriage and the underlying surface.

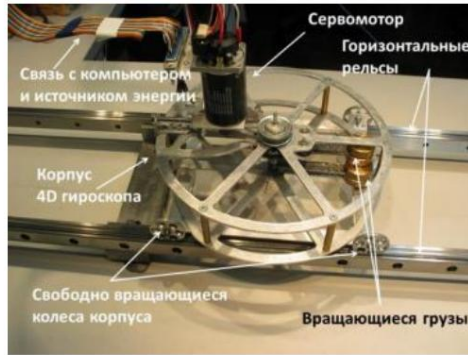
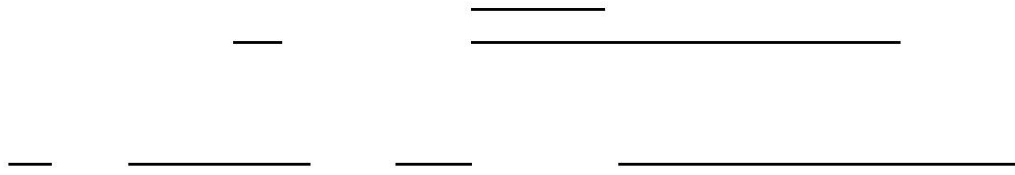


**Fig.9.** 4D gyroscope controlled by a computer program

For the theoretical description of the motion of a 4D gyroscope, the following were used: equations (17), which for our model had the form [3]



For the experimental study of space-time precession, described by equations (26), (27), a 4D gyroscope was created, in which the moment was carried out using a servomotor (Fig. 9), which was controlled by a specially developed computer program. In order to identify the role of the friction forces of the wheels with the underlying surface, theoretical studies of the movement of the 4D gyroscope only due to friction forces were carried out. The theoretical estimate of the work of friction forces on the movement of the center of mass of a 4D gyroscope weighing 1700 grams turned out to be 100 times less than the energy that was observed in the experiment.

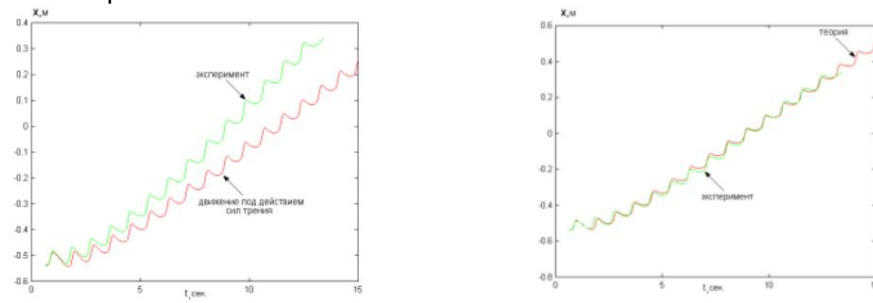


**Fig.10.** Comparison of theory and experiment during the movement of a 4D gyroscope: on the left is Newton's theory taking into account forces and friction; on the right are formulas (26), (27) of nonholonomic mechanics.

To draw a final conclusion about the cause of the 4D gyroscope motion, a theory of the 4D gyroscope motion due to nonlinear friction forces was constructed, and then the resulting theoretical curve was compared with the experimental graph (Fig. 10 on the left). On the right in Fig. 10, the theoretical curve obtained from equations (26) and (27) is compared with the experimental curve. This comparison shows that the cause of the 4D motion is the internal inertial force arising from the control of space-time precession, and not the friction force. We were unable to solve equations (26), (27) analytically, so numerical calculations were performed using the Matlab program, which were compared with the experimental curves (Fig. 10).

A computer program of motion was developed such that the center of mass and the body of the 4D gyroscope moved only forward (Fig. 11). Note that when the frequency changed, the internal momentum of the beginning changed the speed of the center of mass and only then the speed of the body, while the speed of the center of mass "copied" the angular frequency of rotation.

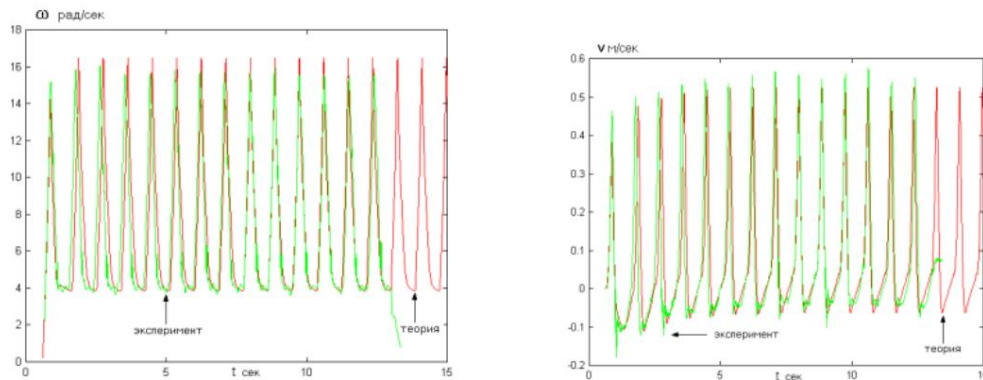


**Fig. 11.** Comparison of theoretical graphs (red curve) obtained using equations (26) and (27) with experimental curves (green curve)

### Nonholonomic mechanics, the discovery of the inertial field and the Unified Field Theory program

Since Newton, inertial forces have been treated ambiguously. Most scientists consider these forces to be "fictitious", so for more than three centuries inertial forces have not been the subject of close study. This omission is mainly due to the fact that inertial forces are generated by rotation (see equation (18)), and a complete description of rotation is impossible without introducing non-holonomic rotational i.e. without describing inertial forces within the framework of non-holonomic coordinates of mechanics. Moreover, inertial forces have a field nature, since their action From this we on an extended material object occurs at each point of the rotating object. come to the conclusion that there is an inertial field and the mechanics of inertial forces has a field nature, being part of field theory. This is also evidenced by Einstein's strong equivalence principle, which states that "a uniformly accelerated body is acted upon by an inertial field equivalent to a uniform

gravitational field". However, this particular case does not at all imply the complete equivalence of inertial fields to the gravitational field.

In 1979, I published a monograph [11] at Moscow State University, in which the equations of the inertial field (A), (B) were first published and the dependence of mass on the angular velocity of rotation of the elements (22) that make it up was found. Equations (A), (B) describe 10-dimensional space-time as a continuous medium with elastic properties. In the formalism (1+3), the splittings of the inertial field equation look as follows [12]

— — —  
which includes the following parameters of elasticity of the medium: rotation, expansion, shear

acceleration ,	A continuous medium described by the equations , has Riemann curvature and torsion (object . From these equations follows a new non-holonomic)
	conservation law

connecting the rotation parameter with the acceleration parameter . Law (28) directly indicates that by changing the rotation of the masses inside the system, it is possible to change the acceleration of its center of mass. Russia's priority in discovering these results was confirmed by a speech in 2005 in Belgium at the International Conference [13] dedicated to the 100th anniversary of the creation of the special theory of relativity. The organizers of the conference highly appreciated the results obtained and issued me a special certificate certifying the priority. It should be noted that the inertial field is the third fundamental physical field (after gravitational and electromagnetic), given in sensations in everyday life. In addition, after appropriate simplifications, equations (A), (B) of nonholonomic mechanics satisfy the principle of correspondence with the equations of Einstein's theory of gravitation, the equations of Maxwell-Lorentz electrodynamics and the equations of quantum field theory, such as the equations of Pauli-Dirac electrodynamics (quantum electrodynamics taking into account spin) [14]. For this it is necessary to hang the equations of the Physical Vacuum, in the spinor basis as [15,8]

In this notation, the equations contain Penrose spinor matrices (spinor indices  
in equations (A) and (B) are omitted),

generalizing Pauli matrices to the case of curved and twisted space A. Here are spinor matrices of Riemannian curvature (the + sign denotes Hermitian conjugation), are spinor Carmel matrices of the field B

inertia (tensor of contortion of the space of absolute parallelism A  
quasi-inertial reference system the density of matter in the integral (22) is expressed If we normalize the field through inertia unity and compare it with the de Broglie wave, then, in the square of the complex field of on this approximation, it will satisfy the equations of quantum electrodynamics Pauli-Dirac. Thus, it turns out that quantum mechanics has a "non-holonomic" nature and describes the dynamics of inertial fields in the approximation of weak inertial fields. In general, equations (A), (B) can be considered as equations of the Physical Vacuum, the excitations of which describe spinning elementary particles with strong gravitational and electromagnetic interaction. The source of these fields is the inertial field, Strong gravitational and electromagnetic fields manifest themselves on a 10-dimensional coordinate manifold as *external* fields, the inertial field should be considered as an *internal* field. It seems that the theory of Physical Vacuum completes A. Einstein's program for the creation of a Unified Field Theory, and all other observed fields and interactions (strong, weak, etc.) that go beyond

the framework of Einstein's program, are imitated by various constructive or phenomenological theories such as the modern Standard Model. As shown by the works on the fundamental description of strong interactions [16], nuclear potentials can be obtained from the solution of the equations of the Physical Vacuum, rather than being entered manually, as has been done to date.

## Conclusion

All physical models are divided into fundamental, phenomenological and constructive. Fundamental theories are of the greatest value, allowing us to understand and correctly interpret physical processes. As for phenomenological and constructive theories, they are preliminary, descriptive in nature and are created to describe new, not yet understood experiments that go beyond fundamental theories. Over time, as theoretical physics develops, any phenomenological or constructive theory dies out and is replaced by a fundamental theory. At the present stage in theoretical physics, two theories are generally recognized and claim to be the "unified field theory": the phenomenological theory - the Standard Model and the constructive theory - string theory. In contrast to these, the theory presented in this article Nonholonomic Mechanics = Theories of Physical Vacuum, claims to be the fundamental unified field theory that explains anomalous phenomena in mechanics, gravity theory and electrodynamics. As an example, this article provides an explanation for the anomalous motion of a 4D gyroscope.

Based on the above analysis, we conclude that the cause of the movement of the center of mass of the 4D gyroscope is the controlled space-time

precession of a gyroscope that moves according to the geodesic equations (26), (27) of the effectiveness , and not under the action of friction, as most space physicists believe. Other examples of the new fundamental theory, brought to the latest technologies, are beyond the scope of this article and will be demonstrated in future publications.

## LITERATURE

1. *Tolchin V.N.* Inertsoid. Inertial forces as a source of motion. Perm. 1977
2. *Olkovsky I.I.* Course of theoretical mechanics for physicists. Moscow: Nauka, 1970.
3. *Shipov G.I.* 4D Gyroscope in Descartes' mechanics. Cyrillic, 2006, p. 74.
4. *Golnik E.R.* Self-sliding of a body with a rotating eccentric on a rough surface of a horizontal plane. Collection of methodological articles on theoretical mechanics, 1980, Voronezh, Issue 10.
5. *Cartan E.* Compt. Rend. 1922. Vol. 174, p. 437.
6. *Euler L.* Discovery of a new principle of mechanics. Notes of the Berlin Academy sciences, 1750, v. 14, pp. 185-217.
7. *Schouten Ya.A.* Tensor analysis for physicists, 1965. Moscow: Nauka, GRFML, p. 455. 8. *Shipov G.I.* Theory of physical vacuum, theory, experiments and technologies, Moscow, Nauka, 1997. 450 p.; *Shipov G.* // A theory of Physical Vacuum, Moscow: ST-Center, 1998. P. 312.
9. *Schouten J.* Ricci-Calculus. B.; Heidelberg: Springer, 1954. P. 516.
10. *Shipov G.I.* Conversations about new (torsion) mechanics. Conversation 2 // "Academy of Trinitarianism", M., EI No. 77-6567, publ. 11659, 22.11.2004. <https://trinitas.ru/rus/doc/0231/006a/02310003.htm>
11. *Shipov G.I.* Problems of the theory of elementary interactions, 1979, Moscow, Moscow State University, Part 1, p. 146.
12. *Ellis G., Van Elst H.*, Cosmological models. Carg`ese Lectures 1999, p.89.
13. *Shipov G.* Decartes' Mechanics – Fourth Generalization of Newton's Mechanics. In "7th Intern. Conference Computing Anticipatory Systems ~ HEC - ULg, Liege, Belgium, 2005, ISSN 1373-5411 ISBN 2-930396-05-9 P.178.
14. *Shipov G.I.* Fundamental results of the theory of Physical Vacuum. Moscow, Pero Publishing House, 2023, 77 p.
15. *Shipov G.I.* Yang-Mills fields in the geometric model of vacuum. Proceedings of the 6th All-Union Conference on General Relativity and Gravitation, Moscow, Lenin Moscow State Pedagogical Institute Publishing House, 1984, p.333. (*Equations of Physical Vacuum were proposed for the first time*).
16. *Gubarev E.A., Sidorov A.N.* Vacuum model of strong interaction. New results. Proceedings of the VI seminar "Gravitational energy and gravitational waves", Dubna, October 26-30, 1993 , from 141.

## **The problem of inertia and rotation of matter. Nonholonomic mechanics**

**G.I. Shipov**

Institute of Vacuum Physics, Moscow  
[warpdrive09@gmail.com](mailto:warpdrive09@gmail.com)

For a complete description of the rotational motion of extended bodies, forces and fields of inertia, the geometry of absolute parallelism A\_4(6) is used, based on a 10-dimensional coordinate manifold of four holonomic and the six nonholonomic rotational coordinates. The equations of motion found in such nonholonomic mechanics take into account the forces and

fields of inertia. Conservation laws generalizing Newton's laws of mechanics are obtained. Within the framework of the new mechanics, a theoretical description of the motion of the Tolchin inertoid and its more advanced model, the 4D gyroscope, is given. It has been experimentally proven that the generalized Tsiolkovsky equation makes it possible to create a fundamentally new vehicle for moving in space without using a traditional jet engine.